



**Investigation of the role of chemical composition on the weathering
and emulsification behaviour of North Sea crude oil**

Joachim Johnson Awaka-ama

A thesis submitted for the degree of

Doctor of Philosophy

School of Life Sciences
Heriot-Watt University
Edinburgh, UK

August, 2011

The copyright of this thesis is owned by the author. Any quotation from the thesis or use of any information contained in it must acknowledge this thesis as the source of the quotation or information.

Abstract

The exploration, production, transportation and refining of petroleum often pose great technical and environmental challenges to the oil and gas industry. It is therefore extremely important to reliably predict and control fluid behaviour, in order to optimize production cost and for purposes of potential environmental pollution in the oil and gas operational activities. The investigations in this work focuses upon North Sea crude oils. In view of the fact that the North Sea crude oils are derived from the same source rock (Kimmeridge), they would be expected to have the same chemistry, but however, they tend to behave differently. The objectives of the research were to develop a better understanding of the effect of temperature and time on evaporation rate and its role in modifying the rate of weathering of North Sea crude oils on seawater. In this research, the chemistry of the oils was investigated to see the relationship to their emulsification behaviour. In the first part of this thesis, the weathering behaviour of four North Sea crude oils were investigated, in particular the evaporation, using a novel evaporation method. It was observed that the rate of evaporation varied between the North Sea oils. Evaporation of emulsified oil differed to unemulsified oil. North Sea crude oils of different states of weathering were emulsified and their viscosities and water contents measured. The four oils produced emulsion types of different viscosities and states of stability. The effects of degree of weathering of oils on emulsion states were assessed. The chemistry of the four North Sea crudes was investigated using a range of analytical techniques. The oils were fractionated by SARA analysis to produce saturates, aliphatic, resins and asphaltene fractions, prior to chemical analyses, using a range of analytical techniques (The crude oils were fractionated and the fractions analyzed for their chemical compositions). The compositions of the four crude oils differed to one another. From these analyses, a number of parameters were selected to characterize the oils. These were polarity, aromaticity and alkyl side chain. These data were used in a modeling study. The asphaltenes from the North Sea crudes investigated were substituted into both synthetic and model oils to study the effect on emulsification. It was observed that the asphaltenes had an effect on the emulsification behaviour. The behavior of modeled asphaltene structures based on the chemical characterization data was found to correlate with the emulsification behavior of the North Sea crudes investigated.

Dedication

This work is dedicated to God, my Jehovah – Jireh (Philippians 4:19).

Acknowledgements

I would like to express my sincere gratitude to my supervisors, Dr. Steve Grigson and Dr. Stephen Euston for their thorough professional guidance and invaluable encouragement throughout this research work.

I gratefully thank fellow graduate students for their intellectual assistance and the enjoyable working environment they provided.

As well, I acknowledge the staff of the Environment Group and EPS, Sean McMenamy, Hugh Barras, Dr. Alan Boyd and Christina Graham for their technical and analytical support. Sincere thanks also to Prof. P. Hughes for constructive comments and suggestions.

My profound and wholehearted gratitude goes to my family for their love, encouragement, total support and prayers without which this work would not have been completed.

I am most grateful to Dr. Swts-Idy for her love, patience and understanding.

I thank my friends and others for their encouragement, even when the road to completion of this project seemed circuitous. To make a definitive list would be difficult indeed, but for those who have given most directly of their time and effort, I offer my sincere thanks. In this respect, I think most especially of Dr. Rosemary, Mohammed Abbas, Mike, Akan Ukwak, John Tinsley, Calum Robb, David, Blaise and others too numerous to mention here. God bless you.

The grant and support from Akwa Ibom State University of Technology (AKUTECH) for this research is gratefully acknowledged.

Declaration

I, Joachim Johnson Awaka-ama, hereby declare that I am the author of this thesis. All the work described in this thesis is my own, except where stated in the text. The work presented here has not been accepted in any previous application for a higher degree. All the sources of information have been consulted by myself and are acknowledged by means of reference.

Joachim Johnson Awaka-ama

ACADEMIC REGISTRY Research Thesis Submission



Name:	Joachim Johnson Awaka-ama		
School/PGI:	School of Life Sciences		
Version: <i>(i.e. First, Resubmission, Final)</i>	First submission	Degree Sought (Award and Subject area)	PhD (Environment)

Declaration

In accordance with the appropriate regulations I hereby submit my thesis and I declare that:

- 1) the thesis embodies the results of my own work and has been composed by myself
- 2) where appropriate, I have made acknowledgement of the work of others and have made reference to work carried out in collaboration with other persons
- 3) the thesis is the correct version of the thesis for submission and is the same version as any electronic versions submitted*.
- 4) my thesis for the award referred to, deposited in the Heriot-Watt University Library, should be made available for loan or photocopying and be available via the Institutional Repository, subject to such conditions as the Librarian may require
- 5) I understand that as a student of the University I am required to abide by the Regulations of the University and to conform to its discipline.

* Please note that it is the responsibility of the candidate to ensure that the correct version of the thesis is submitted.

Signature of Candidate:		Date:	
-------------------------	--	-------	--

Submission

Submitted By <i>(name in capitals)</i> :	JOACHIM JOHNSON AWAKA-AMA
Signature of Individual Submitting:	
Date Submitted:	

For Completion in the Student Service Centre (SSC)

Received in the SSC by <i>(name in capitals)</i> :			
Method of Submission <i>(Handed in to SSC; posted through internal/external mail):</i>			
E-thesis Submitted <i>(mandatory for final theses)</i>			
Signature:		Date:	

Table of Contents

Abstract.....	i
Dedication.....	ii
Acknowledgements.....	iii
Declaration	iv
Research Thesis Submission	v
Table of contents.....	vi
List of Tables	x-xii
List of Figures	xii-xxviii
List of Abbreviations	xix
Appendix A	225-237
Appendix B	238
Appendix C.....	239-279
Appendix D.....	280-284
Chapter 1.0 Introduction.....	1-3
1.1 Crude oil exploration, production and transportation	3-4
1.2 Processes of Offshore Oil and Gas exploration and development drilling	5-6
1.3 The North Sea and Oil exploration and production	6-7
1.4 Sources of oil spill and marine Oil pollution	7-8
1.4.1 Waste discharges from Offshore Oil production	9
1.5 Weathering processes	9-10
1.5.1 Physical transport	10-11
1.5.2 Natural degradation of Oil spills	11-13
1.5.3 Evaporation	13-14
1.5.4 Dissolution.....	15-16
1.5.5 Emulsification	16-17
1.5.6 Dispersion	17-18
1.5.7 Adsorption onto suspended particulate material (SPM)	18-19
1.5.8 Photooxidation	19-20
1.6 Overview of Analytical methods for evaluation of Oil (spill) in the environment	20
1.6.1 Chemical fingerprinting	21-24

1.7 Structural characterization of asphaltenes and its relationship to the weathering behavior of water-in-oil emulsions	24-25
1.7.1 Crude oil components and the chemistry of Asphaltenes	25-26
1.7.2 Some methodologies for studying the structure of Asphaltenes.....	26-30
1.8 Weathering characteristics and Oil spill modeling	30-39
1.9 Research objectives	39
1.9.1 Research outline	40

Chapter 2 Investigation of Effects of Temperature on the Rate of Evaporative Weathering of some North Sea crudes

2.1 Introduction	41- 43
2.2 Experimental	43
2.2.1 Materials	43-44
2.2.2 Glassware cleaning procedure.....	44
2.3 Method	44-46
2.4 Results and Discussion	46
2.4.1 Effect of temperature variation on the rate of weathering of Forties and Brent crude oils.....	46-50
2.4.2 Comparison of Brent crude oils evaporation rates with and without seawater	50-51
2.4.3 Comparison of evaporation of Brent and Forties crude at 30°C	51-52
2.4.4 Compositional changes in Forties and Brent crude oils as a consequence of evaporative weathering	53
2.4.5 GC-FID analyses of fresh/weathered Forties and Brent crude oils on seawater	53-60
2.4.6 Evaporative weathering of Brent crude and Brent crude emulsion on Seawater	60-67
2.4.7 Modeling the effect of temperature on the rate of evaporation of Forties crude oil	67-78
2.5 Conclusion	79

Chapter 3 Water-in-oil Emulsification and stability Measurements for Forties, Brent, Brae A and Stirling crude oils

3.2 Introduction	80-85
------------------------	-------

3.3 Experimental	86
3.3.1 Materials	86
3.3.2 Method	86-87
3.4 Results and Discussion	87-89
3.4.1 Factors influencing the stability of emulsions	90
3.4.2 Effect of viscosity of emulsions	90-92
3.4.3 Influence of crude oil type	92
3.4.4 Effect of shear rate	92-93
3.4.5 Effect of water content of emulsion	93-94
3.4.6 Effect of volume fraction of internal phase	95-96
3.4.7 Influence of temperature	97-98
3.5 Stability classifications of Emulsions	98-100
3.6 Conclusion	101

Chapter 4 Chemical characterization of Forties, Brent Brae and Stirling North Sea Crude Oils

4.2 Introduction	102
4.3 Experimental	102-106
4.4 Materials and Method	106-112
4.5 Results and Discussion	112
4.5.1 Saturates, Aromatics, Resins, Asphaltenes (SARA) fractionation...	112-114
4.5.2 Fluorescence measurements for aromatic hydrocarbon standards and asphaltenes and resins from the crude oils	114-117
4.5.3 Elemental analysis	117-121
4.5.4 Fourier-Transform Infrared (FT-IR) spectroscopy	121-127
4.5.5 ¹ H and ¹³ C NMR (Nuclear Magnetic Resonance)	127-131
4.5.6 GC-FID/ GC-MS analyses	131-132
4.6 Conclusion	133-135

Chapter 5 Crude Oil Fractionation: An investigation of the role of Asphaltenes and Resins in the stability of crude and model Water-in-Oil Emulsification

5.2 Introduction	136-137
5.2.1 Saturate	137
5.2.2 Aromatics	138
5.2.3 Resins	138-139

5.2.4 Asphaltenes	139-142
5.3 Experimental objective	142
5.4 Experimental	142
5.4.1 Materials	142-143
5.4.2 Methods	143-145
5.5 Results and Discussion	145
5.5.1 Effect of Asphaltene/Resin ratios (A/R) on emulsion stabilities of synthetic crude oils	145-150
5.5.2 Characteristics and stability of model crude oil emulsions containing substituted asphaltenes.....	150-157
5.6 Conclusion	158-159
 Chapter 6 Multiphase molecular dynamics modelling of crude oil asphaltene structures	
6.1 Introduction	160-162
6.2 Relationship between surfactants (surface-active agents) and emulsification	163-167
6.3 Methodology	168-170
6.4 Results and discussion	170-183
6.5 Conclusion	184-185
 Chapter 7 Correlation analysis of variables measured in a study of North Sea crude oils	
7.1 Introduction	186
7.2 Background	186-188
7.3 Results and discussion	188-205
7.4 Conclusion	206
 Chapter 8 Integrated discussions of the experimental results	
8.1 Introduction	207
8.2 Background to Oil pollution incidence.....	207-208
8.3 Discussions of experimental results	208-221
 Chapter 9 Conclusions and suggestions for further work.....	
	222-224

List of Tables

Table 1	Specification of crude oils.....	2
Table 2	Parameters from the non-linear regression fit for the data in Figure 4a.....	69
Table 3.1	Viscosity measurement at 10 °C for emulsions (mPa.s) of North Sea crude oils.....	90
Table 3.2	Properties of fresh and weathered crude emulsions.....	91
Table 3.3	Effect of volume fraction on emulsion viscosity.....	98
Table 4.1	Theoretical and experimental maxima in the spectra of aromatic hydrocarbon compounds.....	118
Table 4.2	Functional Group distribution for Forties, Brae A, Brent and Stirling oil fractions from FT-IR analyses indicating various peak heights (cm) at characteristic absorption bands.....	126
Table 4.3	Some major chemical differences in Forties, Brae A, Brent and Stirling crude oil types using various analytical equipment.....	127
Table 4.4	GC-FID <i>n</i> -alkanes in aliphatic fractions of Forties, Brent, Brae A and Stirling crude oil types showing percentage peak heights (mm) relative to <i>n</i> -C ₂₅	138
Table 5.1	Asphaltene/ Resin ratios of synthetic oil emulsions.....	154
Table 5.2	Control synthetic oil emulsion (DHN + 70ml seawater).....	156
Table 5.3	Viscosity of fresh Brent (unemulsified), de-asphaltened Brent, and Brent crude emulsions.....	157
Table 5.4	Viscosities of emulsions (control) of fresh crude oils: 70 ml seawater + 10ml of each crude oil emulsified and measured in SV cup.....	158
Table 5.5	Viscosity measurements, water contents, colour and stability of crude oil fraction combinations in model oil emulsions.....	160
Table 5.6	De-asphaltened original crude oil + Forties asphaltenes.....	161
Table 5.7	De-asphaltened original crude oil + Brent asphaltenes.....	161
Table 5.8	De-asphaltened original crude oil + Brae A asphaltenes.....	161
Table 5.9	De-asphaltened original crude oil + Stirling asphaltenes.....	161
Table 7.1	Showing the correlation of variables in the analyses of some North Sea crude oils	197
Table 7.2	Showing a summary of the significant and not significant correlated variables in the correlation analysis ($p < 0.05$)	199
Table 8.1	Classification of emulsifiers according to HLB values.....	221

Table 8.2 HLB group numbers used in equation (1) calculation for the model asphaltene compounds.....	222
---	-----

List of Tables in Appendix A

Table 2.1 Experimental measurements of Forties crude oil evaporation on seawater.....	229
Table 2.2 Forties evaporation at 20 °C.....	230
Table 2.3 Forties evaporation at 25 °C.....	231
Table 2.4 Forties evaporation at 30 °C.....	232
Table 2.5 Forties evaporation at 40 °C.....	233
Table 2.6 Forties evaporation at 50 °C.....	234
Table 2.7 Mean evaporative mass loss of Forties crude on seawater.....	235
Table 2.8 Percentage (%) evaporation of samples at 12 °C.....	236
Table 2.9 Percentage (%) evaporation of samples at 20 °C.....	236
Table 2.10 Percentage (%) evaporation of samples at 25 °C.....	237
Table 2.11a Percentage (%) evaporation of samples at 30 °C.....	237
Table 2.11b Mean weight loss (g) for Forties evaporation on seawater at 30 °C.....	238
Table 2.12 Percentage (%) evaporation of sample at 40 °C.....	238
Table 2.13 Percentage (%) evaporation of sample at 50 °C.....	239
Table 2.14 Evaporation of Brent crude oil on seawater at 30 °C and measurement of weight loss (g) at intervals.....	239
Table 2.15 Evaporation of Brent crude oil (without seawater) at 30 °C and measurement of weight loss (g) at intervals.....	240
Table 2.16 Evaporation of seawater on Petri dishes at 30 °C and measurement of weight loss (g) at intervals.....	240
Table 2.17 Mean weight loss (g) for Brent evaporation on seawater, Brent (no seawater), and seawater at 30°C.....	241
Table 2.18 Mean weight loss for weathering (evaporation) of Brent crude emulsion on seawater at 30 °C	241

Appendix B

Table 3a Effect of temperature on emulsion stability.....	242
Table 3b Water content (%) of water-in-oil emulsions.....	242
Table 3c Density of crude oil with viscosity of emulsions.....	242

List of Tables in Appendix C

Table 1	Elemental analysis (wt.%) of crude oil fractions.....	243
Table 2	Summary of mean yield (wt.%) of CHN of crude oil fractions by elemental analysis.....	244
Table 3	Hydrogen/ Carbon (H/C) ratios in asphaltene, resin and aromatic fractions of Forties, Brae A, Brent and Stirling crude oils.....	244
Table 4	Yield of various fractions from chromatographic fractionation (SARA analysis) of crude oils.....	280
Table 5	Summary of mean yield (mg) of crude oil fractions from 3 replicate fractionations.....	281
Table 6	Summary of weight percentage (%) yields of fractions from SARA separation of crude oils.....	281
Table 7	Physical appearance of crude oil fractions from chromatographic fractionation.....	282

List of Figures

Figure 1	Flow-chart showing complex impact on higher marine organisms including commercial fish species during offshore oil development.....	4
Figure 2	SARA separation scheme for separation of crude oil into Saturate, Aromatic, Resin and Asphaltene (SARA) components.....	38
Figure 3	Weathering of crude oils on seawater in Petri dishes in the thermostatic water bath.....	47
Figure 4a	Plot of percentage weight loss of Forties crude evaporation at various temperatures.....	49
Figure 4b	Plot of percentage weight loss of Forties crude at 12, 20, 25 and 30 °C.....	49
Figure 5	Plot of mean weight loss for evaporation of Brent crude on seawater, Brent crude without seawater, and seawater samples at 30 °C.....	50
Figure 6	Mean evaporative mass loss for Forties and Brent crude oil on seawater at 30 °C at 0 – 48 hrs interval.....	52
Figure 7a	GC-FID chromatogram of fresh Forties crude oil	

showing the distribution of <i>n</i> -alkanes.....	54
Figure 7b GC-FID chromatogram of fresh Brent crude oil	
showing the distribution of <i>n</i> -alkanes.....	54
Figure 8a Forties evaporation on seawater (SW) at 12 °C (1 h).....	57
Figure 8b Forties evaporation on seawater (SW) at 12 °C (24 h).....	57
Figure 8c Forties evaporation on seawater (SW) at 12 °C (110 h).....	57
Figure 9a Forties evaporation on seawater (SW) at 30 °C (1 h).....	58
Figure 9b Forties evaporation on seawater (SW) at 30 °C (24 h).....	58
Figure 9c Forties evaporation on seawater (SW) at 30 °C (110 h).....	58
Figure 10a Forties evaporation on seawater (SW) at 40 °C (1 h).....	59
Figure 10b Forties evaporation on seawater (SW) at 40 °C (24 h).....	59
Figure 10c Forties evaporation on seawater (SW) at 40 °C (110 h).....	60
Figure 11a 1 h weathering of Brent crude (without seawater) at 30 °C.....	61
Figure 11b 1 h weathering of Brent crude (on seawater) at 30 °C.....	61
Figure 12a 6 h weathering of Brent crude (without seawater) at 30 °C.....	62
Figure 12b 6 h weathering of Brent crude (on seawater) at 30 °C.....	62
Figure 13a 48 h weathering of Brent crude (without seawater) at 30 °C.....	63
Figure 13b 48 h weathering of Brent crude (on seawater) at 30 °C.....	63
Figure 14 Comparison of evaporations between Brent crude	
and Brent crude emulsion showing variations in	
rate of evaporation of oil fractions.....	64
Figure 15a 1 h weathering of Brent crude emulsion on seawater at 30 °C.....	66
Figure 15b 24 h weathering of Brent crude emulsion on seawater at 30 °C.....	66
Figure 15c 48 h weathering of Brent crude emulsion on seawater at 30 °C.....	67
Figure 16 Data for 12 °C evaporation fitted to a two-parameter power law.	
Filled circles are the experimental data	
and the solid line is the regression curve.....	70
Figure 17 Data for 20 °C evaporation fitted to a two-parameter power law.	
Filled circles are the experimental data	
and the solid line is the regression curve.....	71
Figure 18 Data for 25 °C evaporation fitted to a two-parameter power law.	
Filled circles are the experimental data and	
the solid line is the regression curve.....	72
Figure 19 Data for 30 °C evaporation fitted to a two-parameter power law.	
Filled circles are the experimental data and	

the solid line is the regression curve.....	72
Figure 20 Data for 40 °C evaporation fitted to a two-parameter power law. Filled circles are the experimental data and the solid line is the regression curve.....	73
Figure 21 Data for 50°C evaporation fitted to a two-parameter power law. Filled circles are the experimental data and the solid line is the regression curve.....	73
Figure 22 Temperature dependence of coefficient a from equation (1) and Table 2.....	74
Figure 23 Temperature dependence of coefficient b from equation (1) and Table 2.....	75
Figure 24 Linear fit to a vs. T data over the T range 12 – 30 °C.....	76
Figure 25 Linear fit to a vs. T data over the T range 12 – 30 °C.....	77
Figure 26 Common types of crude oil emulsions: Oil-in-water (o/w), water-in-oil (w/o), and less common: water-in-oil-in water (w/o/w).....	82
Figure 27 Formation of water-in-oil emulsion.....	83
Figure 28 Processes taking place in an emulsion leading to breakdown and separation.....	85
Figure 29 Showing water-in-oil emulsions of fresh, 11 %, and 20 % weathered crude oil.....	91
Figure 30 a, b, and c Shows the relationship between the viscosity (Pa.s) and density (gcm^{-3}) of crude oils in fresh oil emulsion, 11% weathered oil emulsion and 20 % weathered oil emulsion respectively.....	93-94
Figure 31 Water content for B(11%) and C(20 %) weathered crude emulsions.....	96
Figure 32(a) and (b) shows the effect of volume fraction of internal phase (water) on emulsion stability of fresh, B(11 % weathered) and C(20 % weathered) respectively. Emulsion viscosity increased as volume fraction increased.....	99
Figure 33 11 % weathered oil (emulsion B) showing the effect of temperature on emulsion stability of emulsion B.....	100
Figure 34 20% weathered oil (emulsion C) showing the effect of temperature on emulsion stability of emulsion C.....	101

Figure 35 (a) showing the mean yields from fractionations in Forties, Brae A, Brent (B) and Stirling (S) crude oils.....	116
Figure 35 (b) The weight % yield of mean values of each fraction.....	116
Figure 36 Showing the comparison of yield of C, H, N analysis of asphaltene (a), Resin (b) and Aromatics (c) fractions isolated by elemental analyses.....	121-122
Figure 37a Comparison of H/C ratios in crude oil fractions (asphaltenes, resins and aromatics) isolated from the 4 oil types by elemental analyses.....	122
Figure 37b Schematic diagram of the proposed mechanism of interactions between resins and asphaltenes. Polydispersed monomers of asphaltenes stack cofacially with resins near the exposed top and bottom surfaces.....	131
Figure 37c The peak heights from the chromatograms of aliphatic fractions from SARA fractionation.....	138
Figure 38 Molecular structure of crude oil resin.....	146
Figure 39 Crude oil asphaltene molecular structures.....	147
Figure 40 Effect of varying the asphaltene/Resin ratio (A/R) on emulsion stability of synthetic oils.....	154
Figure 41 Asphaltene molecular structures showing the high or low aromatic ring, ring heteroatoms and alkyl side chains. These structures were used in the molecular dynamic (MD) simulations.....	175
Figure 42 Plot of density of asphaltene molecules at the water-vacuum interface. The Z-distance (nm) is the distance along the z-dimension normal to the interface.....	179
Figure 43 Plot of density of asphaltene molecules at the decane - water interface. The Z-distance (nm) is the distance along the z-dimension normal to the interface.....	181
Figure 44 (b,c,) of Ha1N and (44d,e) of ha2N showing the structural conformation at the water-vacuum interface and a plot radial distribution (g(r), (Fig 44a) for the adsorbed molecules.....	182
Fig 45 (b,c) of La1N and (45d,e) of la2N showing the structural conformation at the water-vacuum interface and a plot of radial distribution (g(r)), (Fig45a), for the adsorbed molecules.....	184

Figure 46 (a,b) showing the comparison of the ha1N with la1N and ha2N with la2N.....	185
Fig 47 Showing the effect of addition of hydrocarbon chains to the ha1N (Fig 47c,d) and la1N (Fig 47e, f) molecules to the asphaltene layer.....	186
Figure 48 Ha2N and la2N showing the structural conformation of asphaltenes at the decane-water interface and a plot of radial distribution ($g(r)$), (Fig 48a,b,c), for the adsorbed molecules.....	188 -189

List of figures in Appendix

Figure 1 (a-f) Showing the fluorescence emission spectra obtained for the various PAH compounds. The measured emission spectra ranged from ~340 nm – 445 nm. All compounds were in dilute cyclohexane solution.....	245-247
Figure 2 (a-c) Showing the measured fluorescence spectra for asphaltenes of Forties, Brae A and Brent. The spectra indicate the fluorescence ranging from ~300 nm – 600 nm.....	248-249
Figure 3a Showing the FT-IR spectra of Forties asphaltene.....	250
Figure 3b Showing the FT-IR spectra of Brae A asphaltene.....	251
Figure 3c Showing the FT-IR spectra of Brent asphaltene.....	252
Figure 3d Showing the FT-IR spectra of Stirling asphaltene.....	253
Figure 4a Showing the FT-IR spectra of Forties resin.....	254
Figure 4b Showing the FT-IR spectra of Brae A resin.....	255
Figure 4c Showing the FT-IR spectra of Brent resin.....	256
Figure 4d Showing the FT-IR spectra of Stirling resin.....	257
Figure 5a Showing the FT-IR spectra of Forties aromatic.....	258
Figure 5b Showing the FT-IR spectra of Brae A aromatic.....	259
Figure 5c Showing the FT-IR spectra of Brent aromatic.....	260
Figure 5d Showing the FT-IR spectra of Stirling aromatic.....	261
Figure 6a GC-FID of Forties aliphatic fraction.....	262
Figure 6b GC-FID of Brae A aliphatic fraction.....	262
Figure 6c GC-FID of Brent aliphatic fraction.....	263

Figure 6d	GC-FID of Stirling aliphatic fraction.....	263
Figure 7a	^1H NMR spectrum of Forties asphaltene showing signals at different intensities.....	264
Figure 7b	^1H NMR spectrum of Forties resin showing signals at different intensities.....	264
Figure 7c	^1H NMR spectrum of Forties aromatics showing signals at different intensities.....	265
Figure 7d	^{13}C NMR spectrum of Forties asphaltene showing 7 signals corresponding to the different carbon environments numbered (1-7) in the sample in CDCl_3	265
Figure 7e	^{13}C NMR spectrum of Forties resin showing signals corresponding to the different carbon environments in the sample.....	266
Figure 7f	^{13}C NMR spectrum of Forties aromatics showing signals corresponding to the different carbon environments in the sample.....	266
Figure 8a	^1H NMR spectrum of Brae A asphaltene showing signals at different intensities.....	267
Figure 8b	^1H NMR spectrum of Brae A resin showing signals at different intensities.....	267
Figure 8c	^1H NMR spectrum of Brae A aromatics showing signals at different intensities.....	268
Figure 8d	^{13}C NMR spectrum of Brae A asphaltene showing signals corresponding to the different carbon environments in the sample.....	268
Figure 8e	^{13}C NMR spectrum of Brae A resin showing signals corresponding to the different carbon environments in the sample.....	269
Figure 8f	^{13}C NMR spectrum of Brae A aromatics showing signals corresponding to the different carbon environments in the sample.....	269
Figure 9a	^1H NMR spectrum of Brent asphaltene showing signals at different intensities.....	270
Figure 9b	^1H NMR spectrum of Brent resin showing signals at different intensities.....	270

Figure 9c	^1H NMR spectrum of Brent aromatics showing signals at different intensities.....	271
Figure 9d	^{13}C NMR spectrum of Brent asphaltene showing signals corresponding to the different carbon environments in the sample.....	271
Figure 9e	^{13}C NMR spectrum of Brent resin showing signals corresponding to the different carbon environments in the sample.....	272
Figure 9f	^{13}C NMR spectrum of Brent aromatics showing signals corresponding to the different carbon environments in the sample.....	272
Figure 10a	^1H NMR spectrum of Stirling asphaltene showing signals at different intensities.....	273
Figure 10b	^1H NMR spectrum of Stirling resin showing signals at different intensities.....	273
Figure 10c	^1H NMR spectrum of Stirling aromatics showing signals at different intensities.....	274
Figure 10d	^{13}C NMR spectrum of Stirling asphaltene showing signals corresponding to the different carbon environments in the sample.....	274
Figure 10e	^{13}C NMR spectrum of Stirling resin showing signals corresponding to the different carbon environments in the sample.....	275
Figure 10f	^{13}C NMR spectrum of Stirling aromatics showing signals corresponding to the different carbon environments in the sample.....	275
Figure 11a	GC-MS of Forties aromatics fractions.....	276
Figure 11b	GC-MS of Brae A aromatics fractions.....	277
Figure 11c	GC-MS of Brent aromatics fractions.....	278
Figure 11d	GC-MS of Stirling aromatics fractions.....	279
Figure 12	A schematic representation of a Soxhlet extractor, used in the separation and purification of crude oil asphaltenes.....	280

Appendix D

Asphaltene. Annotated mdp File for the Molecular Dynamics (MD) simulation...	283-287
--	---------

List of abbreviations

BTEX	Benzene, toluene and ethylbenzene and <i>o</i> -, <i>m</i> - and <i>p</i> -xylene isomers
PAC's	Phenols, acids and alcohols
TLP	Tension Leg Platform
DDCV	Deep Draft Caisson Vessel
OSPAR	Convention for the Protection of the Marine Environment of the North-East Atlantic
ASCE	American Society of Civil Engineers
ITOPF	The International Tanker Owners Pollution Federation Limited
UNEP	United Nations Environment Programme
PAH's	Polycyclic Aromatic Hydrocarbons
NORM	Natural Occurring Radioactive Materials
HELCOM	The Helsinki Commission
UV	Ultraviolet
EIA	Environmental Impact Assessment
GC-FID	Gas chromatography-Flame Ionization Detection
GC-MS	Gas Chromatography- Mass Spectroscopy
IR	Infrared
FT-IR	Fourier Transform - Infrared
NMR	Nuclear Magnetic Resonance
SARA	Saturates, Aromatic, Resins and Asphaltenes
NOAA	National Oceanic and Atmospheric Administration
BSW	Brent on Seawater
SW	Seawater
O/W	Oil-in-water emulsions
W/O	Water-in-oil emulsions
W/O/W	Water-in-oil-in-water emulsions
H/C	Hydrogen to carbon ratio
DHN	Decahydronaphthalene
A/R	Asphaltene to resin ratio
R/A	Resin to asphaltene ratio
MD	Molecular Dynamics

CHAPTER 1

1.0 Introduction

Crude oil, generally referred to as petroleum, is a complex mixture of hydrocarbons that exist naturally in gaseous (natural gas), liquid (crude oil), and solid (asphalt) states. It is derived from a variety of biochemical compounds present in algae, bacteria, phyto- and zooplankton and higher plants. The conversion and transformation of biochemical compounds (e.g., lipids, fatty acids, proteins, porphyrins, sterols and terpenoids) into petroleum is completed through a selection of maturation processes: diagenesis, catagenesis and metagenesis in time scales of hundreds of millions of years (Peters and Moldowan, 1993). Crude oil is inherently complex in nature with a ubiquitously distributed mixture of thousands of different organic compounds formed from a variety of organic materials that are chemically converted under differing geological conditions. The composition of crude oils can vary substantially depending on the starting organic materials and the maturation history in the source rock and the reservoir (Christensen, 2005).

Crude oils contain primarily carbon and hydrogen (which form a wide range of hydrocarbons from light gases to heavy residues), but also contains smaller amounts of sulfur, oxygen and nitrogen as well as metals such as nickel, vanadium and iron. The infinitely variable nature of these factors results in distinct chemical differences between oils (Wang and Fingas, 2003). Refined petroleum products are fractions usually derived by distillation of crude oil. The variability in the number and form of individual components in the crude oil give the oil different physico-chemical properties (Doerffer, 1992). These specifications of crude oils are given in Table 1.

Table 1 Specification of crude oils

Category	Country	Type	Specific Gravity Kg/l	Viscosity Cs at 38 °C	Pour point °C	Pour point for residue 200 °C + °C
1 High wax content	Gabon	Gamba	0.872	28.5	30	Not relevant
	Libya	Es sider	0.841	5.7	9	Not relevant
	Libya	Libyan h.pour	0.846	12.7	21	Not relevant
	Libya	Sarir	0.847	11.9	24	Not relevant
	Nigeria	Nigerian light	0.844	3.59	21	Not relevant
	Egypt	El Morgan	0.847	13.0	13	Not relevant
	UK	Argyll	0.833	3.2	9	36 ^(b)
	UK	Auk	0.837	5.7	12	35 ^(b)
	UK	Beatrice	0.835	8.15	27	42 ^(b)
	UK	Dunlin	0.850	5.3	3	30 ^(b)
2 Moderate wax content	Qatar	Qatar	0.814	2.55	-18	5/10
	Qatar	Qatar mar.	0.839	4.1	-12	5
	USSR	Muhanovo	0.835	4.18	0	13
	USSR	Romashkin	0.859	6.9	-4	5/7
	Algeria	Zarzaitine	0.816	4.56	-15	5
	Libya	Brega	0.824	3.6	-18	7
	Libya	Zueitina	0.808	2.9	-12	10
	Iran	Iranian light	0.854	6.6	-4	10
	Iran	Iranian heavy	0.869	10.2	-7	7
	Iraq	Northern Iraq	0.845	4.61	-15	10
	Abu Dh.	Abu Dhabi	0.830	3.42	-18	5/7
	Abu Dh.	Abu Dhabi-Z	0.825	2.9	-15	7
	Abu Dh.	Abu Dhabi-U	0.840	3.8	-15	5/10
	Norway	Ekofisk	0.808	2.4	-12	30 ^(a)
	UK	Andrew	0.827	3.3	-12	33 ^(b)
	UK	Brent	0.833	4.6	-6	36 ^(b)
	UK	Magnus	0.828	3.1	-3	30 ^(b)
	UK	Forties	0.842	4.43	-13	33 ^(b)
3 Low wax content	Algeria	Hassi Messaoud	0.802	1.95	< -30	< 5
	Algeria	Arzew	0.809	2.4	< -30	< 5
	Nigeria	Nigerian med.	0.907	14.1	< -30	< 5
	Nigeria	Nigerian export	0.872	5.8	< -30	< 5
	Kuwait	Kuwait	0.869	10.6	-17	< 5
	Saudi Ar.	Arabian light	0.851	5.45	< -30	< 5
	Saudi Ar.	Arabian med.	0.874	9.7	-15	< 5
	Saudi Ar.	Arabian heavy	0.887	19.1	< -30	< 5
	Neutr.Z.	Kaffi	0.888	18.1	< -30	< 5
	Iraq	Southern Iraq	0.847	5.76	-13	< 5
	Oman	Oman	0.861	8.7	-27	< 5
	Venezuela	Tia Juana med.	0.900	16.8	< -30	< 5
4 Very low wax highly viscous	Venezuela	Baccharaquero	0.978	1280	-15/7	-
	Venezuela	Tia Juana Pos.	0.980	2983	-3	-

(a) Sbm = Single buoy mooring; (b) Residue 342 °C+ (648 °F+).

Source: Doerffer (1992): *Oil spill response in the marine environment*

Petroleum hydrocarbons can be broadly divided into saturated, aromatic and polar compounds. Saturates are the predominant class of hydrocarbons in most crude oils and include straight and branched chain saturates (i.e., paraffins) and cycloalkanes (naphthenes). The aromatics are cyclic, planar compounds that resemble benzene in electronic configuration and chemical behavior. The aromatics are mainly comprised of BTEX (the collective name of benzene, toluene, ethylbenzene, and *o*-, *m*- and *p*-xylene isomers), other alkyl-substituted benzene compounds such as naphthenoaromatics and polycyclic aromatic compounds (PACs) including the alkylated C0 - C4- PACs that are characteristic in oil. The polar fraction includes heterocyclic hydrocarbons such as nitrogen, oxygen and sulphur containing PACs, phenols, acids and alcohols (Doerffer, 1992; Dutta and Harayama, 2001).

1.1 Crude oil exploration, production and transportation

The economy of the world is greatly dependent on the exploration, production, transportation and refining of petroleum. Crude oil and refined petroleum products play an important role in the modern society. It creates most of the energy and resources that is needed to run the rapidly developing society. It powers transport, heat and cools buildings, creates industrial and domestic chemicals and provides feedstock for many products.

Oil is a non-renewable resource that is used at a rate of 100 million barrels a day at present with projected estimates that this consumption will double by 2030. Experts have forecast that by 2030, oil will remain the largest source of energy supply at approximately 34% (Exxonmobil, 2010). The exploitation and development of this resource also lead to a wide range of present and future environmental and social cost, both direct and indirect. Widespread use of crude oil and petroleum products inevitably result in intentional and accidental releases to the environment. There is a growing awareness and demand by society to balance the environmental costs against the benefits derived from this resource. A greater percentage of national and international shipping of raw materials and commercial goods in the fast growing world economy will also be transported by marine vessels. Thus, the risk of accidental discharges to the environment – either as crude oil from

production operations or marine fuels from the discharge of maritime cargo vessels – will certainly increase. Waterborne oil spills of unknown origin often occur in rivers, in open water and in coastal waterways, and they range from the continuous leakage from land sources and illegal tank washings at sea to larger spill accidents such as the 2002 *Prestige* oil spill and the Deepwater Horizon offshore installation accident which occurred in April, 2010. World-wide, the number of spills is high (Etkin, 2001; Wang and Fingas, 2003).

Oil spills cause extensive damage to marine life, terrestrial life, human health, and natural resources. Therefore, to unambiguously characterize spilled oils and to link them to the known sources are extremely important for environmental damage assessment, understanding the fate and behavior and predicting the potential long-term impact of spilled oils on the environment, selecting appropriate spill response, and taking effective clean-up measures, as well as reliably monitor remediation.

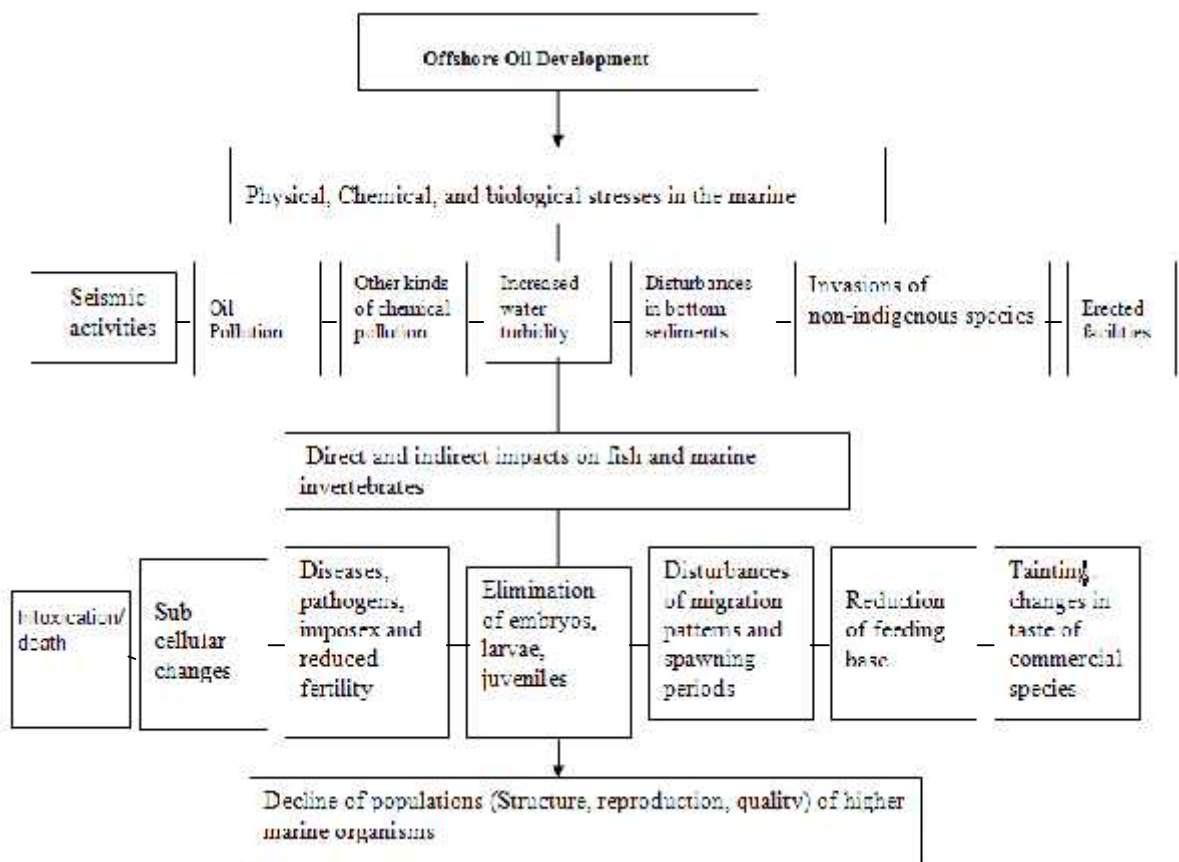


Fig.1 Flow-chart showing complex impacts on higher marine organisms including commercial fish species during offshore oil development (Patin, 1999).

1.2 Processes of Offshore Oil and Gas Exploration and Development Drilling

The two primary phases of drilling operations conducted as part of oil and gas extraction process are exploration and development. Exploratory drilling involves drilling wells to determine the presence of hydrocarbons. Once hydrocarbons have been discovered, additional appraisal or delineation wells are drilled to determine the size of the hydrocarbon accumulation. When the size of a hydrocarbon accumulation is sufficient for commercial development, field development starts. Development wells are drilled for production during this phase. Although the rigs used for each type of drilling may differ, the drilling process for each well is generally similar.

Exploration activities are usually of short duration, involve a relatively small number of wells, and are conducted from mobile drilling rigs. Development drilling usually occurs over a longer interval of time and involves multiple wells to different parts of the reservoir. Depending upon the development concept, these wells may be drilled from a mobile drilling rig or may be drilled from a permanently located facility such as a platform or floating facility such as a tension leg platform (TLP) or deep draft caisson vessel (DDCV). Development wells are drilled to efficiently produce the hydrocarbons contained in the reservoir. They are drilled both as the initial means of producing the field and during the field's life to properly manage withdrawal of reserves and to replace wells that have experienced mechanical problems.

The overall development of offshore oil is associated with increased support vessels and oil tanker traffic and the general environmental impacts of these processes include noise and vibration, solid and liquid production wastes, increased water column turbidity from dredging, disturbance of the sea bed areas, avoidance of the area by marine wildlife such as fish and marine mammals due to construction noise, vibration and the presence of erected facilities, and possible invasions of non-indigenous species carried in ballast water of support vessels and oil tankers (Steiner, 2003; Wills, 2002; Patin, 1999). Offshore oil development may also result in severe environmental stress leading to different biological responses such as complex transformations at all levels of biological hierarchy. The flowchart in Fig.1

illustrates the possible negative impacts on higher marine organisms and commercial fish species.

1.3 The North Sea and Oil Exploration and Production

The North Sea is a dynamic shelf sea with oceanic waters entering from the Straits of Dover in the south of England and from the North Atlantic between the Shetland and Orkney Isles and off the coast of Norway in the north. North Sea waters outflow via the Norwegian Trench (Laane *et al.*, 1996). Within the North Sea, there exists a wide range of subsurface geological formations. The chemistry of the rocks, and in particular the principal source rock, the shale of the Jurassic Kimmeridge Clay Formation, has a significant heavy metal and radioactive content. The metals are often incorporated as sulphides, whereas radionuclide of the natural uranium and thorium decay series are enriched in the more organic-rich fractions of the sediments. The chemistry of the reservoir and cap rocks are also related to the chemistry of the formation fluids (or “brines”). Different provinces within the North Sea have markedly different reservoir brine chemistries (Helgeson *et al.*, 1993). Production of the field requires drilling of the reservoir rocks (and sometimes source rock), that subsequently become mixed with the drilling mud and accumulates on the seafloor contributing to the sediment complexity of the drill cuttings piles.

The North Sea is a coastal region with intensive offshore oil production. The hydrocarbon reserves include several marginal fields, which are either small or deep-water fields. An economical exploitation of these reserves requires the introduction of subsea developments and multiphase fluid transport over long distances. It is therefore extremely important to reliably predict and control fluid behavior, in order to optimize production cost and for purposes of potential environmental pollution in the oil and gas operational activities. However, data from OSPAR reveal that the oil pollution balance in the North Sea is mainly fed by land-based sources (50 %), with offshore production as the second largest source (32%) and maritime traffic the smallest contributor (18 %) to the regional oil pollution balance (OSPAR, 2000). Such perspective is in fact appropriate in helping define

environmental policies for a coastal region with offshore potential. However, the well-known potential of oil tankers to cause large oil spills keep policymakers globally vigilant.

1.4 Sources of oil spill and Marine Oil Pollution:

Incidences of oil spills may arise from both oil tankers and offshore installations. In cases of large spills, the levels of oil pollution results in immediate lethal consequences for plants, birds and mammals and even more environmentally disastrous when the oil washes ashore polluting and accumulating in sediments of shallow coastal zones. It should however be noted that the magnitude of oil discharged into the sea may not necessarily be translated directly into real environmental impact as this depends on the toxicity of the oil and different input rates. Therefore a relatively small but sudden input of oil (e.g. an oil spill caused by a tanker accident) has acute and lethal effects on most marine life, whereas large quantities of oil discharged over longer periods of time (e.g. oil in production water arising from offshore oil exploitation; offshore oil production accidents) may have chronic and sub-lethal impacts (Kloff and Wicks, 2004). Recently, a landmark report from the U.N. Environmental Program (UNEP, 2011), concluded that the pollution from more than 50 years of oil operations in Nigeria's Niger Delta (Ogoniland) region is more far-reaching than thought, and the clean up of the environmentally devastated oil producing Niger Delta region could be world's largest, with a restoration cost estimated at \$1 billion that could take up to 30 years to complete.

In the cases of oil tanker accidents, large spills may arise from maritime traffic after grounding of an oil tanker, collisions with other vessels, and due to cargo fires and explosions. Most of these accidents are usually caused by technical failures and human errors. A myriad of certain extreme conditions such as bad weather, bad maintenance, age of tanker and metal fatigue, some oil tankers may simply break into two. The *Torrey Canyon* oil spill in 1967 involved a 269 metre tanker, which ran aground off the southwest coast of England, releasing approximately 733,000 barrels of Kuwaiti crude. The Exxon Valdez oil spill in 1989, spilled 11.2 million gallons of crude oil in Alaska. The Kuwaiti oil spill (as a result of the Gulf War) in 1991 was estimated at 900 million barrels (ASCE, 1996). This was

recorded as the largest oil spill in human history. The *Braer* Oil tanker ran aground on Shetland's south coast spilling 85,000 tons of Gulfaks North Sea crude oil (Davies and Topping, 1997). In 1996, *Sea Empress* oil tanker ran aground and resulted in the discharge of approximately 72,000 tonnes of Forties Blend North Sea crude oil into the sea around the coast of South-West Wales (SEEEEC, 1998). The *Prestige* accident in 2002 is probably the most recent example of such complicated circumstances (New Scientist, 2003).

Accidental oil spills usually occur during routine terminal operations when oil is loaded and discharged. This normally occurs in ports or at terminals such as offshore production platforms. This source of spill is of greater magnitude and the amount of oil spilled during terminal operations is three orders of magnitude greater than the total amount of oil spilled after accidents with oil tankers (ITOPF website). However, there are several examples of global best practice in port management and tanker traffic control systems, which have minimized the problem to very small proportions using existing technology and careful management. Some examples are the port of Sullom Voe, in the Shetland Islands where the major oil companies agreed to this system in 1979, and the Valdez Marine Terminal in Alaska, which has imposed a zero-tolerance pollution regime after the Exxon Valdez disaster in 1989 (Kloff and Wicks, 2004).

Offshore oil production accidents are another major source of marine oil spill and pollution. Accidents involving offshore oil installations can be caused by many different factors. 'Blowouts' of wells or pipeline ruptures are the best known examples. This is usually caused if a drilling rig encounters a pocket of sub-sea oil under excessive geological pressure or errors leading to technical failures. Examples of major blowouts occurred in 1969 near Santa Barbara (Charter, 2002) and off the Egyptian coast in 2004. The most recent offshore oil installation accident occurred in April 20, 2010 when the offshore drilling rig, Deepwater Horizon operated by Transocean and owned by BP, exploded and sank with oil gushing into the Gulf of Mexico at an estimated 40,000 barrels per day.

1.4.1 Waste Discharges from Offshore Oil Production

There are four possible disposal methods for all waste products arising from offshore oil extraction which include overboard discharge, ship-shore, re-injection or disposal in a platform core or especially drilled underground structures. One of the largest sources of intentional operational discharges includes discharges from vessels (mostly bilge and other oily discharges). Overboard discharge has been identified as the most environmentally damaging (Patin, 1999).

A number of different exploration and production (E&P) chemicals are needed during exploration, drilling and production of oil and gas. These chemicals are required in order to ensure effective and safe drilling and production processes. A fraction of these chemicals may end up in waste streams. Under offshore conditions drill-cuttings and produced water are waste streams that are discharged into the open sea, under environmental constrictions with regard to the content of oil and, in some jurisdictions, other contaminants. The use of E&P chemicals in offshore oil and gas production is thus subject to notification of chemicals from an environmental perspective (Scholten *et al.*, 2000).

1.5 Weathering Processes

This process can best be described as the alteration of the physical and chemical properties of spilled oil through collective effects of a series of natural processes which begin when the spill occurs and continues indefinitely, while the oil remains in the environment. When crude oil or petroleum products are released into the environment, they are immediately subjected to a wide variety of weathering processes (Jordan and Payne, 1980; Doerffer, 1992).

Weathering processes can be divided into physical (e.g., evaporation, emulsification, natural dispersion, adsorption onto suspended particulate material, dissolution and sorption), chemical (photodegradation) and biological processes (microbial degradation) (Wang and Fingas, 1995). Oil components are redistributed (*transported*) in compartments of the environment (e.g., air, water, sediment, soil and biota) during physical weathering

and transformed (*degraded*) during chemical and biological weathering processes. Evaporation and dissolution and, depending on the meteorological conditions, UV degradation are the most important weathering processes immediately (hours - few days) after oil spills on water (Fingas, 1997).

In contrast, biodegradation affects the long-term (months-years) fate of oil (Christensen, 2005). The oil composition and the position of the oil release also significantly influence on the relative magnitudes and importance of each of the processes mentioned above.

1.5.1 Physical transport.

The distribution of oil spilled on the sea surface occurs under the influence of gravitation forces. It is controlled by oil viscosity and the surface tension of water. After a spill of one ton of oil, it can disperse to a slick of 50 m radius within 10 minutes, forming a slick 10-mm thick. The slick gets thinner (less than 1 mm) as oil continues to spread, covering an area of up to 12 km² (Ramade, 1978). During the first several days after the spill, a considerable part of oil transforms into the gaseous phase. Besides volatile components, the slick rapidly loses water-soluble hydrocarbons. The rest - the more viscous fractions - slow down the rate of slick spreading (Ramade, 1978; Baker *et al*, 1990; Dutta and Harayama, 2000).

Further changes take place under the combined impact of meteorological and hydrological factors and depend mainly on the power and direction of wind, waves, and currents. An oil slick usually drifts in the same direction as the wind. While the slick thins, especially after the critical thickness of about 0.1 mm, it disintegrates into separate fragments that spread over larger and more distant areas. Storms and active turbulence speed up the dispersion of the slick and its fragments. A considerable part of oil disperses in the water as fine droplets that can be transported over large distances away from the place of the spill (U.S EPA, 1990).

In Environmental Impact Assessment (EIA) studies, and when planning the most effective response, it is important to have reliable predictions of how specific oil properties will change during an oil spill event. The efficiency of oil spill combat methods (e.g. mechanical recovery, chemical dispersion and/or burning) depends generally on the physical/chemical properties of the oil at the time of action (Reed *et al.*, 2004). Fundamental knowledge of these processes is therefore required to predict this behavior. Modeling algorithms used by oil-spill experts to predict the fate of oil spills have traditionally been designed to answer immediate response questions. Most of them, therefore, are usually applicable only to the first few days after a spill release and may neglect important weathering processes that occur over a longer time frame. These longer term weathering processes are expected to determine the ultimate fate of the spilled oil that remains at sea, and any subsequent impact to the environment (Rainey *et al.*, 2003).

1.5.2 Natural Degradation of Oil Spills

Many micro-organisms possess the enzymatic capability to degrade petroleum hydrocarbons. Some micro-organisms degrade alkanes, others aromatics, and some others aromatic hydrocarbons. Often the normal alkanes in the range C₁₀ to C₂₆ are viewed as the most readily degraded, but low-molecular-weight aromatics, such as benzene, toluene and xylene, which are among the toxic compounds found in petroleum, are also very readily biodegraded by many marine micro-organisms. This is followed by isoalkanes and higher-molecular-weight *n*-alkanes, olefins, monoaromatics, PAHs, and finally, highly condensed cycloalkanes, resins, and asphaltenes (Wang and Stout, 2007). Compounds that are degraded are typically converted into oxidized compounds that can be further degraded, dissolved, or retained within the oil. Following a spill of crude oil or refined petroleum to soils, sediments or open water, different hydrocarbon classes are degraded simultaneously, but at widely different rates by indigenous microbiota (Atlas *et al.*, 1981; Oudut, 1984; Gough *et al.*, 1992; Prince *et al.*, 2003). More complex structures are more resistant to biodegradation, meaning that fewer micro-organisms can degrade those structures and the rates of biodegradation are lower than biodegradation rates of the simpler hydrocarbon structures found in petroleum. The greater the complexity of the hydrocarbon structure, i.e., the higher the number of methyl branched substituents or condensed aromatic rings, the slower the rates of degradation (Atlas, 1995).

The biodegradation of petroleum in the marine environment is carried out largely by diverse bacterial populations, including various *Pseudomonas* species. The hydrocarbon-biodegrading populations are widely distributed in the world's oceans; surveys of marine bacteria indicate that hydrocarbon-degrading micro-organisms are ubiquitously distributed in the marine environment (Roling *et al.*, 2002). Generally, in pristine environments, the hydrocarbon-degrading bacteria comprise < 1% of the total bacterial population. These bacteria presumably utilize hydrocarbons that are naturally produced by plants, algae, and other living organisms. They also utilize other substrates, such as carbohydrates and proteins. When an environment is contaminated with petroleum, the proportion of hydrocarbon-degrading micro-organisms increases rapidly. In particular, in marine environments contaminated with hydrocarbons, there is an increase in the proportion of bacterial populations with plasmids containing genes for hydrocarbon utilization. The proportion of hydrocarbon-degrading bacterial populations in hydrocarbon-contaminated marine environments often exceeds 10 % of the total bacterial population (Atlas, 1995).

The rate of mass loss due to biodegradation is slower than that of evaporation or dissolution and as such the effects of biodegradation on spilled oil's chemistry are not obvious in the short term following a spill (Atlas, 1995). Complex processes of oil transformation in the marine environment start developing from the first seconds of oil's contact with seawater. The progression, duration, and result of these transformations depend on the properties and composition of the oil itself, parameters of the actual oil spill, and environmental conditions (U.S EPA, 1990). The main characteristics of oil transformations are their dynamism, especially at the first stages, and the close interaction of physical, chemical, and biological mechanisms of dispersion and degradation of oil components up to their complete disappearance as original substances. Similar to an intoxicated living organism, a marine ecosystem destroys, metabolizes, and deposits the excessive amounts of hydrocarbons, transforming them into more common and safer substances (Leahy and Colwell, 1990; U.S EPA, 1990).

Over the last 20 years complex chemical equations have been derived to describe the metabolic pathways in which oil is broken down. The general outline of bioremediation pathways for aliphatic and aromatic hydrocarbons has been formulated and continues to be developed in greater detail with time (Glaser *et al.*, 1991). All of these pathways will result in the oxidation of at least part of the original hydrocarbon molecule (Bragg *et al.*, 1994). The content of a particular petroleum mixture will also influence how each hydrocarbon will degrade (Atlas, 1981) and the type and size of each hydrocarbon molecule will determine the susceptibility to biodegradation (Atlas and Bartha, 1993). There are several hundred individual components in every [type of] crude oil, and the composition of each crude oil varies with its origin (Atlas and Bartha, 1993). The difference in composition determines the quality of any particular oil. Petroleum is a complex mixture of hydrocarbons, but it can be fractionated into aromatics, aliphatics, asphaltics and a small portion of non-hydrocarbon compounds (Atlas and Bartha, 1993; Atlas, 1981).

1.5.3 Evaporation

Shortly after a spill has occurred, evaporation is the single most important and dominant weathering process, in particular for the light petroleum products, with regard to mass transfer (molecular partitioning) and to removal of the more toxic, lower molecular weight components from the spilled oil. In the first few days following a spill, the loss can be up to 70 % and 40 % of the volume of light crude and petroleum products. For heavy or residual oils the losses are only about 5–10 % of volume (Doerffer, 1992; Fingas, 1997; Fingas, 2004). Evaporation extensively affects the composition and thereby the total weathering of oil, and evaporation has in several studies been used as a simple model of weathering in the environment or as pre-weathering of oil before further studies of microbial degradation (Wang and Fingas, 1995; Wang *et al.*, 1998). Evaporative loss is controlled by several factors, the most important of which are the composition and physical properties of the oil, the slick surface area and its thickness, the wind velocity and the sea state, air/sea temperature and the intensity of solar radiation. Compound - specific losses are generally difficult to predict. It could be stated that compounds with vapour pressures greater than that of *n*-C₈ compounds will not persist in the slick, whereas compounds with vapour pressures more than those of *n*-C₁₈ compounds do not evaporate appreciably under normal

environmental conditions (Doerffer, 1992). Component – specific concentrations remaining in a slick show the loss of individual compounds due to evaporation and to a lesser extent due to dissolution. Compounds below $n\text{-C}_{14}$ are readily removed. Since the compound-specific data alone do not allow an overall accounting of the total mass balance of a slick, a distillation characterization of weathered crude oil is required (Doerffer, 1992).

Spill volume also influences the relative rate of evaporation. The larger the spill volume, the smaller the evaporation rate, since the surface/volume ratio of the slick thickness increases. Wind speed and ambient temperature has a significant effect on the evaporation rate. The rate of evaporation increases with increasing wind and temperature. There are differences in rates of evaporation for some typical crude oil with different volatility characteristics. It is therefore necessary to classify different crude oils with respect to their evaporative behavior after spillage at sea, based on the expected evaporative loss of crude oil under average conditions (wind speed 8 knots and temperature 7°C) as noted by Doerffer (1992).

As a consequence of the removal of the lighter hydrocarbons ($n\text{-C}_3$ to $n\text{-C}_{18}$, naphthalene and BTEX) through evaporation, the volume of oil decreases, but density and viscosity increases (Douglas *et al*, 1996). The densities of oil are temperature dependent and in most cases the reference temperature for the determination of density is 15°C (Doerffer, 1992). Changes in these factors are important with respect to other weathering processes as natural dispersion, emulsification, dissolution, biodegradation, photooxidation and sinking of oil.

Though evaporation effects on oil composition and behavior have been described in several studies, they are still intensively investigated and modeled because the understanding of this process is crucial for identification of oil spill samples in forensic science using chemical fingerprinting (Chao *et al.*, 2001; Christensen, 2002; Douglas *et al*, 2002; Fingas, 2004). During the weathering processes the oil fingerprint changes, making chemical comparisons between spill and suspected source increasingly difficult as every change has to be assessed and evaluated (Daling *et al.*, 2002).

1.5.4 Dissolution

Most oil components are water-soluble to a certain degree, especially low-molecular-weight aliphatic and aromatic hydrocarbons. Polar compounds formed as a result of oxidation of some oil fractions in the marine environment also dissolve in seawater. Like evaporation, dissolution of the soluble petroleum compounds is component specific and thereby can be used as a process indicator and give valuable information about the complex process (Chao *et al.*, 2001; Prince *et al.*, 2002; Rogers *et al.*, 2000). Dissolution may have important biological consequences, although it is of less importance in terms of the overall mass balance of an oil spill. However, understanding of this process may be important in recognizing the impact of spilled oil on biota, which can uptake dissolved hydrocarbons more readily (Wang and Stout, 2007). The rate at which a hydrocarbon dissolves in water is generally lower than the rate of evaporation and usually the amount of the dissolved oil is less than 1% of the original mass of the spill (Riazi and Enezi 1999; Riazi and Edalat, 1996). The extent of dissolution depends on the point of oil release. Subsurface releases of crude oil, in offshore operations, enhance the dissolution of lower molecular weight aromatic components. As the oil floats upwards through the water column to the surface, the lower molecular weight aromatics, such as benzene partition into the water column and are almost completely removed from the oil mass by the time it reaches the surface, giving elevated (greater than 100 µg/l) levels of benzene when measured directly beneath the water surface.

The amount of the oil hydrocarbons dissolving in water phase from oil slick largely depend on the molecular structure and polarity of a given oil component, and the relative solubility of the oil component in water phase versus its solubility in the oil phase. In general, (1) the aromatic hydrocarbons are more soluble than aliphatic hydrocarbons, (2) solubilities increase as the alkylation degrees of alkylated benzene or PAHs decrease, (3) the lower molecular weight hydrocarbons are more soluble than the high molecular weight hydrocarbons in that class. Therefore, it can be readily understood why the BTEX and lighter alkyl-benzene compounds and some smaller PAH compounds such as naphthalene are particularly susceptible to dissolution or “water-washing” (Doerffer, 1992; Wang and Fingas, 2003). Compared with evaporation, dissolution takes more time. Hydrodynamic

and physicochemical conditions in the surface waters strongly affect the rate of the process (U. S. EPA, 1990).

1.5.5 Emulsification

Of all weathering processes, the formation of emulsions is the only one that promotes the persistence of oil on the surface of water and on the shore – and concurrently retards the weathering processes. Emulsification of crude oils or refined products involves the dispersion of water droplets into the oil medium. As the percentage of water increases (up to maximum 75 to 80 %) the resulting emulsion called “chocolate mousse”, undergoes an increase in viscosity, its effective volume (volume of pollutant) increasing by up to a factor of 4, its density approaching that of the surrounding water and colour changes occurring. They can exist in the marine environment for over 100 days in the form of peculiar “chocolate mousses (Payne and Phillips, 1985). These properties of resulting emulsions make cleanup operations and combustibility more difficult. Emulsions often form a crust of oxidized asphaltene materials that inhibit dissolution, evaporation, photooxidation and biodegradation of hydrocarbons in the bulk oil phase. This therefore preserves the chemical fingerprint of the emulsified oil relative to the non-emulsified oil (Wang and Stout, 2007). Thus, the weathered deposits of mousse, tar and asphalt pavement on the shore may retain some volatile hydrocarbons and biodegradable compounds for long periods of time (Boehm and Fiest, 1982; Payne and Phillips, 1985; Irvine *et al.*, 1999). The evaporation of components from an emulsion is also diminished even when the mousse is exposed to air and sunlight as the weathering continues at a slower rate, converting the oil deposit to a tar mat or asphalt pavement that may be extremely persistent and retain many of the primary and secondary features of the spilled oil for long period of time. The “centres” of the tar balls can contain virtually unweathered oils, several months after the initial oil spill, thereby providing the potential to generate chemical fingerprints with little effect of biodegradation (Wang and Stout, 2007).

The measurable increases in viscosity and specific gravity observed for many water-in-oil emulsions in sea water affect their behavior, including spreading, dispersion, interaction with suspended particulate material, evaporation and dissolution properties (Payne and

Phillips, 1985). Stability of these emulsions usually increases with decreasing temperature (Rønningsen, 1995). Certain oils have the tendency to form stable water-in-oil emulsified mixtures. This tendency appears to depend on wax and asphaltic materials contained in the crude oil. Heavy fuel oils such as the industrial heavy fuel oils spilled by the *Erika* and the *Baltic Carrier* form water-in-oil emulsions slowly. However, many spilled crude oils will rapidly form w/o emulsions when spilled at sea (Lewis *et al.*, 1995a,b). Emulsions formed in this manner will initially have low viscosities, unstable and will tend to revert to the oil residue and water if they are removed from the mixing action of the sea (Daling *et al.*, 2003). Refined petroleum products do not contain waxes and asphalt and thus they do not form stable oil-in-water emulsions and also because surface-tension forces quickly decrease the dispersion of oil (US EPA, 1990). In stabilizing water-in-oil emulsions an important role is played by oxy-generated surface materials, which are generated by photochemical and microbial degradation processes. Surface active compounds are believed to surround the water droplets, which usually range in size from less than 10 micrometres, preventing water/water droplets coalescence and ultimate oil/water phase separation. Additional evaporative and dissolution weathering can be significantly reduced and further degradation by either microbial or photochemical oxidation processes are limited to the exterior surface of tar balls or mousse (Doerffer, 1992). As a consequence of weathering evaporation of the light ends (increase in density), dissolution of surface active components (decrease in spreading coefficient) and emulsification, the rate of spreading will gradually decrease under natural conditions (Doerffer, 1992).

1.5.6 Dispersion

Dispersion of whole oil droplets is an important process in the break-up and disappearance of a surface slick. The sea surface turbulence has a direct impact on the droplet dispersion, although dispersion of oil droplets into the water column or processes of spontaneous emulsification from calm seas can also occur. Natural dispersion is in fact the net result of three separate processes:

- the initial process of globulation, i.e. the formation of oil droplets from a slick under influence of breaking waves;

- the process of dispersion, i.e. the transport of oil droplets into the water column as a net result of the kinetic energy of the oil droplets supplied by the waves and the rising forces;
- the process of coalescence of the oil droplets within the slick.

The physico-chemical parameters which influence these individual contributing processes include the slick thickness, oil/water interfacial tension, density and viscosity. The thinner the slick, the more frequently wave breaking occurs, since the damping effect decreases with thinner slicks and the increased probability of the formation of small droplets (globulation increases), which become permanently dispersed (dispersion increases and coalescence decreases) (Doerffer, 1992). The oil/water interfacial tension affects globulation and coalescence, but does not affect dispersion (transport) of the oil droplets into the water column. The smaller the oil/water interfacial tension, the more likely the formation of oil droplets (globulation increases) and the less the tendency of droplets to coalesce within the slick.

The density and viscosity of the spilled oil also affects natural dispersion. The higher the density of the oil and thus the smaller the density difference between oil and water, the more easily small oil droplets are formed from the slick. The heavier the oil, the more important is natural dispersion. Dispersion of oil droplets increases the surface area, allowing enhanced dissolution of lower molecular weight aromatics, and provides materials which may be ingested by organisms and ultimately deposited in sediments in the faecal pellets.

1.5.7 Adsorption onto suspended particulate material (SPM)

Interaction between spilled oil and suspended particulate material represent an important mechanism for the rapid dispersal and removal of oil from surface waters. Oil spills in nearshore waters with high suspended particulate loads experience rapid dispersal and removal of the oil due to sorption onto suspended particulate matter (SPM) along frontal zones. This mainly happens in the narrow coastal zone and shallow waters where

particulates are abundant and water is subjected to intense mixing. In deeper areas remote from the shore, sedimentation of oil (except for the heavy fractions) is an extremely slow process (U.S EPA, 1990). At concentrations greater than 100 mg/litre massive oil transport may occur with the potential for significant adverse impacts on the benthos. Therefore the adsorption of dispersed oil onto suspended particulates may provide an efficient mechanism for sedimenting fractions of oil mass of up to 15 % (Doerffer, 1992).

1.5.8 Photooxidation

Photo-oxidation is considered to be another most important factor involved in the transformation of crude oil or its products released into the marine environment (Garrett *et al.*, 1998). Rates of photo-oxidation of crude oil are considered to be dependent or directly related to the intensity of ultraviolet radiation from sunlight, oil film thickness but they are also sensitive to ambient temperature (Syndes *et al.*, 2001; Prince *et al.*, 2003). The photochemical degradation yields a great variety of oxidized compounds which are more polar and highly soluble in water than the parent compounds (Payne and McNabb, 1985; Ehrhardt and Douabul, 1989; Ehrhardt and Burns, 1990; Ehrhardt *et al.*, 1992) and thus can be preferentially dissolved from the surface of the spilled oil and diluted in underlying waters.

Several mechanisms are proposed for photochemical oxidation of oil. These include free radical oxidation in the presence of oxygen, singlet oxygen initiation of hydroperoxide formation, and ground – state triplet oxygen combining with free radicals to form peroxides, aldehydes, ketones, alcohols, carbonyls, sulfoxides, epoxides and fatty acids (Larson *et al.*, 1977; Thominet and Verdu, 1984, 1986; Nicodem *et al.*, 1997). Photo-sensitive higher-molecular-weight compounds can form cross-links upon photooxidation, thereby becoming increasingly large and insoluble, and the spilled oil increasingly viscous (Thominet and Verdu, 1984; Daling and Brandvik, 1988). Therefore, photooxidation of petroleum compounds affect the oil by removing the largest and the most substituted PAHs at the highest rate, and the smaller and less substituted the PAH, the slower the

photooxidation rate (Bertilson and Widenfalk, 2002; Garrett *et al.*, 1998), in direct contrast to the effects of evaporation, dissolution and microbial degradation.

However, photooxidation and biodegradation are the only two natural processes that actually destroy petroleum hydrocarbons and remove them from the environment- in many cases forming the same classes of oxygen-containing products. Often, the target oil ingredients of the two degradative processes are different. Under suitable conditions, they act together to degrade oil more rapidly than either of the process working alone (Dutta and Harayama, 2000; Prince *et al.*, 2003).

1.6 Overview of analytical methods for the characterization of Oil (spill) in the Environment

The marine environment may be polluted by oil through a number of anthropogenic and natural sources. Acute anthropogenic sources of oil can be generally classified as either accidental oil spills or intentional operational discharges. Despite the significant contributions of oil and hydrocarbons to the marine environment from chronic anthropogenic sources, oil seeps, and naturally occurring hydrocarbons, the route of entry that particularly promulgate the greatest need for thorough analytical and chemical fingerprint is the acute accidental oil spills and intentional operational discharges.

These acute releases can require expensive response and cleanup measures and damage marine and terrestrial natural resources. The resulting casualty and punitive financial consequences can be substantial (Wang and Stout, 2007). This therefore requires a confident and robust establishment of the source of the spilled oil and again the spatial and temporal extent of any damage.

1.6.1 *Chemical fingerprinting*

Chemical fingerprinting can be defined as a set of techniques applicable in the environmental assessment of complex mixtures, like oil and petroleum products. Chemical fingerprinting includes characterizing (i.e., fuel type), quantifying (i.e., concentration), differentiating (i.e., from a similar source of pollution) and identifying (i.e., trace identity and fate) a spill sample based on its chemical composition (i.e., distribution patterns of different compounds). This is also referred to as Forensic Environmental Geochemistry (Kaplan *et al.*, 1997; Christensen, 2005). Successful forensic investigation and analysis of oil and refined product hydrocarbons in contaminated sites and receptors yield a wealth of chemical “fingerprinting” data. In specific terms, hydrocarbon fingerprinting is very important in:

1. To specifically determine oil source(s) and distinguish spilled oil from background hydrocarbons of biogenic and pyrogenic origin.
2. Determine the fate of oil. Crude oil and refined petroleum products released into the environment are subject to numerous transport and transformation processes (weathering).
3. Monitor petroleum hydrocarbons in compartments of the environment with the aim of assessing the impact on the ecosystem (risk assessment).

These data, in combination with historic, geological, environmental, and any other related information on the contaminated site can, in many cases, help to settle legal liability and to support litigation against the spillers. Petroleum contains thousands of different organic compounds. Successful oil fingerprinting involves appropriate sampling, analytical approaches and data interpretation strategies. A wide variety of instrumental and non-instrumental techniques are currently used in the analysis of petroleum hydrocarbons following oil spills (petrogenic hydrocarbons) and emission/deposition resulting from fossil fuel combustion (pyrogenic hydrocarbons). These techniques include gas chromatography (GC), gas chromatography–mass spectrometry (GC–MS) (Wang *et al.*, 1999; Daling *et al.*, 2002), two-dimensional GC-GC (Frysiner and Gaines, 2002), Gas chromatography with

flame ionization detection (GC-FID) (Wang and Fingas, 2003), high-performance liquid chromatography (HPLC), size-exclusion HPLC, infrared spectroscopy (IR), supercritical fluid chromatography (SFC), thin layer chromatography (TLC), ultraviolet (UV) and fluorescence spectroscopy, GC- isotope ratio mass spectrometry (GC-IRMS) (Mansuy *et al*, 1997; Rogers and Savard, 1999), GC-MS-MS (Munoz *et al.*, 1997), and gravimetric methods.

Of all these hyphenated techniques, GC techniques have proven most effective and the most widely used (Burns *et al.*, 1997; Christensen *et al.*, 2004; 2005) and the primary reason for this is that capillary GC, performed using various column types, can resolve many, but clearly not all, of the hundreds to thousands of compounds in petroleum permitting their detection and identification by a variety of detectors (Wang and Stout, 2007). Compared to the molecular measurements two decades ago, GC methods have now been enhanced by more sophisticated analytical techniques, such as capillary GC–MS, which is capable of analyzing the oil-specific biomarker compounds and polycyclic aromatic hydrocarbons. The accuracy and precision of analytical data has been improved and optimized by a series of quality assurance/quality control measures, and the laboratory data handling capability has been greatly increased through advances in computer technology.

Bulk properties such as total petroleum hydrocarbons (TPH), measured by GC-FID, and gravimetric analysis of the aliphatic, aromatic and polar oil fractions have been used frequently for chemical fingerprinting and for evaluating the effects of oil weathering (Mille *et al*, 1998; Oudot *et al*, 1998; Dutta and Harayama, 2000). Furthermore, GC-FID is often used for screening analysis of mainly *n*-alkanes and polycyclic aromatic hydrocarbons (PAHs), with 2-3 rings. Subjective pattern matching of GC-FID fingerprints were used to assess the changes in composition of the *Amoco Cadiz* oil 13 years after the spill (Mille *et al.*, 1998). GC-FID fingerprints were also used to classify sediment samples, collected 25 years after the *Nipisi* land spill, according to the levels of oil contamination and the extent of weathering. Sediment samples were classified into: a) background

samples, b) highly weathered samples, c) lightly to moderately weathered and d) lightly contaminated with oil and vegetation hydrocarbons (Wang *et al.*, 1998).

The heterogeneity encountered in field samples can be corrected by normalization to a conservative (i.e. a compound that is highly resistant to degradation in the environment) internal marker compound such as 17 α , 21 β -hopane (Bragg *et al.*, 1994; Butler *et al.*, 2001; Prince *et al.*, 1994; Venosa *et al.*, 1997), 17 α , 21 β -norhopane (Oudot *et al.*, 1998) or vanadium (Sasaki *et al.*, 1998). These methods have been used frequently for chemical fingerprinting in weathering studies and to calculate the percent loss of oil or individual analytes (Douglas *et al.*, 1996). Univariate plots of percent loss based on preserved internal markers describe the combined effects of physical, chemical and biological weathering processes. The isolated effects of microbial degradation can only be described in controlled laboratory experiments by subtracting the loss in sterile controls. Conversely, low-molecular-weight hydrocarbons, such as heptadecane, octadecane, pristane, phytane and 2-3 ring PAHs, may in field samples be heavily affected by physical weathering processes (Christensen, 2005).

Several reviews (Sauer and Boehm, 1995; Whitaker *et al.*, 1996; Lundanes and Greibokk, 1994; Kaplan *et al.*, 1997; Wang *et al.*, 1995; Stout *et al.*, 2001, Wang and Stout, 2007; Merdrignac and Espinat, 2007) have been published on the analytical methodologies for comprehensive characterization and identification of oil hydrocarbons, including petroleum biomarkers (e.g. steranes, terpanes and sesquiterpanes) and polycyclic aromatic compounds, using various analytical techniques. Depending on chemical/physical information needs, the point of application and the level of analytical detail, the methods used for oil spill study can be, in general, divided into two categories: non-specific methods and specific methods for detailed component analysis. In the non-specific methods such as the US EPA methods 1614 and 418.1, only groups or fractions of chemical hydrocarbons (for example, measurement of total petroleum hydrocarbons (TPH) and EPA priority polycyclic aromatic hydrocarbons) are determined (Wang and Fingas, 2003).

Heavy oil fractions are of very high complexity and the chemical polydispersity is due to the presence of a broad range of different polarities compounds such as paraffinic, aromatic and heteroatomic molecules. Their main characteristics (high viscosity and significant content of heteroatoms and metals) are in majority related to resins and asphaltenes which constitute the most polar fractions of these oils. From these high functionalized mixtures, specific properties emerge like self-association/aggregation of asphaltenic structures, involving tedious characterization (Merdrignac and Espinat, 2007). The compositional analysis and characterization of heavy oil products has become a key in studies relating to the evaluation of the stability of water-in-emulsions. Asphaltene occupies a central role in hydrocarbon utilization and in water-in-oil emulsification. The asphaltenes and resins are of primary interest due to their polar, surface-active nature and important role in stabilizing emulsions and crude oil processability (McLean and Kilpatrick, 1997; Merdrignac and Espinat, 2007; Sjoblom et al., 2003; Mullins, 2008). Numerous studies carried out on heavy products analyses, were primarily related to asphaltene and to a less extent, to resins.

1.7 Structural characterization of asphaltenes and its relationship to the weathering behavior of water-in-oil emulsions

In the petroleum industry, asphaltenes represent the most enigmatic and yet very important class of compounds, occupying a central role in both the downstream and upstream utilization of hydrocarbon resources. The substantial and increasing importance of asphaltenes mandates detailed understanding of these materials. For instance, the increase in viscosity of crude oil which accompanies increased asphaltene content and the tendency of asphaltenes to phase separate creates significant difficulties in the production and transportation of crude oil. They are best known for the problems they cause as solid deposits that obstruct flow in production system. Again the coating tendencies of asphaltenes long with their heavy metal content interfere with the catalytic processing of crude oils in the downstream process where it increasingly enters the refining processing streams with its potentials to disrupt and clog systems (Groenzin and Mullins, 2000; Akbarzadeh *et al.*, 2007).

However, asphaltenes also cause other challenges to fluid flow: not only do they increase fluid viscosity and density, but they also stabilize oil-water emulsions (Auflem, 2002). Emulsions form when oil and water mix under conditions of agitation. Usually, the mixture is more viscous than its components, and flows less easily. Separating emulsified water and oil is sometimes difficult. A better understanding of the effect of asphaltenes may be the key to preventing the formation of emulsions or tempering the deleterious effects of these mixtures.

Though asphaltenes portend significant production and refining challenges, they also find useful practical applications such as materials for road construction, waterproofing and roofing and as curing agents and corrosion inhibitors. However, from a geochemical standpoint, asphaltenes, like many other hydrocarbon components, have the potential to reveal important characteristics about the reservoir's fluid, history and connectivity (Akbarzadeh *et al.*, 2007).

1.7.1 Crude oil components and the chemistry of asphaltenes:

The asphaltene fraction contains the largest percentage of heteroatoms (O, S, N) and organometallic constituents (Ni, V, Fe) in the crude oil (Sjoblom *et al.*, 2003). Therefore, several authors mentioned metalloporphyrins, derived from chlorophylls and bacteriochlorophylls (Baker and Louda, 1986), as central chemical structure of asphaltene macromolecules (Premovic and Jovanovic, 1997; Marquez *et al.*, 1999; Groenzin and Mullins, 2001; Premovic *et al.*, 2002).

Asphaltenes are polar molecules that can be regarded in some characteristics as similar to the resins (a non-polar crude oil fraction), and is operationally defined not as a chemical class, rather, as a solubility class, namely the fraction of the crude oil precipitating in light alkanes like *n*-pentane, hexane or heptane. The precipitate is soluble in aromatic solvents like toluene and benzene.

The definition of asphaltenes as a solubility class rather than as a chemical class has made them more difficult to study than lighter components. The lighter components of hydrocarbons - saturates and some aromatics - have concisely defined chemical structures. However, the heavier components, asphaltenes and their related compounds, resins, have often been lumped together as residue and most times deemed too challenging for further examination (Akbarzadeh *et al.*, 2007). While their chemical structure has been slow to come to light, the average composition of asphaltenes as a class is fairly well known. Elemental analysis shows they are composed of carbon and hydrogen in an approximate 1 to 1.2 ratio, compared with the 1 to 2 ratio for bulk alkanes.

As far as asphaltene structure is concerned, researchers agree that some of the carbon and hydrogen atoms are bound in ring-like, aromatic groups, which also contain the heteroatoms (Aske, 2002; Mullins, 2007). Alkane chains and cyclic alkanes contain the rest of the carbon and hydrogen atoms and are linked to the ring groups. Within this framework, asphaltenes exhibit a range of molecular weight and composition. This compositional characterization is accepted by nearly all asphaltene specialists, but leaves ample room for debate about the structure or size of individual asphaltene molecules (Mullins *et al.*, 2007).

Due to the complex composition of crude oils, characterization by the individual molecular types is not possible. Instead, hydrocarbon group type analysis is commonly employed (Leontaritis, 1997; Lundanes and Greibrokk, 1994; Groenzin and Mullins, 2000). A convenient laboratory method - the saturate, aliphatic, resin and asphaltene (SARA-separation) [Fig.2] is an example of such group type analysis, separating the crude oils in four main chemical families based on differences in solubility and polarity (Sjoblom *et al.*, 2003).

1.7.2 Some methodologies for studying the structure of asphaltenes:

The statement "If you want to understand function, study structure" (Crick, 1988), readily lends credence to the unrelenting effort among researchers in investigating the multi-component, complex nature of crude oil, particularly asphaltenes, when attempting to characterize the chemistry of crude oil.

The extent to which these heavy hydrocarbon constituents are less well-defined and understood than light ones is partly a reflection of the greater economic value enjoyed by the lighter ends and partly of the tractable experimental methods commonly used for light-end analysis. Standard laboratory methods such as gas chromatography can characterize components of the lighter, simpler hydrocarbon compounds with carbon numbers less than about 36. Even large alkanes are amenable to specialized, hyphenated chromatography. However, in the realm of the asphaltenes, standard methods are often not applicable, so specialist techniques are required to extract accurate information about component structure (Akbarzadeh *et al.*, 2007; Mullins *et al.*, 2007).

The molecular weight of asphaltenes has been a subject of considerable controversy in the last two decades. Various measurements of widely varying petroleum crude oils and their thermally derived residual fractions, as well as different coals, can yield asphaltenes of somewhat different properties and values by as much as a factor of 10 or more (Buenrostro-Gonzalez *et al.*, 2001; Groenzin and Mullins, 2000) and these differences can reveal and lead to a better understanding of asphaltenes, their source crude oils and behaviour.

The list of techniques that have been used to study asphaltenes and other heavy fractions encompasses mass spectrometry, electron microscopy, nuclear magnetic resonance (NMR), small-angle neutron and X-ray scattering, near infrared spectroscopy (NIR), pulsed field gradient-spin echo nuclear magnetic resonance (PFG-SE NMR), ultrasonic spectroscopy, Fourier transform ion cyclotron resonance mass spectrometry (FT-ICR MS), dynamic light scattering, fluorescence correlation spectroscopy, fluorescence depolarization, vapor-

pressure osmometry (VPO) and gel permeation chromatography (Ostlund *et al.*, 2002; Aske *et al.*, 2002; Auflem, 2002; Rodgers and Marshall, 2004). Quantitative IR spectroscopy is useful in identification and quantification of chemical functionalities in complex mixtures such as crude oil. It has been used to estimate the type and amount of different chemical functional groups present in polar fractions of high boiling distillates, in asphaltene fractions, and in acidic, basic and neutral fractions of asphalts (McLean and Kilpatrick, 1997; Spiecker, 2001; Mullins *et al.*, 2007). However, certain basic nitrogen compounds which have poorly defined or weak infrared bands cannot be analyzed by infrared alone (McLeans and Kilpatrick, 1997). ^{13}C nuclear magnetic resonance spectroscopy is also useful as a non-destructive tool in crude oils and petroleum products analyses. This technique is very attractive in that it provides an accurate value of “aromaticity” or aromatic carbon content as a fraction of the total carbon and hence enables an excellent characterization of complex, multicomponent petroleum fractions (Jennings *et al.*, 1992). The Carbon types are observed directly in ^{13}C NMR spectroscopy, and can be readily quantified under appropriate conditions.

Because these methods investigate various aspects of asphaltenes under different conditions, it is not surprising that they have produced disparate models of asphaltene molecules (Mullins *et al.*, 2007). The high resolving power and accuracy of new measurements in asphaltene science relies on such techniques to better understand the structure and function of these complicated compounds. The current state of asphaltene and crude-oil characterization has been likened to a stage in the evolution of protein science; proteins were originally classified by solubility, but now, through the science of proteomics, their fundamental structure, in terms of amino acids, is understood. Similarly, the term “petroleomics” has been coined for the study of the structure of hydrocarbons (Mullins *et al.*, 2007), with the promising future prospect that crude oil will be characterized by all of its chemical constituents. These high-resolution measurements facilitate new understanding of petroleum constituents. The new field of “petroleomics” is based on the premise that sufficiently complete knowledge of the chemical composition of petroleum should enable correlation, and ultimately prediction, of its properties and behavior (Marshall and Rodgers, 2004; Mullins *et al.*, 2007).

Today, two main types of measurements - mass spectrometry and molecular diffusion produce the most consistent evidence on asphaltene molecular weight and size (Mullins *et al.*, 2007). Mass spectrometry induces a charge on the molecule, accelerates the resulting ion in an electromagnetic field, and measures the mass-to-charge ratios. Various types of mass spectrometry have different ways of ionizing molecules and accelerating ions (Marshall and Rodgers 2004; Rodgers *et al.*, 2005). In molecular-diffusion measurements, various techniques, especially fluorescence techniques, track the diffusion of individual molecules (Groenzin and Mullins, 2000). Large molecules diffuse slowly, and smaller molecules diffuse more quickly. Estimates of molecular diameter are interpreted to infer molecular weight by comparison with model compounds.

In the past 10 years since these techniques have become available, the concept of the asphaltene molecule has undergone a transformation. Because the asphaltene solubility classification captures a broad range of molecular structures, it is impossible to define a single molecular structure and size. However, new perspective is emerging that honors results from several measurement types. This latest thinking puts the average molecular weight at about 750 g/mol within a range of 300 to 1,400 g/mol. That is compatible with a molecule containing seven or eight fused aromatic rings, and the range accommodates molecules with four to ten rings (Mullins *et al.*, 2007). There is also evidence that some asphaltenes consist of multiple groups of rings linked by alkane chains (Gray, 2003; Peng *et al.*, 1999). Heteroatoms, which are largely contained in the ring systems, can give the molecule polarity: the polarizability of the fused aromatic-ring systems and the charge separation induced by heteroatoms cause the centers of neighboring asphaltene molecules to stick to each other, while the outer chains are repulsed by the chains of other molecules. Such a structure is consistent with the Yen model suggested more than 40 years ago, which also proposed stacking asphaltene fused-ring systems (Dickie and Yen, 1967). However, the molecular weight of a single molecule is significantly smaller - by a factor of ten - than the average asphaltene molecular weight proposed in the 1980's and 1990's (Mullins *et al.*, 2007).

Only now is the Yen model understood within a framework of asphaltene molecular structure and aggregation. With the knowledge of the size and structure of an individual molecule as a starting point, chemists can now explain how asphaltene molecules behave before they precipitate. This aggregation behavior depends on solvent type. Again, most laboratory studies (Goncalves *et al.*, 2004; Evdokimov, 2006; Mullins, 2009; Akbarzadeh *et al.*, 2007; Mullins and Sheu, 1998) are conducted with asphaltenes dissolved in a solvent, such as toluene, but some are only performed with asphaltenes in their native crude oil.

Chemical characterization gives information on the chemical composition and functional groups in macromolecules. The main analytical tools used in chemical characterization are the liquid chromatography (SARA fractionation, elemental analyses, nuclear magnetic resonance (NMR), infrared spectroscopy (IR), etc. Fluorescence spectroscopy has been applied directly to crude oil or to asphaltene solutions and the absorption/emission behaviors of such a multicomponent system carefully studied (Mullins *et al.*, 1992; Wang and Mullins, 1994; Ruiz-Morales and Mullins, 2009). Several authors have reported the utilization of the various analytical tools in characterizing crude oil fractions. Some of the applications that have been published in use of NMR include structural study of residues or asphaltenes (Hamid, 2000; Masuda *et al.*, 1996; Sharma *et al.*, 2000a, b). In a related study, McLean and Kilpatrick (1997) had studied four different crude oils – Arab Heavy, Arab Berri, Alaskan North Slope, and San Joaquin Valley, using the analytical tools to investigate the elemental composition, polar functional groups and carbon types by FT-IR and ^{13}C and ^1H NMR. An indirect measure of the polarity of subsequent groups attached to the aromatic core of these molecules may also be provided by the FT-IR analysis. Other studies include the characterization of residues, resins and asphaltenes fractions of different polarities (Nalwaya *et al.*, 1999; Buenrostro-Gonzales, 2001).

1.8 Weathering characteristics and oil spill modeling

The weathering process undergone by a spilled crude oil or refined product is determined or governed by a wide variety of processes immediately after a spill as discussed above. All of these processes are time - dependent and must be described by dynamic models (Fingas,

1995; Daling and Strom-Kristiansen, 1999). As mentioned earlier; evaporation is the most important process that oils undergo immediately after a spillage. An understanding of evaporation is important both from the practical viewpoint of cleaning up spills and for developing predictive models (Fingas, 1995a). Many spill models incorporate evaporation as a component of their prediction and at times evaporation is sometimes the only transformation process included in oil spill prediction models (Fingas, 1995). Over the years, significant progress has been made in the identification of factors affecting water-in-oil emulsification (Bridie *et al*, 1980a, b; Zagorski and Mackay, 1982; Payne and Phillips 1985, Walker *et al.*, 1993a,b, 1995b, Fingas and Fieldhouse, 2003), and these and other studies have been summarised in a review by Fingas and Fieldhouse (2006). Also, an important and recent improvement in modelling emulsion formation have been reviewed and presented by Fingas and Fieldhouse (2006) and Fingas (2007). State-of-the-art models include some, but not all of these models at varying degrees of sophistication, but field or laboratory experiments designed to test or calibrate models, as contained in considerable literature has, however not reliably addressed certain areas in weathering process (Daling and Strom, 1999; Riazi and Al-Enezi, 1999; Mearns and Simecek-Beatty, 2003). An identifiable area is the paucity of data yet, regarding (a model that predicts) the weathering rate, specific to individual crude oils, at different wind speeds and temperature, the existence and persistence of physical processes important for modelling oil behaviour on the sea surface.

The effects of physical processes are in the literature investigated for various purposes which include enhancement of the prediction of the movement and spreading of oil in case of spills, where fast and effective methods are essential for a successful operations (Fingas,1997); to establish confidence and more accuracy in positive matches when performing forensic oil spill fingerprinting (Wang *et al.*, 2004) and importantly to have better knowledge of the movement of toxic compounds in the environmental compartments (NOOA, 2005).

Weathering effects are primarily measured using chromatographic methods as GC-FID or GC-MS. However, effects of weathering have also been described on the basis of more simple measurements. Fingas (1997) has determined the effect of evaporation, and the relationship between rate and time of evaporation of a crude oil, on the basis of weight. Similar investigations have been conducted with changes in volume (Riazi and Enezi, 1999), and with changes in total hydrocarbon content (THC; Sauer *et al.*, 1998).

Recently, important gaps in the research literature have been identified which places focus aimed towards investigations into the key micro-scale processes influencing the weathering of oil which included oxidation and photo-oxidation (Lee, 2003; Prince, *et al.*, 2003; van der Meer, 2005; Mearn and Simecek-Beatty, 2003). Most importantly, Reed (2007) also reported that researchers identified and prioritized areas of urgent research need and the gap in understanding water-in-oil emulsification i.e. to predict weathering process rates solely from oil composition. In addition, the need to understand rheology of weathered oil apart from the viscosity, amongst other specific processes as they relate to the long-term weathering of oil, in order to improve extended forecasts about the fate and effect of oil from major and deep-water oil spills and the efficacy of various response options. Focus was also on the review of resolving the uncertainties in modelling, simulation and field monitoring in order to improve the spill response activities as reported by Reed *et al.*, 2009.

Different approaches have been taken in the past for mixing of oil products for performance testing, without paying sufficient attention to the changes in the composition of the oil due to weathering. Nordvik (1995) reported that in the past, test methods and standards for performance and effectiveness testing of equipment and products have, in general, used relatively fresh crude oil and oil products as test fluids and therefore, had provided only a snapshot of oil weathering and performance data from an early stage of a spill. Performance data that includes testing of equipment and materials over a wide range of viscosities and weathering stages of oils is required in order to establish windows-of-opportunity and effectiveness for different countermeasure techniques, such as mechanical recovery, chemical treatment by dispersants or emulsifiers and in-situ burning (Nordvik, 1995).

The changes in oil properties as functions of time can be measured by use of a step-wise oil weathering method which was developed initially by IKU-SINTEF as a laboratory method for effectiveness testing of dispersants (Daling *et. al.*, 1990). This weathering method determines oil properties at different degrees of distillation, representing boiling points of 150, 200, and 250°C. These oil residues correlate with evaporation over time on the sea surface. The periods of 1-3 hrs, 12-24 hrs, and approximately 1 week were selected as critical time periods, depending on oil characteristics and environmental conditions at the time of a spill. Oil weathering data from fresh oil and step-wise weathered fractions is used to predict pour point, flash point, density, viscosity of oil, and the degree of emulsification (Daling and Strom, 1999).

Mohammad and Al-Enezi (1999), had investigated the evaporation of Kuwaiti crude oil by pouring a thin layer of oil on vessels filled with water and placed on roof-top for 7 days. The oil residue in each of the vessels was taken, at the rate of one vessel per day, to the laboratory to evaluate and measure the volume of oil sunk to the bottom of the vessel, as well as the rate of oil evaporation. Fernandez-Varela *et al.*, (2005), had weathered crude oil on metallic plates under atmospheric conditions on a shaker for three months. Samples were taken at pre-set intervals. Also, Mehta (2005), had conducted evaporation by spreading crude oil on a corrugated plate supported by angle irons, and inclined at an angle to form a framework that simulated wave action. A continuous flow of the spread oil was ensured by a peristaltic pump to circulate oil, in a cycle, from a container over the corrugated plate. Evaporation was determined in terms of volume loss throughout the experiment at the test conditions.

Another method of evaporation simulation is gas stripping which involves bubbling air at the rate of 2 litres per minute for about 50hrs through a given weight of oil at a constant temperature. The weight of the oil remaining is recorded at regular intervals. This method was undertaken by National Chemical Emergency Centre AEA Technology, Abingdon, UK (Davies, 2001).

Warren Springs Laboratory, in collaboration with the Institute of Offshore Engineering, Heriot-Watt University, UK, conducted a 2-year long study and sea trials into the spill behavior of some North Sea crude oils (Walker *et al.*, 1993). Their study involved a laboratory weathering and emulsification experiments, the fingerprinting of 39 different North sea crude oils, oil spill modeling, sea trials and a review of response options to oil spill. The main objective for the sea trials was to use the data generated from these to determine how closely the weathering experiments conducted in the laboratory approximate natural conditions. In the Warren Springs laboratory weathering simulation, crude oil was distilled at 175 °C and 250 °C which was designed to produce oil similar to weathered oil sample after 1 hour and 50 hours at sea respectively. The correlation was determined from previous studies by Warren Springs Laboratory (Buchanan and Hurford, 1988) which suggested that after 1 hour a spilled oil sample would lose the *n*-alkane components up to and including C₉, and after 2 days the sample would lose *n*-alkanes components up to and including some C₁₃. The results from the investigation showed that distilling crude to a maximum vapour temperature of 175 °C produced a residue corresponding to 1 hour weathering and, similarly, distillation to 250 °C produced a 50 hours equivalent weathered residue.

Other researchers have also used the distillation method to simulate the weathering of oil (Daling *et al.*, 1990). In the past decades, series of field experiments have formed the basis for the continuous evolution of the algorithms used in the SINTEF-Oil weathering model (SINTEF- OWM). This, in combination with a standardized laboratory investigation, including bench-scale (“step-wise”) weathering, chemical dispersibility investigation and mesoscale flume basin weathering study of each specific oil, form the basis input to the model (Daling and Strom, 1999). The strength of the SINTEF- OWM model lies in its use and verification of oil weathering data. The model predicts changes in oil characteristics based upon an empirical approach from data obtained from experimental spills at sea of specific crude oils, crude oil data derived from a comprehensive step-wise weathering test procedure and laboratory flume tank testing. The experimental results lead to subsequent development and modification of algorithms and use of correlation factors for individual oils (Nordvik, 1995).

A small-scale laboratory procedure to characterize the weathering properties of different oils has been refined and standardized (Strom-Kristiansen *et al.*, 1993; Daling *et al.*, 1997). To isolate influence of different weathering processes (i.e. evaporative loss, photo-oxidation and water-in-oil emulsification), Daling and Strom-Kristiansen (1999) prepared oil residues and water-in-oil emulsions (altogether 16 weathered samples) prepared in a "step-wise" way from the fresh oil. These weathered samples represented various stages (weathering times) at sea. The samples were characterized to determine the changes in physico-chemical and emulsifying properties as well as the chemical dispersibility (Daling *et al.*, 1990). The experimental data created from this laboratory investigation formed a basic input for predicting the weathering behavior of the different oils at sea by use of the SINTEF-OWM model (Daling and Strom-Kristiansen, 1999).

When studying weathering effects on different oils, it is important that the oils are exposed to weathering conditions as realistic as possible. van der Meer (2005) had noted that the results from experimentally produced aged hydrocarbon mixtures more accurately reflect those found in the field after an oil spill. A meso-scale flume basin was developed by SINTEF (Nordvik, 1995; Daling and Strom-Kristiansen, 1999), carefully designed to characteristically simulate the weathering processes (i.e., evaporative loss, photo-oxidation, natural dispersion, emulsification, dissolution etc.) which take place at sea. The flume basin had provided reliable conditions for studying the weathering properties of different oil types and testing the performance of dispersants. It also acted as a link between bench-scale laboratory studies and full-scale field experiments and correlations between the SINTEF flume experiment and ground-truth data (i.e. data collected on location) from field experiments (Strom-Kristiansen *et al.*, 1997), has become an important tool to the small-scale weathering procedure as data input to the SINTEF-OWM model for investigating and predicting oils' behaviour at sea (Daling and Strom-Kristiansen, 1999).

Researchers have developed different approaches to predicting changes in oil properties due to weathering during the past decades (e.g. ITOPF, 1987). In many cases, these models are based on a set of "mixing rules", where various physical oil properties are derived on

the basis of composition change caused by evaporation of the lighter oil components. Algorithms based on such simple mixing rules may be relevant for prediction of some properties, such as density, but are less relevant for other properties, such as viscosity and pour-point (Johansen, 1991). As a consequence, an empirical model approach has been used in the development of the SINTEF-OWM (Daling *et al.*, 1990; Aamo *et al.*, 1993). The SINTEF-OWM calculates the changes in oil properties due to weathering under user-specified environmental conditions (oil/water-in-oil emulsion film thickness, sea state and temperatures) and based on data from the standardized laboratory weathering methodology (Daling and Strom-Kristiansen, 1999).

Further research in kinetic weathering model has been advanced. Short and Heintz have developed a first-order loss-rate (FOLR) kinetic model of PAH weathering to evaluate 7767 environmental samples collected for the Exxon Valdez oil spill for the presence of spilled oil (Short and Heintz, 1997). The modeled PAHs included the 14 most persistent compounds of 31 analyzed by GC-MS. Parameters included loss-rate constants related to energy required for PAHs to escape from petroleum and a quantitative index of weathering. The model accounts for 91% of the temporal variability of modeled PAH concentrations. Short has applied this model to four independent case studies (Short, 2002). The approach used in these case studies evaluates a goodness-of-fit metric between the measured hydrocarbon composition of an environmental sample and a suspected source after correcting for PAH weathering loss based on FOLR kinetics.

Malmquist (2006) in his laboratory investigations of *in vitro* short-term (0-192hrs) weathering of some processes – evaporation, dissolution, photooxidation and microbial degradation of a heavy fuel oil placed directly on petridishes stored in a dark room, had evaluated by means of GC-MS, the relative chemical compositional changes in the remaining oil as a function of temperature and time. Gomha (2004) had also reported the consequences of evaporative losses in relation to compositional changes in Hunton and Glenpool oil samples in the Oklahoma oil field and also crude oil samples from a Chinese oil field. During emulsification, the physical properties and characteristics of oil spills

change extensively. The basic principle is that water-in-oil emulsions are stabilized by the formation of asphaltene layers around water droplets in oil and subsequently, several studies have reviewed emulsions and concluded that the asphaltene content is the single most important factor in the formation of emulsions (Sjoblom *et al.*, 2003; Kilpatrick and Spiecker, 2001). Fingas and Fieldhouse (2006) in their study had also weathered the test oils to different percent evaporated losses in developing their emulsification model.

Several workers have studied emulsification by using model oils or modified crude oils and water-in-oil emulsions formed from crude oils of different origins (McLean and Kilpatrick, 1997; Schorling *et al.*, 1998; Hemmingston *et al.*, 2005). These studies found that there is an increase in stability as viscosity increases. Viscosity also correlated with the SARA data taken on the crude oils. A recent study by Fingas and Fieldhouse (2009) had characterized the water-in-oil (emulsion) types in some crude oils and petroleum products, relating the products formed to the starting oil properties. These studies have shown the importance of components such as asphaltenes and resins to have pronounced effects on crude oil emulsion stabilization. It is therefore of interest to isolate and characterize these components according to their specific chemical characteristics in order to understand their roles and mechanism in emulsion formation. The SARA analyses is one of the most convenient and generally accepted method used to separate the crude oil into four major fractions: saturates, aromatics, resins and asphaltenes (SARA), based on their solubility and polarity (McLean and Kilpatrick, 1997; Jiang *et al.*, 2000; Auflem, 2002; Bastow *et al.*, 2007) and are utilized extensively in the oil industry and in environmental forensics (Kircher, 1989; Moldowan *et al.*, 1995; Peters *et al.*, 2005). There are many variations in the recommended procedures but the basis for the method is that asphaltenes are removed by precipitation with a paraffinic solvent such as *n*-pentane or *n*-heptane, and the deasphalted oil is separated into saturates, aromatics and resins by chromatographic fractionation (Miller, 1982; Vasquez and Mansoori, 2000; Aske *et al.*, 2001).

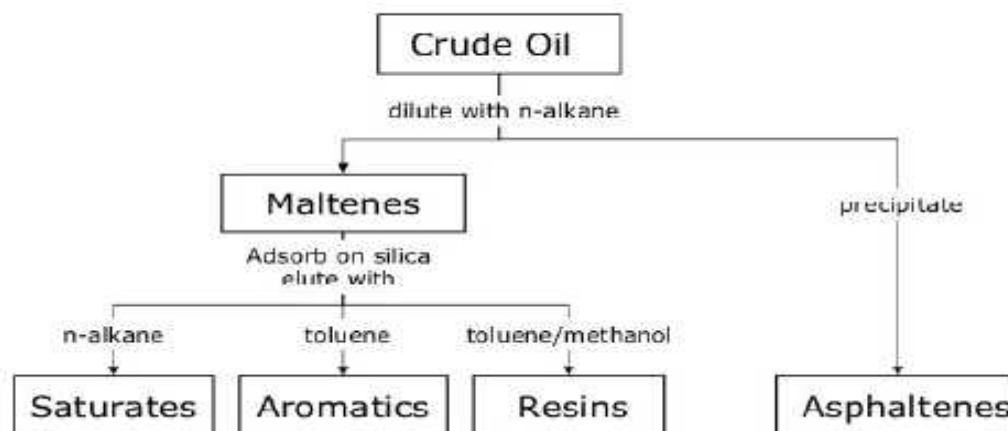


Fig.2 SARA-separation scheme for separation of crude oil into saturate, aromatic, resin and asphaltene (SARA) components (Auflem, 2002).

In SARA fractionation, after separation by addition of *n*-alkane, the remaining components, called maltenes, are then further fractionated by passing the mixture through a column. Each component is removed from the column by flushing with various solvents. Saturated hydrocarbons, or saturates, are removed by flushing with *n*-alkane. Resins are a solubility class, and somewhat similar to asphaltenes. They are the nonvolatile polar component of crude oil that is soluble in *n*-alkanes and insoluble in liquid propane (Akbarzadeh *et al.*, 2007).

The SARA fractionation method has found great utility in combination with high-performance liquid chromatography [HPLC] (Ali and Nofal, 1994; Fan and Buckley, 2002; Hammami *et al.*, 1998; Aske *et al.*, 2001). In a normal-phase liquid chromatographic process, a nonpolar mobile phase permeates through a porous solid stationary phase (polar) usually in the form of small particles, packed into cylindrical column. The sample is injected into the mobile phase, travels through the column, and is retained by the stationary phase mainly depending on polarity. Adsorption interactions between sample components, the mobile phase, and the stationary phase can be manipulated by the choice of mobile and stationary phases and flow conditions (Mullins *et al.*, 2007). High performance liquid chromatography (HPLC) also find useful application in this process due to its simplicity

and speed of analysis compared to the ASTM procedures for SARA separation, which are based on liquid chromatography (LC) [ASTM Method D4124,1991;D2007,1993] (Aske *et al.*, 2001). Fluorescent indicator adsorption (FIA) and thin layer chromatographic methods combined with flame ionization detection (TLC-FID) have also been used for class determination. However, the FIA method is time consuming and the results are strongly dependent on the operator. TLC-FID also requires a thorough knowledge on the limitations of the system (Lundanes and Greibrokk, 1994). Researches in the behavior and fate of oil has been dominated by investigations into the composition of the oil (Fingas, 1997), but relatively not much of this process as a function of the environment has been studied.

1.9 Research Objectives

The main objectives of this research were to develop a better understanding of the effect of temperature and time on the rate of evaporation and compositional profiles and its role in modifying the rate of weathering of North Sea crude oils on seawater. The research is also intended to carry out broad characterization of the crude oils to investigate the effect of oil chemistry on emulsification behavior and to gain insight into which parameters govern the emulsion stability characteristics of North Sea crude oils. In order to understand the process of water-in-oil emulsions, particular emphasis in this study will be the investigation of the role of asphaltenes and resins in the emulsification characteristics of crude oils.

The quantitative information derivable from this work will assist in the understanding of the fate and behaviour of the oil in the environment after a spill in relation to temperature and emulsification, as a function of the oil chemistry and will provide data for generation of algorithms describing the evaporative weathering of oils.

1.9.1 Research Outline

The respective chapters of this thesis can be generally identified with one of the research objectives described in Section 1.9. The thesis consists of nine chapters with each chapter (apart from Chapter 9), respectively containing its own introduction - description of the relative topics, theories and literature review and scopes aimed at achieving the objectives of the research, experimental sub-section, results and discussion, and conclusion.

A general introduction and review of related literature is given in Chapter 1. An investigation of effects of weathering of some North Sea crudes is given in Chapter 2. The aspects of crude oil emulsification and stability are presented in Chapter 3. In Chapters 4 and 5, the chemical characterisation of crude oils using a range of analytical techniques is described and reinforces the important view of the chemistry and qualitative study of crude oils/ emulsion behaviour.

A modelling of proposed asphaltene structures, based on the analytical results of this study is presented in Chapter 6, while Chapter 7 contains a correlation analysis of measured variables. An integrated discussion based on experimental data obtained from preceding chapters in this work, and in the light of results and theories from the literature is presented in Chapter 8. The final conclusions and suggestions for future work is given in Chapter 9.

CHAPTER 2

INVESTIGATION OF EFFECTS OF TEMPERATURE ON THE RATE OF EVAPORATIVE WEATHERING OF SOME NORTH SEA CRUDES

2.1 Introduction

Evaporation is one of the foremost weathering processes for most oil spills, either at the surface or in the subsurface, and is a key process that significantly modifies the composition of spilled oil in the marine environment. Oil spilled at sea will normally be degraded by a number of biological and physicochemical processes, some of which act quickly and others more slowly such that the rate of degradation depends, not only on the initial composition of the spilled product, but also on the environmental conditions which may favour the predominant effect of one process over others. Fates and effects of pollutants in the environment are the result of complex relations among physical, chemical and biological variables and parameters, some of which are well known while others remain less certain (Reed, 2005).

A key component in oil and gas exploration and production is a risk analysis and robust contingency plan for oil spill which needs to propose the most effective operational response techniques and therefore the application of those best suited to any spilt hydrocarbon. This gives realistic options for containing and effectively combating the spill appropriately and with due consideration to the spill scenario and surrounding conditions. In the marine environment, the basic and crucial points in oil spill combat consist in understanding and predicting the fate of the pollutant in the natural environment, what physical and chemical changes it will undergo, and deducing from this the most pertinent, efficient methods of oil spill response to be deployed. On a wider perspective, modelling of environmental processes and systems occupies a central role in development planning

and also plays key roles in research, allowing testing of hypotheses, identification of research needs, and increasing understanding of the natural phenomena.

Most oil spill behaviour models include evaporation as a process and in the output of the model. Mackay *et al.*, (1980) developed semi empirical equations to describe the weathering processes. Subsequently, these equations were incorporated into the fate sub-model of a natural resource damage assessment modelling system for marine and coastal areas (Reed, 1989). This sub-model was designed to estimate the distribution of a contaminant on the sea surface, and to predict water column and sediment concentrations. Further work was carried out by Sebastiao and Soares (1995) in which they transformed the time dependent weathering algorithms of Mackay *et al.*, (1980) and Reed (1989) into a system of differential equations and this effort solved a system of model equations numerically to describe spreading (area growth), evaporation, volume balance accounting for the volume lost by evaporation and by natural dispersion into the water column, water incorporation and viscosity increase with time. However, the complexity of environmental models is continuously increasing in approach and its rapid growth in recent years has been boosted by developments in computer sciences and the availability of remotely sensed and *in situ* environmental data. These data have supplied the capability to calibrate and test increasingly complex model systems made feasible by the developments in the computational domain. It is also noted that the evaluation of environmental impacts and risks associated with pollutant releases to the marine environment is the key to achieving a balanced approach to management of natural resources and industrial and urban operations (Reed, 2005).

For oil spilled in the marine environment, evaporation is a process that is fundamentally affected by temperature. Contingency plans regarding the oil spill scenario is usually addressed by means of predictive computer models available on the market and these make use of algorithms of varying complexity, some of which have been validated experimentally via laboratory work, extensive testing or sometimes via actual sea trials at sea (Merlin and Poutchkovsky, 2004). Although oil spill models have improved significantly over the last 20 years, their capability for modelling of some physicochemical processes still remains weak (Nazir *et al.*, 2008). It is important to note that in all cases, the

validation has been obtained for only a limited number of oils, which are scarcely ever the ones concerned in the oil spill contingency plan to be devised and therefore such software models are always “speculative” to a greater or lesser degree and such predictions not always as reliable as they might be (Fingas, 1995; 1997; Gomha, 2004; Weaver, 2004; Merlin and Poutchkovsky, 2004).

Crude oil is a multi-component mixture which varies from source to source. In order to generate reliable predictions regarding weathering process of some specific types of crude oil, experimental simulation aimed at the investigation of the effects of temperature over a wide range of time on the rate of evaporative weathering of some specific North Sea crudes, and their associated emulsions was carried out. Evaporation rates are important in investigating the rate of loss of crude oil, in source identification, the oil behaviour at sea and assessment of hazards arising from the spillage. Investigating the compositional profiles is particularly important in forensics, where it can be valuable in correlating the spilled oil to the source of the crude and also in estimating the date of the spillage event and therefore ascertaining accurate spilled oil-to-source correlation. Evaporation also changes the density of the oil and affects its emulsification. This chapter addresses the relationship of the effect of temperature and time on the evaporation rate of two North Sea crude oils investigated in this study.

2.2 EXPERIMENTAL

2.2.1 Materials

Crude oils from the Forties and Brent oilfields were received from petroleum companies in the North Sea, United Kingdom and used as oils for these experiments. These crude oils are important by their high production volume and therefore would have a high spill potential (Law and Kelly, 2004; Edwards and White, 1999). The crude oils were used as received from petroleum companies and were stored in sealed containers in a refrigerated room at 10°C. Before use for the experiments, the oil samples were removed from the cold room and shaken vigorously for 30 min. to ensure homogeneity of the sample. All crude oils were returned to room temperature before sampling. The seawater for evaporation and

emulsification experiments was 35ppt saline water obtained from St. Andrews, Scotland. Other materials included glass petridishes (100 x 15 mm) from Fisher Scientific - England, digital thermometer, analytical balance (Mettler AT261 DeltaRange),, thermostatic water bath, cooling coil, airflow meter, Electromantle Me Heater (Fison Scientific, England), Top Drive Macerator propeller (Townsend & Mercer Ltd, Croydon, England), Kilner jars, shear homogeniser, 900mL glass beakers, 3ml scintillation vials, HPLC grade *n*-pentane and toluene (Fisher Scientific – England, sodium sulphate anhydrous (Na₂SO₄) from J.T. Baker, Holland.

2.2.2 Glassware cleaning procedure

To minimize interference in analyses from contaminated glassware, a cleaning procedure was adopted according to the method of Henderson, (1999). The cleaning procedure was followed for all glassware used for sample preparation throughout this research. The procedure involved 1 hour washing of glassware at 50⁰C with Decon (Decon Laboratories Limited, Sussex, and UK.) and three subsequent rinses with tap water. This was followed by one rinse with 3% HCl, two rinses with tap water and one rinse with distilled water after which glassware was allowed to dry before a final rinse with dichloromethane (DCM). Any residual DCM was left to evaporate in a fume cupboard.

2.3 Method

Samples in all experiments were prepared in replicates. The mass of three petridishes (100 x 15mm) labelled 1, 2 and 3 were determined on an electronic balance and recorded. 20ml of filtered seawater (35 g/L, filtered to 1 micron) was measured into each of the petridishes and mass recorded. Forties crude oil (3.5 g) was carefully added to form a thin film on the surface of the seawater in the petridishes. The petridishes were then carefully placed in a clockwise geometry (initially determined to provide the most even airflow and evaporative rate) on the surface of the water in the thermostatic water bath. The weathering experiments were carried out in the water bath over a range of temperatures ranges: 12, 20, 25, 30, 40, and 50 °C respectively. The water bath was placed in a fume cupboard as a measure to comply with Health and Safety requirement and to ensure airflow over the samples. The

initial film thickness of the oil and the airflow rates were kept constant during the experiment. The airflow speed in the fume cupboard was determined with an airflow meter and constantly checked to ensure that it was maintained at 0.77 m/s. At pre-determined intervals, each petridish was removed and immediately weighed on a mass balance and the evaporative mass loss at these specified time recorded for each. Small quantity of samples were carefully taken with a Pasteur pipette from the surface of the weathered oil in each of the Petri dishes at timed intervals of 0 h, 1 h, 2 h, 3 h, 4 h, 5 h, 6 h, 24 h and 48 h, 96 h, and 110 h respectively, and placed into 3 ml scintillation vials. 2 ml of *n*-pentane was added to vials to dissolve the samples and a small amount of anhydrous sodium sulphate (Na_2SO_4) added as a drying agent to absorb possible water uptake taken up during sampling. The samples of the oil taken were further analysed by Gas Chromatography using a flame ionisation detector (GC-FID), in order to check the compositional changes in the hydrocarbon distribution in the oil.

The GC-FID instrument used in this work was a Thermo Quest Trace GC, Manchester, England equipped with a Flame Ionisation Detector (FID) and using a hydrogen air flame. The capillary column was a 5 % PH ME Siloxane manufactured by Hewlett Packard (= HP5). The column was 30m long and its film thickness is 0.25 μm with column internal diameter (ID) of 0.25 mm. The carrier gas was helium at a flow rate of 1.5 ml/min. From the dissolved samples (2 ml *n*-pentane was added to achieve appropriate concentration for GC analysis) a 1 μl aliquot was removed and injected onto the column. The oven programme was set such that the sample was injected at 40 °C where it was held for 1min. It was then heated from 40 to 300 °C at 5 °C a minute. Once at 300 °C it was held there for 30 minutes.

Three sets of further experiments were carried out at 30 °C. These used 3.5 g crude oil and 20 ml of filtered seawater, Brent crude on its own and seawater on its own. The objective of these experiments was to observe whether the presence of seawater affected the rate of evaporation of crude oil. The experimental conditions were as before with sampling and measurements for the three different experiments carried out at similar intervals for a

maximum of 48 h (0-48 h). The samples taken from oil on seawater and crude oil without seawater evaporations respectively were further analysed by gas chromatography. A sample of fresh Brent crude oil (unweathered) was also analysed on the GC-FID for comparison.

Water-in-oil emulsions were prepared using fresh and 20 % weathered samples of the crude. The emulsions were formed in order to investigate the rate of evaporation of volatile components from the crude emulsions formed, in relation to the unemulsified sample of weathered crude oil. The oil was weathered as follows: 150 g of fresh Brent crude was measured into a glass beaker and heated gently on a hot plate, at a temperature of 35 °C for 6hrs to achieve a 20 % weathering (weight loss) of the crude oil. This represents crude oil that has undergone a 20 % weathering. The residue was then used for the preparation of water-in-oil emulsion. Using a measuring cylinder, 700 ml of seawater (35 g/L) was measured and poured into a wide-mouthed 900 ml Kilner jar. The weathered oil residue (96.60 g) was poured into the Kilner jar containing the seawater and a high shear homogenizer with 6 mm rotor-stator head set at speeds ranging from 800 xg, was used to vigorously stir the oil-water mixture. The apparatus can control rotor speed from ~500 to 1200 xg and maintain speed regardless of applied load. During the mixing, most of the seawater was brought from the bottom of kilner jar and blended with oil. The unit was located in a temperature controlled cold room at 10 °C. This rotational speed was sufficient to vigorously stir the mixture, resulting in a high water uptake rate (Walker *et al.*, 1992). Mixing was carried out for 45 min, with stops at specific times for observation. When a specific end point was reached, as observed by the colour change of the emulsion formed, the mixing was concluded (Walker *et al.*, 1992; Hokstad *et al.*, 1993). The prepared emulsions were stored at 10 °C until taken for further analysis.

2.4 RESULTS AND DISCUSSION

2.4.1 Effect of temperature variation on the rate of weathering of Forties and Brent crude oils.

Evaporative loss can be a significant process in the weathering of many crude oils, especially light crude oil, and can lead to a loss of up to 50-60 % of its bulk composition

(Brandvik and Faksness, 2009). In addition to wind speed, the rate at which crude oil is lost by evaporative weathering can also depend on the temperature, compared to other physico-chemical weathering phenomena, since evaporation is a surface phenomenon. Evaporation depends on the boiling point (i.e. vapour pressure), which is generally inversely related to the molecular weight for groups of related compounds (Chao *et al.*, 2001); therefore the low molecular weight compounds in the crude oil will evaporate most rapidly.

Evaporation of Forties Crude at different temperatures (12-50 °C)

The results of the measurements of evaporation of Forties crude oil on seawater at temperatures ranging from 12-50 °C at timed intervals are shown in Table 2.1 – 2.6. Table 2.7 gives a summary of the mean mass loss. Table 2.8 – 2.13 shows the percentage (%) evaporation on each of the sample petridishes in each experiment. Tables 2.1 – 2.13 are shown in Appendix A. Figure 3 shows the experimental set-up used in the evaporative weathering of the crude oils in this study.



Fig. 3 Weathering of crude oils on Seawater in petridishes in a thermostatic water bath. D1, D2 and D3 represent each of the petridishes containing the crude oil samples and seawater.

The mean weight losses of Forties crude due to evaporative weathering at different temperatures and time are given in Fig 4a. The data shows the mass loss due to evaporation decreases as the temperature of the weathering decreases. The degree of evaporation was seen to be more at 50 and 40 °C, where the rate of evaporative loss of volatile (lighter)

fractions recorded were higher as indicated in Fig 4a, compared to lower temperatures of 30, 20 and 12 °C respectively. Also, a significant observation in the evaporative loss was that in the 12 °C – 30 °C temperature ranges, the evaporation rate was rapid in the first few hours (1-6hrs) after which it progressed at a much slower rate. At higher temperatures (40-50 °C), the rate of evaporation appeared to progress at a constant rate. This observation within the temperature range 12-30 °C is in agreement with studies conducted by Merlin and Poutchkovsky (2004) and Fingas (1995). As the evaporation continues the rate decreases following 1st order kinetics, but simultaneously the viscosity of an oil slick increases whereby the rate of removal of compounds from the slick decreases further (Sebastiao and Soares, 1995). This did not appear to be the case at elevated temperatures i.e. 40 and 50 °C.

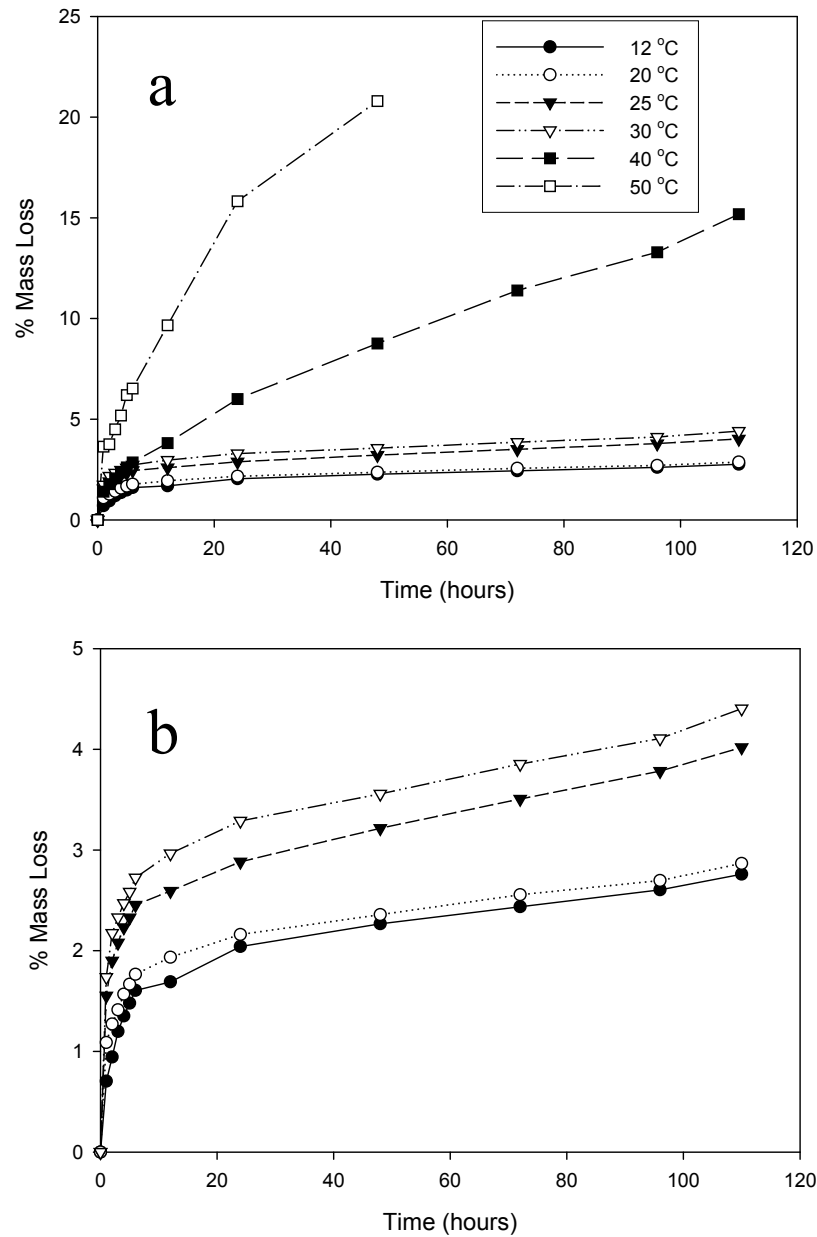


Fig. 4a Showing the percentage weight (mass) loss of Forties crude evaporation at various temperatures (as shown in legend); and 4b shows the plot of percentage weight (mass) loss for 12, 20, 25 and 30°C only.

There is a general consensus that as the oil weathers, in this case due to evaporation, the physical properties of the oil will also change (Lewis and Daling, 1995). As the light fractions evaporate the specific gravity becomes higher (Daling and Brandvik, 1991). Again, evaporation will also cause the pour point values to increase due to the increased

concentration of heavy waxes caused by evaporation (Durell *et al.*, 1993; Daling and Brandvik, 1991). Evaporative weathering may also have an effect on the viscosity of the oil. As the lighter fractions evaporate the heavier fractions remain and the viscosity increases (Durell *et al.*, 1993; Merlin and Poutchkovsky, 2004). In condition of low or reduced temperatures, the initial viscosity of the oil is higher, and conducive to a reduction in the rate of evaporation. At this lower temperatures and low evaporation, the relative polar component concentration increases only moderately. Determining how the parameter of viscosity changes as a result of the effect of temperature refines the assessment of how further oil weathering phenomena such as emulsification will result. This is because evaporative loss due to the effect of temperature will change the viscosity and consequently affect emulsification and stability of such emulsions.

2.4.2 Comparison of Brent crude oils evaporation rates with and without seawater

In the mass loss experiments, at similar temperature of 30°C, the evaporation of Brent crude evaporated on seawater (BSW) proceeded at a much faster rate compared to the rate of evaporative mass loss from sample of Brent crude without seawater (B). This is shown in Fig. 5.

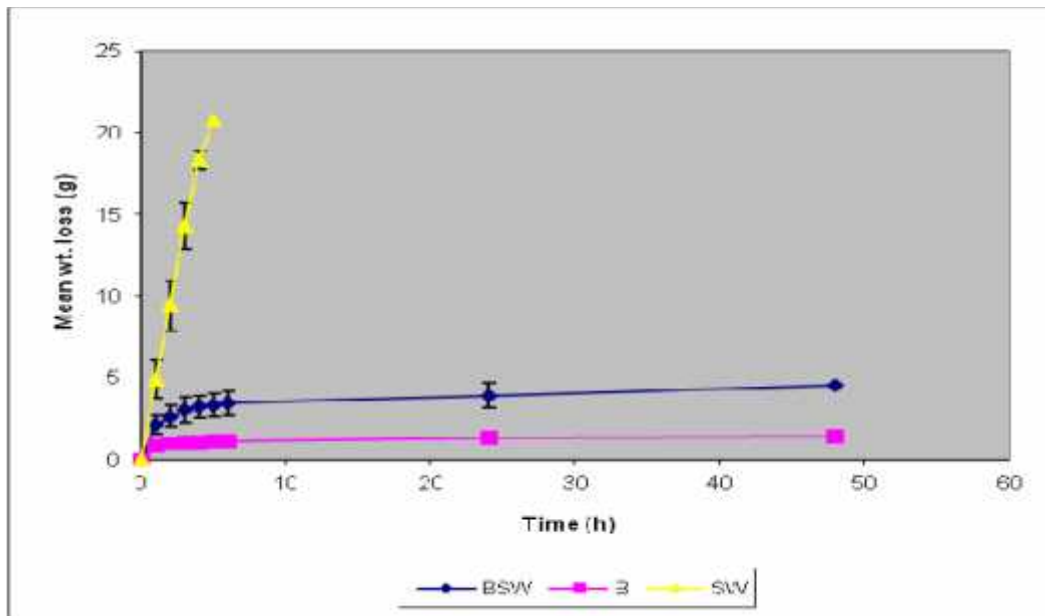


Fig. 5 showing mean weight loss for evaporation of Brent crude on seawater, Brent crude without seawater) and seawater samples at 30°C evaporation.

BSW = Brent crude on seawater; B = Brent (without seawater); SW = Seawater

This difference in the rate of evaporative mass loss can be apparently attributed to the many components of crude oil evaporating at different linear rates with respect to time. This premise is further supported by Fingas (1997) which relates the time dependence of crude oil evaporation particularly in rates and mass loss. Typically due to differences in densities of crude oil (0.84 g/cm^3) and that of seawater (1.03 g/cm^3), crude oil floats on water and also this may be due to differences in molecular weight leading to differences in boiling points. Apparently, both the dispersed seawater and the Brent crude phase evaporates and may contribute to the measured sample mass loss when crude oil evaporates on seawater. N-heptane (C_7H_{16} , a normal alkane) has a boiling point of 98°C ; C_8H_{18} , iso-octane, has a boiling point of 99°C ; benzene has a boiling point of 80°C . In theory, hydrocarbons with boiling points $>100^\circ\text{C}$ evaporates slower than water. The experiment also sought to empirically investigate the effect of weathering on spilled crude oil on seawater to evaluate if this process effectively inhibit or slow the rate of evaporation of its components.

As can also be seen in Fig. 5, the rate of evaporation of seawater sample on its own (SW) at the same temperature of 30°C was considerably faster where after 5hrs there was complete evaporation of the seawater from the petridishes compared to Brent crude on seawater (BSW) and Brent crude without seawater. Crude oil contains thousands of compounds with different boiling points, vapour pressure and volatilities and this may contribute to the rate limiting (less fast) trend in evaporation as these different components will evaporate from the surface at rates specific to its boiling points and volatilities. This is also supported by the gas chromatography data as discussed in Section 2.4.5.

2.4.3 Comparison of evaporation of Brent and Forties crude at 30°C

Fig.6 shows the mean evaporations recorded for Brent and Forties crude oils at a temperature of 30°C over the timed duration of 0-48 h. This indicates a clear and significant difference in the rate of evaporation of the lighter fractions for the Forties crude compared to Brent crude at similar timed intervals, showing a higher rate of evaporation for the Brent crude.

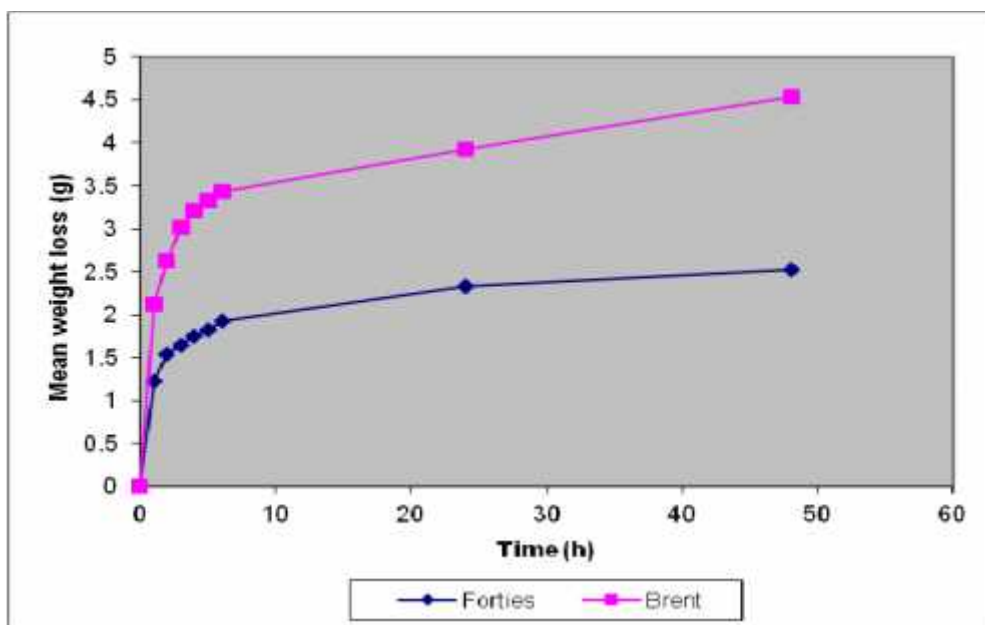


Fig 6 showing the mean evaporative mass loss for Forties and Brent crude oils on seawater at the temperature of 30 °C at timed intervals of 0-48 h. The variation in the rate of evaporation of volatile fractions between Forties and Brent crude oils is indicated.

The observed variation in the rate of mass transfer of volatile fractions between these two crude oils can be as a result of the differences in the chemistry of the specific oils. This result agrees with studies by Evers *et al.* (2004) where the authors also showed differences in evaporation rate in predictive weathering properties of five different oils.

To further understand the phenomenon of crude oil evaporation, the results of the experiments to investigate the effects of temperature on the rate of evaporative mass loss of Forties crude oil was subjected to computational modelling to enhance the prediction of the rate of mass loss of the volatile fractions of crude oil at different temperatures and time. The modelling of the process is discussed in this Chapter, in Section 2.4.7.

2.4.4 Compositional changes in Forties and Brent crude oils as a consequence of evaporative weathering

Results indicating the chemical compositional changes in Forties crude oil based on simulated evaporative weathering and GC-FID analyses of the samples taken at specified time for the different experimental temperatures are shown in the chromatograms contained in this Chapter, (Fig.7a – 10c and 11a – 13b). A determination of the evaporative rate can be measured by means of the modifications to the oil's composition as determined by (gas chromatography analyses) and this provides information on the volume and weight of the oil that is eliminated over time from the surface of seawater by volatilisation (Merlin and Poutchkovsky, 2004). The chromatograms primarily indicate the changes in the saturated hydrocarbon distribution of the oil samples. To facilitate a comparison of the composition and weathering trends between North Sea crude oil samples, with respect to the fresh oils, gas chromatography analyses of the sub-samples taken at timed intervals from the weathering experiments, were carried out.

2.4.5 GC-FID analyses of fresh / weathered Forties crude oil on seawater

Gas chromatography-flame ionisation detection (GC-FID) was used to determine the degree of weathering (by molecular carbon number) resulting from the evaporation. The chromatograms show a homologous series of normal alkanes ranging in carbon number from $n\text{-C}_8$ and C_{35} in the crude oil. As the oil is weathered, the relative peak heights of saturated hydrocarbons or compounds known to be affected by weathering such as n -alkanes should change.

Fig 7a and 7b respectively shows the saturated hydrocarbons of fresh Forties and Brent crude oils which have not undergone weathering. The chromatograms each show that the saturated hydrocarbons of the crude oils mainly distribute between $n\text{-C}_8$ and C_{35} with most abundant n -alkanes found in the $n\text{-C}_{10}$ to $n\text{-C}_{16}$ range.

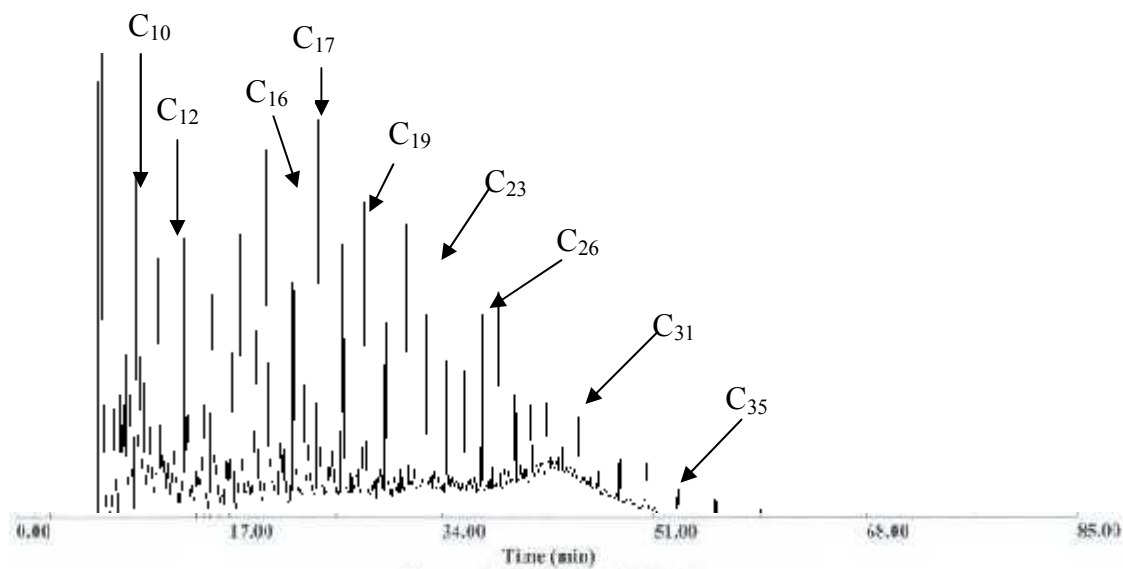


Fig. 7a GC-FID Chromatogram of Fresh Forties crude oil (unweathered) showing the distribution of *n*-alkanes (*n*-C₁₇) and pristane

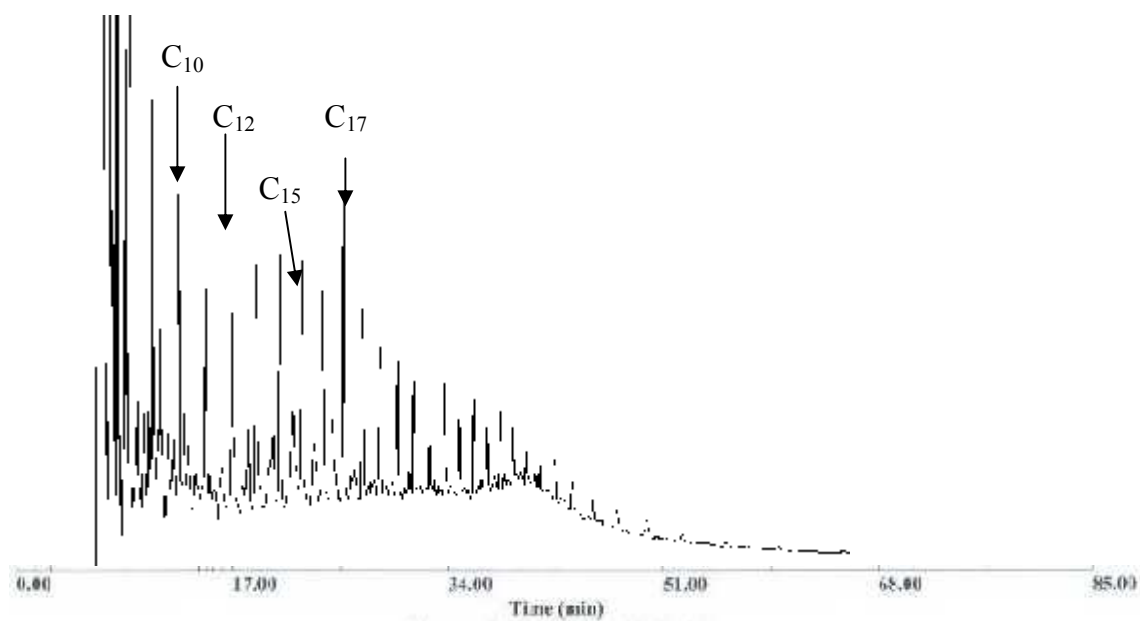


Fig.7b GC- FID chromatogram for fresh Brent crude oil (unweathered) showing the distribution of *n*-alkanes (*n*-C₁₇) and pristane

The main chemical components of the light crude oils are *n*-alkanes and isoprenoids and the aromatic compounds are the less abundant chemical components in the oil (Ma *et al.*, 2007; Jensen, 2000). Comparisons between fresh samples of Forties and Brent and the weathered samples indicated the extent of weathering across the GC-FID chromatograms. The hydrocarbon evaporation signatures can be quantitatively estimated by inspection of the GC-FID chromatogram. This is possible because hydrocarbon retention time on a non-polar GC stationary phase accurately predicts volatility from an oil mixture (Bidleman, 1984; Wang and Fingas, 2003; Arey *et al.*, 2005).

In these experiments, evaporation with time at the various temperatures was seen to systematically remove compounds along the first part of the chromatogram (Fig.8a – 10c) for the weathered Forties crude, corresponding to increasing hydrocarbon boiling point. Compounds in crude oil that boil at temperatures below ~ 270 °C, or have vapour pressure greater than about 0.1 mmHg, tend to rapidly evaporate from the surface of spilled crude oil (Stiver and Mackay, 1984; Fingas, 1995). Alkanes from methane to *n*-C₁₅ and one-and-two ring aromatics ranging from benzene through alkynaphthalenes are included in this category (Wolfe, 1994). The chromatograms illustrate the loss of the *n*-alkanes over time. Pristane and Phytane are examples of isoprenoids present in alkane fraction of crude oil. The concentrations of these compounds are generally large. The ratios *n*-C₁₇/pristane and *n*-C₁₈/phytane peaks are normally unaltered during the initial stages of weathering and therefore serve as internal standard compounds when investigating oil weathering. This enables the identification of other *n*-alkanes appearing at regular intervals in the chromatograms. In general, at all temperatures of weathering the low carbon number *n*-alkanes are removed first, indicated by a progressive mass loss or removal of peaks along the first part of the chromatogram.

After 1 hour at the lower temperature of evaporation (12 °C Fig. 8a), the chromatogram revealed distribution of *n*-alkanes within the *n*-C₁₀ (*n*-decane) to *n*-C₃₀ (*n*-triacontane) region in the Forties crude oil. However, 24 h of weathering of the Forties crude at the same temperature of 12 °C (Fig.8b) indicated significant weathering as shown by removal

of compounds along the first part of the chromatogram. The results in these experiments are consistent with studies by Reddy *et al.*, (2002); Arey *et al.*, (2005) which also showed that evaporation systematically removes oil components along first part of a gas chromatogram. The part of the chromatogram indicating evaporative weathering showed progressive loss of *n*-alkanes with time and after 110 h of weathering, the *n*-alkane profile (Fig.8c) showed a rapid advance of the evaporation front evident in the weathering and mass loss of volatile compounds up to *n*-C₁₃ (*n*- tridecane) indicating significant weathering of the Forties crude.

Experiments conducted at higher weathering temperatures of 20-50 °C indicated a clear and significant increase in loss of compounds with increasing hydrocarbon volatility. It is evident that the evaporation process is accelerated with increased temperature throughout the course of the sampling period. The mass loss trend also showed an increase loss of volatile component with time. Fig 9a - 10c shows the compositional changes for the samples at evaporative temperatures of 30 and 40°C respectively and the chromatograms revealed a higher magnitude of weathering and hydrocarbon volatility with time. Similar sampling time was maintained for the experiments at all temperatures. The part showing evaporation in the chromatogram indicated a more pronounced loss of *n*-alkanes up to *n*-C₁₅ (*n*-pentadecane) with increased weathering time. The hydrocarbon removal pattern reflects that evaporation dominated mass loss during the first few hours and this effect was more at higher evaporative temperatures (25-50 °C) than those experiments conducted at lower temperatures (12-20 °C).

The GC chromatograms indicated that analyses of the weathered Forties and Brent crudes exhibited variability in the evaporation of volatile components. The volatile components in Forties and Brent crude evaporated at different boiling ranges. This difference reflects that Forties and Brent crude samples showed unique physical weathering as shown in the profiles. The variability was also highlighted in the fresh samples of the oil (Fig. 7a and 7b). Fig.7a – 10c and 11a – 13b shows the GC-FID chromatograms of the distribution of hydrocarbons in samples analysed from fresh and weathered Forties and Brent crude oils on respectively.

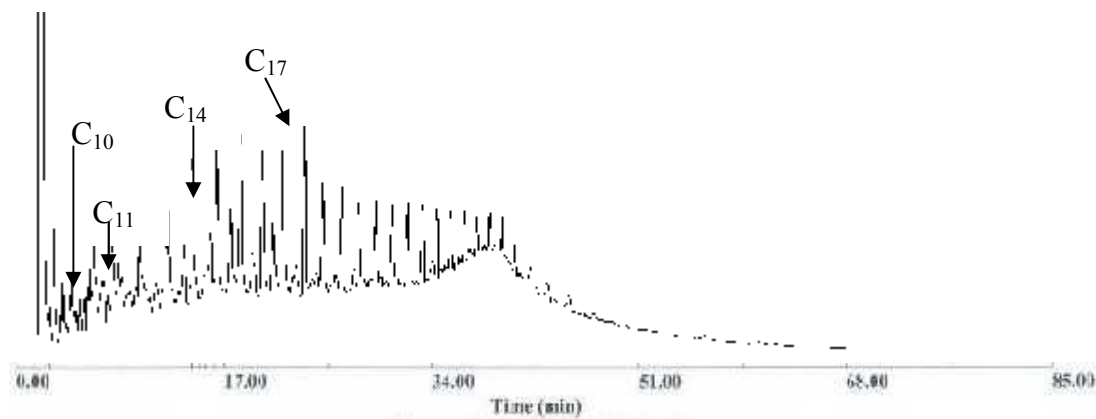


Fig. 8a Forties evaporation on SW at 12 °C (1 h)

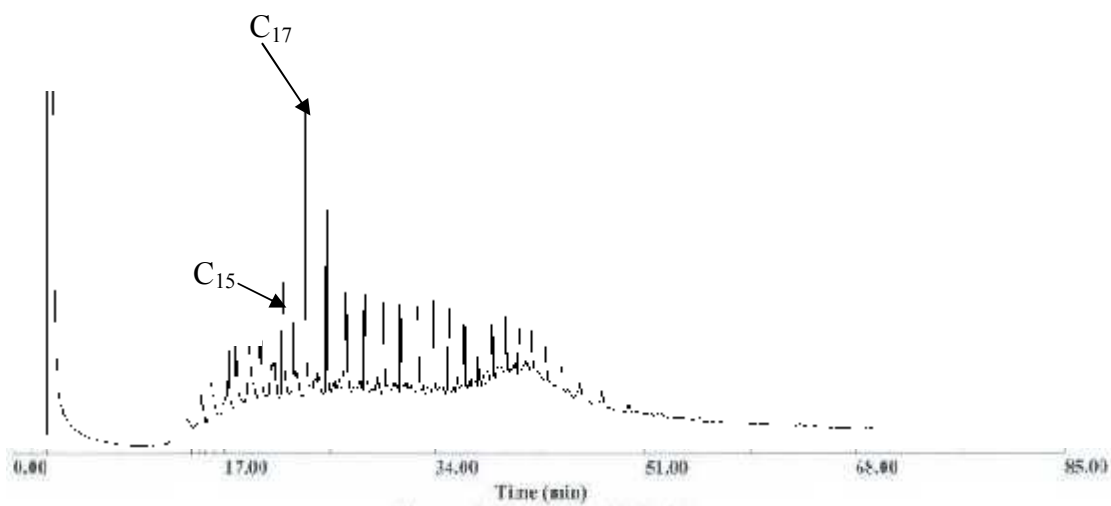


Fig. 8b Forties evaporation on SW at 12 °C (24 h)

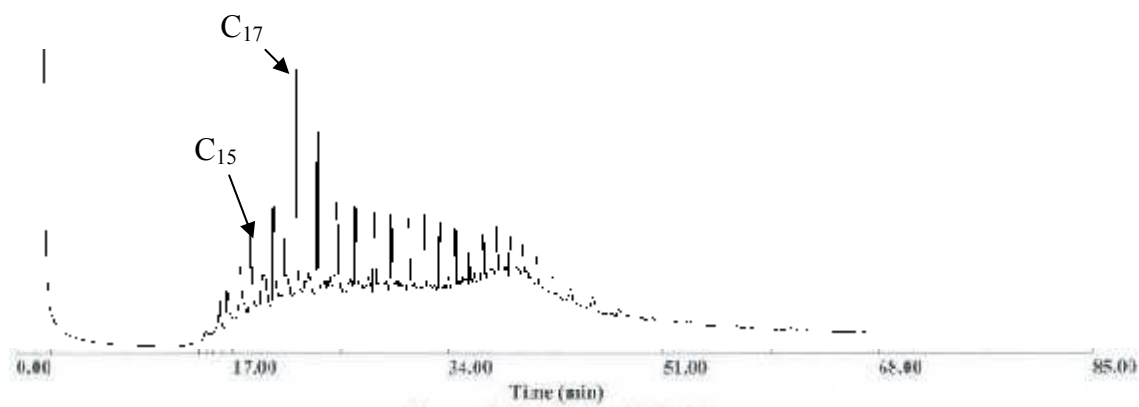


Fig. 8c Forties evaporation on SW at 12 °C (110 h)

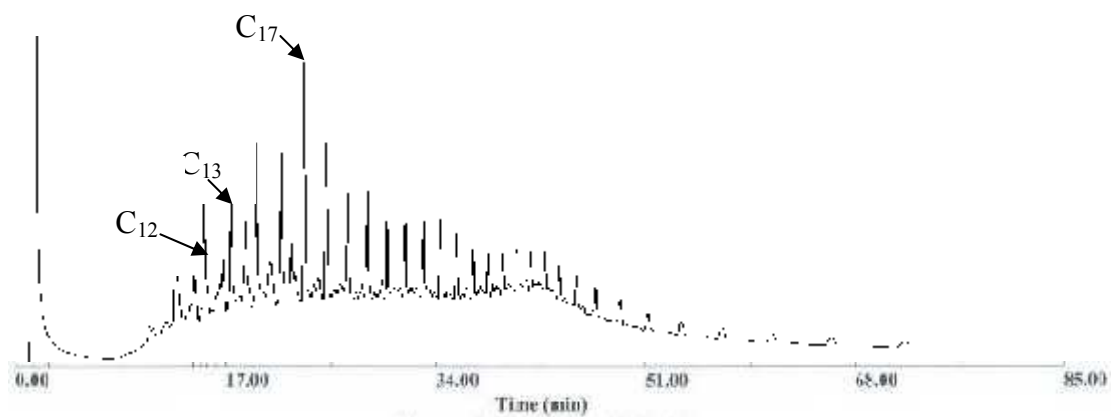


Fig. 9a Forties evaporation on SW at 30 °C (1 h)

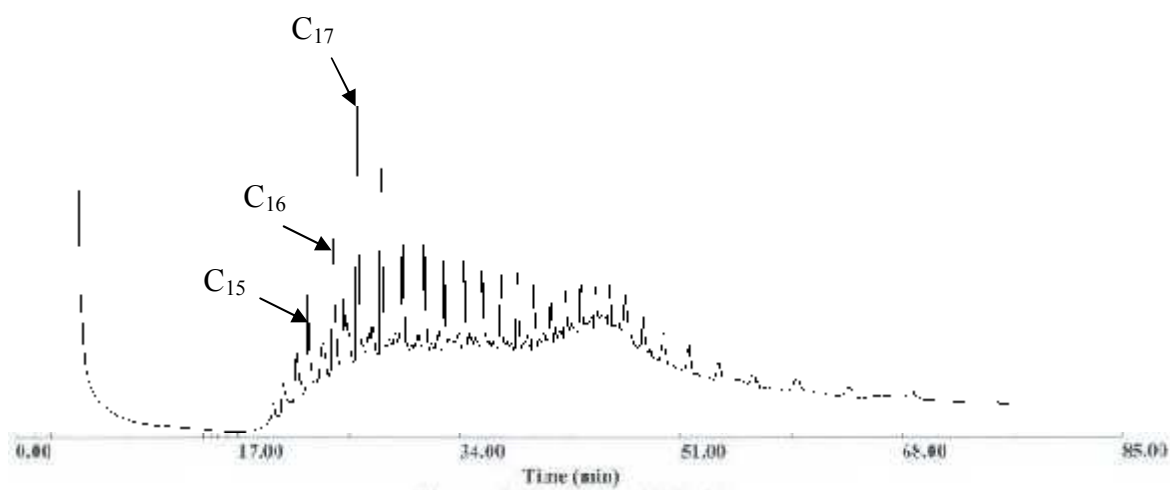


Fig. 9b Forties evaporation on SW at 30 °C (24 h)

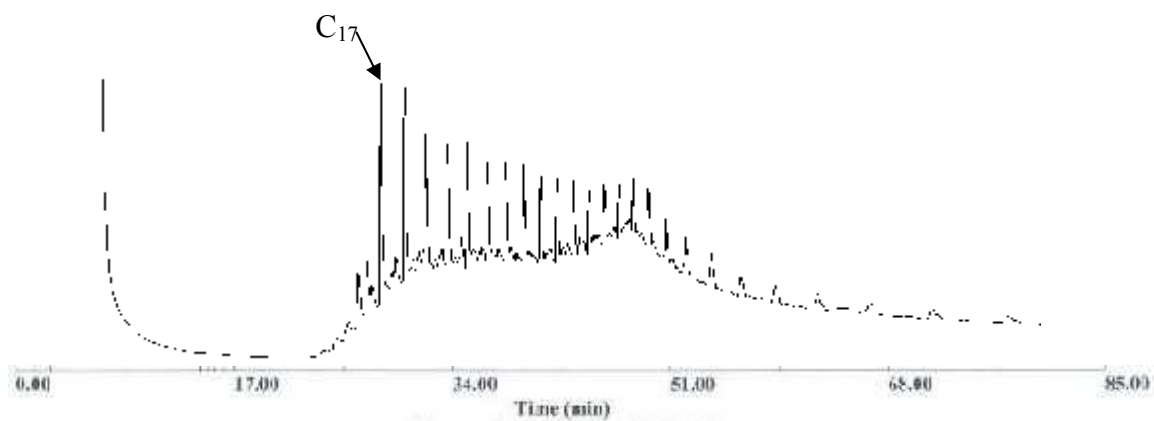


Fig. 9c Forties evaporation on SW at 30 °C (110 h)

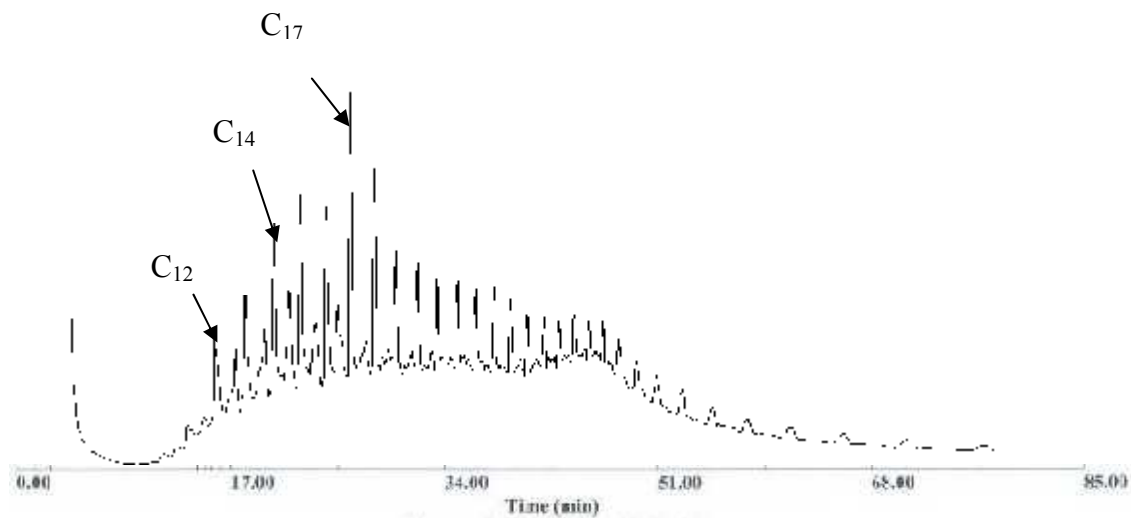


Fig. 10a Forties evaporation on SW at 40 °C (1 h)

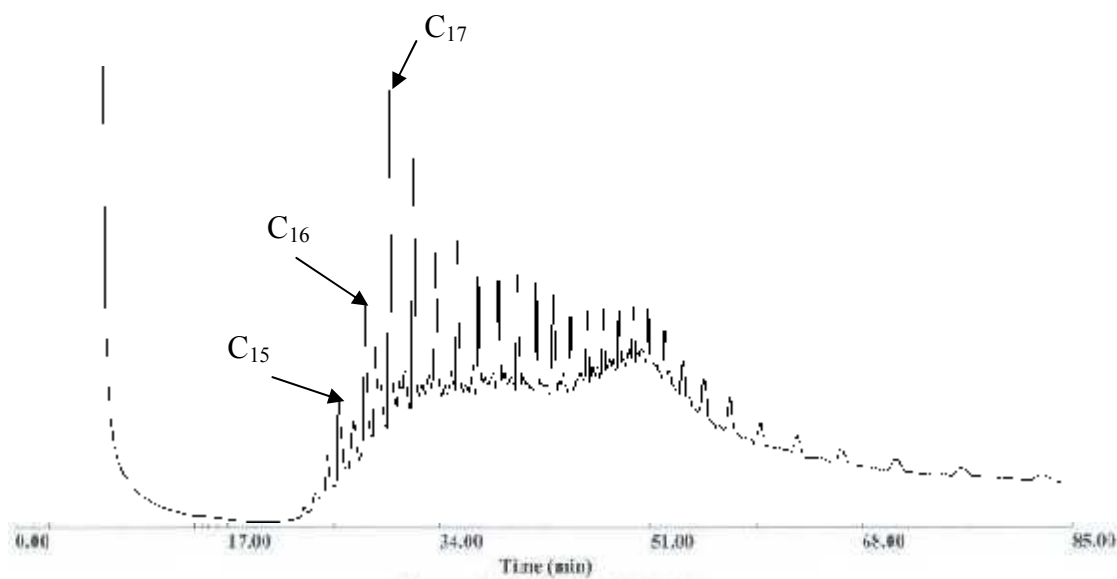


Fig. 10b Forties evaporation on SW at 40 °C (24 h)

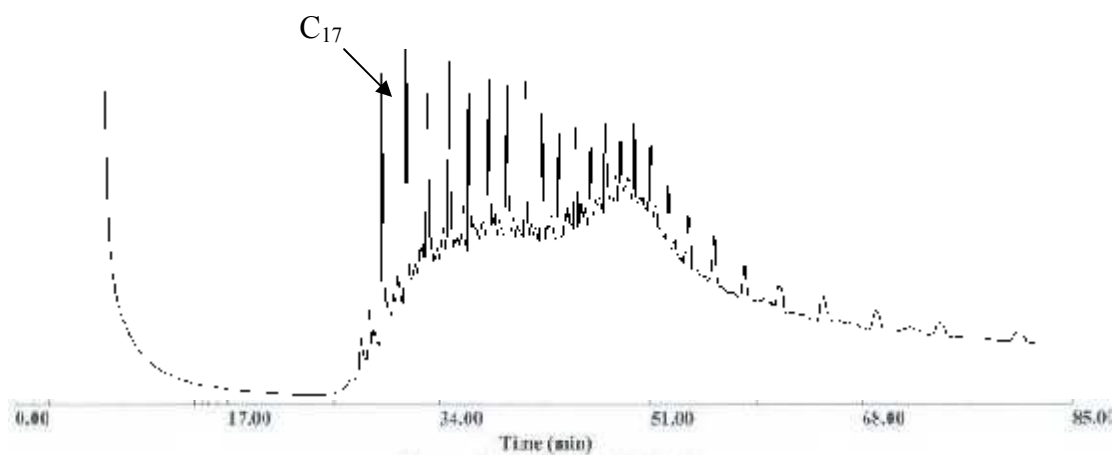


Fig. 10c Forties evaporation on SW at 40 °C (110 h)

2.4.6 Evaporative weathering of Brent crude and Brent crude emulsion on Seawater.

The experiments described in Section 2.4.2 investigated the evaporation of Brent crude in the absence of seawater compared to its evaporation on seawater at the temperature of 30°C. The mass loss of seawater used in the evaporative weathering was evaluated to compare the evaporation of crude oil on its own in the absence of seawater to the rate of weight loss of volatile components when crude oil is evaporated on seawater. A unique and convenient laboratory approach developed in this research was the evaporation of crude oil on seawater in Petri dishes placed in thermostated water bath. A review of several weathering methods, including small-scale laboratory and industrial-scale procedures have been given in Chapter 1, Section 1.8. As reported by other researchers, the results from experimentally produced weathered hydrocarbon mixtures accurately reflect those found in the field after an oil spill. This experimental approach was aimed at determining the effects that these parameters may have on the evaporative mass losses of components independently of each other i.e. (crude oil, crude oil + water, and water-in-oil emulsions respectively), and the rate at which each of these three separate components evaporate and most importantly how mass loss from crude oil (hydrocarbon evaporation) compares to crude oil on seawater in the weathering process.

The results of these experiments are given in Table 2.14- 2.16, shown in Appendix 1. The differences in the rates of evaporation in the experiments are also shown in Fig 5. The comparison is further enhanced by the quantitative assessment of the GC-FID chromatograms analyses of the samples (Fig.15a – 15c).

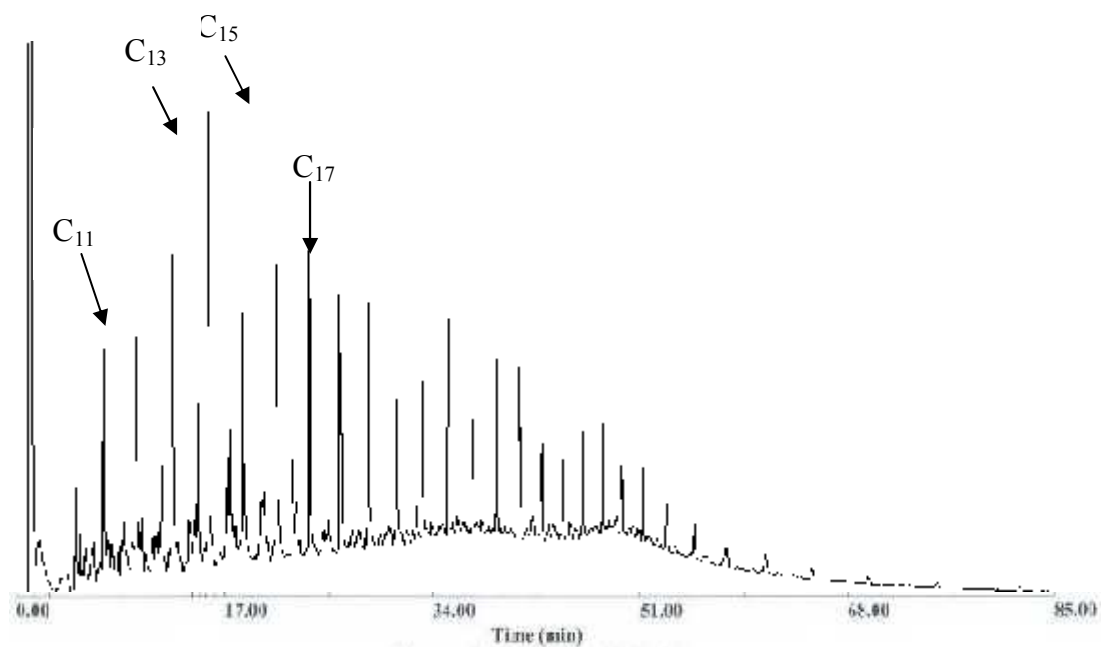


Fig. 11a 1 h weathering of Brent crude (without SW) at 30 °C

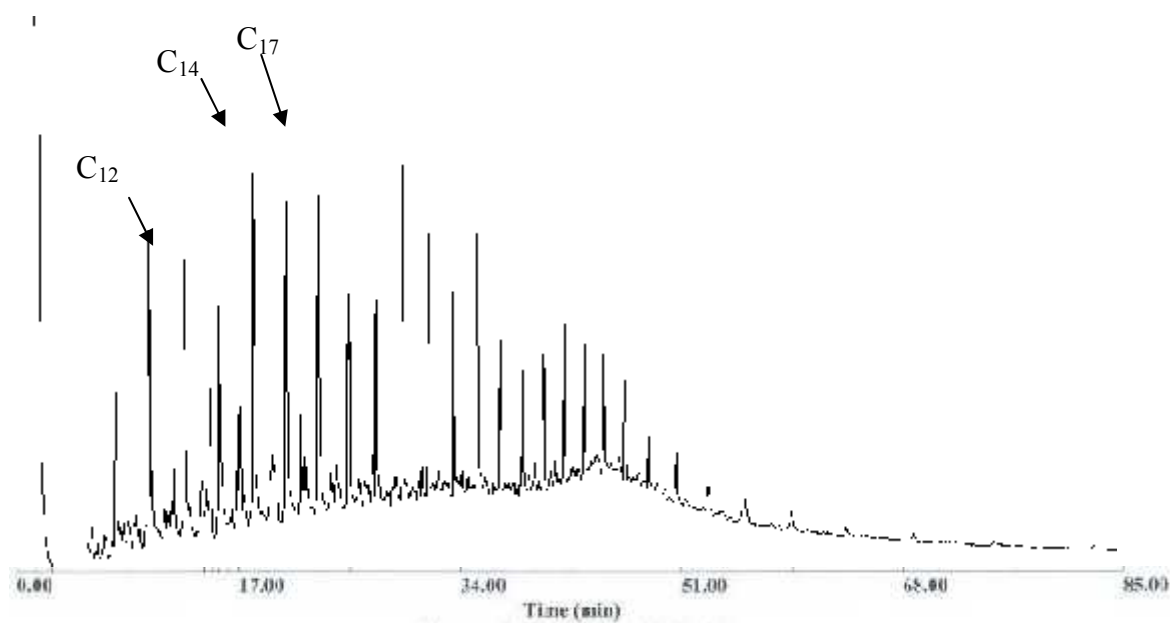


Fig. 11b 1 h weathering of Brent crude on SW at 30 °C

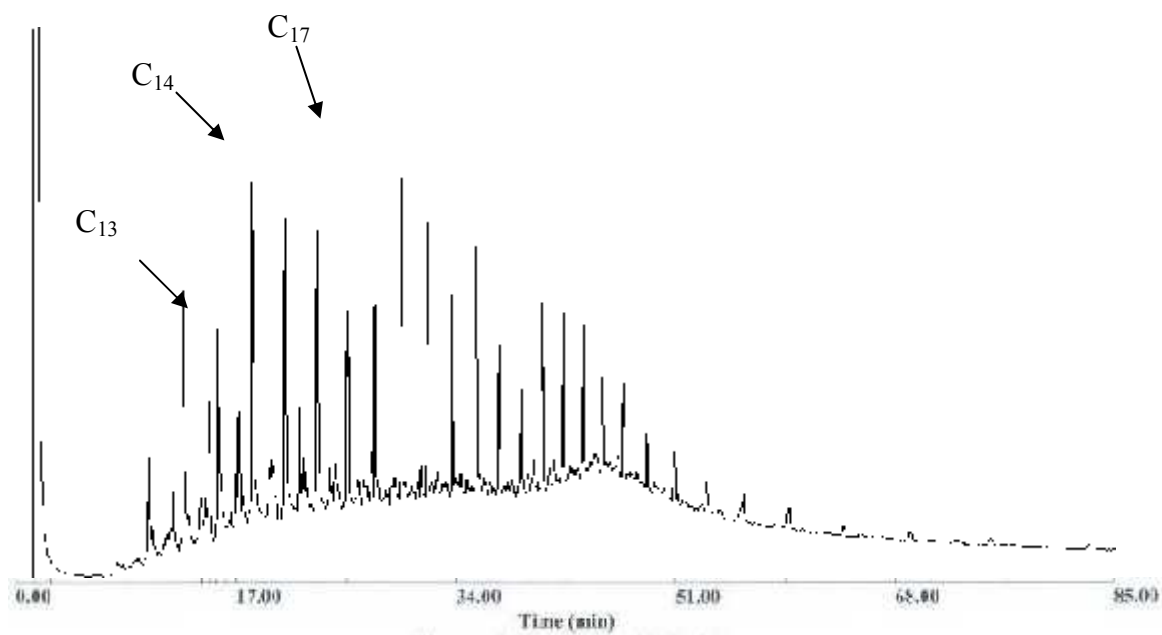


Fig. 12a 6 h weathering of Brent crude (without SW) at 30 °C

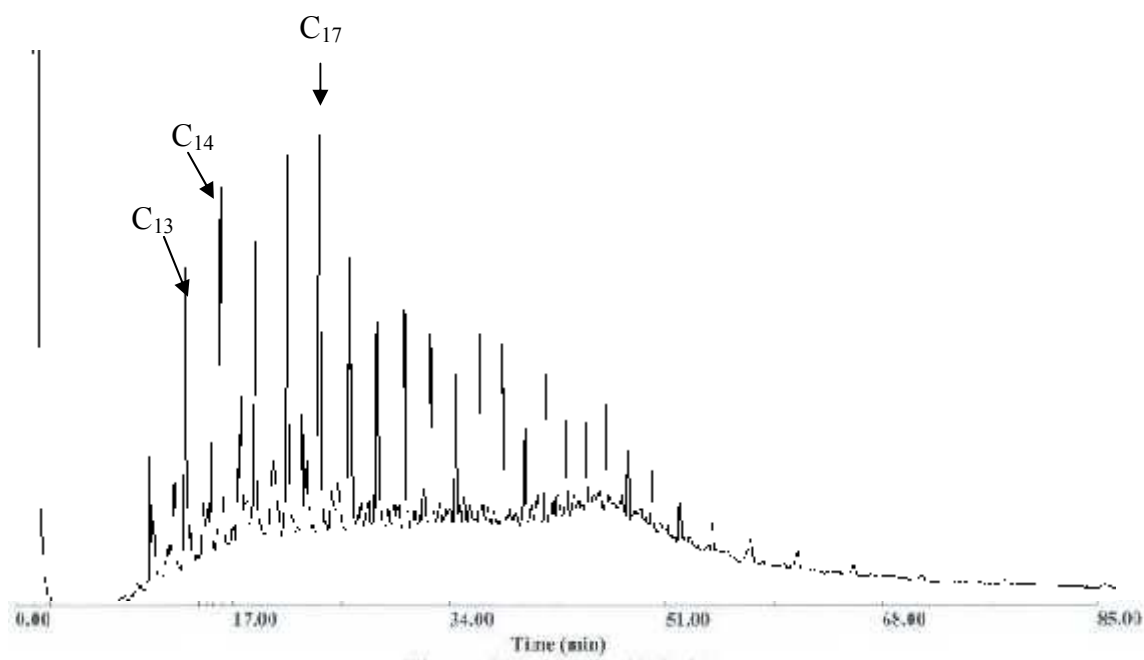


Fig. 12b 6 h weathering of Brent crude on SW at 30 °C

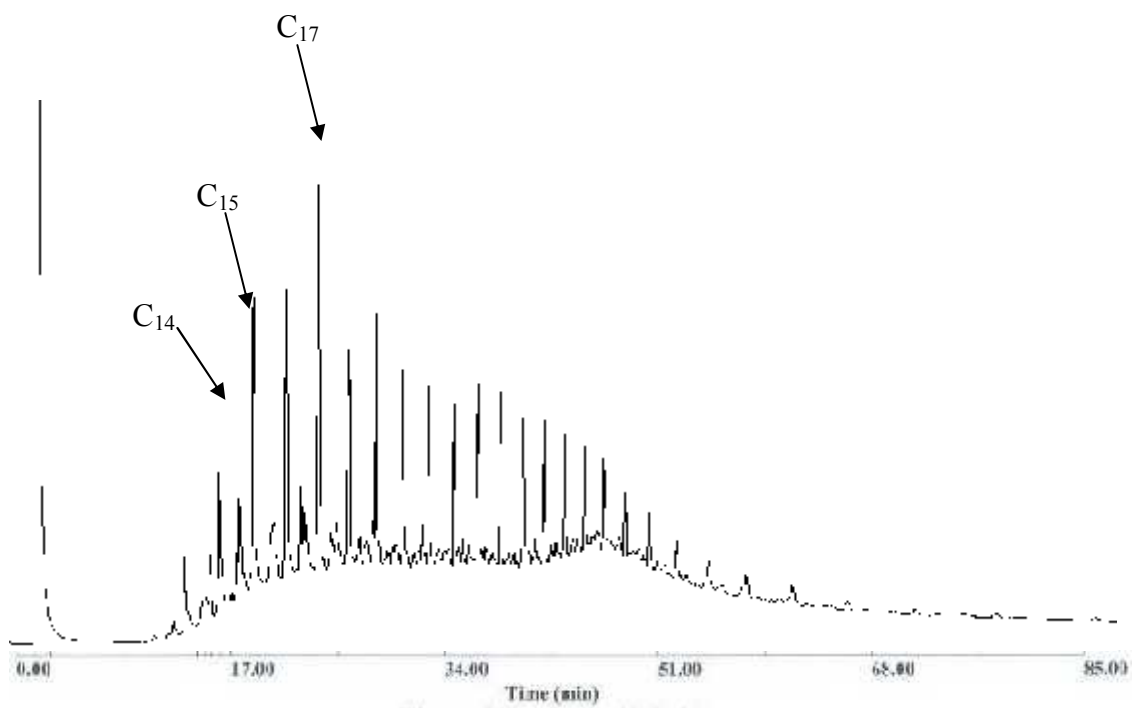


Fig. 13a 48 h weathering of Brent crude (without SW) at 30 °C

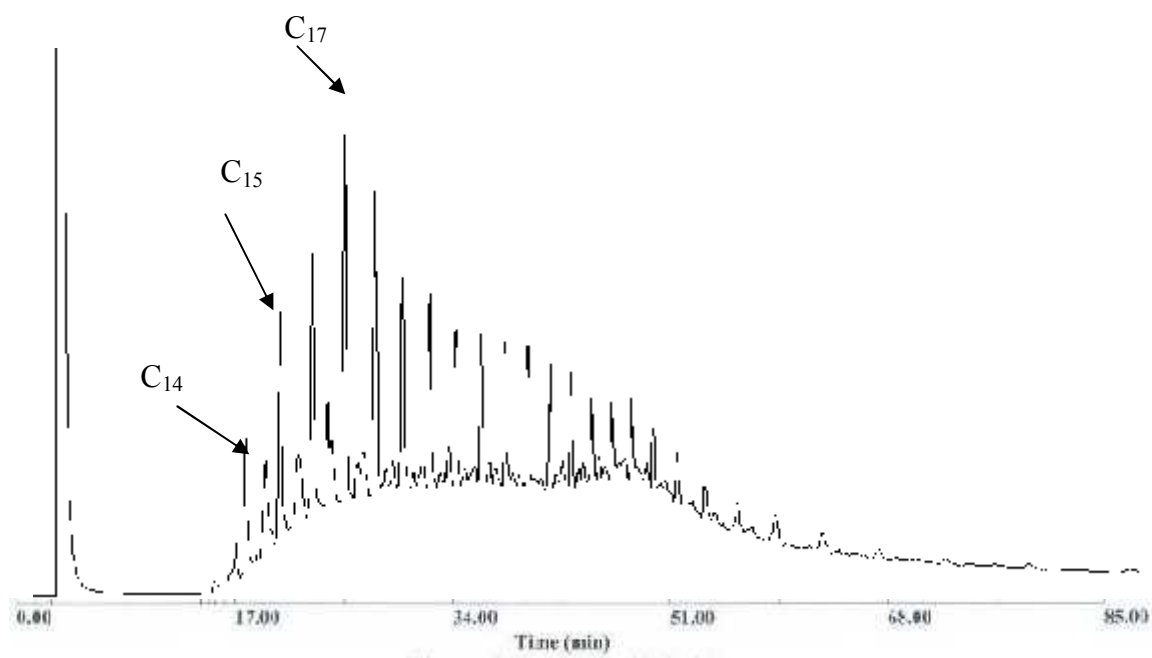


Fig. 13b 48 h weathering of Brent crude on SW at 30 °C

Experiments by Ross and Buist (1995) had found out that oil evaporation is reduced when oil is mixed with water to form stable water-in-oil emulsion. Emulsification increases the overall volume and slick thickness and the increasing water content contributes in the inhibition of evaporation. For a given thickness, evaporation decreases as the water content increases because the liquid phase resists mass transfer in emulsified oil (Xie *et al.*, 2007). In order to investigate the rate of evaporation of volatile components from the Brent crude emulsion formed as stated in Section 2.3.3, in relation to the unemulsified sample of weathered oil, 3.5 g of the emulsion formed was put on seawater in petridishes placed in a water bath at 30 °C and evaporated using the same experimental conditions for the evaporation of in the case of the unemulsified sample. Weighing was carried out to determine the evaporative weight loss at specific times, and sub-samples were taken and placed into 3ml vials for GC-FID analyses.

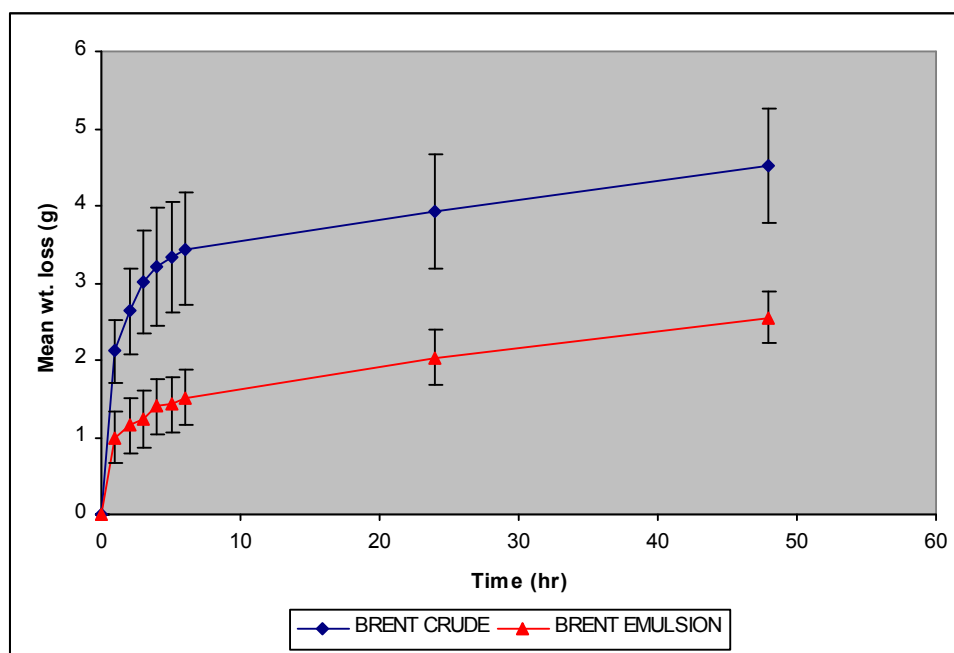


Fig. 14 Comparison of evaporation between Brent crude oil and Brent crude emulsion showing the variation in rate of evaporation of oil fractions.

Fig. 14 shows the difference in the evaporative weight loss of Brent crude and water-in-oil emulsion derived from the same crude. (i.e. Brent crude emulsion). Both samples were weathered at the same experimental conditions to enable a direct comparison of loss of volatile compounds from each sample.

At the selected temperature of 30 °C, the weight loss of 2.12 g recorded for Brent crude was twice as much as the low weight loss of 1.0g measured for the Brent emulsion. The difference in evaporation between the Brent crude and the emulsion showed steady progression with increasing weathering time. After 48 h, a weight loss of 4.53 g was recorded for Brent crude compared to a lower 2.55 g weight loss for its emulsion. It can be seen from this trend that there was considerable differences in volatility for the Brent crude and its water-in-oil emulsion even at the same experimental temperature (30 °C). The explanation here is that increased oil thickness or volume due to emulsification will reduce the evaporative loss from the emulsified oil (Brandvik and Faksness, 2009). The experimental data agree with oil evaporation simulations studies by Xie *et al.*, (2007) which showed similar effect on loss of lighter fractions. This is considered significant when assessing the removal by weight from the water surface with time from both samples and the evaluation of the residual volume (oil not evaporated). Gas chromatographic (GC) analyses of the Brent (Fig.11a - 13b) and Brent emulsion (Fig15a-c) samples also elucidated the chemical compositional changes resulting from evaporative weathering. A comparison of the chromatogram at 1hr evaporation showed a distinct weathering of *n*-alkanes in the emulsion (Fig15a) ranging up to *n*-dodecane (*n*-C₁₂). At 1 h, Brent crude emulsion (Fig15a) was more weathered than Brent crude on seawater (Fig 11b). After 48hrs sampling, analysis again indicated a higher loss of volatile components in the Brent emulsion (Fig15c) where there was an effective weathering, removing the volatile *n*-alkanes up to *n*-C₁₄ compared to the Brent crude on seawater, which did not reveal as much weathering of the compounds (Fig13b). The GC chromatograms showed that emulsified crude evaporated more quickly than crude on seawater at both 1hr and 48 h of weathering.

Nazir *et al.* (2008) had also found in a weathering simulation of Statfjord crude oil that evaporation considerably depletes the fractions of volatile compounds in crude oil. Although findings by other researchers (Brandvik and Faksness, 2009) suggest that emulsified oil should weather more slowly due to increased oil thickness, the results from the experiments in this work appear to contradict this opinion. However, these results are consistent with the findings of Arey *et al.*, 2007; National Research Council, 2003) which suggested that different weathering processes such as evaporation, emulsification,

biodegradation, etc. affects and have independent effects on the removal of volatile compounds. It can be theorised therefore, that in a water-in-oil emulsion, the concentration of the lighter hydrocarbon in the oil phase tends to be increased, the heavier molecules with surfactant properties concentrating at the oil-water interface. This hypothesis may explain the higher rate of evaporation in the emulsified oil.

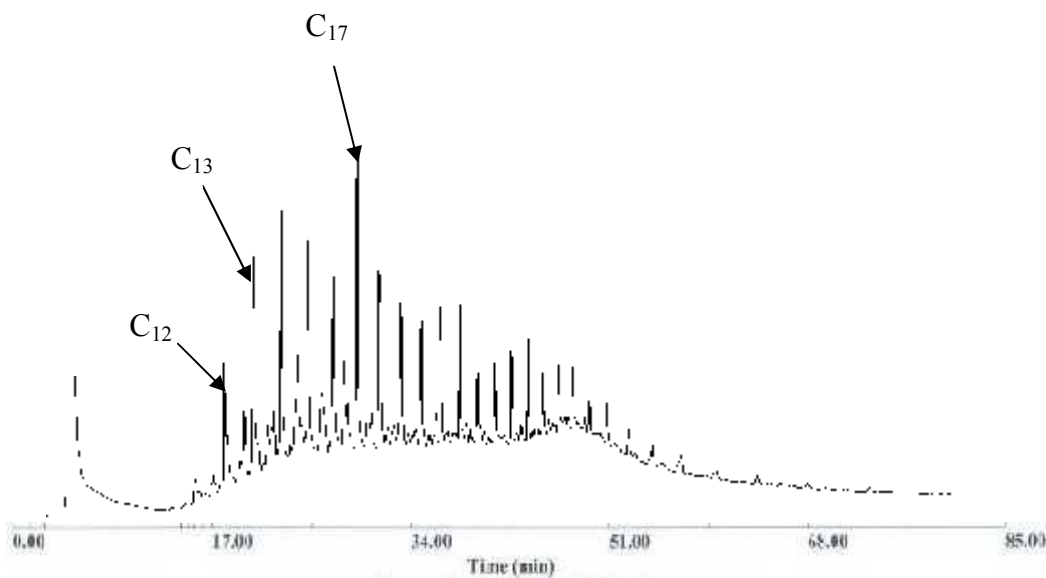


Fig 15a 1 h weathering of Brent crude emulsion on seawater at 30 °C

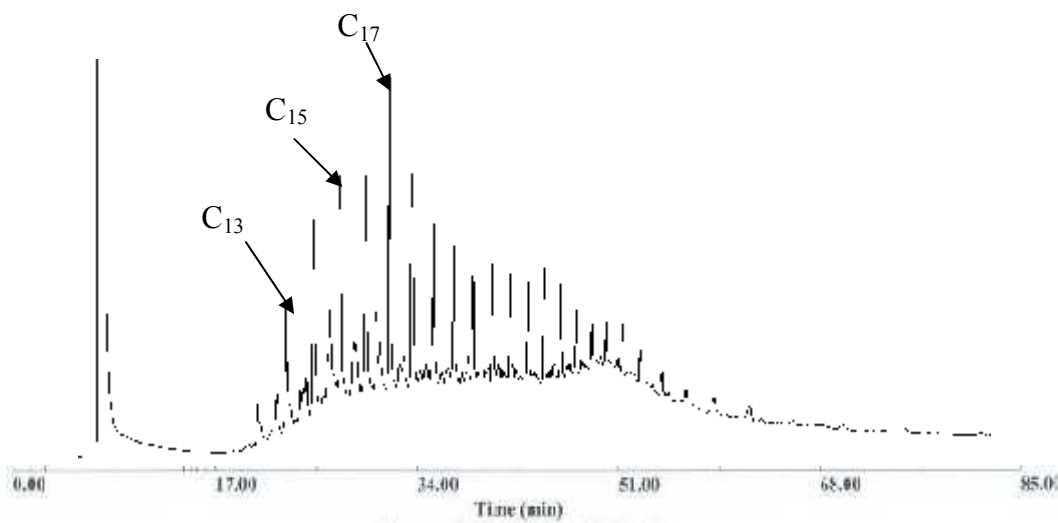


Fig 15b 24 h weathering of Brent crude emulsion on seawater at 30 °C

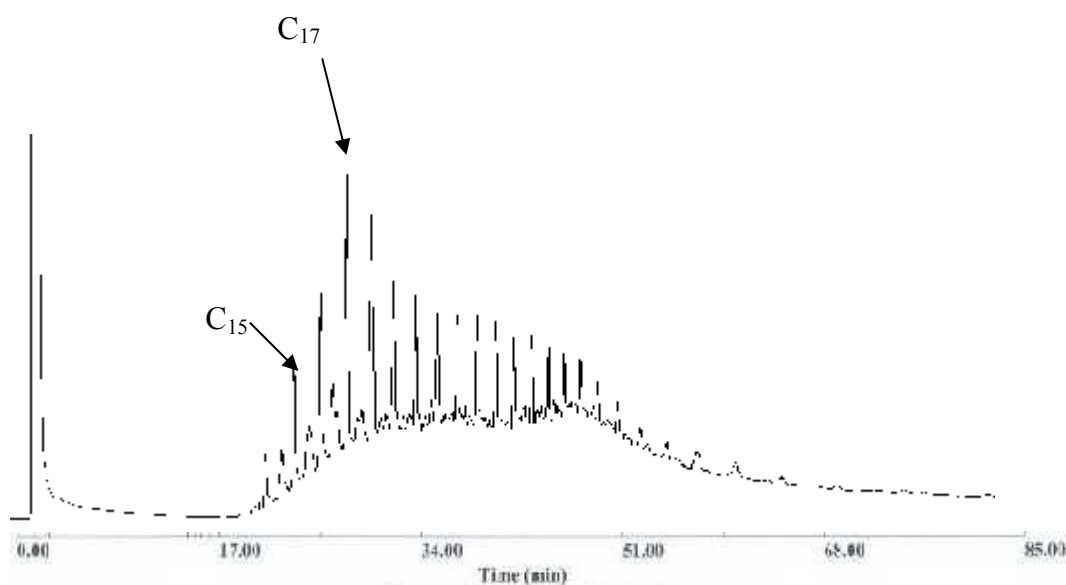


Fig. 15c 48 h weathering of Brent crude emulsion on seawater at 30 °C

2.4.7 Modeling the effect of temperature on the rate of evaporation of Forties crude oil

Good reliable true boiling point curves are fundamental for reliable predictions of evaporation but also for other weathering properties. API (1999) lists 10 weathering processes for fate and transport of a surface slick situation and among these processes, assuming the slick has been at sea for only a few days and under calm sea conditions, evaporation is considered among the four of particular importance in the overall oil budget (Sebastiao and Soares, 1995; Evers *et al.*, 2004). Other key factors that affect the weathering process of an oil slick include spreading, natural dispersion and emulsification. These processes including others, such as dissolution, photo-oxidation and biodegradation have been extensively discussed in Chapter 1, Section 1.5. An extensive use of these parameters is built into oil spill simulation models to enhance the capability of forecasting the short-term and long term behaviour of spilled oil, in order to provide responders the information for contingency plans to be adapted to the type of crude oil in a possible spill scenario (Merlin and Poutchkovsky, 2004; Wang and Stout, 2007; Nazir *et al.*, 2008). The efficacy and application of these oil spill models by oil spill responders in prevention and clean-up is contingent on the availability of the necessary basic data representing

parameters such as the oil's distillation characteristics (oil type, oil properties, volume and rate of spillage), and environmental parameters (wind speed, temperature etc.), corresponding to a volume or weight fraction which can be removed by distillation at various temperatures. Oil and petroleum products evaporate in a slightly different manner than water and the process is much less dependent on wind speed and surface area (Fingas, 2010). As stated previously in Section 2.4.1, the rate of evaporation can be very rapid (about 60 %) after a spill and then slows considerably.

The modeling approach used in this study draws upon the works of other researchers (Sebastiao and Soares, 1995; Nazir *et al.*, 2008) in modelling oil slick physico-chemical weathering process such as evaporation using simple algorithm and the required parameters that are readily available from distillation data. SigmaPlot, a scientific graphing and data analysis software package that allows the creation of graphs was used in integrating the data, enabling the modelling of the evaporative weathering process.

The dependence of temperature and time for evaporative weight loss for Forties crude oil was investigated. The experiments consisted of measurements of the oil weight loss at various temperatures of evaporation. The results of the experimental simulation aimed at investigating the rate of evaporative weight loss of Forties crude oil and modeling of the parameters studied: time and temperature (wind speed was constant) is presented here. The data, previously presented in Section 2.4.1, and a numerical modeling scheme is proposed here to evaluate the effect of temperature and time on the rate of evaporation of crude oil, a multi-component mixture. The primary aim is to use the modeling scheme to predict the rate of evaporative weight loss of Forties crude at any particular temperature as a function of time.

Data for the percentage weight loss from a sample of Forties crude evaporated (weathered) at various temperatures are shown in Fig 4 **a** and **b** (Section 2.4.1).

In Figure 4a, the data for 12, 20, 25 30, 40 and 50 °C are presented, whilst in 4b the data for 40 and 50 °C are omitted.

The data in figure 4a and 4b were fitted to a two parameter power law of the form,

$$\% \text{ mass loss} = a \times \text{time}^b \quad (1)$$

Where a = the slope to the x and y line fit to the log plot; b = power law coefficient for each of the six temperatures using the curve fitting function in SigmaPlot. The coefficients a and b calculated for each temperature are shown in Table 2. A comparison between actual and predicted data (predicted data are generated using equation (1) with the fitted coefficients a and b from Table 2, and are shown as a regression curves in Figs 16-21.

Table 2. Parameters from the non-linear regression fit for the data in Fig. 4a

Temperature (°C)	a	b
12	0.9418 ± 0.0477	0.2281 ± 0.0136
20	1.1891 ± 0.0298	0.1831 ± 0.0070
25	1.6909 ± 0.0421	0.1762 ± 0.0070
30	1.9220 ± 0.0445	0.1687 ± 0.0065
40	0.9937 ± 0.0636	0.5724 ± 0.0149
50	2.6399 ± 0.1906	0.5386 ± 0.0221

Equation (1) is of limited use as a predictive model for mass loss from Forties crude samples since it does not include the effect of temperature. To introduce temperature as well as time as a variable in equation (1) we require some way of relating temperature to the coefficients a and b in equation (1) and Table 2. Figures 22 and 23 are plots of coefficients a and b as a function of temperature (T). In Figure 22 we can see that a increases as T increases in an approximately linear fashion. The point at 40 °C however does not fit with this trend, and is considerably lower than the value at 20, 25 30 and 50°C. Coefficient b , Figure 23, does not show any obvious relationship with T . It decreases slowly as T is increased from 12 to 30 °C and then jumps abruptly at 40 and 50 °C. A possible explanation for the abrupt jump in coefficient b , is probably due to certain highly volatile components in the crude that may have rapidly evaporated at 40 and 50 °C, resulting in coefficient b not fitting the trend. It would appear that any relationship between a , b and T will only be valid over a limited temperature range. Plotting Figures 22 and 23 again, but only up to 30 °C (Figures 24 and 25) we can see that both a and b can be fitted to

a linear regression curve, and appear to be a linear function of T. The linear equations for these fits are,

$$a = 0.05717T + 0.1944 \quad (2)$$

$$b = -0.0033T + 0.2604 \quad (3)$$

If these are substituted into Equation (1) in place of a and b, we get the following equation that is valid for the temperature range 12-30 °C only.

$$\% \text{ mass loss} = (0.0571T + 0.1944) \times t^{(-0.0033T + 0.2604)} \quad (4)$$

This can be used to predict percentage mass loss at any time and any temperature in the range 12-30°C.

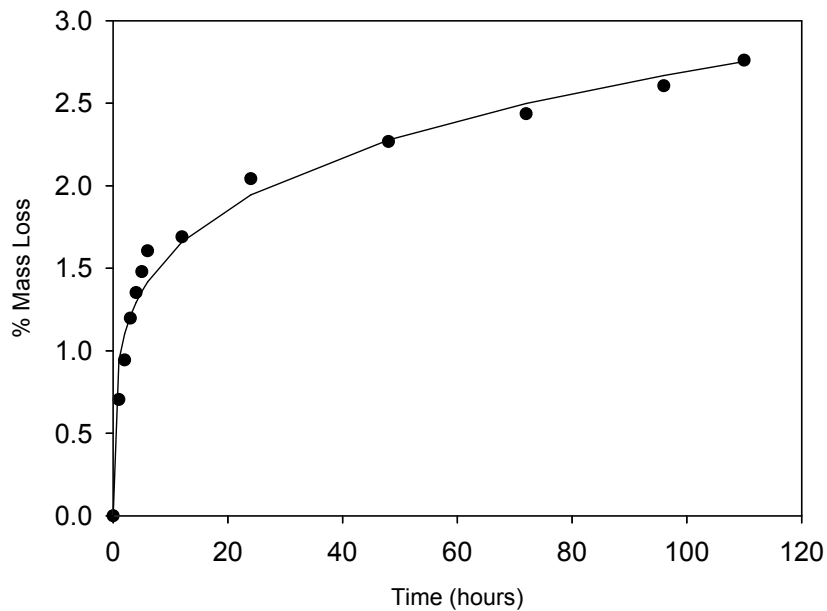


Figure 16 – Data for 12 °C evaporation fitted to a two-parameter power law. Filled circles are the experimental data and the solid line is the regression curve.

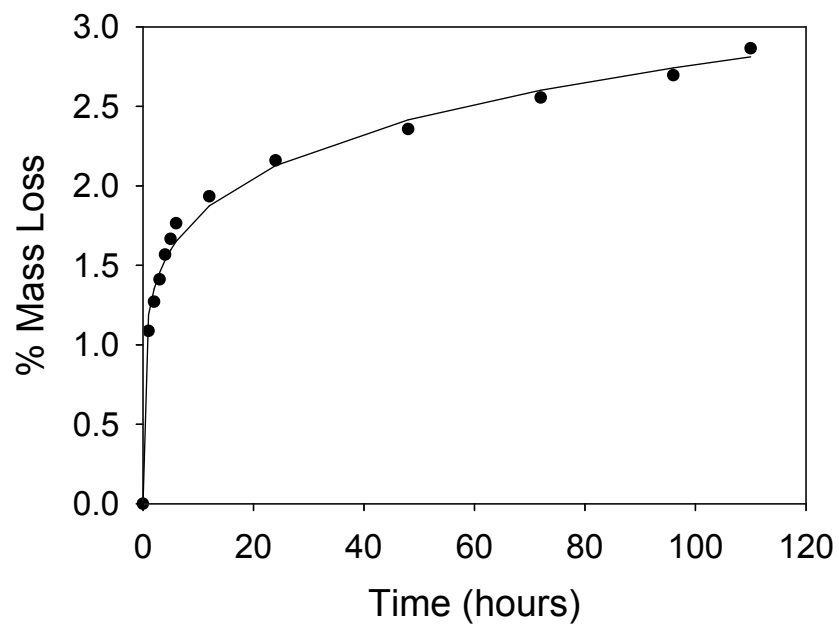


Figure 17 – Data for 20 °C evaporation fitted to a two-parameter power law. Filled circles are the experimental data and the solid line is the regression curve.

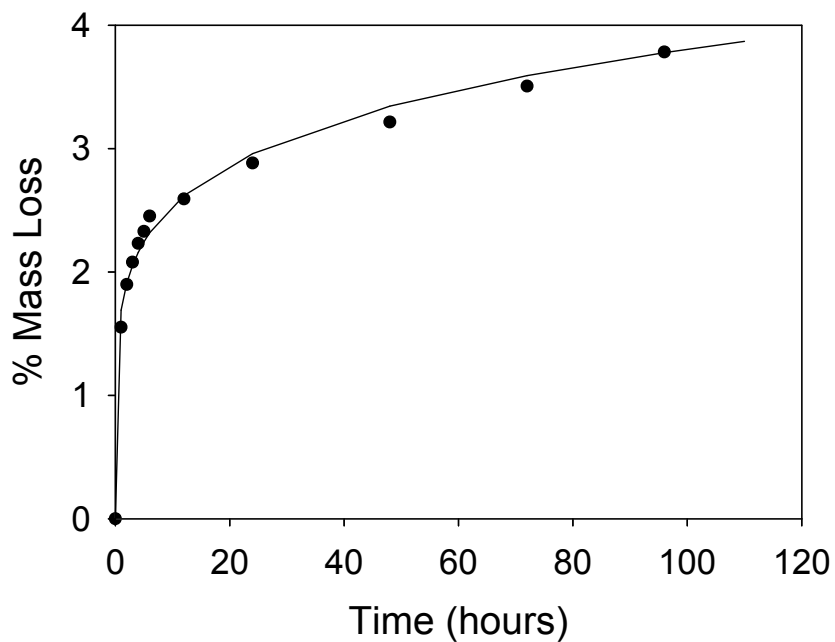


Figure 18 – Data for 25 °C evaporation fitted to a two-parameter power law. Filled circles are the experimental data and the solid line is the regression curve.

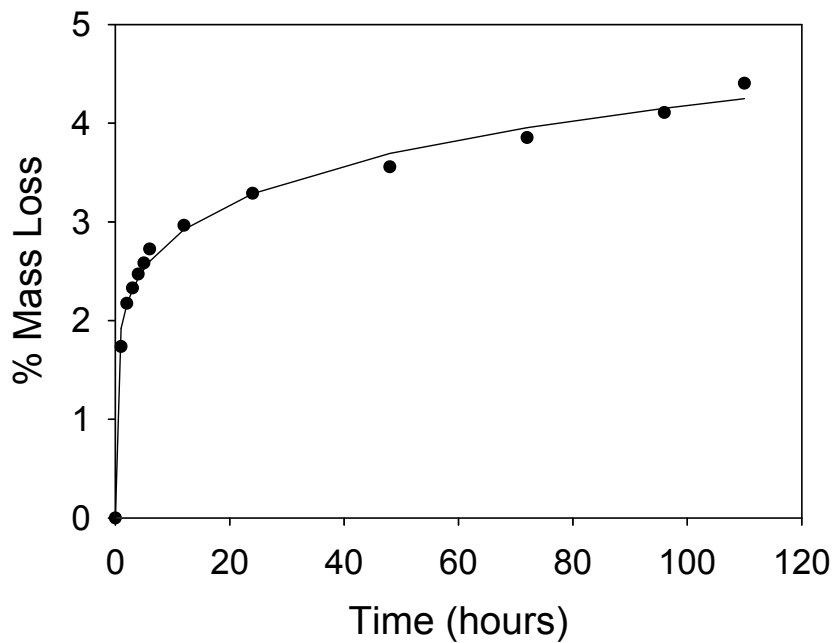


Figure 19 – Data for 30 °C evaporation fitted to a two-parameter power law. Filled circles are the experimental data and the solid line is the regression curve.

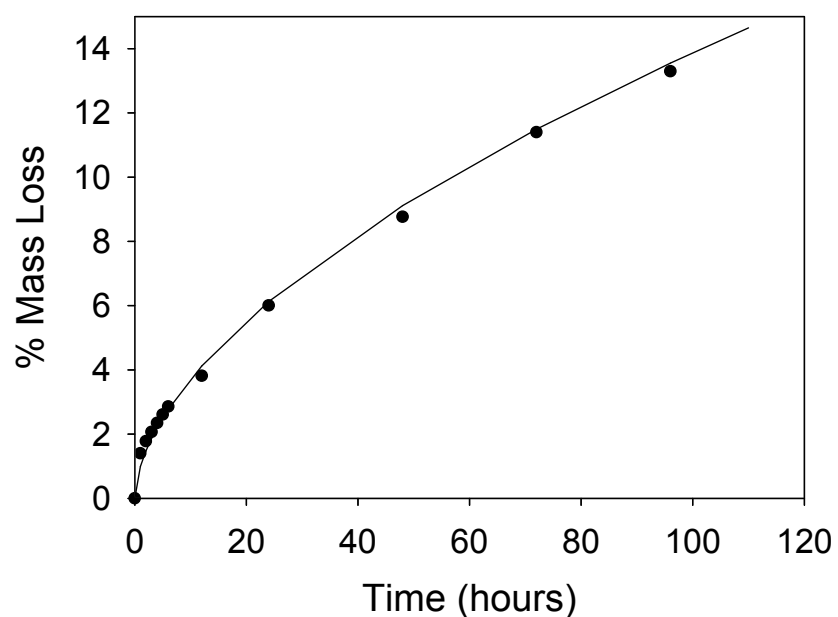


Figure 20 – Data for 40 °C evaporation fitted to a two-parameter power law. Filled circles are the experimental data and the solid line is the regression curve

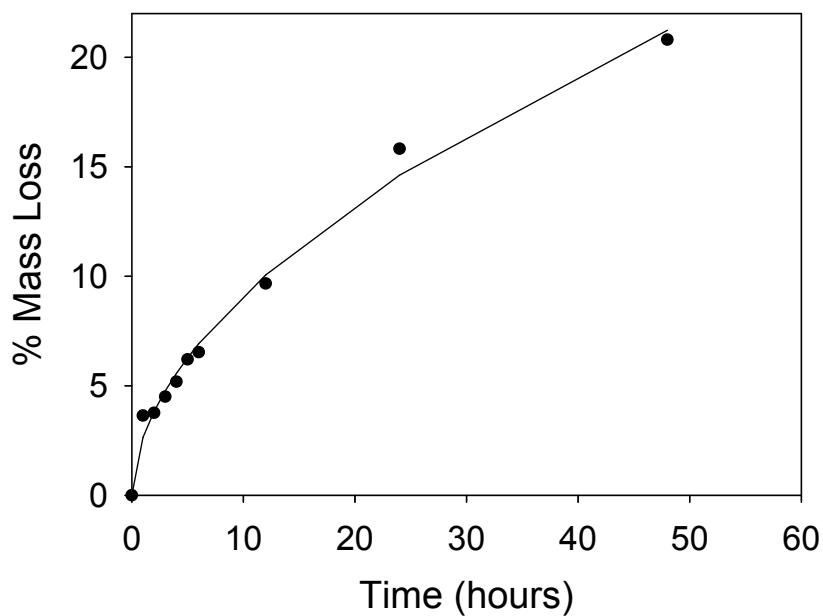


Figure 21 – Data for 50 °C evaporation fitted to a two-parameter power law. Filled circles are the experimental data and the solid line is the regression curve.

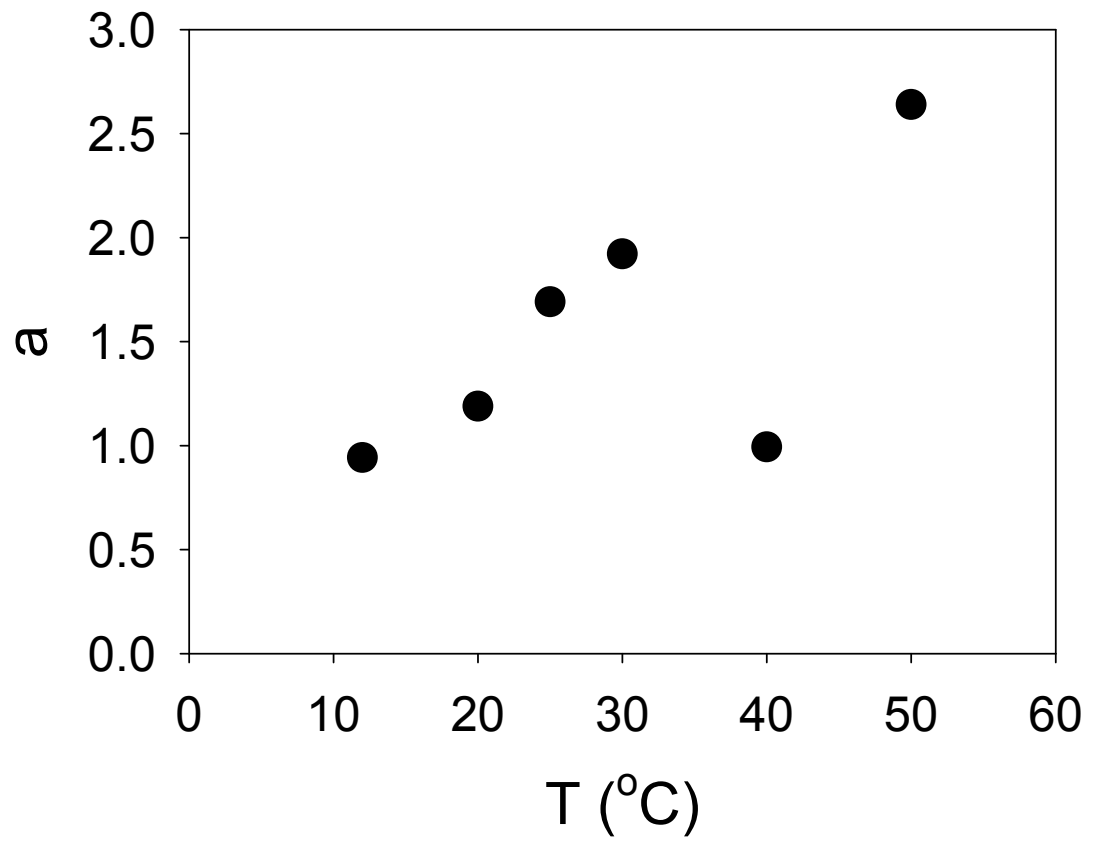


Figure 22 – Temperature dependence of coefficient a from Equation (1) and Table 2.

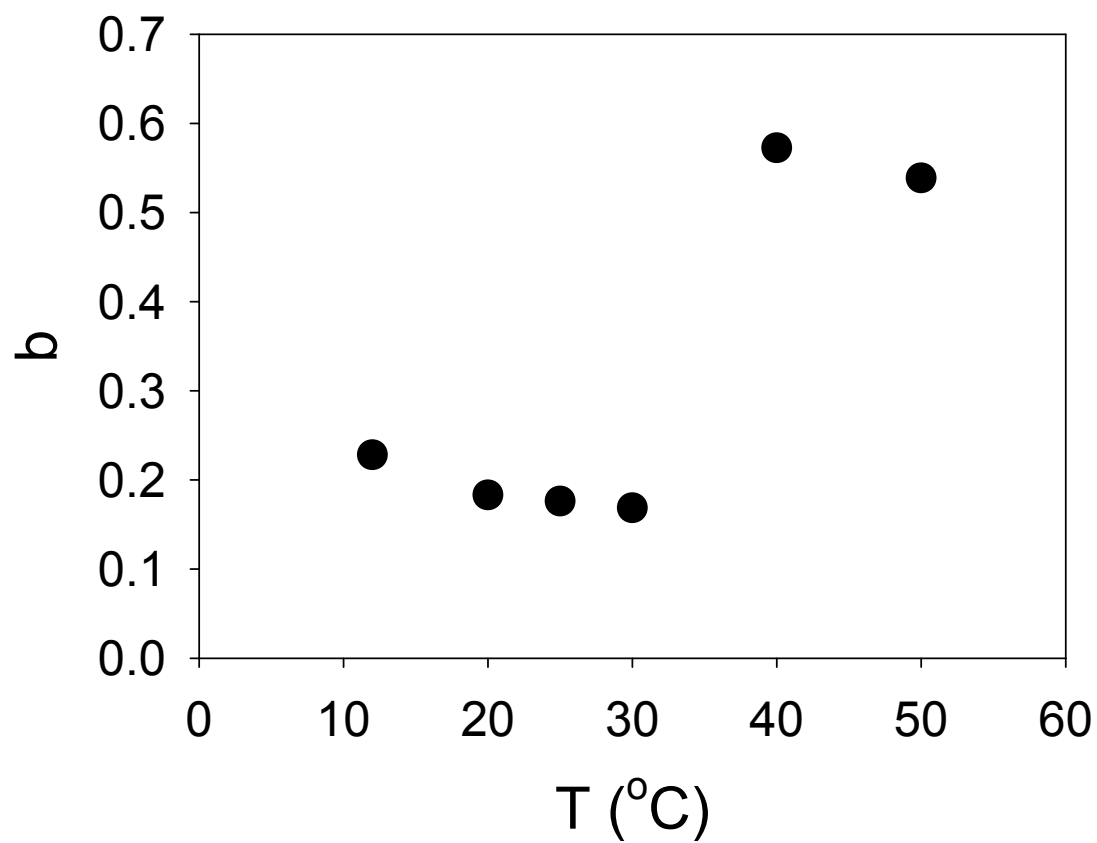


Figure 23 – Temperature dependence of the coefficient b from Equation (1) and Table 2.

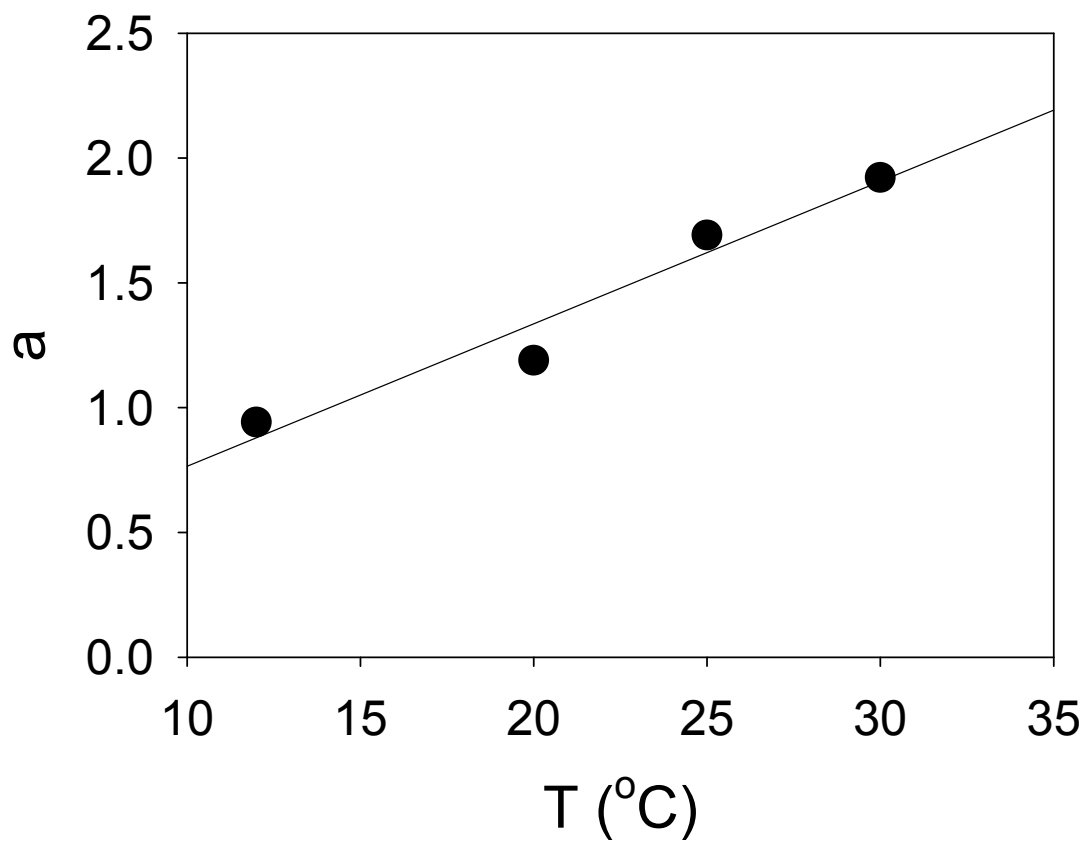


Figure 24 – Linear fit to a vs. T data over the T range 12-30 $^{\circ}\text{C}$.

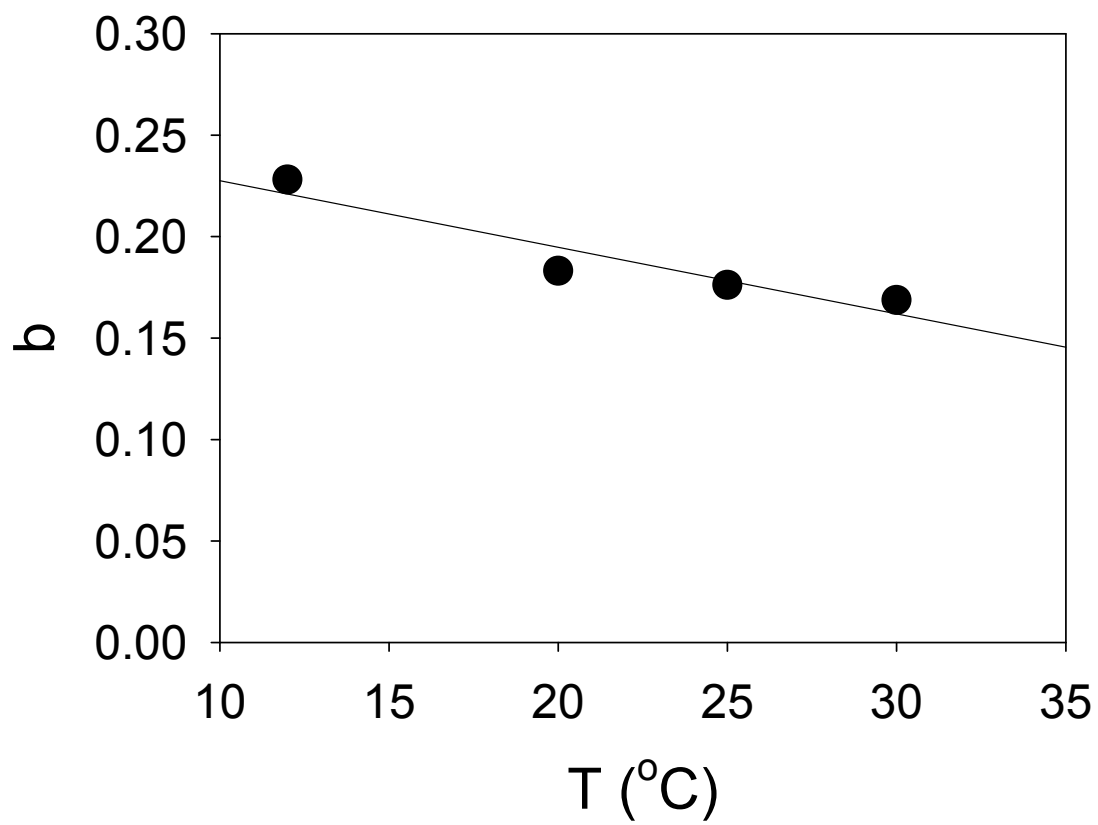


Figure 25 - Linear fit to a vs T data over the T range 12-30 $^{\circ}\text{C}$.

It is reported that the evaporation of most oils follows a logarithmic curve with time, whereas some oils such as diesel fuel, however, evaporate such that it can best be modeled as a square root of time, at least for the first few days (Fingas, 2010; Yanfei *et al.*, 2010). According to Fingas (2010b) the reasons for this are simply that diesel fuel, jet fuel, kerosene, and the like, have a narrower range of compounds that evaporate at similar yield rates, which are a summation of a square root. The implication is that the evaporation rate slows rapidly in both cases. The results of rate of evaporative loss, given in this Chapter followed a power law and gives good agreement with results of similar previous studies (Fingas, 2004; Brandvik and Faksness, 2009) by other researchers.

Crude oil properties can change significantly with the extent of evaporation. A recent report by Fingas (2010) has stated that if about 40% (by weight) of an oil evaporates, its viscosity could increase by as much as a thousand – fold. Likewise, its density could rise by as much as 10% and its flash point could decrease by as much as 400% according to Fingas (2010). Explanations for the viscosity increase by as much as a thousand-fold is that the viscosity of crude oil is largely determined by the amount of lighter and heavier fractions that it contains. The greater the percentage of light components such as saturates and the lesser the amount of asphaltenes, the lower the viscosity. Thus, as with other physical properties, viscosity is affected by temperature, with a lower temperature giving a higher viscosity (Fingas, 2010). Therefore, the extent of evaporation of crude oil can be the most important factor in determining properties of oil at a given time after a spill, and in changing the overall behaviour of the oil.

Akay (1998) has given a detail representation regarding the rules of emulsion viscosity. As given by the author in his study, the viscosity of emulsion increases primarily with increasing oil phase, anioinic/non-ionic concentration ratio, extension rate for phase inversion and the number of mixer units and the viscosity profile of the emulsions in an extended shear rate ($1\text{-}1000\text{ s}^{-1}$) indicated that the viscosity tends to reach a constant value when the shear rate is large. Akay (1998) explained the observations using the colloidal theory of viscosity in concentrated dispersions (Goodwin, 1987) and takes into account the

deformability of droplets using the modified form of the Krieger-Dougherty equation (Krieger, 1972) for shear-dependent viscosity.

The effect of evaporation on crude oil on viscosity and emulsification behaviour was investigated and is presented in the next Chapter.

2.5 Conclusion

1. Crude oil on water and oil alone (i.e. oil on its own) appear to weather at similar rates, although oil on its own evaporated more quickly than oil on seawater.
2. Emulsified oil evaporates more quickly than unemulsified oil.
3. Oil evaporation rates with temperature follows an equation: $\% \text{ mass loss} = (0.0571 T + 0.1944) \times t^{(-0.0033 T + 0.2604)}$ from 12°C up to 30°C but at 40 °C and 50°C appears to deviate and does not fit this trend.
4. Oil evaporation rates increases with temperature.
5. Brent and Forties crude oils evaporate at different rates. Brent crude oil exhibited a higher rate of evaporation of the volatile fractions compared to Forties crude oil at similar experimental conditions.

CHAPTER 3

3.1 WATER-IN-OIL EMULSIFICATION AND STABILITY MEASUREMENTS FOR FORTIES, BRENT, BRAE A AND STIRLING CRUDE OILS

3.2 Introduction

There has been considerable interest in emulsions in the petroleum industry where they typically constitute undesirable consequences in various stages of exploration, production, equipment handling cost, transport and conventional spill equipment. Emulsification as one of the major oil weathering processes for marine oil spill, transforms fresh crude oil with low viscosity to an often brown highly viscous water-in-oil emulsion with several undesirable alterations to the original spilled oil. Daling *et al.*(2003) noted that the appearance and texture of oil slicks at the sea surface can be very different for different crude oils and degree of weathering. Therefore, continuous oil slicks may be observed at an early stage after release, but weathering process will transform the slicks into a patchy appearance consisting of broken fragments of highly emulsified oil.

An emulsion is usually defined as a system consisting of a liquid dispersed in another immiscible liquid, as droplets of colloidal sizes ($\sim 0.1\text{-}10\text{ }\mu\text{m}$) or larger. If the oil is the dispersed phase, the emulsion is termed oil-in-water (o/w) emulsion, conversely, if the aqueous medium is the dispersed phase, it is termed water-in-oil (w/o) emulsion (Cormack, 1999; Auflem, 2002). The surface of each droplet is an interface between hydrophobic and hydrophilic molecules. In the emulsified state, the interfacial area between the dispersed droplets and the bulk phase represents an increase in the systems free surface energy, *i.e.* by energy input and re-coalescence of the dispersed phase occurring simultaneously with reduction in the systems free energy. However, this classification is not always appropriate as other types such as multiple emulsions of the type oil-in-water-in-oil (o/w/o), may also be found (Sjoblom *et al.*, 2003). This is illustrated in Figure 26.

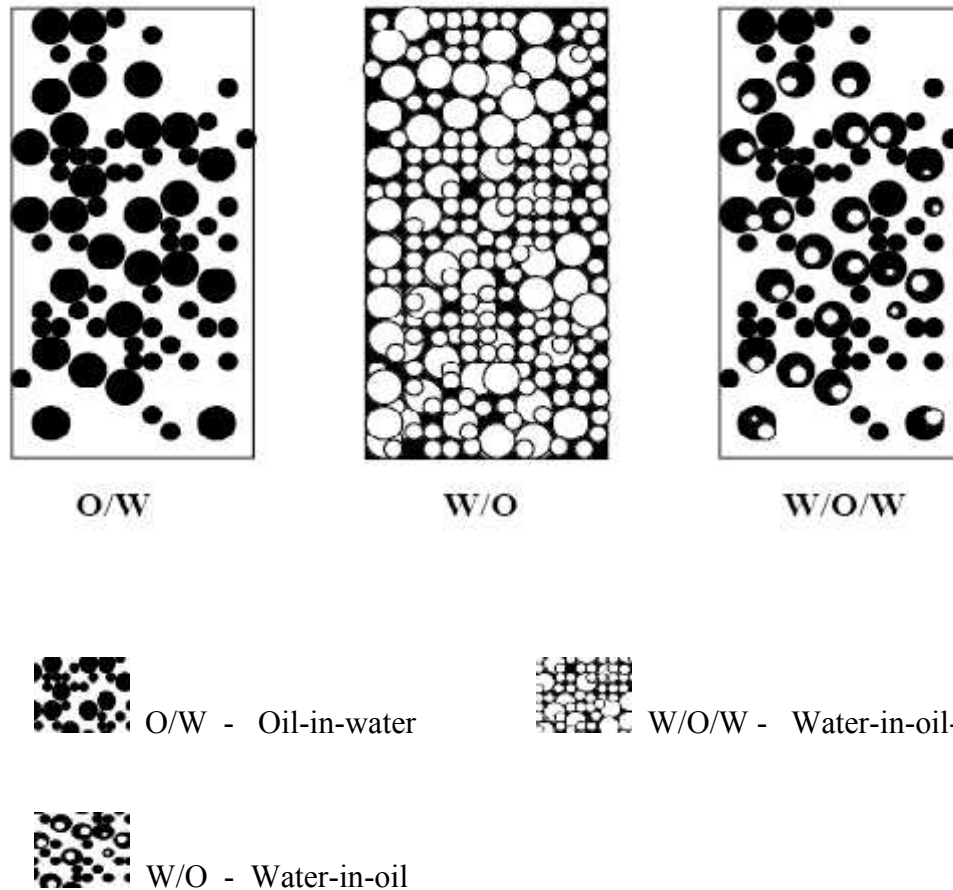


Fig. 26 Common types of crude oil emulsions: oil-in-water (o/w), water-in-oil (w/o), and less common: water-in-oil-in water (w/o/w). (Spiecker, 2001)

Crude oil tends to form water-in-oil emulsions (Cormack, 1999; Fingas and Fieldhouse, 2009). The four distinct states of w/o emulsions that have been identified are: stable, meso-stable, entrained water and unstable. The different classes can be distinguished by stability over time, visual appearance, as well as rheological measurement (Fingas and Fieldhouse, 2004; 2009). Figure 27 illustrates these categories. Stable emulsions are reddish-brown solid-like materials and typically increase their viscosity with time (i.e. a stable emulsion can maintain its viscosity over the length of time the emulsion is allowed to stand or kept). The basic principle is that the stability derives from the strong visco-elastic interface caused by asphaltenes and resins (Mullins *et al.*, 2007; Fingas and Fieldhouse, 2009). Meso-stable w/o emulsions has properties that lie between stable and unstable emulsions and the lack of sufficient quantities of asphaltenes, or too many destabilizing materials such as smaller

aromatics inhibits it to achieve a complete stable state. Meso-stable w/o emulsions are reddish-brown viscous liquids and generally degrades fairly completely within one week (Fingas and Fieldhouse, 2004; 2009). Also entrained water-in-oil types are visually black viscous liquids most often produced from heavier oils (oil density $> 0.92 \text{ g/cm}^3$). Unstable emulsions are the emulsions that breakdown to water and oil immediately after mixing, due to insufficient water particle interaction; an insignificant amount of water may be retained by the oil, particularly if the oil is viscous but in only relatively short time (Sjoblom *et al.*, 2003; Fingas and Fieldhouse, 2009).

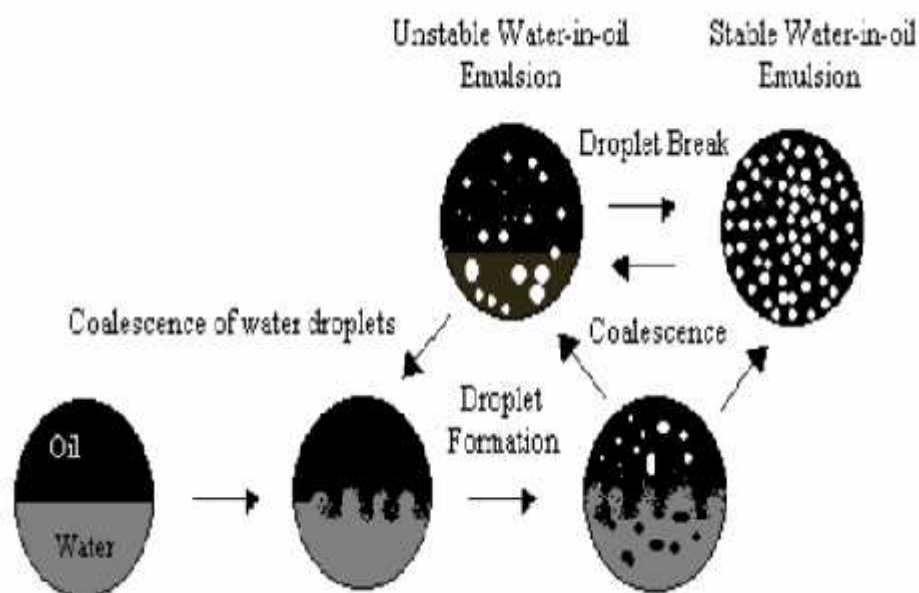


Fig. 27 Formation of water-in-oil emulsion (Modified from Lee, 1999)

The general opinion consequently, is that emulsions are inherently never completely thermodynamically stable and will seek to minimize the surface area by separating into the different phases (Cormack, 1999; Auflem, 2002, Fingas and Fieldhouse, 2009). Emulsions tend to separate only when the droplets merge with each other, or with the homophase continuum that gradually forms. A number of processes that facilitate the separation or breakdown of emulsions have been identified (Becher, 1983; Sjöblom, 1996, Sjöblom *et al.*, 2003; Cormack, 1999; Spiecker and Kilpatrick, 2004). This is illustrated in Fig. 28. Creaming/sedimentation create a droplet concentration gradient due to a density difference

between the two liquid phases, leading to close packing of the droplets (gravity separation); the droplets remain separate even when they touch. Aggregation of droplets may be said to occur when they stay very close to one another for longer time than if they were no attractive forces acting between them. Flocculation is the formation of three-dimensional clusters which have not yet coalesced. Coalescence or breaking of the emulsion occurs in two stages of film drainage and film rupture and is the process whereby the thin liquid film of the continuous phase which separates the flocculated droplets drains allowing fusion to form larger droplets. In order to have film drainage, there must be a flow of fluid in the film and a pressure gradient present. However, when the interfacial film between the droplets has thinned to below some critical thickness, it ruptures, and the capillary pressure difference causes the droplets to rapidly fuse into one droplet. Hence, the properties of the thin film are of uttermost importance for the separation. If the droplets deform (from spherical), the area of the interface increases and consequently the drainage path in the film also increases, resulting in lower drainage rates (Auflem, 2002). Ostwald ripening, first described by Wilhelm Ostwald in 1896, is a thermodynamically-driven process which describes the dissolution of small crystals or soluble particles and the redeposition of the dissolved species on the surfaces of the larger crystals or soluble particles. The process occurs because the smaller particles have a higher surface energy than the larger particles, giving rise to an apparent higher solubility (IUPAC Recommendations, 2007). The mechanism of Ostwald ripening occurs when the dispersed phase has significant solubility in the continuous phase and there is a wide distribution of droplet size with a large proportion in the submicron region, at the expense of smaller ones, resulting in differential rates of solution (Cormack, 1999). Phase inversion may occur when the dispersed phase concentration is high and the surfactants present are not suited to favour stability, leading to dispersed phase becoming the continuous phase and *vice versa*.

Low interfacial tension, volume fraction of the dispersed phase and especially viscosity which is temperature dependent, are other factors that may also influence the stability of emulsion. Hence, the stability of emulsions is the degree to which the above spontaneous processes are inhibited, usually by the presence of a suitable emulsifier.

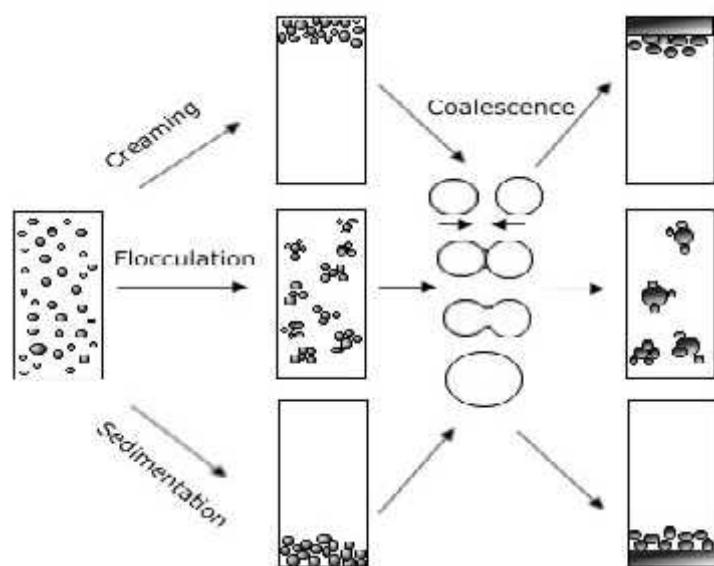


Fig 28 Processes taking place in an emulsion leading to emulsion breakdown and separation (Auflem, 2002).

With w/o emulsions arising from the inadvertent contact of oil and water on the other hand, the general industrial interest in petroleum studies has been in finding ways to destabilize and break them into their constituent parts as separate continuous phase. Formation of emulsions changes the properties and characteristics of oil drastically (Cormack, 1999; Xie *et al.*, 2007; Fingas and Fieldhouse, 2009). This process is of environmental and operational importance as the resultant emulsion characteristically changes the overall behavior of the spilled crude oil. Operational and technical challenges occur in making informed decisions in the selection and application of the most suitable oil spill treatment including the deployment of special handling equipment type, and must be resolved to provide relevant and effective countermeasures.

Emulsion behavior, in terms of stability is relevant to the water-in-oil system in a number of ways. Therefore, w/o emulsions when formed may be of varying degrees of stability depending on crude oil type. Currently, as noted by Reed, 2007, limited knowledge to date thereof, in crude oil emulsification has continued to attract research.

Most of the characteristic properties of crude oil are temperature-variable. The density, viscosity, crystalline wax content, all play a significant role in the stability of emulsions formed. Viscosity decreases with increase in temperature. Cormack, 1999 reported that for water the sensitivity is about 3% per °C and 10% per °C for many crude oils. Emulsion stability may therefore be expected to decrease with increase in temperature because a reduction in the viscosity of the continuous phase would increase the rate of collision of the dispersed phase droplets. Moreover, the density difference between the aqueous and oil phases usually increases. Hence, temperature change may affect emulsion stability. Spilled crude oil that is stranded on coastal beaches typically undergoes photooxidation process. It has been reported (Klein and Pilpel, 1974; Prince *et al.*, 2004) that photooxidation not only contributed to emulsion stabilization but also to the creation of tar balls. In general, oxidation (although not necessarily the introduction of oxygen), however introduces oxygen atoms into the hydrocarbon molecules of the oil and in so doing, produces hydrophilic groupings which produce the surface-active properties necessary for the stabilization of emulsions. Once the emulsion has formed, oxidation process will slow down and this will be particularly so of the tar balls, oxygen access being largely restricted to the outer surfaces of the material and the outward surfaces of emulsion droplets that have been broken up by wave action (Cormack, 1999).

These factors amongst others are therefore important in determining the fate of the pollutant that has reached the shoreline. Moreover, their amenability to treatment with demulsifiers in the course of recycling or final disposal will consequently depend on the stability of the individual oil emulsions. The industry has developed technology that facilitates, to a greater extent, the recovery of spilled crude oil on seawater and the eventual separation of the seawater from the crude oil. In the light of recycling, it should be noted that such recovered oil, having lost its volatile components by evaporation while exposed on the sea surface, will nonetheless resemble the original cargo or crude and will facilitate its disposal through various recycling options. In principle, such recovered oil could be processed with normal feedstock at the refineries if the specifications of the recovered oils are appropriate, or utilized to raise steam for heating at oil-fired power stations. It can also be mixed with coal in coal-fired power stations or used in fluidized bed incinerators to generate electricity. If the oil proves to be unusable for such productive use, other recycling

options include its use in road and related surfacing or final landfarming disposal of the liquid oil or contaminated solids.

Given the general consensus of opinion among researchers that crude oils may form w/o emulsions dependent upon its characteristics (Fingas and Fieldhouse, 2009; Sjoblom *et al.*, 2003; Sjoblom *et al.*, 1990; Cormack, 1999), the experiments in this chapter were aimed to investigate the influence of rheological properties, water contents and overall stability in emulsification in four North Sea crude oil types (Forties, Brent, Brae A and Stirling) and to ascertain their behavior after formation. These oils were selected as previous research (Walker *et al.*, 1992) indicated that their rheological properties differed when emulsified with seawater.

3.3 Experimental

3.3.1 Materials

Forties, Brent, Brae A and Stirling North Sea crude oils were used in the emulsion formation and analyses, Electromantle Me Heater, analytical balance (Mettler AT261 DeltaRange), Dean & Stark apparatus, hot plate, MBL Morander density bottle (B.S 733); (Thermo Scientific, England), HPLC grade toluene, anti-bumping granules (fused alumina, Fison Scientific, England), Top Drive Macerator propeller (Townsend & Mercer Ltd, Croydon, England), Haake Viscotester VT500.

3.3.2 Method

The procedure for emulsion formation given in Chapter 2, Section 3.3 was repeated for forming water-in- oil emulsions for all four types of crude oil investigated in this section. As a pre-treatment prior to emulsification, the oils were weathered in a fume cupboard to give a weight loss of 11% and 20% respectively. The oil samples were placed on a hot plate (35°C) in a fume cupboard with an air velocity of 0.77ms^{-1} to obtain evaporative weight loss. 20% weathering was achieved for Forties and Brent crudes at ~6 h and Brae A and Stirling crudes at ~3 h, 20 min. 11% weathering was achieved for Forties and Brent crudes

at ~12hrs; Brae A and Stirling crude at ~17 h, overnight at room temperature. The methodology was similarly used by Fingas and Fieldhouse (2006). Emulsions were formed from the respective weathered oil residues. Water-in-oil emulsions formed with 11% and 20% weathered-oils in this study will be referred to as Emulsions B and C respectively. The emulsions were collected from the vessels (Kilner jar) with a Teflon spatula for measurements of viscosity and water content. Each crude oil density was measured by pycnometry using MBL Morander 50cm³ density bottles (B.S 733). A pycnometer is a standard vessel for measuring and comparing the densities or specific gravities of liquids or solids.

Viscosity measurements were carried out using a Haake VT 500 Viscotester, the viscometer maintained at 10°C temperature. This is because the emulsions were formed at 10 °C which is the average North Sea temperature. With the use of a Teflon spatula, an appropriate quantity of the emulsion was placed in the SV1 cup to the designated mark and allowed to thermally equilibrate at 10°C for 10min. The viscometer was operated with the following ramp times: one minute to target shear rate of s⁻¹; one minute at target shear rate (s⁻¹). Viscosity was measured as a function of shear rate by increasing the shear rate linearly from 0 to 178.1 s⁻¹. Starting with the lowest shear rate, the viscosity data were obtained across the shear rate range and the viscosity reported at a standard shear rate of 8.9 s⁻¹ (Institute of Petroleum, 1986). The viscosity measurement was taken when the emulsions formed was left to settle for 24 h. The viscosities are reported at all ten different shear rates measured. A Dean & Stark apparatus was used for measurement of water contents in the emulsions (ASTM D95). Water content was reported as weight percentage.

3.4 Results and Discussion

Rheological data based on the four samples of crude oil emulsions are summarized in Table 3.1. The densities of the starting oil, water contents and emulsion properties measured for the water-in-oil emulsions are shown in Table 3.2. Several factors are known to affect the stability of water-in-crude oil emulsions and their overall classification (type of emulsion). These are viscosity, density, temperature and water content. These parameters were measured in the crude oils and their water-in-oil emulsions to investigate the type of

emulsions that will be formed by Forties, Brent, Brae A and Stirling crudes. These emulsion types were considered in relation to the starting crude oil properties, prior to emulsion formation, in order to further understand their behaviour after emulsification.

Table 3.1 Viscosity measurements at 10°C for fresh and emulsions (mPa.s) of North Sea Crude Oils

Shear rate (s ⁻¹)	Fresh crude (unemulsified)				Fresh crude (emulsified)				11% Weathered (B)				20% Weathered (C)			
	Forties	Brent	Brae A	Stirling	Forties	Brent	Brae A	Stirling	Forties	Brent	Brae A	Stirling	Forties	Brent	Brae A	Stirling
1.78	10340	790	890	904	11300	8190	9100	9430	17300	8210	10800	13400	43700	8430	15600	23300
2.225	998	674	750	890	9900	6890	7470	7390	11400	6980	8530	10300	32400	7090	12100	15800
3.56	790	518	690	882	7430	4360	4710	4570	7260	3840	5350	6490	21400	4360	7910	10700
4.56	670	509	678	876	5860	3270	3730	3690	6040	3410	4240	5380	17300	3660	6520	8280
8.90	655	496	653	870	3470	1710	1890	1900	3290	1980	2360	3010	10000	2040	4060	4610
17.8	643	492	644	858	1840	872	660	961	1810	970	1210	1680	5130	1100	2230	2610
44.5	638	478	595	849	917	346	375	310	896	390	551	851	2560	526	1180	1450
53.4	640	470	590	837	494	292	322	322	782	268	459	739	2100	459	1000	1290
89.0	635	453	483	796	390	181	192	195	562	201	319	528	1790	309	711	958
178.1	633	442	481	792	264	85	93	97	373	113	185	355	874	192	489	646

Table 3.2 Properties of fresh and weathered crude Emulsions

Emulsions	Colour	Initial density of oil (gcm ⁻³)	vol. % Water Content	Stability	Texture
<i>Fresh crude viscosity @ 8.90s⁻¹</i>					
Forties	Light Brown	0.8713	25.0	Unstable	Mobile
Brae A	Dark Brown	0.8713	20.0	Unstable	Mobile
Brent	Dark Brown	0.8713	34.5	Unstable	Mobile
Stirling	Brownish Brown	0.8713	17.8	Unstable	Mobile
<i>11% Weathered (B)</i>					
Forties	Light brown	0.8713	63.1	Stable	Not Mobile
Brae A	Dark brown	0.8576	35.0	Meso-stable	Mobile; creamy
Stirling	Brownish- black	0.8434	60.0	Entrained water	Mobile; greasy
Brent	Dark brown	0.8342	40.1	Unstable	Fairly mobile; oil-like
<i>20% Weathered (C)</i>					
Forties	Light brown	0.8713	82.9	Stable	Not mobile
Brae A	Dark brown	0.8576	75.0	Stable	Not mobile
Stirling	Brownish-black	0.8434	78.0	Stable	Not mobile
Brent	Dark brown	0.8342	54.0	Unstable	Fairly mobile; oil-like

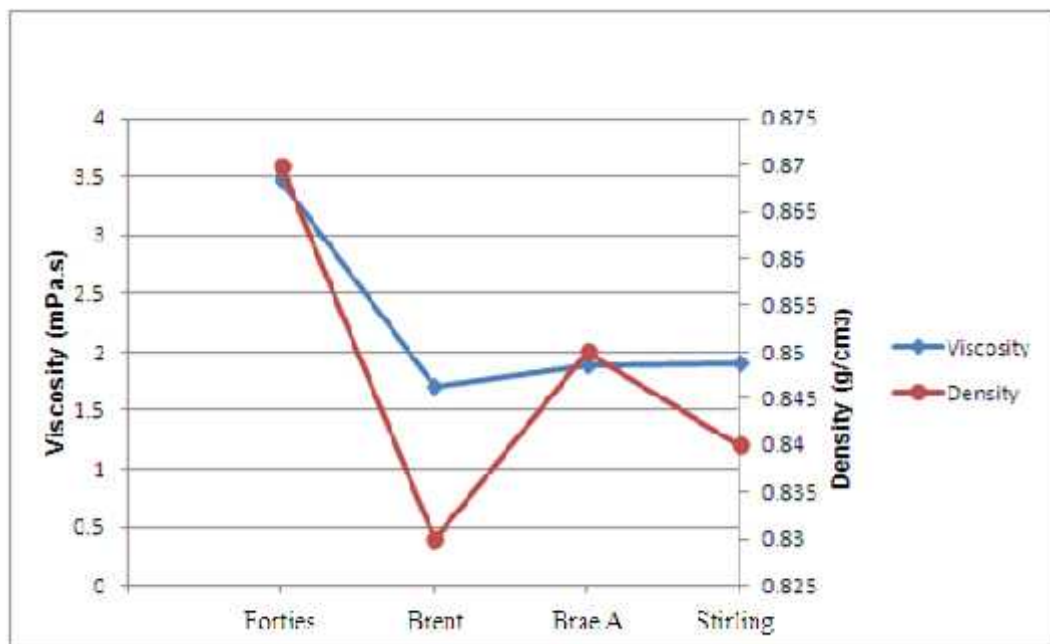


Fig. 29 Showing water-in-oil emulsions of fresh, 11%, and 20% weathered crude oil. The emulsions formed from the differently weathered oil showed water separated as a different phase from the emulsions.

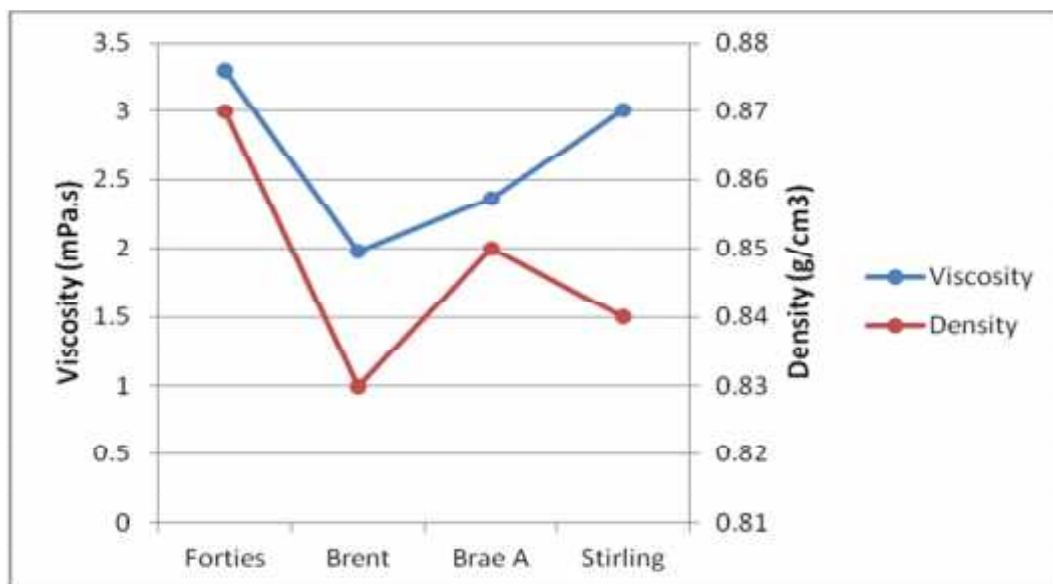
3.4.1 Factors influencing the stability of emulsions

3.4.2 Effect of viscosity of emulsions

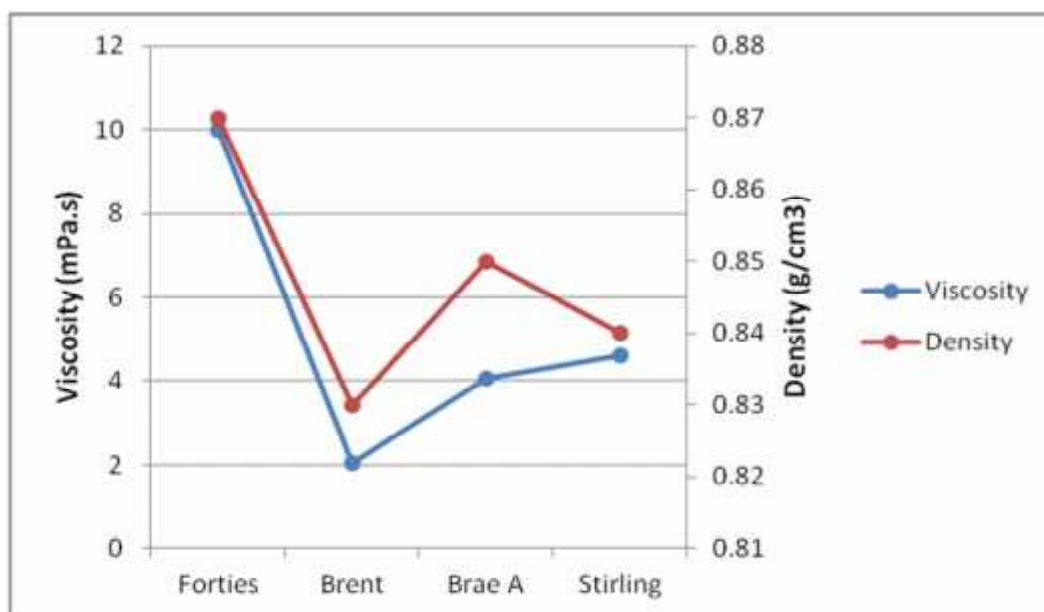
The viscosity of a liquid can be described as a measure of its resistance to flow. As indicated in Table 3.1, emulsions formed from the Brent, Brae A and Stirling fresh crude oils which had not undergone “weathering” gave similar viscosities (1710, 1890 and 1900 mPas⁻¹) at 8.90 s⁻¹. However, the viscosity of fresh Forties emulsion was significantly higher, approximately by a factor of 2. The viscosities of the fresh, and 11% weathered Forties were similar at 3470 and 3290 mPas⁻¹ respectively. The fresh, 11% and 20% weathered Brent emulsions all had similar viscosities of 1710, 1980 and 2040 mPas⁻¹ respectively. The viscosities of fresh Brae A and 11% weathered Brae A emulsions were similar, 1890 and 2360 mPas⁻¹ respectively. It however showed a marked increase in emulsion viscosity to 4060 mPas⁻¹ in the 20% weathered Brae A. The viscosities of fresh, 11% and 20% weathered Stirling emulsions showed a gradual increase, measuring 1900, 3010 and 4610 mPas⁻¹ in the viscosities of fresh, 11% and 20% weathered crude emulsions. The variation in the viscosities for the oil emulsions was indicative of the differences in the characteristics of the crude oils, and their propensity for emulsion formation and stability. The results indicated that crude oils which gave higher viscosities measured tend to form more stable emulsions. The higher the viscosity of the emulsions, the more stable the emulsions formed. In general, Brent crude which produced lower viscosity measurements was seen to produce unstable emulsions compared to the stable emulsions formed with Forties crude which had a correspondingly higher viscosity in the emulsion formed from it. These results agree with similar findings (Mehta, 2005; Fingas and Fieldhouse, 2004, 2009). Mesostable emulsions were formed from the fresh and 11% weathered Brae A and Stirling crudes. As earlier stated, meso-stable water-in-emulsions is a class of emulsion that lie between stable and unstable emulsions and generally degrades fairly completely within a few days of its formation. The stability, which is a measure of the tendency at which emulsions breakdown owing in part to its viscosity, may affect the emulsions. It was found that oils with low viscosity emulsions also had correspondingly lower densities as indicated in Table 3.2, and this may have influenced the stability of the emulsions.



(a)



(b)



(c)

Fig 30 (a), (b) and (c) shows the relationship between the viscosity (PaS) and density (g cm^{-3}) of crude oils in fresh oil emulsion, 11% weathered oil emulsion and 20% weathered oil emulsion respectively.

However, it is reported (Cormack, 1999) that oils with low density that form low viscosity emulsions, which contain a significant amount of asphaltene and wax may have other natural constituents (mixed surfactants) in the oil exhibiting synergistic effects to stabilise water-in-oil emulsions, thereby overriding the influence of low viscosity of the oil and density. Generally, a relationship exist where the less dense the oil, the less viscous the oil is, and its emulsion product. The effect of viscosity and density in relation to the stability of emulsions was clearly seen in Forties and Brent crudes. Forties crude emulsion with viscosity of 10000 mPa.s^{-1} formed the most stable emulsion compared to Brent crude emulsion with a much lower viscosity of 2040 mPa.s^{-1} both measured at the same shear rate using 20% weathered samples (Table 3.1).

3.4.3 Influence of crude oil type

The data suggest that there exist oil-specific differences between the viscosities of emulsions based on the different oils as well as the variations in the viscosities of the individual (fresh) crude oils (Table 3.1 and 3.2). This was clearly evident in the stability

of the emulsions from the different crudes in this study. High molecular weight oils generally has a higher percentage of compounds with large number of carbon atoms and hence a high boiling point and molecular weight (SEG, 2008). It has also been found that high molecular weight oils are more viscous with a resultant stable emulsion (Ronningsen, 1995). In general, at low temperatures, viscosity is dominated by wax formation therefore waxy, paraffinic oils tend to be more viscous and emulsions derived from such oils are more likely governed by wax formation other than other factors (Cormack, 1999).

3.4.4 Effect of shear rate

The viscosity of the water-in-oil emulsions decreased with increasing shear rate as indicated in Table 3.1. A uniform shear rate range was maintained for the viscosity measurements in the emulsions of the four crude oils. In general, crude oil emulsions are non-Newtonian, shear thinning at low temperatures ($<25^{\circ}\text{C}$). Certain materials have variable viscosity depending on the degree of inducement to flow to which they are subjected. The inducement to flow is referred to as deformation, and the rate of deformation dictates rheological properties including viscosity. Such materials are said to exhibit non-Newtonian properties or to be thixotropic. Since materials have to be induced to flow in order for the tendency to flow (viscosity) to be measured, viscosity for non-Newtonian material such as water-in-oil emulsions varies with shear rate and is often quoted at stated shear rates used during viscosity measurement. Water-in-oil emulsions may tend to exhibit viscoelasticity (a property of materials that exhibit both viscous and elastic characteristics when undergoing deformation) at low shear rate, though this effect is mostly transient (Cormack, 1999; Ronningsen, 1995) and may not have a significant effect on the stability of the emulsions. However, the measure of elasticity includes extensional viscosity, normal stress difference and elastic recoil.

3.4.5 Effect of water content on emulsion formation

The influence of water content on the stability of the water-in-oil classes are depicted in Fig. 31 and Table 3.3. Fresh crude emulsions showed closely similar water contents of

20.0% and 17.8% for Brae A and Stirling crudes respectively, whereas the water contents were 34.5% and 25.0% for Brent and Forties respectively. Emulsions B showed closely similar water contents of 63.1% and 60.0% for Forties and Stirling crude emulsions respectively. The water contents for Brae A and Brent crudes emulsions were lower: 35% and 40.1% respectively. Water contents for emulsions C were similar in Forties, Brae A and Stirling and were higher than the water content in Brent emulsion as indicated in Fig 31. Statistical analysis ($p < 0.05$) showed a positive correlation (0.66) between the viscosities of the fresh crude and the water content of the 11.0% weathered oil emulsion. Similarly, the viscosities of the fresh crude showed good correlation (0.63), with the water content of the 20.0% weathered oil emulsion. There was a good significant correlation (0.91), between the viscosity of 11% weathered crude emulsion and 11% weathered emulsion water content.

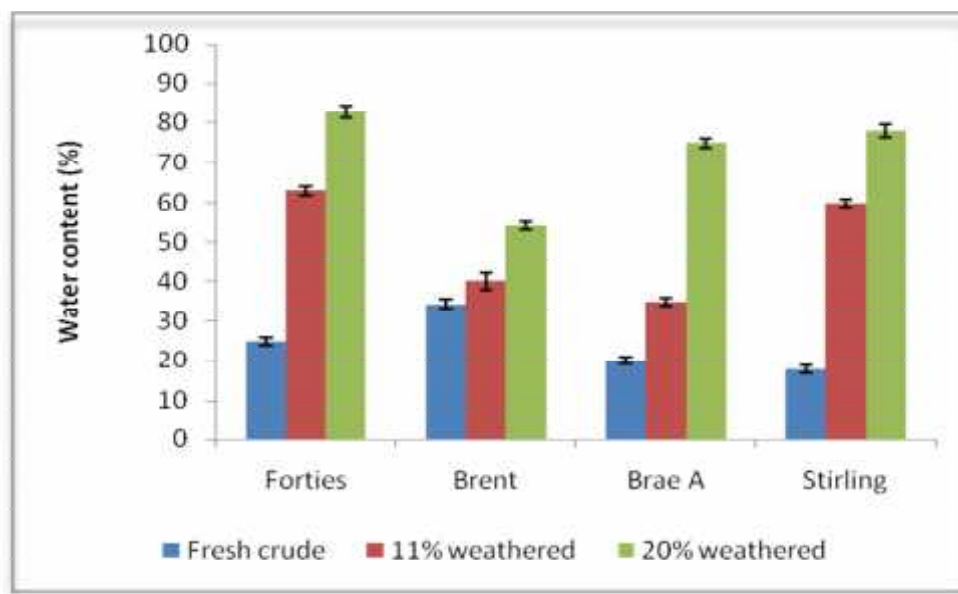


Fig.31 Water content for fresh, B(11%) and C(20%) weathered-crude emulsions

In general, water-in-oil emulsions with high water contents produced more stable emulsions. It is thought that at this point, when an emulsion has been formed, the small water droplets are closely packed and virtually in contact except for the interface structure of the stabilising molecules and a thin film of oil (Cormack, 1999). Higher water contents increases the cohesion and coalescence of droplets but more so,

stabilisation by emulsifier components may also be the controlling factor (Cormack, 1999; Abdurahman and Yunus, 2006). Most researchers have determined the stability of water-in-oil emulsions by gauging the water uptake and have reported water contents ranging from 20-90% (Kilpatrick and Spiecker, 2001; Gu *et al.*, 2002; Dicharry *et al.*, 2006; Yarranton *et al.*, 2007; Fingas and Fieldhouse, 2009, Abdurahman and Yunus, 2009). For emulsions at higher water contents, the droplets may become more closely packed leading to more energy dissipated in droplet interaction and deformation therefore resulting in more accelerated increase in viscosity. Indeed, 20% weathered Forties crude has the highest water content (82.9%) and emulsion viscosity (10000 mPas^{-1}). Viscosity and droplets interaction and deformation are thus linked and hence may have an effect on the stability of the water-in-oil emulsions.

3.4.6 Effect of volume fraction of internal phase

The effect of volume fraction of the internal phase (water) on the stability of the w/o emulsions of the four oil types was studied in relation to the emulsions viscosity. The volume fraction is expressed below Table 3.3 and relates the viscosity of the emulsions to the water content of the internal phase as illustrated in Fig 32 (a, b). The effect of volume fraction is shown in Table 3.3 for the emulsions B and C respectively.

Table 3.3 Effect of volume fraction on emulsion viscosity

	11% Weathered (B)				20% Weathered (C)			
	Forties	Brent	Brae A	Stirling	Forties	Brent	Brae A	Stirling
Vol. % Water content	63.1	40.1	35.0	60.0	82.9	54.0	75.0	78.0
Volume ratio (Φ)	1.71	0.67	0.54	1.5	4.85	1.17	3.0	3.55
*Emulsion viscosity μ_e (Pas⁻¹)	3.29	1.98	2.36	3.01	10.0	2.04	4.06	4.61
*Fresh oil emulsion viscosity μ_o (Pas⁻¹)	3.47	1.71	1.89	1.9	3.47	1.71	1.89	1.9
μ_e/μ_o	0.948	1.157	1.248	1.584	2.881	1.192	2.148	2.426

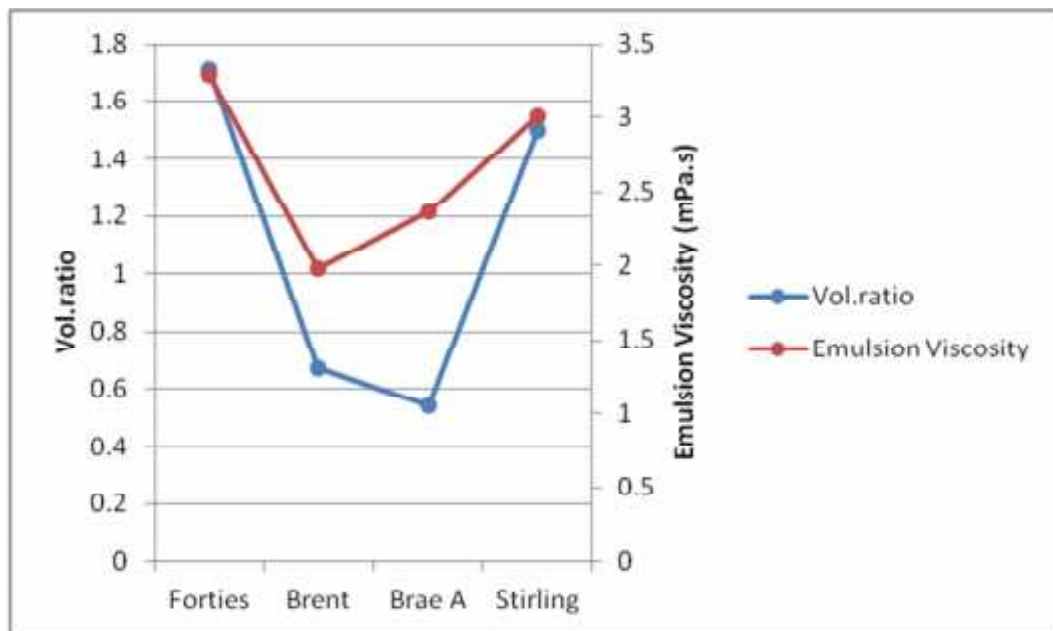
*Note: Viscosity selected at shear rate of 8.90 (s⁻¹) in Pas⁻¹

The volume ratio of internal phase was derived by expressing the ratio of the % water content in relation to 100%. i.e. for volume ratio in 11% weathered Forties: Water content = 63.1%, subtracting 63.1 from 100.0 (100 – 63.1) = 36.9

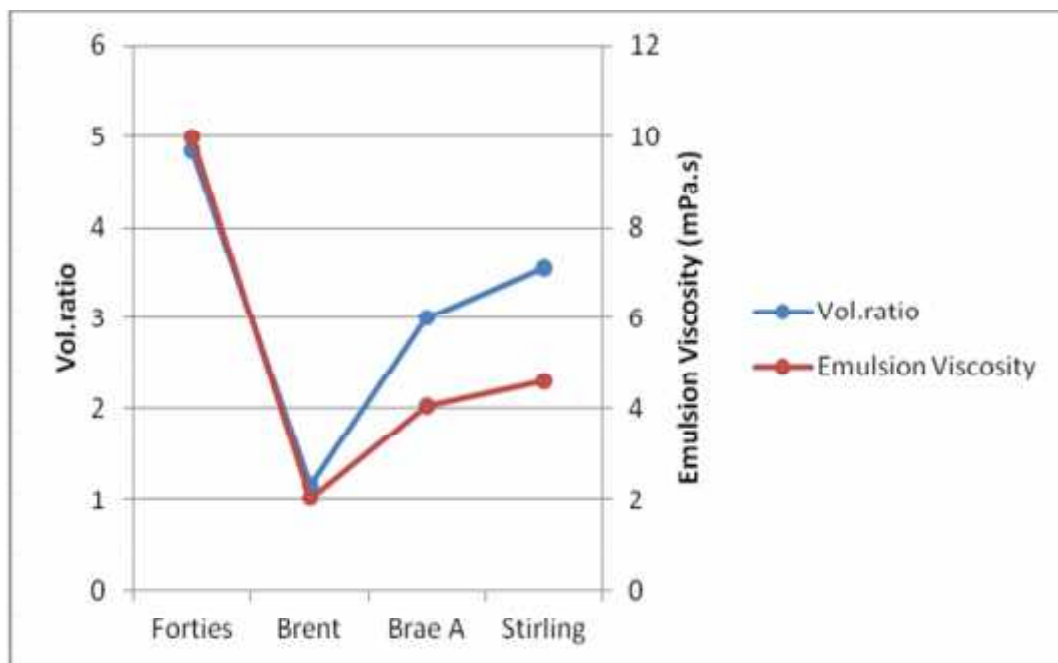
Hence, 63.1/36.9

= 1.71 (volume ratio of internal phase)

μ_e/μ_o = is a derivative that represents the ratio of the emulsion viscosity to the fresh oil emulsion viscosity. This indicates the degree or factor by which the emulsion differs to the fresh oil in viscosity.



(a)



(b)

Fig.32 (a) and (b) shows the effect of volume fraction of internal phase (water) on emulsion stability of B (11% weathered) and C (20% weathered) respectively. Emulsion viscosity increased as volume ratio increased.

Fig 32 (a, b) indicates that the viscosity of the emulsions increased markedly as the volume ratio of the internal phase (Φ) increases in both emulsions B and C, with the

exception of Brae A in emulsion B. The increase in viscosity resulted in progressive contribution to the stability of the water-in-oil emulsions. As shown in Table 3.2 and 3.3, of greater significance, Forties crude emulsion exhibited a high viscosity leading to a stable emulsion. The stability of water-in-oil emulsions can be measured based on the viscosity of the emulsions. Based on the viscosities of the water-in-oil emulsions in relation to the volume fractions of the internal phase, a stability trend for the emulsions of the four oils was indicated as Forties > Stirling > Brae A > Brent.

3.4.7 Influence of temperature

Some crude oils do not form stable water-in-oil emulsions until they lose certain amount of volatile compounds through evaporation (Fingas and Fieldhouse, 2009). It was observed in evaporation studies discussed in Chapter 2 that the rate of evaporation of volatile hydrocarbons increased with temperature. This followed a linear curve up to 30°C above which the evaporation did not fit linearly. For these experiments, the emulsions were formed and the viscosities observed at 10°C, the average North Sea temperature as shown in emulsions B, (Fig 33).

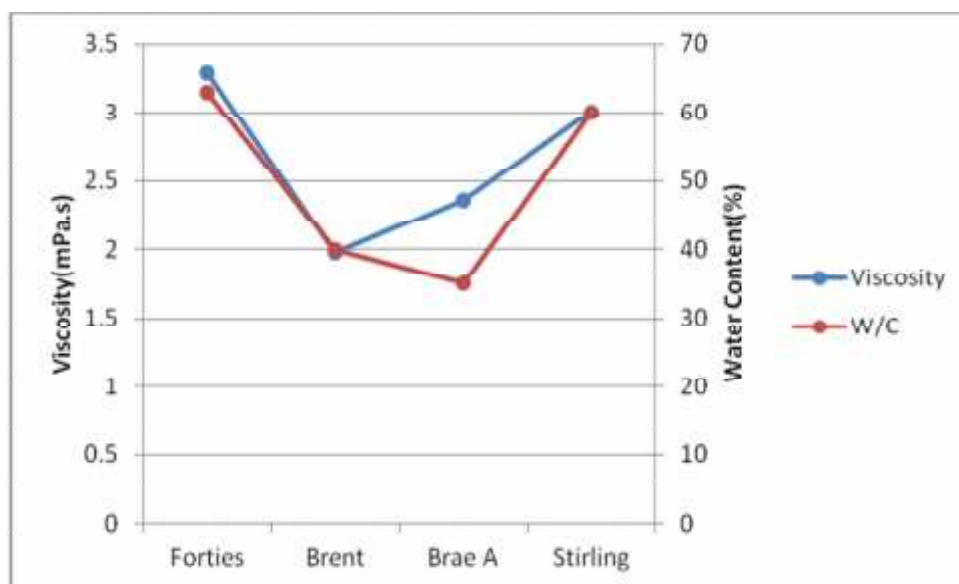


Fig 33. 11 % Weathered-oil (Emulsion B) showing the effect of temperature on emulsion stability of emulsion B. *Note: Viscosity expressed in $\text{Pa}\cdot\text{s}^{-1}$

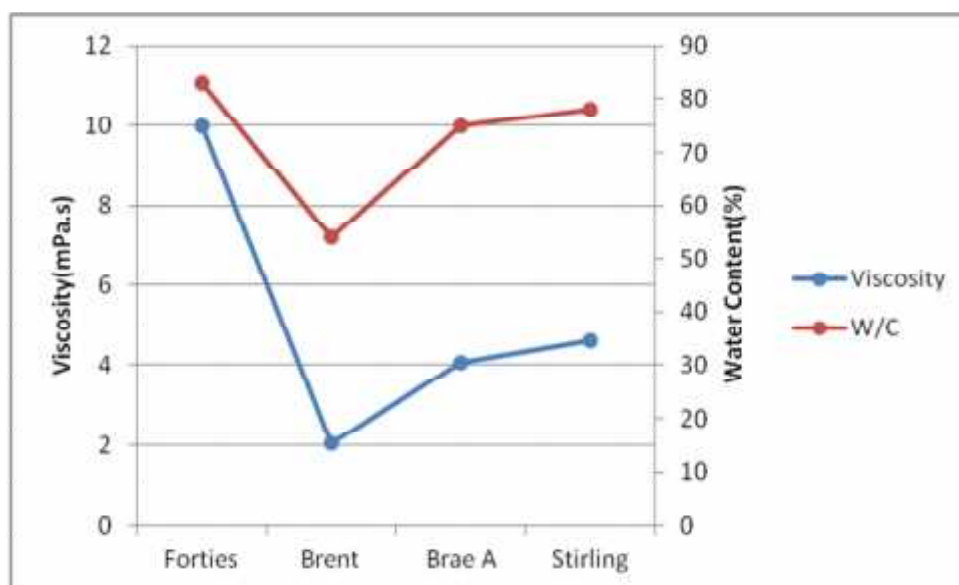


Fig 34 20% Weathered-oil (Emulsion C) showing the effect of temperature on emulsion stability of emulsion C. *Note: Viscosity expressed in Pa^{-1} .

A number of characteristic properties of crude oil are dependent on temperature and this can have a very significant effect on emulsion rheology. Density, viscosity, crystalline wax content all contribute to the stability of the w/o emulsions formed. A change in temperature may indirectly alter and cause changes in interfacial tensions, viscosities, nature (hydrophilicity-lipophilicity) of the surfactants and in the thermal agitation of the molecules. Weathering the oils by 11% prior to emulsion formation had resulted in the above changes in the characteristic of the oils and in the viscosity in particular as can be seen in Fig 33. As a consequence of removal of the lighter hydrocarbons through evaporation, the density and viscosity increased. As emulsions tend to be sensitive to temperature changes, the stability of the w/o emulsions formed are also influenced by the temperature at which the emulsions are formed. Generally, emulsion stability decreases when temperature is increased, during and after formation (Abdurahman and Yunus, 2006).

3.5 Stability classifications of Emulsions

The stability of water-in-oil emulsions classes for Forties, Brae A, Brent and Stirling crudes may be assessed by viscosity measurements, water-uptake and visual appearance (colour and texture) as shown in Table 3.1 and Appendix C.1).

Four distinctive emulsion states were observed: stable water-in-oil emulsions; meso-stable water-in-oil emulsions; entrained water; and unstable water-in-oil emulsion. These emulsion states were previously defined in Section 3.2 of this chapter. Considerable differences were exhibited in the emulsion states from the four crude oil types, as summarised in Table 3.2. The viscosity of the stable emulsions markedly increased from that of the starting (fresh emulsified) oil viscosities (Table 3.2 and 3.3). For all cases of the crude oils, with the exception of Brent, higher viscosities were recorded for emulsion C samples compared to fresh or B samples. For example, the viscosity of Forties emulsion increased by a significant degree, a factor of 3, from 3290 mPas⁻¹ to 10000 mPas⁻¹ (at a shear rate of 8.90 s⁻¹, Table 3.1) and starting oil density of 0.87 gcm⁻³ (Table 3.2). Forties crude formed stable emulsions which had a light-brown (chocolate) colour and semi-solid appearance in both emulsion categories B and C. The water content (the amount of water taken up by the continuous phase) was retained in the emulsions over a period of several months, and the emulsions remained stable without breaking. These results agree with findings by Fingas and Fieldhouse (2009), who also reported similar high water uptake in stable w/o emulsions. They also noted an average oil viscosity of 3.0 Pas⁻¹ (3000 mPas⁻¹) and similar density of the crude oil for the formation of a stable emulsions. This agreed with the data from this research, all stable emulsions having viscosities > 3,000 mPas⁻¹. The Forties oil, which had the highest percentage water contents (63.1% and 82.9%), produced the most viscous emulsions.

Meso-stable emulsions formed were a dark brown viscous liquid and mobile in texture. A meso-stable emulsion was formed with 11% weathered Brae A crude, which had a water content of 35.0%. The oil however attained a stable state in emulsion C, with a significant increase in water content (75.0%) and viscosity as shown in Table 3.2 and 3.3. The increased water content and viscosity are important factors which changes the stability of emulsions, and this was evident in the Brae A emulsion samples. The Brae A oil which formed the meso-stable emulsion had a density of 0.85 gcm⁻³ and an emulsion viscosity (2360 mPas⁻¹ measured at 8.90 s⁻¹). Fingas and Fieldhouse (2009) had noted

similar minimum properties such as an average oil viscosity of 3000 mPas^{-1} , as necessary for formation of meso-stable emulsions. The minimum properties may be considered to be the range of viscosity and oil density required for the formation of a meso-stable emulsion. It is however noted that meso-stable emulsions do not retain water taken up for long period and the water content in the emulsion may reduce considerably over time, leading to a change in the stability of the emulsion (Fingas and Fieldhouse, 2004; 2009). This was also observed for Brae A emulsions.

Another emulsion stability class formed by Stirling crude was entrained-water, a mobile and greasy black-brownish viscous liquid with a water content of 60.0% and viscosity of 3010 mPas^{-1} for the 11% weathered-oil emulsion B. The water content increased to 78.0% with a corresponding increase in viscosity (4610 mPas^{-1}) for emulsion C. Both emulsions had a starting oil density of 0.85 gcm^{-3} . A significant change in the stability of the Stirling emulsion from meso-stable to stable emulsion was observed in emulsion C, apparently due to the higher water uptake (78.0%) measured in the more weathered-oil emulsion sample.

Brent crude formed unstable emulsions in both emulsions B and C respectively. The unstable emulsions were dark brown in appearance with a fairly mobile texture. The emulsion properties are shown in Table 3.2. The water content increased from 40.1% to 54.0% with a corresponding increase in the emulsion viscosities as shown in Table 3.3 for the two categories (B and C) of weathered-oil emulsions. It was observed that the slight increase in viscosity (from 1980 to 2040 mPas^{-1}) in emulsion C corresponded with an increased water content (54.0%), though the emulsion formed remained with an inability to hold significant amounts of water.

Interestingly, weathering the Brent crude did not result in a significant increase in emulsion viscosity. Fingas and Fieldhouse (2009) in their studies had characterised the unstable emulsion class by its inability to hold significant amount of water. In these experiments it was observed that stable emulsions all had water contents of $> 54\%$.

3.6 Conclusion

Rheological measurements and properties of Forties, Brea A, Brent and Stirling crudes and its emulsion products have been investigated in this study. Various parameters known to influence the stability of water-in-oil emulsions have been studied in the emulsions formed using fresh, slightly weathered (11%; emulsion B) and more weathered (20%; emulsion C) samples. The crude oils yielded four distinct water-in-oil emulsions with varying stability classes: Stable, meso-stable, entrained water and unstable emulsions. The emulsions showed significant differences in terms of viscosity and water content. The following observations were made:

1. The four North Sea crude oils produced emulsions of different viscosities, water content and stabilities.
2. Four different emulsion states were observed: stable water-in-oil emulsions; meso-stable water-in-oil emulsions; entrained water; and unstable water-in-oil emulsions.
3. Emulsion viscosity increased with degree of oil weathering and water content.
4. There appeared to be a positive correlation between the density of the crude and the viscosity of the emulsion formed.
5. The most stable emulsions had the highest water content and viscosities.

The four North Sea crudes investigated were derived from the same source rock and had similar physical properties. Their differing emulsification behaviour may reflect differing chemical compositions, in particular their resins and asphaltenes which are known to play a role in oil emulsification. This was investigated in the next Chapter.

CHAPTER 4

4.1 CHEMICAL CHARACTERISATION OF FORTIES, BRENT, BRAE A AND STIRLING NORTH SEA CRUDE OILS

4.2 Introduction

Crude oils are complex mixtures of molecules encompassing a broad range of shapes and sizes (Tissot and Welte, 1984; Mullins and Sheu, 1988). They include molecules which are alkanes and relatively simple, to asphaltenes, which are complex and may interact strongly with one another (Mullins and Sheu, 1988). The properties of crude oils, including viscosity and phase behaviour are determined by the composition. Oil emulsification is an important process in crude oil phase behavior and a better understanding of the factors that affect their formation lies in an in-depth knowledge of the structures and interactions of the crude oil components. Of the crude oil fractions, asphaltenes and resins are reported to play an important role in hydrocarbon utilization, emulsion formation and stability. As stated earlier, the asphaltenes and resins are of primary interest due to their polar, surface-active nature and important role in stabilizing emulsions and crude oil processability (McLean and Kilpatrick, 1997; Merdrignac and Espinat, 2007; Mullins, 2001, 2008). Chemical characterization gives information on the chemical composition and functional groups in macromolecules. A number of techniques that probe these oil fractions have been outlined earlier in Chapter 1.7.2 of this study.

There have been advances, though certainly not comprehensive, in current knowledge in asphaltene and resin studies, where these fractions have been shown to have varied distributions of heteroatom functionality and presence of carboxylic acids, carbonyl, phenol, pyrroles, and pyridine functionality (Ignasiak *et al.*, 1977; Boduszynski *et al.*, 1980; Spiecker, 2001; Mullins *et al.*, 2007). For example, asphaltenes were fractionated from two Saudi Arabian crudes (Arab Heavy and Arab Berri) into acids, bases and residue fractions and analyzed by elemental microanalysis, ^1H and ^{13}C NMR, and

infrared spectroscopy (Hassan *et al.*, 1988). Their study revealed the predominance of some proportion of various fractions of the fractionated crude over other subfractions and in most cases these dominant fractions constituted nearly half of the original sample. The highest content of nitrogen was found in the base fraction of the Arab Heavy asphaltenes. The NMR spectra indicated a higher percentage of aromatic hydrocarbon atoms in the Arab Berri base fraction compared to Arab Heavy asphaltenes. There were also disproportionate H/C ratios where the ratios increased from one subfraction to another. The acids and bases from Arab Heavy asphaltenes had higher hydrogen/carbon ratios than those from Arab Berri asphaltenes. Such results and several others in the literature demonstrate the uniqueness and distinctiveness that can exist between fractions of generic asphaltenes and resins.

The four North Sea crudes investigated for their emulsification behaviour in Chapter 3 were characterized to further elucidate their chemical compositions of asphaltenes and other subfractions by Ultraviolet-fluorescence spectroscopy (UV-fluorescence spectroscopy), elemental microanalysis, Fourier transform infrared (FT-IR) spectroscopy, Nuclear Magnetic Resonance (NMR) spectroscopy, GC-FID/GC-MS and Saturates, Aromatic, Resins and Asphaltenes (SARA) fractionation.

The preliminary step was in the fractionation of the crude oils to obtain chemically distinct fractions, reasonable yields and reproducibility. Refinement of the experimental procedures ensured steady improvement in the yield fractions. A further objective was to understand the structure of asphaltenes and resins and how these vary in the different crude oil types even though they are all derived from the same source rock (Kimmeridge Clay) and consequently their composition should be expected to be similar. The analyses also investigated if the chemical or physical difference lies in the amount of asphaltenes and resins in each oil type. The comprehensive characterization of the oil properties could enable a further understanding of oil emulsification. It may also be useful to fluid chemist modelers in using structural characteristics of asphaltenes and other hydrocarbon components in predictive composition models for asphaltene behavior

regarding the propensity for emulsion formation and stability. This is discussed in Chapter 3 of this work. The information derived from these analyses was further used with model oil emulsion studies in the subsequent chapter to probe and give valuable insight into the mechanism through which crude oil emulsification and stability may proceed in the oil samples in this study.

Asphaltenes are highly absorptive in the visible spectrum, even into the near-infrared, while standard polycyclic aromatic hydrocarbons (PAHs) with four fused rings or fewer are all colourless. Asphaltenes therefore possess some large chromophores (Ruiz-Morales and Mullins, 2009). A chromophore is a chemical group capable of selective absorption resulting in the colouration of certain organic compounds. As a prelude to the characterization and analyses of the asphaltene component by optical techniques, an initial experimental study of the absorptivities and fluorescence spectroscopy of some aromatic compounds was carried out in order to provide background information on the optical range of interest for petroleum asphaltenes. Many recent studies have utilized various optical techniques to extensively study and understand the fluorescence of the asphaltene fraction of crude oil. A review of the historical development of those applications, as well as prior low and high-resolution mass spectrometry of petroleum, have been given by Smith *et al.*, (2007). One of the merits offered by use of optical spectroscopic techniques is that the samples are not destroyed since they are simply illuminated by a light beam.

A common (laboratory) definition of asphaltenes is that they are toluene soluble, *n*-heptane insoluble (Mullins, 2008). Asphaltene solution investigations have been conducted in pure toluene solvent (Goncalves *et al.*, 2004; Evdokimov, 2006; Mullins, 2009) and in *n*-heptane-toluene mixtures (Auflem, 2002; Rajagopal and Silva, 2004). Electronic spectra, obtained using UV-f spectrofluorometer, are usually measured on very dilute solutions, and more so for crude oil asphaltene which characteristically self-aggregate at high concentrations (Goncalves *et al.*, 2004; Mullins *et al.*, 2007).

The selection of appropriate solvents is an essential requirement for optimum absorbance and fluorescence performance when probing organic samples (Kemp, 1991; Evdokimov, 2006). The electronic spectra are usually measured on very dilute solutions and the solvent must be transparent within the wavelength range being examined (i.e. wavelength limit), since a strongly absorbing solvent will allow very little light to pass through the cells, and may lead to the photomultiplier not recording proper spectrum but a noisy background. The lower-wavelength limit for common spectroscopic-grade solvents are given by Kemp (1991). Below these limits the solvents show excessive absorbance and sample absorbance will not be recorded linearly. Certain wavelength limits, for instance, are given for some solvents for electronic spectroscopy: hexane (210 nm); diethyl ether (210 nm); and carbon tetrachloride (265 nm) etc. (Kemp, 1991). Some reasons have been given by Mullins (2006), that all fluorescence spectra of asphaltenes lack much emission from aromatics with one or two rings, at the 290 nm and 310 nm respectively and also from three-ring aromatics, although it is also stated that there is more emission here than for one and two-ring aromatics (Ruiz-Morales and Mullins, 2009). The reasons given are that, either the chromophores are not present in abundance in asphaltenes or they are present but predominantly undergo radiationless emission in asphaltenes. Small chromophores emit short wavelength light.

It is possible to study polycyclic aromatic hydrocarbons (PAH's) by their characteristic electronic absorption and fluorescence emission spectra and the interrelation between the PAH's, crude oil asphaltenes and resins can be ascertained. This is because the electronic absorption and emission spectra of asphaltenes are distinct and unique for each ring structure, and in particular recent research findings (Mullins *et al.*, 2009; Ruiz-Morales, 2002; 2004; Gutman and Ruiz-Morales, 2007) have explored and developed systematic rules governing the optical absorption spectra of PAHs in terms of the number of fused rings, their heteroatom content and configuration.

In the initial experiments described in this Chapter, six model aromatic compounds, ranging from two-ring (1-Methylnaphthalene) to seven fused aromatic rings (Coronene) in three different organic solvents and various concentrations respectively were studied by UV-fluorescence in order to investigate the electronic absorption and emission spectra given by these standard aromatic compounds prior to asphaltene solution studies in these solvents. These aromatic compounds (PAHs) were selected in terms of having acceptable ratios of isolated double-bond carbon/sextet carbon (Ruiz-Morales, 2004). A sextet carbon has only six electrons in its outermost valence shell instead of the eight valence electrons that ensures maximum stability (octet rule). Studies have established that aromatic sextet carbon dominates asphaltene PAHs, most probably due to the significantly enhanced stability of sextet carbon over that of isolated double-bond carbon [within the Clar representation],(Ruiz-Morale, 2004; 2007, Gutman and Ruiz-Morales, 2007). Moreover, recent asphaltene studies have indicated that the major characteristics of the optical absorption and fluorescence emission spectra of asphaltene are understandable in terms of PAHs with most probable 7 fused rings and a distribution of 4-10 rings (Ruiz-Morales and Mullins, 2007; Ruiz-Morales *et al.*, 2007).

Experiments in this study as shown in this Chapter, gives an illustration of the experimental and theoretical PAH distribution in aromatic compounds and principal maxima in UV-fluorescence spectra of the standard compounds. The experimental data in this study, and the theoretical data from previous studies given in the literature by other workers (Kemp 1991; Casper and Meyer, 1983; Ruiz-Morales and Mullins, 2009; Lakowicz, 2010), shows good agreement as discussed in this Chapter.

4.3 Experimental

4.4 Materials and methods

Forties and Brent crudes (BP, UK), Brae A crude (Marathon Oil Ltd. UK), Stirling Oil, UK. The crude oil samples used for the analyses were virgin crudes and did not undergo any processing or alteration prior to separation of the different fractions. Other materials include: aromatic standard compounds: 1-methylnaphthalene, phenanthrene, chrysene,

pyrene, perylene, coronene, spectrophotometric grade and HPLC grade dichloromethane (DCM), cyclohexane, toluene, tetrachloroethylene (Fisher Scientific, England), quartz glass cell (10 x 10mm; HELMA, United Kingdom), 250 ml and 500 ml round-bottom flasks (QUICKFIT, England), 125ml conical flasks; 60cm x 1cm Pasteur pipette (PYREX, USA), analytical balance (Mettler AT261 DeltaRange), volumetric flasks (Fisher Scientific, England), scintillation vials (12mm x 45mm; Chromacol Ltd. UK), anti-bumping granules (fused alumina); Fisons Scientific, UK., GFC filter paper (Whatman No.42), HPLC grade *n*-heptane, *n*-pentane, alumina, silica gel, potassium bromide (KBr) from Fisher Scientific, UK; cotton wool, ceramic Buchner funnels, high-purity glass microfiber thimbles (QUICKFIT, UK), rotary evaporator unit, UV-f spectrofluorometer (Shimadzu, RF-540; equipped with Shimadzu Data Recorder, DR-3).

Sample preparation of model PAH for UV-fluorescence analysis

Stock standard solutions of the aromatic compounds described in Material were prepared as follows: 10 mg of each compound was measured into a 10ml volumetric flask and made up to the mark with dichloromethane (DCM), giving concentrations of 500 mg/l for each aromatic standard. 50 μ l of stock standard in DCM was gently evaporated to dryness and redissolved in cyclohexane, toluene and tetrachloroethylene respectively. The resultant concentrations of 5 μ g/ml of each stock solution were preserved for analyses. The solutions were further serially diluted to different concentrations (ranging from 4 mg/l – 160 μ g/l) and analyzed on the UV-fluorescence. For the asphaltene and resin spectroscopy, optical properties of dilute solutions were kept at a concentration of 5 μ g/ml since further dilution did not change the fluorescence emission spectra.

Optical emission spectra of samples were measured using a UV-fluorescence spectrofluorometer (Shimadzu, RF-540), equipped with light filters consisting a Xenon Short arc lamp as excitation source for the fluorescence measurement. The spectra and total fluorescence intensity were recorded on a Shimadzu Data Recorder DR-3. A quartz glass cell with path length 10x10 mm was used for the solution samples. The samples

were initially scanned at an excitation wavelength of 254 nm and emission scan ranging from 264 nm – 900 nm.

Extraction and purification of crude oil asphaltenes

Separation of asphaltenes from crude oils

The crude oils were shaken vigorously to ensure homogeneity. British standard test method, IP-143 was used to determine the heptane insoluble asphaltene content of the crude petroleum. It is known that asphaltene may absorb some maltene (resins and oil fractions) during the *n*-heptane precipitation process. This is prevented with fractionated asphaltenes using a Soxhlet extraction to purify the asphaltene, with apparently no contamination of occluded resin and such other *n*-heptane soluble materials in the maltene (Trejo *et al.*, 2004; Groenzin and Mullins, 2000). An illustration of a Soxhlet extractor set-up is shown in Appendix 3, Figure 12. 3 x 1g of each crude oil was measured on a Mettler AT261 DeltaRange analytical balance (accurate to 0.0001 g) into three 500ml round-bottom flasks, and 100ml *n*-heptane (100:1 volumetric ratio) was added. Anti-bumping granules (fused alumina) was added into the mixture and heated under reflux for 120 min. The sample/solvent mixture was allowed to cool and filtered through with a GFC filter paper (Whatman No.42). The asphaltene precipitated during reflux was trapped in the filter paper. The flasks were thoroughly rinsed with hot *n*-heptane (2 x 20 ml) and the aliquot added to the filter. This two-stage filtration was to ensure complete removal and transfer of the asphaltenes that may have adhered to the flasks surface.

Separation of wax constituent from the asphaltenes

In order to separate the waxy constituents from the asphaltenes the filter paper, with the use of forceps, was placed in the Soxhlet apparatus, which served as the extraction unit, and then refluxed with 50 ml *n*-heptane for 60 min. These fractions of the *n*-heptane were retained for further quantification and analyses. Thereafter, the flasks were replaced and again refluxed with 160 ml toluene until all the asphaltenes was dissolved from the filter paper. This was ascertained when the solvent wash in the Soxhlet unit

became clear and colorless. The solvents were then reduced to small volume in a rotary evaporator and transferred to pre-weighed 20 ml scintillation vials (12 mm x 45 mm). The solutions were then reduced to dryness at ~100°C under vacuum to obtain pure solid free-flowing asphaltene. The vials were immediately re-weighed to determine the yield of asphaltene. 10ml of the following solvents: toluene; cyclohexane; and tetrachloroethylene respectively were added to each vial to provide sample concentrations, 200mg/L and stored in the absence of light ready for analyses.

Chromatographic separation of crude oil into Saturates, Aromatic, Resin and Asphaltene (SARA Analysis)

Chromatographic separation was carried out for the four North Sea crude oil types (Forties, Brae A, Stirling and Brent) to give the following fractions: Saturates, Aromatics, Resins and Asphaltenes (SARA). A total of three replicate fractionations were performed for each of the crude oil types. This fractionation process is also known as SARA analysis. The standard procedure for separating asphaltene as given by the IP-143 method, and detailed above, was used in the precipitation and fractionation of asphaltenes. The supernatants (maltenes) were concentrated to small volumes (1 ml) using a rotary evaporator at 30°C under reduced pressure and transferred to 20 ml vials. The saturate, aromatics and resin fractions were transferred to columns and extracted with solvents of increasing polarity (McLean and Kilpatrick, 1997; Auflem, 2002; Spiecker *et al.*, 2003; Bastow *et al.*, 2007). Three replicates fractionations were carried out in order to extract sufficient quantity for further quantification and for statistical analysis.

Standard column preparation

Standard columns were prepared using glass columns (Pasteur pipette 60 cm length x 1 cm internal diameter – PYREX, USA) fitted with a Teflon tap, each plugged with approximately the same size of cotton wool to ensure it occupies the same volume in each column. The columns were packed with 6g silica gel (chromatographic silica gel, 35 – 60 mesh) and 6 g of Alumina, and made uniform by slowly pouring in three bed volumes of *n*-pentane, with occasional tapping of the of the column to minimise trapped

air in the silica and prevent plug formation. The solvent in the column was drained down to the top of the silica gel/ alumina, avoiding damage to the prepared column, and collected into a 125 mL conical flask. This was to eliminate super-fine particles and any air trapped in the silica gel matrix.

Separation of saturate (aliphatic) and aromatic fractions

The maltene (filtrate) from each crude oil sample was carefully transferred into the top of the column. The aliphatic fraction was eluted with 60 ml HPLC grade *n*-pentane under gravity, initially using small aliquots (2 x 100 µl) of the sample to produce a concentrated band. To ensure a complete quantitative transfer of the sample into the column, the sample container was rinsed with 3 x 50 µl portion of the *n*-pentane and poured in allowing each portion to drain down the column. With the use of low boiling point solvents to prevent any loss of volatile compounds, the aromatic fractions were eluted using a mixture of 100 ml 60:40 (v/v) *n*-pentane: dichloromethane (Béhar *et al.*, 1989; Al Darouich *et al.* 2005), allowing each of the aliquot to elute from the column. A thorough rinsing with 3 x 50 µl portion of the solvent mixture was carried out to completely transfer the sample into the column. The eluate was collected into 125 mL conical flasks, and the colours from each fraction were noted. Three replicates fractionations were carried out in order to extract sufficient quantity for further quantification and for statistical analysis.

Separation of resin fractions

On complete fractionation of the saturate and aromatic fractions, a more polar binary solvent mixture (50ml 1:1 (v/v) toluene: methanol) was used to elute the resins. The solvents was then reduced to small volume under gentle stream of nitrogen and the eluates transferred to pre-weighed 20 ml scintillation vials (12 mm x 45 mm) with the use of 1ml of the *n*-pentane : DCM solvent, using a pipette. The aliphatic and aromatic fractions were carefully reduced at 30°C to constant weight minimise the loss of volatiles, and the resins fraction reduced at 50°C on a hot plate under gentle stream of nitrogen in a fume cupboard. The vials containing the eluates were reweighed on a chemical balance to determine the percentage mass based SARA - distribution of the

extracted fractions from each crude oil type. The percentage yield for each fraction of saturate, aromatic, resin and asphaltenes from each oil type was determined from the standard method (IP-143). The eluates were made up to 1.5 ml with *n*-pentane for the aliphatic and 1.5 ml hexane for the aromatics and resins to provide sample concentrations ready for GC-MS analysis (Bastow *et al.* 2007; Al Darouich *et al.* 2005). Three replicate fractionations were carried out in order to extract sufficient quantity for further quantification and for statistical analysis.

Elemental Analysis

Elemental composition analyses for carbon, hydrogen and nitrogen (C, H, N) and aggregate weight of the crude oil asphaltenes and resin fractions were determined using a 440 Elemental Analyzer from Control Equipment Corporation. The instrument was first calibrated with a suitable standard such as sulfamethazine and acetanilide (ASTM D5291).

FT-IR Spectroscopy

Fourier-transform infrared (FT-IR) spectra of the crude oil fractions were recorded on a Perkin Elmer Spectrum RX FT-IR System instrument in the transmission mode. The spectra were averaged from the accumulation of 32 scans with a resolution of 4 cm⁻¹ in the 4000-600 cm⁻¹ region. In the technique, samples were prepared by homogenizing with spectroscopic grade KBr and were run as KBr discs. The spectra were acquired relative to the KBr disc. Peak positions and areas were determined using the integrated software package in the instrument. This method obtains qualitative information about the relative amounts of functional groups such as pyrrolic nitrogen, saturate, aromatic, carbonyl carbon and sulfoxides.

¹H and ¹³C NMR

¹H and ¹³C NMR spectra were recorded using a Bruker DPX 400 spectrometer observing ¹H at 400MHz and ¹³C at 100MHz. Samples were dissolved in deuteriochloroform in 5 mm o.d. tubes and observed at 25°C. For ¹H spectra the spectral width was 20 part per

million (ppm) centred on 5ppm, and 64 scans were collected into 64K data points with a pulse interval of 4.19 sec. For ^{13}C spectra the spectral width was 240ppm, centred on 105ppm, and several thousand (typically 20 000) scans were collected, usually overnight, into 32K data points with a pulse interval of 2.18 sec. ^1H BB - decoupling was applied throughout, using the WALTZ-16 composite pulse decoupling sequence. Integration traces were recorded on the ^1H NMR spectra, and in general, this permits a quantitative estimate to be made of the relative amounts of each component in a mixture and also is a valuable quality control procedure in industrial laboratories. However, because of the low concentration of materials available the ^{13}C spectra were recorded without compensation for relaxation time or Nuclear Overhauser effect (NOE), so the intensities are not quantitative. Both techniques (^1H and ^{13}C NMR) were used in order to obtain structural information on the asphaltene and resin samples of the crude oils.

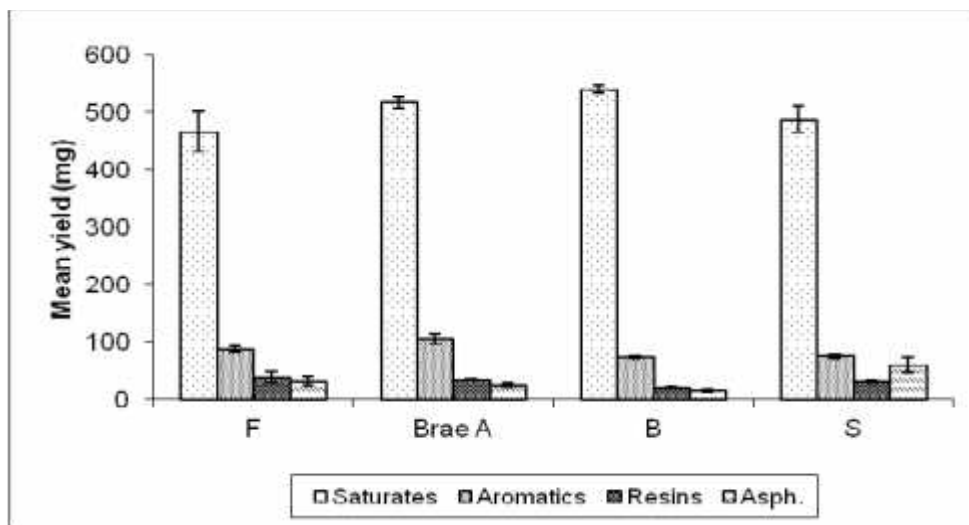
GC-FID/ GC-MS

GC-FID and GC-MS analyses of the aliphatic and aromatic fractions of the crude oils were carried out using Thermo Quest Trace GC, with a Flame Ionisation Detector (FID) and Gas Chromatography coupled to Mass Spectrometry (GC/MS). Detailed description of the GC-FID system has been given in Chapter 2.3.3. An aliquot of 1ml in *n*-pentane was prepared and 0.5 μl injected on-column mode into the GC. The GC-MS chromatograms of the aromatic fractions were obtained using an HP 6890 gas chromatograph system coupled with an HP 5972 A Mass Selective Detector with an HP Chemstation data handling package. The fractions were separated on an HP5 (30m length, 0.25 mm ID, 0.25 μm film thickness) capillary column in the splitless mode. The injector was initially set at 50°C, then heated to 250°C at rate of 120°C/min and kept at 250°C. The temperature was programmed to be initially held at 50°C for 15 min then increased by 3°C/ min to 250°C and held at this temperature for 30min. Helium was used as a carrier gas. The injected volume was 1 μl .

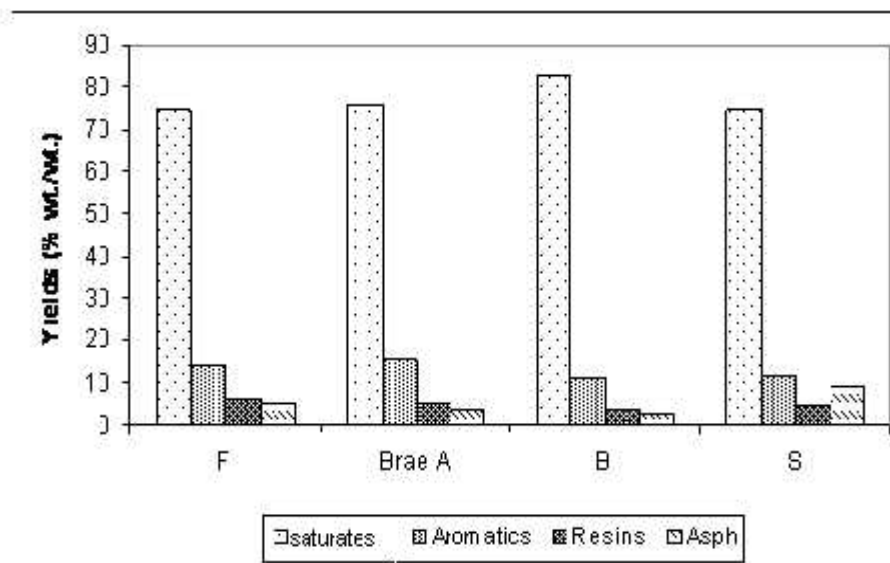
4.5 Results and Discussion

4.5.1 Saturates, Aromatics, Resins, Asphaltenes (SARA) Fractionation

Yields of various fractions from fractionation analyses are shown in Appendix C, Table 4 and 5 and Fig 35(a) respectively. A summary of the weight percentage (%) yields of each fraction is also given in Appendix C, Table 6 and Fig 35 (b)



(a)



(b)

Fig 35 (a) showing the mean yields from fractionations in Forties, Brae A, Brent (B) and Stirling (S) crude oils. The weight % yield of mean values of each fraction is shown in (35b).

The various fractions of the samples on complete elution from the column yielded a common colour pattern. The visual appearances of some fractions were visibly different, as summarized in Appendix C, Table 7.

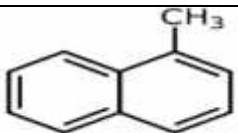

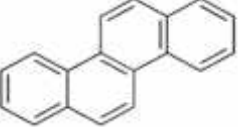
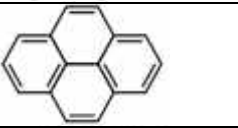
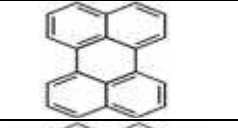

As expected, in all four crude samples, the aliphatic (saturates) fraction was the most abundant, followed by the aromatic component, with much less resins and asphaltenes. Brent yielded the highest amount of aliphatics compared to Forties, Brae A and Stirling. All four crude oil samples yielded a similar amount of aromatic in the fractionation. Brae A yielded a higher amount of aromatic component than Forties whereas the aromatic constituents in Stirling and Brent samples were similar.

The percentage yield of the resin fractions was higher in Forties, and was twice the amount yielded by Brent, with the lowest resin yield. Also Brae A yielded a higher resin fraction than Stirling. The followed trend can be given for the crude oil resin: Forties > Brae A > Stirling > Brent. However, the percentage yields of asphaltenes shown in Fig 35(b) indicated a considerably higher amount in Stirling compared to Forties, Brae A and Brent. The following trend can be given for the percentage asphaltene yield: Stirling > Forties > Brae A > Brent. Also, the total polar fraction (asphaltenes + resins) was much higher in Stirling sample (13.94) compared to a much lower content in Brent (5.67). Forties and Brae A samples yielded total polar fractions of 11.43 and 8.83 respectively. The amount of total polars (asphaltenes + resins) as shown in these results may indicate the characteristic emulsion forming capacity and stability in the different crude oil sample. Stirling and Forties samples with very high asphaltene contents from the result shown above, would form stable emulsions, whereas the results also indicated that Brent crude sample which had comparatively lower asphaltene content would exhibit the least propensity for emulsion formation and stability.

4.5.2 Fluorescence measurements for aromatic hydrocarbon standards and asphaltenes and resins from the crude oils

In crude oil spectroscopy, the electronic absorption and emission spectra of asphaltene are unique and characteristically distinct. An important and seemingly ongoing debate has been in ascertaining the types of polycyclic aromatic hydrocarbons (PAH's) contained in petroleum asphaltenes. Recent studies (Ruiz-Morales and Mullins, 2009) have investigated the main features of the UV absorption spectra of asphaltenes using PAH model compounds with a wide variety of distribution of aromatic ring systems. However, in this study, the UV-fluorescence emission spectra of aromatic compounds and asphaltenes were investigated.

Table 4.1 Theoretical and experimental principal maxima in the spectra of Aromatic Hydrocarbon compounds

Hydrocarbon compound	Structure	*Theoretical Principal maxima(nm)	**Experimental Principal maxima(nm)
1-ring methyl-naphthalene		450	335
3ring: Phenanthrene		294.23	350
4 ring: Chrysene		348.05	360
4 ring: Pyrene		343.28	360
5 ring: Perylene		~434	400
7 ring: Coronene		396	420

*(UV- absorption. Kemp, 1991; Ruiz-Morales and Mullins, 2009); **Experimental principal maxima measured UV-fluorescence

Using the synchronous scanning mode and a 10 nm wavelength incremental interval over the range λ_{ex} 254 – 875 nm, λ_{em} 264 – 885 nm, emission and fluorescence measurements were carried out for the aromatic standard solutions at different concentrations, ranging from 4 mg/L – 160 μ g/L. Synchronous excitation-emission spectra were recorded for samples in cyclohexane, toluene and tetrachloroethylene solutions respectively. The fluorescence intensity showed some variations when the spectra were recorded in the different solvents. Fluorescence emission spectra of tetrachloroethylene indicated poor emission. It is reported by Ralston *et al.* (1996) that chlorinated solvents can reduce fluorescence lifetimes somewhat by the heavy atom effect, where the intrinsic lifetimes refers to the lifetime of the fluorophore in a particular solvent when unperturbed by other quenching and energy transfer effects. However, fluorescence emission for six different aromatic compounds in cyclohexane solution were observed with good fluorescence emission band ranging from 340 nm – 445 nm (Appendix C, Fig 1a - f). There appeared to be a trend which showed a general increase in wavelength of emission maxima with ring number. However, this was not observed in the coronene compound (Appendix C, Fig 1f). Shift in the emission band was not observed when the solutions were diluted to lower concentrations and scanned at 15 nm and 25 nm wavelength intervals respectively. This indicated that the PAH solutions were able to give emission and fluorescence measurable at these spectral range. However, good emission and fluorescence measurements were obtained at 4 mg/L concentration of the aromatic standard compound within a range of spectral maxima in cyclohexane solution. In general, the PAH's (aromatic standards) with high number of fused aromatic rings, especially coronene (7-rings) (Appendix C, Fig 1f), exhibited electronic emission in the ~450 nm range were asphaltenes often fluoresce according to previous studies (Ruiz-Morales and Mullins (2009).

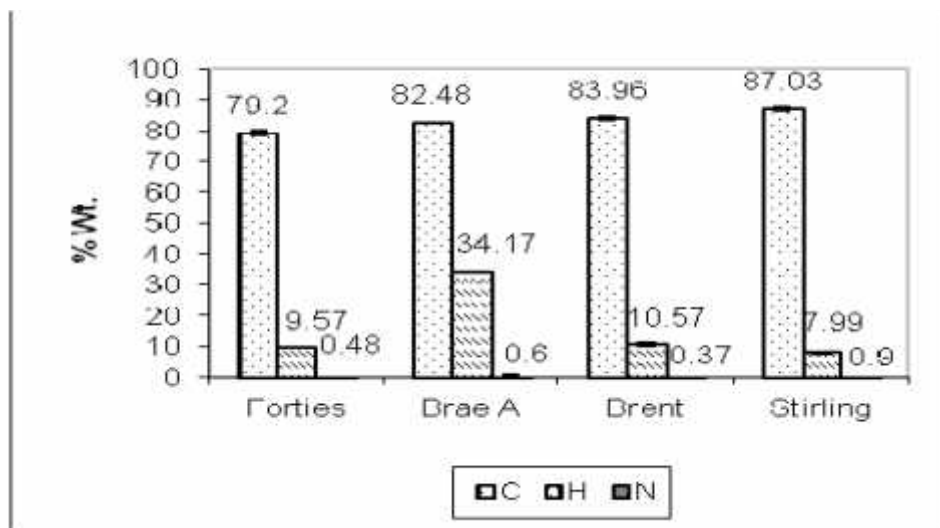
The fluorescence emission spectra can be used to ascertain population distributions of different sized aromatic rings (Ralston *et al.*, 2006) and this was also used in this study to investigate if asphaltenes derived from different crude oil types give similar fluorescence. The UV-f spectra of asphaltenes of the crude oils in this study are shown in Appendix C, Fig 2 a - c. Though some studies have shown that asphaltenes lack much

UV- fluorescence for smaller ring aromatics at certain wavelengths, these spectra are very typical for asphaltenes exhibiting fluorescence maxima in the ~ 450 nm range. The experiments were carried out using very dilute solutions (4 mg/L to 160 μ g/L concentrations) and at λ_{ex} 254 – 875 nm; λ_{em} 264 – 885 nm range. Fig 2 a - c in Appendix C shows the spectra for the asphaltenes samples respectively. Forties asphaltene indicated fluorescence with emission maxima at ~ 460 nm. Brent asphaltene exhibited good fluorescence emission maxima at about 460 nm with some spectral emission at ~ 400 nm. The result indicated that the emission maxima in the Forties asphaltene corresponded with the emission maxima in the perylene standard compound. The results here are consistent with a similar study by Ruiz-Morales and Mullins (2009), where electronic absorption of asphaltenes were observed at ~ 450 nm using dilute sample solutions. However, Brae A asphaltene indicated multiple emission maxima in the ~ 350 nm to 430 nm with rather low intensity, in contrast to the emission maxima in Forties and Brent asphaltenes respectively. Though these results may indicate relatively small populations of small aromatic ring systems in asphaltenes, as opposed to larger ring systems, it is difficult to completely ascertain these population ratios due to the molecular complexity of asphaltenes and again the somewhat unknown optical constants of the contributing structures. Relatively broad spectral bands were observed in Stirling asphaltene solution, even at the most dilute concentration possibly reported for asphaltene fluorescence. These broad spectral bands were also observed for the resin fractions of all samples. Intramolecular energy transfer and quenching may have an increasing impact on the fluorescence lifetimes of asphaltene at high concentrations. Using dilute asphaltene concentrations, these effects were not detectable, hence it is apparent that the fluorescence emission spectra of the Forties, Brae A, Brent and Stirling asphaltene solutions are intrinsic and therefore inherently belong to the optical character of the investigated crude oil asphaltenes samples.

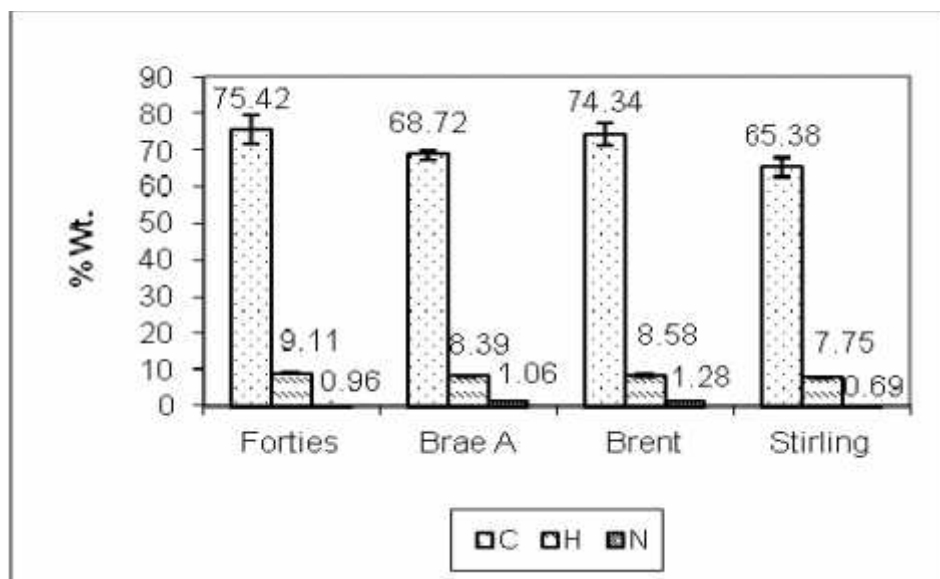
4.5.3 Elemental analysis

The elemental compositions of carbon (C), hydrogen (H) and nitrogen (N) of the polar fractions (i.e. asphaltenes, resins) and the aromatic fractions of the Forties, Brae A,

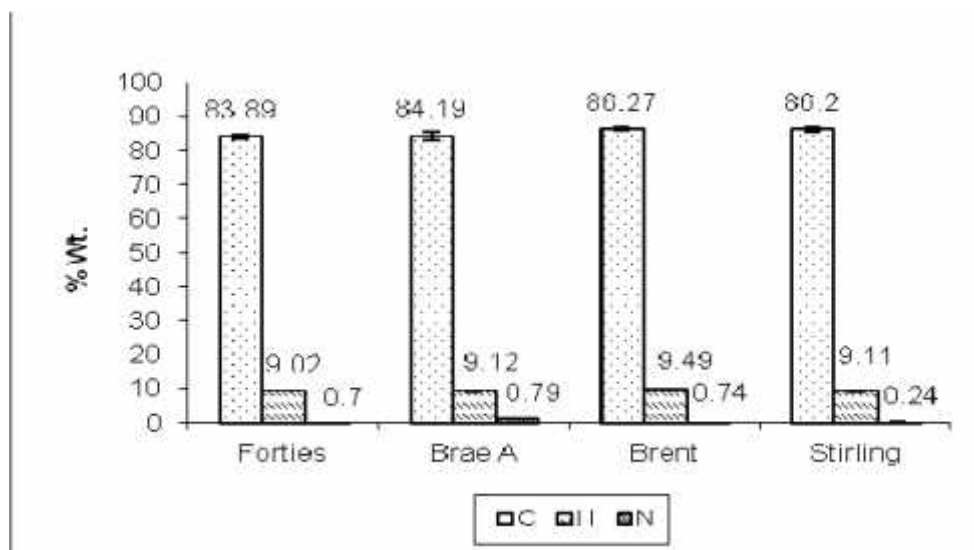
Brent and Stirling crudes were measured. The values in terms of mean parameter values of %C, %H, %N and compositions hydrogen/carbon ratios (H/C), along with their calculations, are shown in Appendix C (Table 2) and Fig.36 (a - c) and Fig 37 respectively. These results, as indicated in the elemental compositions, reveal significant difference in the four crude oils.



(a) Asphaltene



(b) Resin



(c) Aromatics

Fig 36 showing the comparison of yield of C, H, N analysis of Asphaltene (a), Resin (b), and aromatics (c), fractions isolated from the 4 oil types by elemental analyses.

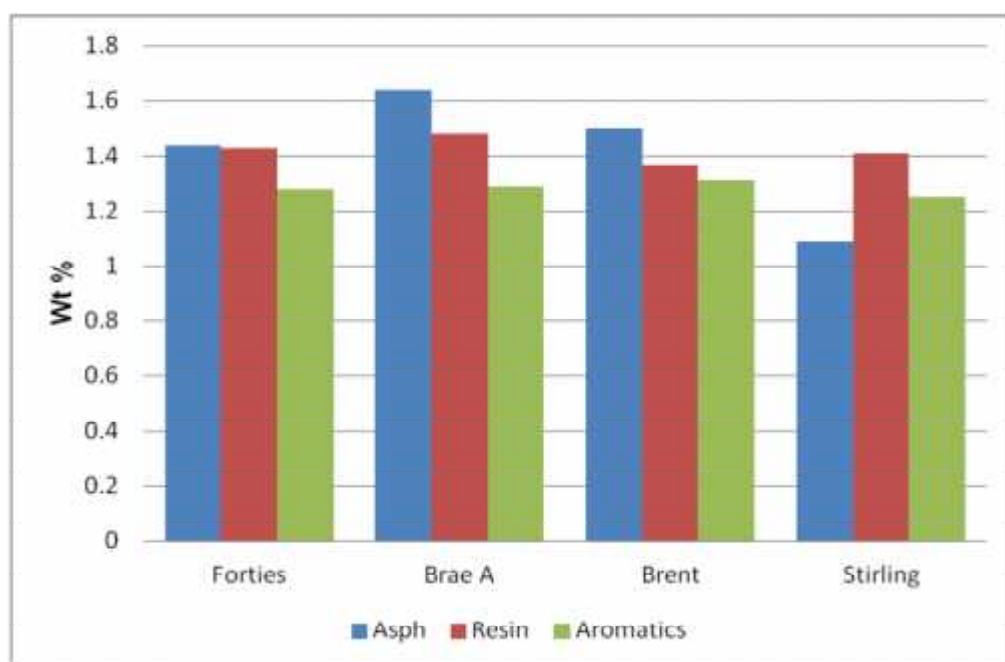


Fig 37a Comparison of H/C ratios in crude oil fractions (asphaltenes, resins and aromatics) isolated from the 4 oil types by elemental analyses.

The results of the elemental analyses indicate that the % C content was significantly greater in the aromatics fraction than in resin fractions in Brae A and Stirling, but only slightly greater in Forties and Brent. The % C was similar in Brae A, and same in Stirling asphaltene and aromatic samples respectively, as shown in Appendix C, Table 1 and 2. Again, the results also indicated a significantly lower % C measured in Stirling resin (65.38%) compared to resin fractions of other samples as shown in Fig 36(a – c). A lower %H compared to % C was measured in the aromatics, asphaltene and resin fractions of the four crude oils and the lower value of % H to % C in the aromatic fraction is consistent with similar findings by other researchers on the elemental analysis of crude oil fractions (McLean and Kilpatrick, 1997; Trejo *et al*, 2004; Elsharkawy *et al.*, 2008; Merdignac and Espinat, 2007).

Fig 37a and Appendix C (Table 3) indicates the H/C ratios in the fractions of the four oil samples. As can be seen in Fig 37, the H/C ratio was similar (1.44 and 1.43) respectively in the asphaltene and resin fractions of Forties sample. The result showed considerably the highest H/C ratio in Brae A asphaltene (1.64) and resin (1.48) compared to the fractions in Forties, Brent and Stirling respectively. Similarly, the H/C ratio was considerably higher in Brae A asphaltene compared to the resin and aromatic fractions of the same oil. In contrast, a greater difference was indicated in the H/C ratio between Stirling asphaltene and its resin and aromatic fractions where the H/C ratio was significantly higher in the resin fraction. This result in the Stirling crude sample indicated that the resin fraction contains less aromatic hydrogen whereas the asphaltene counterpart contained the highest aromatic hydrogen in the fractions of the four crudes in general. The H/C ratio in asphaltene fractions followed the trend: Brae A > Brent > Forties > Stirling whereas the H/C ratio in the resin fraction was: Brae A > Forties > Stirling > Brent. The trend in H/C ratio in the aromatic fraction was: Brent > Brae A > Forties > Stirling.

Spiecker (2001) had also investigated the elemental compositions in Arab Heavy, Canadon Seco and Hondo crude oils, and Elsharkawy *et al.*(2008) also studied the elemental compositions in crude oils from the Kuwaiti Burgan oil field, and reported similar variations in H/C ratio of some crude oil fractions. It is reported (Spiecker, 2001) that decreased aromaticity in crude oil resins confers a considerably higher solubility in more aliphatic solvents than asphaltenes. The H/C ratio highlights the differences in terms of the aromaticity factor and number of aromatic carbons in the asphaltene, resin and aromatics fractions of the four oil types. The results indicated that the asphaltene in Brae A can be seen to be more aliphatic (i.e., higher H/C value) and/or less condensed than the asphaltene fractions of the other three oil types. An important finding in the result revealed that the H/C ratio in Stirling asphaltene fractions was significantly lower than the other three oils. A lower H/C value suggests the possibility of a more aromatic character in the crude oil fraction as reported by McLean and Kilpatrick, 1997; Speight, 2004. The results of the asphaltene values measured in this study also agree well with findings by Spiecker (2001) where H/C ratios in the range between 1.0 and 1.2, which was found in Stirling asphaltene only, may indicate that much of the asphaltene backbone consists of fused aromatic carbon interspersed with polar functional groups containing 5 to 7 heteroatoms, according to Spiecker (2001). In all, the elemental analyses indicated a consistent high values among the H/C ratios of the polar fractions, except the asphaltene in Stirling crude, in contrast to the lower H/C ratios in the aromatic fractions of the crudes. The exception specific to Stirling is most probably due to the low content in functional groups that also enables strong hydrogen bonding interactions between resins and asphaltenes as was further confirmed by FT-IR analysis which revealed low functional groups in the Stirling asphaltene. The low functional group also conferred a lower polarity on the Stirling asphaltene.

Nitrogen (N) content may indicate the polarity in oil fractions (McLean and Kilpatrick, 1997; Speight, 2004). The %N in the resins fractions of the four oil types in this study varied from 0.69 to 1.28%, whereas the %N in the asphaltene and aromatic fractions in the four oil types varied from 0.37 to 0.90% and 0.24 – 0.79% respectively. Resins contain polar heteroatoms. As indicated in Fig 36 (a-c) and Appendix C (Table 2), Brent

crude with 1.28 %N in the resin fraction was apparently the most polar of the four crude oils, and Stirling the least polar.

The %N content in each of the oil fractions was generally significantly higher in the resins compared to the asphaltene and aromatics fractions with the exception of Stirling. The most significant difference in the %N was measured in Brent crude with 1.28% for the resin, 0.37% for the asphaltene and 0.74% for the aromatics fractions respectively. The trend in %N content in the resin fractions was: Brent > Brae A > Forties > Stirling. The trend in the asphaltene fraction was: Stirling > Brae A > Forties > Brent whereas the trend in the aromatics fraction was: Brae A > Brent > Forties > Stirling.

4.5.4 Fourier-Transform Infrared (FT-IR) spectroscopy

Fourier-Transform Infrared (FT-IR) spectroscopy is a useful technique for determining the chemical composition of crude oil asphaltene and resin fractions. Information regarding the polar functional group distributions can be drawn from this analytical technique (Anderson, 1994; Spiecker, 2001; Mullins *et al.*, 2007) and also the analyses of the oil fractions can reveal many groups capable of forming hydrocarbon bonds. Several investigations have indicated the presence of carboxylic acids, carbonyls, phenols (O-H) and pyrrolic and pyridinic nitrogen (N-H) (Boduszynski *et al.*, 1980; McLean and Kilpatrick, 1997; Mullins and Sheu, 1998; Merdrignac and Espinat, 2007). The functional group distribution from the FT-IR analyses in this study is given in Table 4.2

Table 4.2 Functional Group distribution for Forties, Brae A, Brent and Stirling oil fractions from FT-IR analyses indicating various peak heights (cm) at characteristic absorption bands.

Functional group		CH ₂ CH ₃ (saturate)	C=C, C=O (carbonyl)	OH and NH (pyrrole)	C-O,C- N,-CH stretching	C-H (aromatic) bending region
Peak wave number (cm ⁻¹)		~3000	~1375 - 1700	~3500	~1000	~800
<i>Crude oil type</i>	<i>Fraction</i>					
Forties	<i>Asph.</i>	9.4;8.5	3.2; 3.8; 6.2; 1.6; 1.8	4.5	1.6	2.0
	<i>Resin</i>	7.0; 6.5	2.8; 3.0; 1.8	2.0	1.5	0.4
	<i>Arom.</i>	2.5	0.5; 2.0; 0.5			0.5
Brae A	<i>Asph.</i>	5.9; 9.3; 5.4	1.3; 1.3; 2.0; 1.0; 0.6	3.0	0.5; 0.5; 0.5	0.2; 0.2
	<i>Resin</i>	7.0; 5.5	1.0; 3.0; 1.8	1.7	1.5	1.3
	<i>Arom.</i>	6.4; 5.0		1.6	2.0	
Brent	<i>Asph.</i>	5.0; 4.0	1.0; 2.0; 0.9	1.2		0.2
	<i>Resin</i>	3.0; 2.7	0.2; 0.3; 1.4; 0.4	1.0	0.2; 0.3	0.1; 0.2
	<i>Arom.</i>	7.0	2.0; 6.0; 2.4			2.8
Stirling	<i>Asph.</i>	10.0; 6.1	2.5; 3.6; 2.5	2.5	2.0	
	<i>Resin</i>	8.0; 6.5	2.5; 3.7; 2.0		1.8	
	<i>Arom.</i>	3.7; 3.0	0.6; 2.0; 0.6	0.5		0.3

N/B: Multiple values indicate more than one peak in each functional group.

Table 4.3 Some major chemical differences in Forties, Brae A, Brent and Stirling crude oil types using various analytical equipment

Property	Crude oil type			
	Forties	Brent	Brae A	Stirling
Alkyl side chain (FT-IR, NMR, Elemental analysis)	<i>Medium</i> +++	<i>Large</i> ++++	<i>Medium</i> +++	<i>Small</i> ++
Amount of condensed aromatic rings (UV-f, Elemental analysis, NMR)	<i>Medium</i> +++	<i>Medium</i> +++	<i>Small</i> ++	<i>Large</i> ++++
Carbon type in each fraction (NMR): <i>Asph:</i> <i>Arom:</i> <i>Resins:</i>	<i>10</i> <i>15</i> <i>18</i>	<i>12</i> <i>16</i> <i>24</i>	<i>9</i> <i>9</i> <i>18</i>	<i>14</i> <i>16</i> <i>14</i>
Total carbon types	<i>43</i>	<i>52</i>	<i>36</i>	<i>44</i>
Polarity (Elemental analysis, NMR, FT-IR)	++ (<i>polar</i>)	++++ (<i>most polar</i>)	+++ (<i>polar</i>)	+ (<i>least polar</i>)

NB: (+) represents the degree of polarity and alkylation

FT-IR transmission spectra were obtained for the asphaltenes, resins and aromatics fractions of Forties, Brae A, Brent and Stirling crudes. The spectra exhibited bands of variable intensities in the regions ranging from $\sim 500 - 3600 \text{ cm}^{-1}$. The spectra of the asphaltene samples are shown in (Appendix C, Fig 3 a – d), the spectra of the resin samples are shown in (Appendix C, Fig 4 a – d) and the spectra of the aromatic samples are shown in (Appendix C, Fig 5 a – d) respectively, with the peaks that enable the identification of specific functional groups relevant to asphaltene aggregation, as shown in each spectrum.

In nearly all of the samples analyzed, the saturates (CH_2 & CH_3) were relatively the most abundant followed by the least abundant in the (O-H) and (N-H) contents. The low concentrations of the O-H and N-H groups in the asphaltenes and resins and their near absence in the aromatic fractions were significant. This is because these groups are often considered important for asphaltene aggregation phenomena through hydrogen bonding as reported in related research studies (Kardim and Sarbar, 1999; Spiecker, 2001; Elsharkawy *et al.*, 2008). Indeed, Spiecker (2001) had reported that the most plausible mechanism of asphaltene aggregation included hydrogen bonding between functional groups and other charge transfer interactions.

Two apparent qualitative similarities were observed in all the spectra where they all exhibited large absorbance intensities (up to 60.52%) for the aliphatic $\text{CH}_2\text{-CH}_3$ stretches in the wavelength region from ~ 2800 to 3000 cm^{-1} , with exception of the aromatic samples of Forties and Stirling and the resins of Brent, respectively. Secondly all the samples showed large absorbance intensities (11- 60%) in the CH_3 bending region in the $1380 - 1500\text{ cm}^{-1}$. In addition, the spectra also showed that the asphaltenes and resins contained absorbances in the free O-H stretch. These were absent from the aromatic fractions.

Clearly, the spectra revealed certain significant differences mostly in the bending region ($1380 - 1500\text{ cm}^{-1}$) and the C-O, C-N stretching regions ($\sim 1000\text{ cm}^{-1}$) and C-H-bending region ($700 - 900\text{ cm}^{-1}$) among the asphaltenes, resins and aromatics samples of the same oil type. In the Forties, Brent and Stirling oil types, the asphaltenes (Appendix C, Fig 3a, 3c and 3d), resin (Appendix C, Fig 4a, 4c and 4d) and the aromatics samples (Appendix C, Fig 5a, 5c and 5d), exhibited more identifiable absorbance bands in the CH-bending regions and the stretching regions. An exceptional case in the spectra was indicated in the Brae A aromatic spectra, where only a singular low intensity absorbance in the C=O (carbonyl region) was recorded (Appendix C, Fig 5b). However, in contrast, several characteristic absorbances in the C=O region were exhibited in the asphaltene and resin spectra of the Brae A (Appendix C, Fig 3b and Fig 4b).

Forties aromatic fraction showed characteristic absorption corresponding to C-H and three C=C stretch appeared at 1600 cm^{-1} , 1455 cm^{-1} and 1376 cm^{-1} respectively (Appendix C, Fig 5a). A typical characteristic of most aromatic compounds is the near absence of bands at $\sim 700\text{ cm}^{-1}$ C-H bending region (Kemp, 1991). Here, a singular band appeared at 746 cm^{-1} . However, Brae A aromatic showed characteristic absorption corresponding to C-H stretch appearing at 2923 cm^{-1} . Also, one C=C stretch appeared at 1456 cm^{-1} . Characteristically, no bands appeared at the C-H region as shown in (Appendix C, Fig 5(b)). This was very characteristic of aromatic compounds as reported by Kemp, 1991. Brent aromatic showed C=C stretches at 1601 cm^{-1} , 1456 cm^{-1} and 1376 cm^{-1} . A singular C-H band appeared at 746 cm^{-1} (Appendix C, Fig 5(c)). Stirling aromatic showed characteristic absorption corresponding to C-H stretch appearing at 2923 cm^{-1} and 2852 cm^{-1} . Three C=C stretches appeared at 1599 cm^{-1} , 1456 cm^{-1} and 1376 cm^{-1} . One C-H stretch appeared at 747 cm^{-1} (Appendix C, Fig 5(d)). A close similarity was indicated in the characteristic absorptions of Forties and Stirling aromatics, though the spectra in Brent resins however revealed a higher characteristic absorption in the CH-bending region and the stretching regions. It was also seen that the Brent resin had a characteristic absorption at 1657 cm^{-1} (Appendix C, Fig 4c), assigned to the amide group ($1670 - 1620\text{ cm}^{-1}$). Amide groups are highly polar (Weast, 1980), and the Brent resin fraction was therefore considered to be the most polar of the four resin fractions investigated. In addition, the differences were greater and more pronounced when comparing the spectra of fractions from the different oil types. In the aromatic fractions of the oil types, significant difference were indicated in the spectra of the various oil types with Brae A aromatics sample showing the lowest characteristic absorption bands in the bending region as can be seen in Appendix C, Fig 5(b).

In the asphaltene samples (Appendix C, Fig 3 a - d), the spectra showed bands of variable intensities for the four oil types. Brent asphaltene sample showed the lowest characteristic absorption appearing at 1611 cm^{-1} , 1462 cm^{-1} and 1377 cm^{-1} in the CH-bending region and the stretching regions compared to Forties, Brae A and Stirling oil types. Brae A asphaltene sample showed a higher characteristic absorption corresponding to C=C stretch appearing at 1650 cm^{-1} , 1614 cm^{-1} , 1460 cm^{-1} , 1378 cm^{-1}

and 1270 cm^{-1} . Forties asphaltene sample showed characteristic absorption band appearing at 1691cm^{-1} , 1605cm^{-1} , 1460cm^{-1} , 1374 cm^{-1} and 1261cm^{-1} . All the spectra of asphaltenes in the four oil samples showed characteristic absorption corresponding to CH_2CH_3 stretch. The spectra also showed differences in the wide and distinct distribution in the functional groups, and variable intensities by a measure of each peak height in the spectra of the characteristic absorption of the various samples. The peak height of absorption in each functional group in the asphaltenes, resins and aromatic fractions of the four oil samples, together with the different functional groups, are shown in Table 4.2.

Based on the FTIR spectra, clear difference can be seen in the wide distribution of bands of variable intensities in the various fractions of the different crude oil types analyzed. These results may enhance the investigation and understanding of the interactions between the polar components (i.e., asphaltenes and resins) and the aromatics fractions in each crude oil type. Mingyuan *et al.*, (1992), had separated resins and asphaltenes and studied the FT-IR spectrum and the emulsions formed by each fraction. The fractions were tested in model systems for their emulsion-forming tendencies. Model emulsions were stabilized by both asphaltene and resin fractions, but the asphaltene fractions were much more stable.

Crude oil resins are known to enhance the dispersion of asphaltenes (McLean and Kilpatrick, 1997; Mullins *et al.*, 2007).

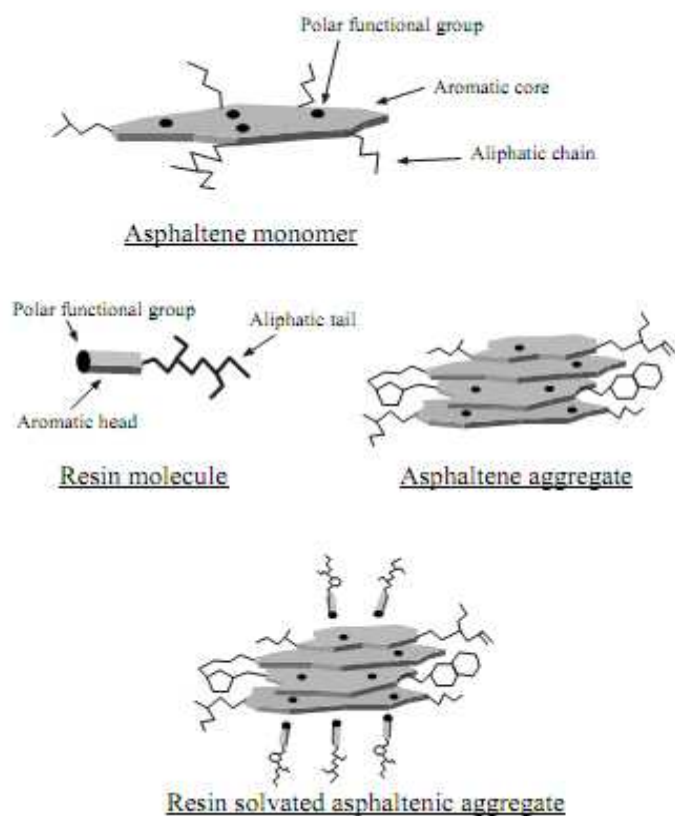


Fig 37b. Schematic diagram of the proposed mechanism of interactions between resins and asphaltenes. Polydispersed monomers of asphaltenes stack cofacially with resins near the exposed top and bottom surfaces. (Adapted from Spiecker, 2001)

However, despite being claimed as one of the substances that is crucial to the stabilization of water-in-crude oil emulsions, studies by Kilpatrick *et al.*, (2001) have suggested otherwise. Based on their study, resins are not necessarily essential for stabilization of the rigid film encapsulating the water droplets. This notion is also supported by Auflem (2002) who argues that the asphaltenes tend to aggregate when the water phase is introduced to the oil system while resins are likely to shed and do not participate in the formation of interfacial film. In addition to this, investigations by Schorling *et al.*, (1999) have shown that water-in-crude oil emulsion stability increases

with decreasing resin/asphaltene ratio which suggests the importance of asphaltenes over resins. Studies have reported that a determining factor in the solubilizing character of the resins appears to be hydrogen bonding (Hagen *et al.*, 1989; Elsharkawy *et al.*, 2008), though the solubility may not necessarily be a function of its general carbon-hydrogen skeleton and its chemical functionality alone but depends on interactions with other substances that may act as co-solvents. Hydrogen bonding between a phenolic hydroxyl group in a resin molecule and a proton bonded to oxygen (e.g., pyrrole, pyridine, carboxylic etc.) in the asphaltenes molecule leads to a resin-asphaltene agglomerate (McLean and Kilpatrick, 1997). These aggregations, and in general the nature of dispersion of the asphaltenes, are known to have a significant effect on the emulsification character of a specific crude oil type (Spiecker, 2001; Auflem, 2002). As asphaltenes are considered the most aromatic portion of crude oil, the aromaticity of the resins and the crude medium can also affect the solubility of the asphaltenes. The functionality of the asphaltene constituents is generally defined in terms of several commonly occurring natural product types that are more in sync with the recognized maturation pathways than any of the structures previously conceived. The compositions in terms of compound class, the functionality and aromaticity of the polar surface-active resins and asphaltenes and the aromatics constituents as shown in the FT-IR spectra of the four different crudes oils in this study may be practically useful in furthering the understanding between the scope of interaction and emulsifying potential of crude oils.

4.5.5 ^1H and ^{13}C NMR (Nuclear Magnetic Resonance)

Nuclear Magnetic Resonance (NMR) is an analytical tool that is concerned with the magnetic properties of certain atomic nuclei, notably the nucleus of the hydrogen atom (proton), and that of the Carbon -13 isotope of the carbon. The use of NMR to study a molecule enables the record of the differences in the magnetic properties of the various magnetic nuclei present, and to determine, to a greater extent, the positions of these nuclei within the molecule (Kemp, 1991). It is also possible to deduce the number of different kinds of environment there are in the molecule, and normally how many atoms are present in each of these environments, and which atoms are present in neighbouring groups.

As given in Chapter 1, Section 1.7.2, ^{13}C nuclear magnetic resonance spectroscopy is a useful non-destructive tool in crude oil and petroleum product analysis. This technique is very attractive in that it provides an accurate value of aromatic carbon content as a fraction of the total carbon and hence enables an excellent characterization of complex, multicomponent petroleum fractions (Jennings *et al.*, 1992). The excellent resolving capability, enhanced sensitivity and accuracy of the NMR analytical technique have been utilized in chemical characterization of petroleum fractions. Several authors have reported the utilization of the NMR in crude oil studies, and some of the applications that have been published in the use of the NMR include structural study of residues or asphaltenes (Hamid, 2000; Masuda *et al.*, 1996; Sharma *et al.*, 2000a, b; Merdrignac and Espinat, 2007). The Carbon types are observed directly in ^{13}C NMR spectroscopy, and can be readily quantified under appropriate conditions.

The aim of the analyses in this section was to explore the aspects of polar (asphaltene and resin) and aromatic chemical structure that gives a unique character to these fractions, especially the asphaltenes of crude oil. A set of asphaltenes, resins and aromatics isolated from the four different crude oil types were investigated to study the different peripheral and internal carbon in aromatic ring systems (i.e. structural parameters in the aromatic and aliphatic carbon) in order to identify key chemical parameters that particularly differentiate, by way of specific identity, the asphaltenes, resins and the aromatics of one crude oil type from another. The spectra were divided into two general regions for analysis: the aromatic region (110 – 160 ppm) and the aliphatic region (5-60 ppm). A sharp peak appeared in all spectra at 77.5 ppm corresponding to the sample deuterated chloroform used as a standard solvent in NMR spectroscopy.

^1H and ^{13}C NMR of Asphaltene Fractions

The ^1H NMR spectra of Forties, Brae A, Brent and Stirling asphaltene samples indicated a close similarity in all the spectra. This is shown in Appendix C, Fig 7a, 8a, 9a, and 10a respectively. However, the ^1H spectrum for Stirling asphaltene fraction indicated a high intensity peak at the region of 2.4 ppm. This observation of hydrogen in the H_α region

for Stirling asphaltene was absent in the fractions from Forties, Brae A and Brent asphaltenes. The spectra are able to distinguish between aromatic hydrogen (H_{ar}) and aliphatic hydrogen in the different positions in a branch (H_{α} , H_{β} , and H_{γ}). Seidl *et al.*, 2004; and Merdrignac and Espinat, 2007 have shown that the chemical shift range applied to identify the different hydrogens is as follows: 0.5–1 for H_{γ} , 1.0–2.0 for H_{β} , 2.0–4.0 for H_{α} , and 6.0–9.0 for H_{ar} .

Several relatively sharp resonances with varied carbon types were observed for the ^{13}C spectra of the asphaltenes. All the asphaltenes samples contained substantial proportion of aromatic to aliphatic carbon, supporting the widely held opinion in asphaltene studies that asphaltene consist primarily of fused aromatics with an aliphatic periphery. A common similarity in the spectra of the four samples was in the very high signal for carbon type exhibited at 30 ppm. Clear and considerable differences were revealed in the spectra in the aliphatic region ranging from 0 - 60 ppm. There were more carbon types; ten (10) for Stirling asphaltene fraction (Table 4.3) and (Appendix C, Fig 10a) in contrast to seven (7) for Forties and nine (9) carbon types each for Brae A and Brent asphaltenes fractions respectively. This is of significance as it tends to highlight the structural differences in the carbon backbone of these crude oil asphaltene fractions. The aromatic region of 110 – 180 ppm was characteristically broad and featureless for the Brae A asphaltene, whereas the spectrum of the Stirling asphaltene revealed four (4) peaks representing carbon types with comparatively higher intensities in contrast to Forties with three (3) carbon types of low intensity and Brent asphaltene fractions respectively.

It can be observed clearly from the ^{13}C NMR spectra, an indication of more aromatic rings in Stirling crude asphaltene compared to Brae A and Forties asphaltenes. The differences are more pronounced for Stirling asphaltene. The analysis also revealed a higher aromaticity factor in Stirling asphaltene in comparison to fractions from Forties and Brae A. Importantly, this evidence from the NMR spectrum is of great complementary significance and strongly supports the results and deductions regarding

the significantly lower hydrogen/carbon (H/C) ratio of Stirling asphaltene (suggesting a more aromatic character) as previously discussed in Section 4.5.2 of this Chapter. From a chemical comparison standpoint, these differences observed in the spectra of the analysed fractions may indicate a more complex chemical structure in the Stirling asphaltene.

^1H and ^{13}C NMR of Resins fractions:

The resins fractions isolated from Forties, Brae A, Brent and Stirling crudes respectively were analysed by NMR spectrometry. This is shown in Appendix C, Fig. 7b, 8b, 9b and 10b respectively. Again, subtle differences were observed for the ^1H NMR spectra of the resin fractions, with the spectra of Brae A and Brent resins indicating low intensity peaks at 3.5 ppm and 4.3 ppm regions respectively (Appendix C, Fig.8b and 9b). This feature was not observed in the ^1H NMR spectra of Forties and Stirling crude resins.

The two major carbon types, aromatic and aliphatic as described earlier in Section 4.5.4 of this Chapter, were distinguished in the ^{13}C NMR spectra. The spectra revealed differences in the chemical nature of the resins (Appendix 3, Fig.7e - 9e and 10e) respectively. In the aliphatic regions (0 – 60 ppm) a total of sixteen (16) carbon types were observed for the resin fraction from Forties (Appendix C, Fig 7e); fifteen (15) carbon types from Brae (Appendix C, Fig.8e) and eleven (11) carbon types for Stirling resins (Appendix C, Fig.10e) fractions respectively. The aromatic region of 110 – 180 ppm indicated a similarity in the number of carbon types for Brae A and Stirling resins, with both having three (3) carbon types and the peaks observed at similar regions of the spectra respectively.

However, the spectra revealed, even with varying peak intensities, clear and considerable differences in the aromatic region for Brent resin, in comparison with resin fractions of the other oil types. A total of twenty four (24) peaks for carbon types were indicated with 17 carbons in the aliphatic region between 0 – 60 ppm and 7 carbons in

the aromatic region (110 – 180 ppm) of the Brent resin sample (Appendix C, Fig 9e). In contrast, two (2) carbon types were observed in the spectrum of aromatic region for Forties resin fraction. The analyses above also reveals the differences in aromaticity factor in the three resin fractions. An important result in the spectra was the fact that the resins exhibited much more content of aliphatic carbon, compared to the asphaltenes and aromatics, which corresponds to large alkyl chains and limited fused aromatic ring presence. Again, the high content of aromatic carbon also in the resins, which makes it less aromatic than asphaltenes, would probably promote good interaction that may lead to ready solubilization of the asphaltenes. This observation is also in agreement with previous findings reported by Spiecker (2001).

¹H and ¹³C NMR of Aromatics fractions:

In order to further investigate the structural character of the crude oil samples, the aromatics fractions of the Forties, Brae A, Brent and Stirling crudes were analysed. ¹H NMR spectra of the aromatics samples are shown Appendix C, Fig 7c - 10c respectively. The spectra revealed very close similarities in all four oils. However, the spectra for Brent aromatics indicated a peak with high intensity at 0.2 ppm as shown in Appendix C, Fig 9c.

The ¹³C NMR spectra of the aromatic fractions of Forties, Brae A, Brent and Stirling are shown in Appendix C, Fig 7f - 10f respectively. All of the spectra indicated very high spectral signals at 30 ppm of the aliphatic region (110 - 180 ppm) in the samples. The aromatic region (110 – 180 ppm) was broad and featureless for all four samples. The aromatic samples showed obvious differences in the chemical nature of the four crude oil types as indicated in the ¹³C NMR spectra. Sixteen carbon types were observed in both Brent and Stirling aromatics samples respectively (Table 4.3) and (Appendix C, Fig 9f and 10f) in the 110 - 180 ppm region whereas Forties aromatics contained fifteen carbon types. Comparatively, Brae A aromatics indicated the least number (9) of carbon types. The significance of the differing number of carbon types is that it indicates the different peripheral and internal carbon in aromatic ring systems (i.e. structural parameters in the aromatic and aliphatic carbon). The ¹H and ¹³C NMR analyses of the various fractions of the four crude oil types have shown some structural information on

the organic structures of the samples. However, the overall ^1H and ^{13}C spectra of the asphaltenes, resins and aromatics samples of the crude oils analysed indicate obvious chemical differences, as shown in Table 4.3, which may help explain the differing emulsification behaviour of the four crude oils. They may also find very valuable application for oil spill fingerprinting.

4.5.6 GC-FID/ GC-MS analyses

GC-FID and GC/MS analyses of aliphatic and aromatics fractions of Forties, Brae A, Brent and Stirling crude oil samples were carried out. Qualitative data for aliphatic and aromatic hydrocarbons in the range of $n\text{-C}_9$ to $n\text{-C}_{28}$ were obtained for both fractions in all the samples. The chromatograms for the aliphatic fractions are shown in Appendix C, Fig 6a – d, while the chromatograms for aromatic fractions are shown in Fig. 11a – d, respectively. The GC-FID chromatograms revealed the aliphatic samples of the four crude oil types contained a homologous series of normal alkanes but each indicated a distinct normal alkane profile. Close inspection of the chromatograms also revealed some differences in the relative abundance of the n -alkanes, measured by the peak heights in the four oil fractions.

Table 4.4 GC-FID of *n*- alkanes in aliphatic fractions of Forties, Brent, Brae A and Stirling crude oils types showing percentage peak heights (mm), relative to *n*- C₂₅

<i>n</i> -alkanes	Peak height (mm)			
	Forties	Brent	Brae A	Stirling
C ₉	37.5	62.5	0	0
C ₁₀	125	275	33.3	60
C ₁₁	200	375	106.7	300
C ₁₂	375	750	220	520
C ₁₃	312.5	625	200	480
C ₁₄	312.5	625	233.3	500
C ₁₅	300	625	200	500
C ₁₆	325	400	233.3	480
C ₁₇	306.3	437.5	226.7	400
C ₁₈	281.3	375	233.3	380
C ₁₉	268.8	375	200	370
C ₂₀	237.5	312.5	180	320
C ₂₁	187.5	250	133.3	250
C ₂₂	168.8	187.5	133.3	220
C ₂₃	143.8	175	100	190
C ₂₄	125	125	100	150
C ₂₅	100	100	100	100
C ₂₆	93.8	62.5	60	90
C ₂₇	56.3	50	40	50
C ₂₈	31.3	25	0	0

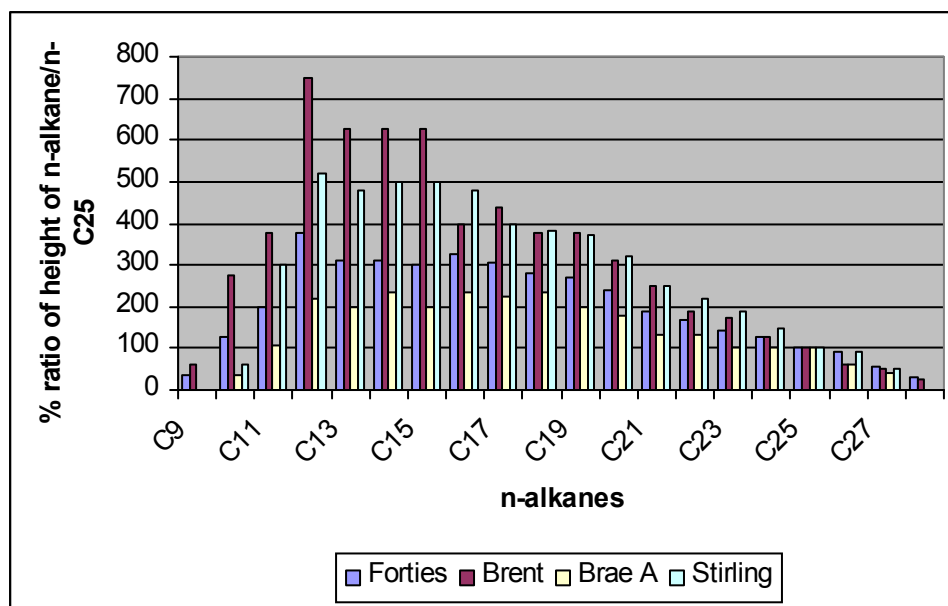


Fig.37c The peak heights from the chromatograms of aliphatic fractions from SARA fractionation (Appendix 3, Fig 6a – d) shown as percentage of the ratio of the height of the *n*-alkanes to the height of *n*- C₂₅

The peak heights in the aliphatic fractions of the four oils are shown in Table 4.4 and Fig 37b. Forties and Brent aliphatic samples contained the most abundant compounds compared to Brae A and Stirling aliphatic samples as shown in Appendix C, Fig 6a - d respectively. The aromatic hydrocarbon distributions are shown in Figures 11(a-d) in Appendix C. The fractions are dominated by 2-5 ring PAH and their alkyl homologues. The distributions from Forties to Brae A were very similar, indicating a fairly even distribution of peaks across the chromatogram. The Brent crude contained a greater abundance of naphthalenes and phenanthrenes compared to higher molecular weight PAH whereas the opposite was true for Stirling. Overall, the chromatograms suggest that all four crudes contained the same compounds but with differing abundance.

4.6 Conclusion

1. The analyses of the crude oils by SARA fractionation yielded four distinct fractions namely: saturates, aromatics, resins and asphalttenes.
2. The aliphatic was the most abundant of all fractions in the four crudes with the highest percentage yield in Brent crude. Brae A yielded the highest percentage of aromatic, while Forties yielded the highest percentage of resins, whereas Stirling yielded the highest percentage of asphalttenes.
3. In the UV-fluorescence analysis, emission spectra were obtained for six different aromatic compounds from 340 nm – 445 nm and there appeared to be a trend which showed a general increase in wavelength of emission maxima with ring number, the exception of coronene. Good UV-fluorescence emission was obtained for the aromatic standard compounds in cyclohexane solution.
4. Both Forties and Brent asphalttenes exhibited fluorescence with emission maxima at ~460 nm which corresponded to that of the perylene standard compound, whereas Brae A asphaltene exhibited multiple UV-fluorescence emission of low intensity, ranging from ~350 – 430 nm.
5. From the CHN elemental analysis, the results indicated the asphaltene fraction from Brae A could be seen to be more aliphatic and/or more less condensed than the aromatic fractions from the other three oils.
6. Brent crude was the most polar, and Stirling the least polar of all four crudes.
7. From the FT-IR analysis, the saturates (CH_2 & CH_3) were relatively the most abundant, and the least abundant was the (O-H) and (N-H) constituents. The low contents of O-H and N-H groups were of significance since these groups are often considered important for asphaltene aggregation.

8. All the spectra of asphaltenes in the four oil samples showed characteristic absorptions corresponding to the CH_2CH_3 stretch.
9. The FT-IR spectra revealed a wide and distinct distribution in the functional groups and variable intensities. The spectra also revealed more alkyl side chain in Brent than in the other three oil types.
10. As crude oil resins are known to enhance the dispersion of asphaltenes, the nature of its interaction, alongside other constituents may have a significant effect on emulsification character of a specific crude oil type.
11. The results may enhance the understanding of the polar components (asphaltenes and resins), and the aromatic fractions in the four different oil types, and may be practically useful in giving insight into the scope of interaction of the different constituents and emulsification character of the crude oils.
12. The results of the ^1H NMR spectra indicated close similarity in all asphaltenes of the four crude oils. The spectra were able to distinguish between aromatic hydrogen and aliphatic hydrogen.
13. The ^{13}C NMR spectra revealed that all the asphaltene samples contained substantial proportion of aromatic to aliphatic carbon.
14. From the NMR spectra the resins were seen to exhibit much more aliphatic carbon than asphaltenes and aromatics, which correspond to large alkyl chains and limited fused aromatic presence.
15. The overall ^1H and ^{13}C spectra of the asphaltenes, resins and aromatics samples of the crude oils analysed indicated obvious chemical differences, which may also find very valuable application for oil spill fingerprinting.

16. The GC-FID showed that the aliphatic samples of the four crude oil types contained a homologous series of *n*-alkanes with some differences in the relative abundances of the *n*-alkanes. The GC-MS showed that the aromatic fractions are dominated by 2-5 ring PAH and their alkyl homologues, with similar distributions for Forties and Brae A. A greater abundance of naphthenes and phenanthrenes were contained in Brent crude. In general, the chromatograms suggest that all four crudes contained the same compounds but with differing abundances. These results will complement and enhance the understanding of the profound effects of these compositions on emulsions formation and stability.

CHAPTER 5

5.1 AN INVESTIGATION OF THE ROLE OF ASPHALTENES AND RESINS IN THE STABILITY OF CRUDE AND MODEL WATER-IN-OIL EMULSIFICATION

5.2 Introduction

In the petroleum industry, current researches suggest that specific crude oil compositions are likely to contribute a fundamental role in water-in-oil emulsion stability. Emulsion stability is widely used to describe the persistence of an emulsion in the environment, and has been identified as an important characteristic of water-in-oil emulsions. The crude oil emulsifying agents include native sub-classes such as resins, asphaltenes as well as hydrocarbon waxes. Although the interfacial relationship between asphaltenes and resins has been conventionally cited as the predominant factor that determines stability in crude oil emulsions, there exist disagreements however, regarding the fundamental role played by these key crude oil solubility classes in the emulsification process.

Many researchers have studied emulsification by using model oils or modified crude oils, while some researchers studied emulsions as thin layers of droplets (Fingas and Fieldhouse, 2009; McLean and Kilpatrick, 1997; Hemmingston *et al.*, 2005). Given the well recognized researched opinions that the stability of emulsions is an interplay between the heavy components (asphaltenes, resins, porphyrins, etc.,) and waxes, it is worthy to state that typically in a crude oil without water, the asphaltenes are dispersed by the lighter components and are therefore prevented from precipitation (Mullins and Sheu, 1998; Premuzic and Lin, 1999; Spiecker *et al.*, 2003). When water is mixed into the crude oil a new interface is created leading to a new distribution of the heavy components. It is reported that resins are more interfacially active than the asphaltenes, which means that these molecules will initially cover the fresh water-in-oil interface. As a consequence of this, the solubility conditions of the asphaltenes will drastically change and a precipitation will occur. With a lot of aqueous droplets present the asphaltene

particles will accumulate at the surface of the droplets with a very high total surface area. In this way, there are possibilities to rigidify the “monolayer” of resins initially adsorbed at the interface. The central mechanism will therefore be both steric and particle stabilization (Mullins and Sheu, 1998).

Crude oil fractionation is an important necessary step in separating the multi-component mixture of the hydrocarbons into its various fractions. A conventional and convenient method of achieving the separation is by fractionating the crude oil into four major fractions to obtain the following fractions: saturates, aromatics, resins and asphaltenes (SARA) as a function of their solubility and polarity in paraffinic and specific solvents. A detailed description of the fractionation process has been given in Chapter 4, Section 4, and basically involves the removal of asphaltenes by a combination of solvent induced precipitation, followed by column chromatographic separation of the maltenes (deasphalted oil) into saturates, aromatics and resins. The amounts of each fraction can then be determined by the gravimetry.

5.2.1 *Saturates*

In the four classes of compounds derived from the fractionation, only the saturates are clearly distinguishable from the rest of the compounds in the hydrocarbon mixture. This is because the absence of π - bonds allows the saturates to be readily differentiated from the aromatic constituent as a function of the differences in polarities of the components. π – bonds, or π - π interaction is a noncovalent interaction between organic compounds containing aromatic moieties, and act strongly on flat PAH's such as Coronene because of the many delocalized π -electrons in the orbital configuration. The aromatics and heteroatom compounds in the maltenes have different degrees of condensation and constitute a compositional continuum in respect of molecular weight and polarity (Auflem, 2002). Saturates fractions are nonpolar and consist of normal alkanes (*n*-paraffins), branched alkanes (iso-paraffins) and cyclo-alkanes (naphthenes). The saturates fraction constitutes the largest single source of hydrocarbons or waxes generally classified as paraffin wax, microcrystalline wax or petrolatum (Lira-Galeana and Hammami, 2000).

5.2.2 Aromatics

Aromatics are hydrocarbons which are chemically and physically very different from the paraffins and naphthenes of the saturates, containing one or more ring structures similar to benzene. The atoms are connected by aromatic double bonds (Hammami and Ratulowski, 2004).

5.2.3 Resins

Resins are defined as the non-volatile and polar fraction of crude oil that is soluble in *n*-alkanes (e.g. pentane) and aromatic solvents (e.g. toluene) and insoluble in liquid propane. They are known to peptize asphaltenes. Structurally, they are similar to asphaltenes, but with lower molar mass and lower heteroatom content. Higher hydrogen/carbon ratios compared to asphaltenes have also been reported (Auflem, 2002). Resins are thought to be molecular precursors of asphaltenes. They are very important in the stability of petroleum by preventing the separation of the asphaltene constituents as a separate phase (Li *et al.*, 1997; Premuzic and Lin, 1999). The polar heads of the resins surround the asphaltenes while the aliphatic tails extend into the oil. After asphaltenes, resins are the most polar and aromatic fractions in crude oil and have been suggested to contribute to the overall solubility of asphaltenes in crude oil by creating a solvating layer on the polar and aromatic portions of the asphaltenic aggregates in the oil solution (Nalwaya, 1999; Spiecker and Kilpatrick, 2001). Spiecker and Kilpatrick have shown that the addition of resins at the ratios of 2:1 (resins: asphaltenes) or less could increase the stability of water-in-oil emulsions by as much as twice. Other studies have noted that the resins and asphaltenes are somehow tied together in emulsion stability. Sjoblom *et al.* (2007) in their work had noted that a significant aspect of the stability differences in emulsions can be explained by the interactions between asphaltenes and resins. They concluded that asphaltenes are believed to be suspended as colloids in the oil with some stabilization by resins. Each particle is believed to consist of one or more sheets of asphaltene monomers and absorbed resins to stabilize the suspension. Under certain conditions, the resins can desorb from the asphaltenes leading to increased asphaltene aggregation and precipitation of the larger asphaltene aggregates. This premise has led several authors to

note that there is significant interplay between asphaltenes and resins and that resins solvate the asphaltenes in water-in-oil emulsions (Murgich and Strausz, 2001; Spiecker *et al.*, 2003). Thus, resins play an important role in precipitation and crude oil emulsification. A proposed molecular structure of resins is depicted in Fig.38 based on chemical analyses.

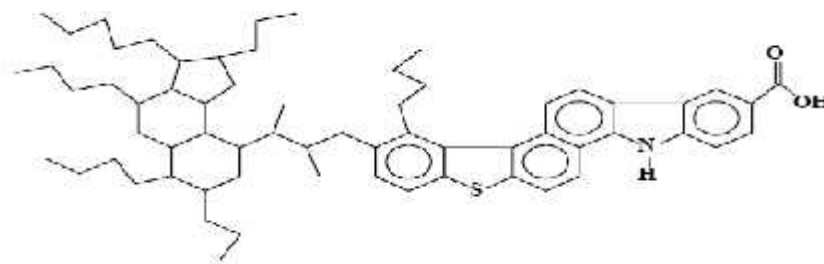


Fig.38 Molecular structure of crude oil resin (Adapted from Spiecker, 2001).

5.2.4 Asphaltenes

Asphaltenes are arbitrarily defined as the portion of crude oil that is insoluble in *n*-alkanes such as *n*-heptane or *n*-pentane but soluble in toluene, benzene or dichloromethane (Hammami *et al.*, 2000; Stankiewicz *et al.*, 2002; Mullins *et al.*, 2007). In general, asphaltenes are characterized by fused ring aromaticity, aliphatic side chains, and polar heteroatoms containing functional groups and trace metals (e.g., Ni, V, Fe). Presently, the actual chemical structure of asphaltenes has been difficult to define using existing analytical techniques and therefore remains an important area of ongoing research and contention. Until recently, the molecular weight of asphaltenes was believed to be ~ 3000 g/mol. However, current research suggests the molecular weight averages about 750 g/mol (Groenzin *et al.*, 2003; Mullins *et al.*, 2007; Strausz *et al.*, 2008). However, a recent and somewhat tenable argument by Creek (2005) is that structure is important provided it is related to function and reactivity, and suggested the consideration of an integrated approach, rather than a stylized “molecule” for asphaltenes. Based on chemical analyses, average asphaltene structures are illustrated in Fig. 39.

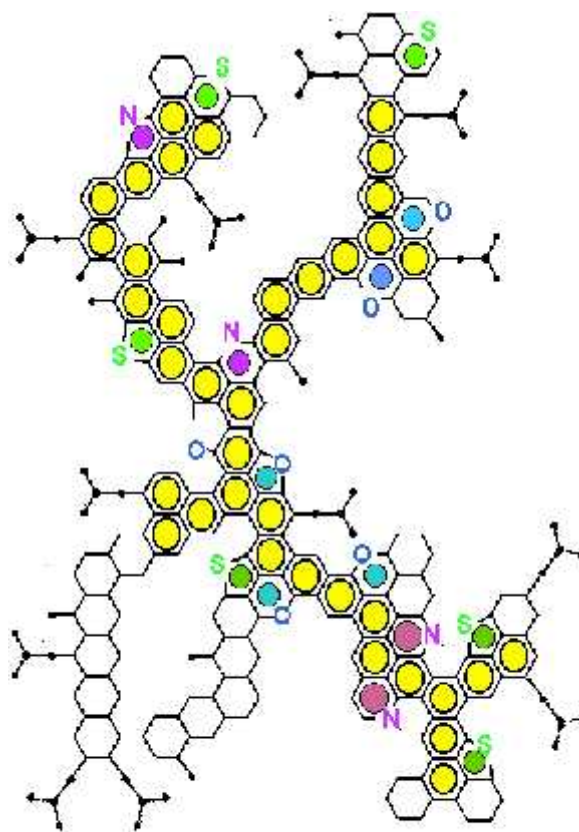


Fig. 39 Crude oil asphaltene hypothetical molecular structures (Adapted from Aske, 2002).

Asphaltenes play an important role in crude oil emulsification and stability. The scope of knowledge of water-in-oil emulsion formation is currently strongly limited by the extent of knowledge of asphaltenes and resins themselves (Sjoblom *et al.*, 2003; 2007). Several researchers have noted that there are differences in the stability of emulsions, depending on the fractions of asphaltenes taken and also by the amount of asphaltene aggregation (Spiecker *et al.*, 2003; Abdurahman and Yunus, 2006; Schorling *et al.*, 1999). A number of studies by some workers have also reviewed the results of research on emulsions formation with the general conclusion that the asphaltene content is the most important factor in emulsion formation. Kokal (2002) studied several factors causing the formation of emulsion in oil fields and found that there is a strong correlation of asphaltene content of crude oil with emulsion stability. Even in the absence of any other compounds that may act in synergy (i.e. resins, waxes and aromatics), asphaltenes were found to be

capable of forming rigid cross-linked elastic films which are the primary agents in stabilizing water-in-crude oil emulsions. It was noted that the exact conformations in which asphaltenes organize at the oil-water interfaces and the corresponding intermolecular interactions have not been fully elucidated (Kilpatrick, 2001; Spiecker, 2001). Generally, suggestions often proposed as explanation are H-bonding between acidic functional groups (such as carboxyl, pyrrolic and sulfoxide), electron donor-acceptor bonding between transition metal atoms and electron-rich polar functional groups, or some other type of force such as π -bonding between delocalized π electrons in fused aromatic rings (Fingas and Fieldhouse, 2008). Moreover, research in petroleum asphaltenes in relation to water-in-oil emulsions has in recent years seen a leap in new perspectives and results. However, of these investigations, only a few have broadly studied the asphaltene subfractions in relation to emulsion behavior and even fewer on crude oils from the North Sea Oilfields.

Schorling *et al.* (1999) had investigated the influence of resin type and the asphaltene/resin ratio on emulsion stability in model oils. They found that the influence of resins in the presence of asphaltenes on the properties of emulsions was independent of the origin or source of the resins and, also that high resin/asphaltene ratios decrease the emulsion stability. By contrast, Midttun *et al.* (2000), had investigated the effect of crude oil resins with various polar characters on the stability of water-in-oil model emulsions containing asphaltenes, at different ratios. They found that resins with different polar character have different effects on the emulsion stability, and at the asphaltene/resin ratio of 1 and 5:3 the resins in some cases lead to an emulsion stability higher than that of a similar emulsion stabilized by asphaltenes only, while at asphaltene/resin ratios of $\sim 1:3$, the emulsion stability was reduced by the resins. Their research concluded that the effect on emulsion stability when combining two different resin fractions depended on the resin types combined as well as the relative amount of resins and asphaltenes. Emulsion formation and stabilizing effects of the asphaltene and resin fractions of oils from the Saudi Arabian fields have also been studied by Kadim and Sarbar (1999). Their results showed evidence of crude oil properties having a direct correlation with the tendency of these fractions to form stable emulsions. On the other

hand, effects of demulsifiers on water-in-oil emulsions have been investigated in oils from Malaysian and Middle East oilfields by Abdurahman and Yunus (2009) and a strong connection in performance was established between some emulsifiers and coalescence. Fingas and Fieldhouse (2009) had extensively characterized emulsion types from crude oil products from Canadian oil fields and correlated the emulsion stability with starting oil composition and properties.

Again, literature has revealed that a bulk of these researches has been selectively dominated by studies on the interfacial activities of asphaltenes and resins in the drilling and production aspects of petroleum production, thereby relegating to the background the effects of these crude oil components on emulsification after oil spillage and the huge environmental and economic cost that may arise from it. An in-depth understanding of asphaltene subfraction chemistry and behavior in crude oil emulsions will clearly enhance the overall knowledge in crude oils studies and interfacial emulsion forming properties.

5.3 Experimental objectives

Experiments in this chapter will investigate whether crude oil asphaltenes and resins of different North Sea crude oils have different influences on the stability of the water-in-oil emulsions obtained. The experiments involve the isolation of asphaltene fractions from each oil type and recombination with the other oils to investigate if substituting the asphaltenes from one oil to another will have an effect on the emulsification characteristics of the resultant “model oil”. The influence of varying the ratios of crude oil asphaltenes to resins on emulsification, as well as the effect of varying the asphaltene/resin ratios in a solution of decahydronaphthalene, used as a synthetic oil (composed of decahydronaphthalene (DHN) and *n*-heptane), was also investigated.

The emulsion forming capability and stability of the emulsions formed from these experiments was studied in relation to the corresponding asphaltenes and resins

subfractions used, in view of the fact that asphaltenes and resins from different crude oil types can have wide and distinguishable properties that may determine their overall chemical and physical properties.

5.4 Experimental

5.4.1 Materials

Dean & Stark apparatus, Top Drive Macerator propeller (Townsend & Mercer Ltd, Croydon, England), Thermo Haake Viscotester VT500, 150mL glass beakers (Fisher Scientific – England), analytical balance (Mettler AT261 DeltaRange), seawater (filtered to 1 micron, St. Andrews, UK), HPLC grade *n*- heptane, HPLC decahydronaphthalene (Sigma-Aldrich), North Sea crude oils (Forties, Brae A, Brent, Stirling), 20 mL scintillation vials.

5.4.2 Method

Asphaltenes and resins fractions were isolated from Forties, Brae A, Brent and Stirling North Sea crude oils by the SARA fractionation technique. Details of the precipitation and SARA fractionation are given previously in Chapter 4, Section 4. The isolated subfractions formed the basis for model oil formation.

Fractionation and recombination of Brent crude oil was initially carried out, and the viscosities and water contents were measured. The objective was to see whether emulsions formed from fractionated crude oil will retain, or have the same viscosity and water content as originally measured in the whole oil. Thereafter, four sets of experiments were carried out where the deasphalted crudes were combined with Forties, Brent, Brae A and Stirling asphaltenes fractions respectively and their subsequent emulsification behaviour investigated. Synthetic oils with varying asphaltene/resin contents were also prepared. The objective was to investigate the effect of the ratios of asphaltene/resin fractions on the emulsification behaviour of the crude oil.

For these experiments, the experimental setup was scaled down from those described in Chapter 2, Section 3.3, with the use of 70ml seawater and 10 ml oil fraction to form water-in-oil emulsions with the four different crude oil types. The water contents were measured as described in Chapter 3, Section 3.2. Viscosity measurements were carried out on a Thermo Haake Viscotester VT500 fitted with a standard NV cup measuring system. The same proportion in weight of asphaltenes fractions as obtained in the original crude, ‘donor crude’, from fractionations was used in preparing the combinations in the model oils, i.e. the total amount of asphaltenes obtained in each oil was added to a deasphalted fraction of another oil, ‘recipient oil’.

As an initial step, synthetic oil, a solution of 10ml decahydronaphthalene (DHN) and 23.3 ml *n*-heptane, was added to 70 ml seawater in a glass beaker to prepare an emulsion and kept as control. The viscosity of the control emulsion was measured.

For each of the emulsions formed in the above experiments, water content was measured by Dean & Stark method (ASTM D95), and reported as weight percentage.

Fractionation and recombination of Brent crude oil

To investigate and determine the possibility of emulsions formed from fractionated crude oil to retain, or have the same viscosity and water content as originally measured in the whole oil (i.e. when the crude oil was not separated by fractionation). Brent crude oil was randomly selected and 10 ml of the crude was measured into a 500 ml round-bottom flask. 250 ml *n*-heptane was added and the solution was refluxed in a Soxhlet apparatus for two (2) hours. The solution was filtered through with Whatman No. 42 filter paper and the filter paper was then refluxed with 100 ml *n*-heptane for one (1) hour. The 250 ml and 100 ml *n*-heptane extracts were combined giving a total of 350ml solution, containing 10ml of the Brent crude dissolved in it. The filter paper was then refluxed with 150 ml toluene until all the asphaltene was dissolved from the filter paper into the toluene. This was ascertained when the solution in the Soxhlet apparatus was

colourless. The 350 ml *n*-heptane extract was re-combined with the 150 ml toluene extract and the solution was reduced to 10 ml using a rotary evaporator, resulting in a re-constituted crude oil. The weight was ascertained by weighing on an analytical balance (Mettler AT261 DeltaRange). Emulsions were formed with the 10 ml re-constituted crude oils and another emulsion with that of the deasphalted crude oil. The viscosities and water contents were measured to determine if the viscosities and water contents had changed in the resultant emulsion or were retained, as originally obtained in the whole crude.

Preparation of crude oils with substituted asphaltenes

The asphaltene fractions and the deasphalted solutions (maltenes) from the soxhlet extractions of each of the four North Sea crudes were selectively combined in a sequence, with an exchange of the asphaltene fractions in each case to form model oils. Emulsions were formed with the model oils and the ability to form stable water-in-oil emulsions were assessed by measuring the viscosity and water contents. The sequence of the asphaltene substitutions into non-native deasphalted oils is given in Table 5.5

Preparation of synthetic oils with varying asphaltene/resin contents

Four synthetic oils were initially prepared as follows: 10 ml of decahydronaphthalene was measured into 150 ml glass beaker. 23.3 ml of *n*-heptane was added and the solution stirred for a few minutes with a glass stirrer. Thereafter, 100mg of asphaltene and 50 mg of resin fractions (ratio of 1:0.5), both from Forties crude, were added to the solution and stirred vigorously to mix. The mixture was allowed to stand for 30 min to equilibrate. The four synthetic oil solutions were vigorously stirred using a high shear homogenizer with 6 mm rotor-stator head set at speeds ranging from 800 - 1200 xg to mix the solution. The procedure was repeated with asphaltenes and resins fractions from Brent, Brae A and Stirling crude oil types. The viscosities and water content for the emulsions formed from each solution were measured. The experiments were again carried out with 50mg asphaltene and 100mg resins (ratio of 0.5:1) of the four oil samples to form model oils with similar *n*-heptane and decahydronaphthalene

concentrations. The model oils were designated as A, B, C and D denoting Forties, Brae A, Brent and Stirling in the two asphaltene/resin ratios respectively.

5.5 Results and Discussion

5.5.1 Effect of Asphaltene/Resin ratios (A/R) on emulsion stabilities of synthetic crude oils

In order to determine the effects of the ratio of asphaltene to resin concentration on emulsion stability, synthetic oil emulsions were prepared in the presence of asphaltene to resin (A/R) ratios of 1:0.5 and 0.5:1 respectively. The synthetic oils contained a pre-determined volume of *n*-heptane and decahydronaphthalene as given in the method section (5.4.2) in order to give the synthetic oils a better and approximate correspondence to crude oil emulsions from whole oil. The viscosities of the emulsions were measured and the stabilities of the synthetic oils were gauged by measuring the percentage (%) water content as shown in Table 5.1. Some emulsions do not retain their water content over a long period and the water content may change over time, leading to a change in the stability of the emulsion. Most researchers (Kilpatrick and Speicker, 2001; Yarranton *et al.*, 2007; Fingas and Fieldhouse, 2009) have determined the stability of emulsions by gauging the water content. Asphaltenes and resins act as emulsifying agent that reduces the interfacial tension and induces repulsion between molecules in an emulsion. Hence, the asphaltene/ resin ratio can be a valuable parameter to predict the stability of water-in-oil emulsions (Abdurahman and Yunus, 2009; Schorling *et al.*, 1999). Resins generally increase the solubility of asphaltenes in crude oil and reduce the asphaltene interaction with water droplets.

In the experiments reported in this Chapter, the stability of the various emulsions measured was gauged by water content.

Table 5.1 Asphaltene/ Resin ratios of synthetic oil emulsions

Shear rate (s ⁻¹)	Asphaltene/Resin ratio (A/R); 1:0.5				Asphaltene/Resin ratio (A/R); 0.5:1			
	Viscosity (mPas ⁻¹)				Viscosity (mPa s ⁻¹)			
	Forties (A)	Brae A (B)	Brent (C)	Stirling (D)	Forties (A)	Brae A (B)	Brent (C)	Stirling (D)
10.82	160	138	147	170	138	96	122	160
15.53	145	120	127	158	82.11	79	101	140
21.64	82.4	70.4	77.1	84.20	69.24	54	66.3	78.1
27.05	70.1	58.1	64.8	68.4	58.3	46	51.0	64.3
54.10	38.4	30.0	32.8	43.1	32.0	24	23.8	36.8
108.2	22.4	20.6	19.8	32.0	18.4	12	16.2	28.04
270.5	14.8	11.20	11.9	22.6	11.1	6.4	9.44	20.32
324.6	12.05	9.84	10.01	13.10	9.30	4.3	8.21	10.12
541.0	11.8	8.55	9.57	11.54	8.10	2.1	7.40	9.24
1083.0	9.36	6.90	7.48	9.11	6.21	0.88	5.81	7.01
Water content (%)	35.0	40.0	24.0	50.0	21.0	32.0	19.5	43.4

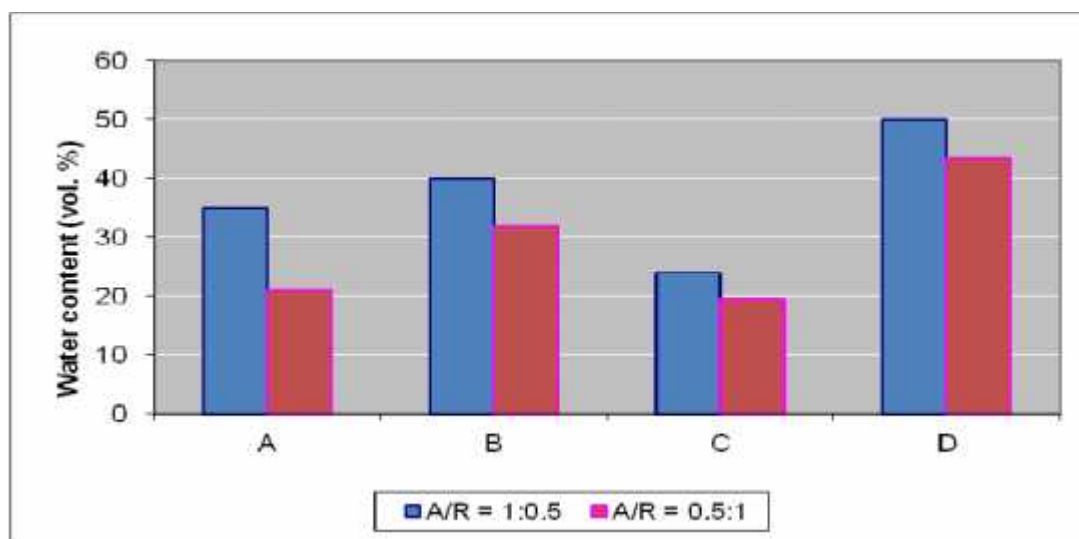


Fig. 40 Effect of varying the Asphaltene/ Resin ratio (A/R) on emulsion stability of synthetic oils

As can be seen in Fig. 40 when using an A/R ratio of 1:0.5 and water content as a measure of emulsion stability, synthetic oil emulsion D formed with Stirling asphaltene and resin was the most stable, with water content of 50.0 %, whereas synthetic oil emulsions A, B and C were less stable, with corresponding lower water contents of 35.0 %, 40.0% and 24.0, % respectively. Similarly, for the A/R ratio of 0.5:1, the synthetic oil emulsion containing Stirling asphaltene and resin yielded a more stable emulsion with water content of 43.0 %, compared to the less stable emulsions obtained from A, B and C synthetic oils, with 21.0%, 32.0% and 19.5% water contents, respectively. A Microsoft Excel for statistical test showed that at the A/R ratio of 1:0.5 there was a significant correlation ($p < 0.05$) of 0.522 between the viscosities and water content, whereas the correlation was lower (0.380), at the A/R ratio of 0.5:1. This correlation indicates that viscosity increases with water content at higher asphaltene in the A/R ratio, and viscosity decreases when the asphaltene ratio is lower, i.e. at the A/R ratio of 0.5:1.

From Figure 40, it can be seen that the water content increases with decreased resin content i.e. R/A ratio. It was found that the amount of water separation (water content) decreased with decreasing asphaltene/resin (A/R) ratio, i.e. at a higher asphaltene in the A/R ratio, the emulsion stability increases in the synthetic oil emulsions. It was interesting to note that the more stable synthetic oil emulsions (D) in both A/R ratios (1:0.5 and 0.5:1 respectively) were also observed to have yielded higher viscosities in comparison to A, B and C as indicated in Table 5.1.

The viscosities (at a shear rate of 10.82 s^{-1} in Table 5.1) were all relatively low (range 96 – 170 mPas^{-1}) but higher than the control as shown in Table 5.2.

Table 5.2 Control synthetic oil emulsion (DHN + 70ml Seawater)

Shear rate (s^{-1})	Viscosity (mPas^{-1})
10.82	88.0
15.53	74.2
21.64	63.3
27.05	29.4
54.10	17.6
108.2	8.14
270.5	7.32
324.6	6.65
541.0	6.04
1083.0	5.5
Water content (%)	9.45

The result also showed that the viscosity of the deasphalted Brent (Table 5.3) was higher (978 mPas^{-1}) at 8.9 s^{-1}), than any of the viscosity of the synthetic crudes shown in Table 5.1. It was important to note that the viscosity and water content of the re-constituted Brent (rB), was similar to that of the original fresh Brent crude (Table 5.3).

Table 5.3 Viscosity of fresh Brent (unemulsified), de-asphaltene Brent, and re-constituted Brent crude emulsions

Shear rate (s ⁻¹) (SV Cup)	Viscosity (mPas ⁻¹)		
	Fresh Brent (A)	Deasphaltene Brent(B)	Re-constituted Brent (rB)
1.78	8190	10100	7900
2.225	6890	7210	6920
3.56	4360	4120	4240
4.56	3270	2610	3100
8.90	1710	978	1670
17.8	872	884	790
44.5	346	592	410
53.4	292	383	362
89.0	181	246	210
178.1	85	122	98
Water content (%)	65	52	60.1

For comparison, the control synthetic oil emulsion had a viscosity of 88.0 mPaS at 10.82 s⁻¹ (Table 5.2) and, interestingly, a much lower water content (9.5%). The viscosities of the control and synthetic oil emulsions were measured using the NV cup of the Viscometer, as a standard viscosity measurement tool, resulting in the shear rate range as shown in Tables 5.1 - 5.2. In general, the emulsions formed with a combination of Stirling asphaltene and resin, fresh and deasphaltene Brent respectively, were more stable compared to that of the control emulsion. This result indicated that the viscosity directly related to the asphaltene concentrations in the different crudes. It can be seen clearly from these results, an indication of the substantial contributory effect that the asphaltene concentration will have on the overall emulsion stability. This effect may be attributed to a lower interfacial activity of the crude oil resins compared to that of the

asphaltenes as similarly reported in related studies by Abdurahman and Yunus, 2009; Schorling *et al.*, 1999; Sjoblom *et al.*, 1992, where it was found that high resin-asphaltene ratio (R/A) decreases emulsion stability. Moreover, the effects of the interfacial activity of the crude oil asphaltenes and resins can also be seen in the increased viscosities of the synthetic oil emulsions (Table 5.1) containing these subfractions in comparison to the viscosity of the control emulsion (without the asphaltenes and resins) given in Table 5.2.

5.5.2 Characteristics and stability of model crude oil emulsions containing substituted asphaltenes

Table 5.3 shows that when a North Sea crude is fractionated and then re-constituted, an emulsion of similar viscosity and water content to the original oil is produced.

Table 5.4 shows the viscosity and water contents of emulsions produced from the four North Sea crude oils in the scaled down experiments. The viscosity at a shear rate of 8.9 s^{-1} will be used in the discussion.

Table 5.4 Viscosities of emulsions (control) of fresh crude oils: 70 ml Seawater + 10 ml of each crude oil emulsified and measured in (SV cup) respectively.

Shear rate (s^{-1})	Viscosity (mPas^{-1})			
	Fresh Forties	Fresh Brent	Fresh Brae A	Fresh Stirling
1.78	15200	41800	19200	97200
2.225	11300	33500	15100	72500
3.56	8120	20500	9500	40100
4.45	6670	16800	7370	28400
8.90	3820	9660	4460	11200
17.8	2180	5160	2160	4000
44.5	1190	2570	1020	1780
53.4	1010	2240	984	1240
89.0	779	1540	718	981
178.1	526	1010	462	712
Water content (%)	30.0	28.0	61.0	72.0
Colour	Light Brown	Dark Brown	Dark Brown	Very dark brown
Stability	Fairly stable	Unstable	Stable	Stable

At the shear rate of 8.90 s^{-1} , the water contents of the fresh crudes tended to increase with viscosity. However, fresh Brent, with the lowest water content, produced an emulsion with one of the highest viscosity (Table 5.4). This suggests water content alone does not always determine the resultant viscosity of an emulsion.

Table 5.5 shows the viscosity, water content, colour and stability of the model oil emulsions. Table 5.6-5.9 compare the viscosity and water contents of the original and model (asphaltene substituted) crudes.

Table 5.5 Viscosity measurements, water contents, colour and stability of crude oil fraction combinations in model oil emulsions

Shear rate (s ⁻¹)	F.asph + dBrent	F.asph + dBrae A	F.asph + dStirling	Brent asph + dForties	Brent asph + dBrae A	Brent asph + dStirling	Brae A asph + dForties	Brae A asph + dBrent	Brae A asph + dStirling	Stirling asph + dForties	Stirling asph + dBrae A	Stirling asph + dBrent
1.78	14700	15900	44600	19600	21100	25700	33200	21500	20100	30700	27900	28400
2.225	10200	12600	28700	15100	17700	21500	23400	17000	16400	25700	23200	24600
3.56	7910	8910	18200	10200	10700	13500	15200	10700	10300	17200	15900	18300
4.45	5940	6550	14900	8170	8740	11100	12700	8800	8340	14000	12900	14100
8.90	2980	3820	9290	6480	5740	8950	5270	4430	4250	11400	10880	10490
17.8	2460	2020	5200	2450	2500	3200	3810	2200	2120	5740	3980	8630
44.5	1300	966	2620	1110	1240	1470	1940	892	828	3580	1930	5500
53.4	992	805	2240	949	1060	1270	1620	762	695	2060	1670	2280
89.0	701	549	1560	656	722	848	1100	469	425	954	1130	964
178.1	580	326	977	396	442	499	706	235	217	630	645	595
W/C (%)	23.5	46.0	65.0	45.0	35.0	40.0	32.0	38.0	42.0	35.0	20.0	40.0
Colour	Dark Brown	Dark Brown	Very dark brown	Dark Brown	Dark Brown	Dark Brown	Dark Brown	Very dark Brown	Very Dark Brown	Very Dark Brown	Very Dark Brown	Dark Brown
Stability	Fairly Stable	Stable	Very Stable	Unstable; mobile	Unstable	Unstable; mobile	Stable	Unstable; mobile	Unstable; mobile	Stable	Unstable	Very Stable

N/B: F.asph represents Forties asphaltene. dBrent represents deasphaltened Brent crude. dBrae A represents deasphaltened Brae A crude. dStirling represents deasphaltened Stirling crude. Brent asph. represents Brent asphaltene. dForties represents deasphaltened Forties. S.asph represents Stirling asphaltene. W/C represents water content (%). Stability as determined by (%) water content.

Summary of the addition of asphaltenes and comparison of viscosities and water contents (*in italics*) of original oil emulsions and model oil emulsions. The arrows (↑ and ↓) indicate an increase or decrease in viscosity of the model oil.

Table 5.6 Deasphaltened original crudes + Forties asphaltenes

	Forties	Brent	Brae A	Stirling
Original	3820 <i>30.0</i>	9660 <i>28.0</i>	4460 <i>61.0</i>	11200 <i>72.0</i>
Forties + Original		2980 ↓ <i>23.5</i>	3820 ↓ <i>46.0</i>	9290 ↓ <i>65.0</i>

Table 5.7 Deasphaltened original crude + Brent asphaltenes

	Brent	Forties	Brae A	Stirling
Original	9660 <i>28.0</i>	3820 <i>30.0</i>	4460 <i>61.0</i>	11200 <i>72.0</i>
Brent + Original		6480 ↑ <i>45.0</i>	5740 ↑ <i>35.0</i>	8950 ↓ <i>40.0</i>

Table 5.8 Deasphaltened original crude + Brae A asphaltenes

	Brae A	Forties	Brent	Stirling
Original	4460 <i>61.0</i>	3820 <i>30.0</i>	9660 <i>28.0</i>	11200 <i>72.0</i>
Brae A + Original		5270 ↑ <i>32.0</i>	4430 ↓ <i>38.0</i>	4250 ↓ <i>42.0</i>

Table 5.9 Deasphaltened original crude + Stirling asphaltenes

	Stirling	Forties	Brae A	Brent
Original	11200 <i>72.0</i>	3820 <i>30.0</i>	4460 <i>61.0</i>	9660 <i>28.0</i>
Stirling + Original		11400 ↑ <i>35.0</i>	10880 ↑ <i>20.0</i>	10490 ↑ <i>40.0</i>

The results given in Table 5.6 shows the viscosities and water contents of the model oils formed from the combination/substitution of asphaltene fractions isolated from the four

different crude oils in combination with the deasphalted fractions of each specific crude oil type

Deasphalted original crudes + Forties asphaltenes

The viscosities of the model oil emulsions formed with Forties asphaltenes in combination with the deasphalted fractions of Brent, Brae A and Stirling crudes were comparatively less viscous than the initial viscosities of fresh Brent, Brae A and Stirling crudes respectively (Table 5.6). This drop in viscosity was most significant for the deasphalted Brent (2980 mPas⁻¹ compared to 9660 mPas⁻¹ measured initially in the emulsion derived from the unaltered Fresh Brent). The viscosity of the model oil consisting of Forties asphaltene and deasphalted Brae A, was similar to the original Brae A crude. Similarly, the viscosity of the Forties asphaltene with deasphalted Stirling was only slightly lower (9290 mPas⁻¹ compared to a higher viscosity of 11200 mPas⁻¹ measured in the fresh Stirling emulsion). The results indicated that the water contents of the fresh crude emulsions (Table 5.4) were higher than the water contents obtained when Forties asphaltene was combined with deasphalted Brent, Brae A and Stirling respectively to constitute model oils. Forties asphaltene mixed with deasphalted Brae A yielded a higher water content (46.0%) compared to the water content of fresh Forties emulsion (30.0%). Forties asphaltene with deasphalted Stirling, had water content of 65.0%, which interestingly yielded a very stable model oil emulsion (Table 5.5).

Deasphalted original crude + Brent asphaltenes

A viscosity of 6480 mPas⁻¹ was measured at the shear rate of 8.90 for the model oil consisting of Brent asphaltene substituted into deasphalted Forties as indicated in Table 5.7. The model oil emulsion viscosity was significantly lower than the fresh Brent emulsion. However, the model emulsion formed was unstable with water content of 45.0 %. With Brent asphaltene and deasphalted Brae A, a higher viscosity of 5740 mPas⁻¹ was measured for the model oil compared to a viscosity of 4460 mPas⁻¹ measured for Brae A emulsion (Table 5.4). A possible explanation for this increase in viscosity of the model oil emulsion can apparently be attributed to the higher interfacial activity of the Brent asphaltene component within the deasphalted Brae A emulsion blend, which may suggest a possible override of the Brae A asphaltene by the Brent

asphaltene in the emulsion. The model oil emulsion formed was unstable, with a water content of 35.0 % (Table 5.7). An unstable model oil emulsion with lower viscosity of 8950 mPas⁻¹ and water content of 40.0% was measured for Brent asphaltene combined with deasphalted Stirling (Table 5.7). This contrasts to a viscosity of 11200 mPas⁻¹ and 72.0% water content obtained for the unaltered fresh Stirling emulsion. It is important to note that asphaltenes isolated from unaltered Stirling crude, with the exception of Stirling asphaltene combined with deasphalted Brae A, generally exhibited a high tendency to form stable water-in-oil emulsions as indicated in Table 5.5. This result indicated that the emulsion derived from a blend of deasphalted Stirling with Brent asphaltene fraction, was effectively reduced in viscosity resulting in an unstable emulsion possibly due to the overriding interfacial activity of the Brent asphaltene in the model oil emulsion formed.

Deasphalted original crude + Brae A asphaltenes

The effect of the asphaltene type on emulsion viscosity was also clearly shown in the model oil emulsion consisting of Brae A asphaltene in combination with deasphalted fractions of Forties, Brent and Stirling crudes. A clear indication of the effect of asphaltene type was exhibited in the viscosity measured in Brae A asphaltene added to deasphalted Brent and Stirling fractions, with a sharply decreased viscosity in the model oil emulsions (Table 5.8). The Stirling model oil emulsion was unstable, with a reduced water content of 42.0%. The result indicated that deasphalted Stirling in combination with asphaltene fractions of another oil type yielded an emulsion viscosity value close to the unaltered donor oil type. The combination of Brae A asphaltene with deasphalted Brent yielded an unstable model oil emulsion, with a sharply decreased viscosity of 4430 mPas⁻¹, but increased water content. Again, the viscosity of the model emulsion was similar to that of the donor oil (Table 5.8). A stable model oil emulsion with 32.0 % water content and an increased viscosity of 5270 mPas⁻¹ was measured in Brae A asphaltene in combination with deasphalted Forties crude. The viscosity of the model oil was observed to be higher than both the initial viscosities of both the Fresh Forties and Brae A emulsions.

Deasphalted original crude + Stirling asphaltenes

The asphaltenes from the Stirling crude significantly increased the viscosities of both deasphalted Forties and Brae A crude. Both emulsion viscosities were similar to the original Stirling crude. Although both oil emulsions had relatively high viscosities, they were unstable. The fresh Stirling emulsion was stable, with a high water content of 72.0% (Table 5.4). Interestingly, the water content of the Brae A model oil was significantly lower than the fresh oil, even though the viscosity had more than doubled.

Discussion

From the series of chemical analyses on the asphaltene fractions of the four crude oils, as discussed previously in Chapter 4 Section 4.5, and summarized in Table 4.3, it was indicated that the asphaltenes are comprised of a widely distributed functional groups, and specific differences in the amount of condensed aromatic rings, alkyl side chains, heteroatoms, hydrogen/carbon (H/C) ratios, polarity and the number of carbon types in each fraction (Chapter 4, Table 4.2). These characteristics tend to determine their overall chemical and physical properties, which ultimately influence the nature, stability and behaviour of emulsions formed from these crude oil types. Though these differences between the chemistry of the asphaltenes were sometimes subtle, their behaviour in emulsion formation were significant. Midttun *et al.* (2000) had reported on the influence of polar functional groups in resins and asphaltenes intermolecular interactions, to either stabilize or destabilize emulsions, depending on the ratio of each surfactant fraction.

Abdurahman and Yunus (2006) in their studies, compared to the results in these experiments, had also found that emulsions formed with isolated asphaltenes were more stable than emulsions derived from a mixture of surface-active agents (asphaltenes + resins). A possible explanation for this can be deduced from the composition of resins, which consist of naphthenic aromatic hydrocarbons, generally aromatic ring systems with alicyclic chains (Schorling *et al.*, 1999), and containing very small amounts of polar compounds (such as nitrogen or oxygen) relative to the asphaltene fractions, as reported earlier in Chapter 4, Section 5.2 of this work. The indication in the analyses in this work and supported by similar observations by Schorling *et al.* (1999), is that these heteroatoms found more abundantly in asphaltenes, may have a potentially significant

contributory role in the stability of water-in-oil emulsions. The interfacial behaviour of the heteroatoms and aromatic ring systems in asphaltene was investigated in modelled asphaltene structures and is presented in Chapter 6.

From the investigations of the influence of different asphaltenes on the rheologic behavior of emulsions, it was shown that the viscosities of the model emulsions tended to be dependent on the type of asphaltenes. Further, the stability of the model oil emulsions, gauged by the percentage (%) water content, changed significantly when asphaltene fractions were isolated (deasphaltenation), from the whole (i.e. original) crude. In contrast, Schorling *et al.* (1999) had reported that the origin and type of crude oil resins, which peptizes (i.e. disperses asphaltenes into a colloidal state), therefore contributing to emulsion stability, had no effect on the viscosity and stability of model oil emulsions.

5.6 Conclusion

The ratios of asphaltenes to resins fractions investigated using a synthetic oil system, showed a correlation with the tendency of these components to form stable emulsions, with high resin/asphaltene ratio leading to a corresponding decrease in emulsion stability.

1. The stability of the synthetic oils, A, B, C, and D varied with varying A/R ratios. At a high asphaltene/resin ratio (A/R ratio), the synthetic oil D was more stable than A, B, and C.
2. The water content decreased with decreasing asphaltene/ resin ratio (A/R).
3. At a high A/R ratio of 1:0.5, the synthetic oil emulsion was more stable than the stability, as determined by percentage water content, at the A/R ratio of 0.5:1
4. The viscosity and water content of the re-constituted crude was similar to that obtained for the original fresh crude indicating that fractionated crude can be re-combined to produce an emulsion with characteristics similar to the original fresh crude.
5. Viscosity of crude oil emulsions is directly related to both the water content and asphaltene of the crude. A high water content and high asphaltene tends to increase the viscosity of crude oil emulsions.
6. The viscosities and water content of the 'model oil' emulsions were a resultant of the overriding effect of the asphaltene of the 'donor oil' on the 'recipient oil', where the donor oil either increased or decreased the viscosity and water content obtained in the model oil emulsions. The viscosities and water content of the 'model oil' tended to either reduce, or increase on the other hand, following the addition of asphaltenes of the 'donor oil' (i.e. asphaltenes from another crude oil type).
7. Forties and Stirling asphaltenes, with the exception of Stirling asphaltene in deasphalted Brae A, produced the more stable model oil emulsion in all the four crude oil types investigated, although Forties asphaltene in deasphalted Brent emulsion was fairly stable.

8. The strength or stability of the model oil emulsions can be related to the chemistry, in particular the asphaltene subfractions of the crudes.

9. The investigations have revealed that the overall stability characteristic of crude oil emulsions were considerably affected by the addition of external asphaltenes into a deasphalted crude, which either produced a stable or unstable emulsions, and to a large extent, dependent on the type of asphaltenes, although the asphaltenes were isolated from various North Sea crude oil types derived from potentially similar geologic origin or source rock (Kimmeridge).

CHAPTER 6

MULTIPHASE MOLECULAR DYNAMICS MODELLING OF CRUDE OIL ASPHALTENE STRUCTURES

6.1 Introduction

As stated previously in Chapter 5, Section 5.2.4, asphaltenes are arbitrarily defined as the portion of crude oil that is insoluble in *n*-alkanes such as *n*-heptane or *n*-pentane but soluble in toluene, benzene or dichloromethane (Hammami *et al.*, 2000; Stankiewicz *et al.*, 2002; Mullins *et al.*, 2007). The asphaltenes generally are characterized by fused ring aromaticity, aliphatic side chains, and polar heteroatoms containing functional groups and trace metals (e.g., Ni, V, Fe).

Asphaltenes are heavy hydrocarbon molecules that form colloidal suspension in the oil, stabilised by resins adsorbed on their surface. Each particle is believed to consist of one or more sheets of asphaltene monomers and absorbed resins to stabilize the suspension (Sjoblom *et al.*, 2007). A number of factors such as changes in pressure, temperature and composition may alter the asphaltene/ resin association and may cause precipitation, with a wide range of implications for water-in-oil emulsification. Studies have shown that asphaltenes are found to be capable of forming rigid cross-linked elastic films which are the primary agents in stabilizing water-in-crude oil emulsions, and is reported to form monomolecular layers at the air/water interface (McLean *et al.*, 1998; Spiecker, 2001; Fingas, 2010). It is noted that the exact role of waxes and inorganic solids in either stabilizing or destabilizing emulsions is not well known (Fingas, 2010).

The adsorption of asphaltenes on solids is the result of favourable interactions of the asphaltene species or its aggregates with chemical species on or near the mineral surface. The relevance of adsorption of asphaltenes on mineral surfaces is that it enhances the understanding of phase separation and reservoir wettability in geochemical aspects of crude oil production, and also the adsorption phenomena may influence the mechanism of film formation of water-in-oil emulsification. A number of interaction forces, individually or in combination with each other, can be responsible for it. The major forces that can contribute to the adsorption process include electrostatic

(Coulombic) interactions, charge transfer interactions, van der Waals interactions, repulsion or steric interactions and hydrogen bonding (Murgich, 2002).

However, the exact conformations in which asphaltenes organize at the oil-water interfaces and the corresponding intermolecular interactions have not been fully elucidated (Kilpatrick, 2001; Spiecker, 2001). In support of earlier work by McLean *et al.*, (1998), a recent study by Fingas and Fieldhouse (2008), have proposed an explanation on the adsorption of molecules, stating H-bonding between acidic functional groups (such as carboxyl, pyrrolic and sulfoxide), electron donor-acceptor bonding between transition metal atoms and electron-rich polar functional groups, or some other type of force such as π -bonding between delocalized π electrons in fused aromatic rings, as probable intermolecular forces that may influence molecular adsorption.

Though significant progress has been made in determining both structural and aggregation properties of asphaltenes (Mullins and Sheu, 1988; Buenrostro-Gonzalez *et al.*, Groenzin and Mullins, 2000; Tanaka *et al.*, 2004; Andreatta *et al.*, 2005; Mullins, 2010), however, the understanding of self-association phenomena, especially on a molecular level, is still incomplete. Most recently, to underscore the importance of understanding the interfacial conformation of asphaltenes and its extended role in either stabilizing or destabilizing oil-in-water emulsions, Fingas, (2010) reported that researchers have suggested that specific experimental designs to test these concepts are currently needed to understand the phenomenon on a molecular level. It is also noted that such knowledge would aid in the design of chemical demulsifiers.

Several authors have mostly reported the modelling of asphaltene precipitation in crude oil production. A review of these has been given by Nghiem (1999); Akbarzadeh *et al.*, (2007), to include a solubility model, thermodynamic colloidal model, thermodynamic micellization model and a solid model. It is reported that to date, most of the above asphaltene-precipitation models have been tested only on limited set of experimental results Akbarzadeh *et al.* (2007), although most authors claim that their models could give reasonable predictions. It should be noted however, that these models were developed before the emerging consensus on asphaltene molecular weight and structure,

as discussed in Chapter 1.7.2. Mullins and Sheu (1998) have also studied the structure of asphaltenes in terms of self-association mechanism, and concluded that the self-association of asphaltenes appear to be different due to the fact that asphaltenes, as a solubility class, potentially have very different structures among themselves. The similarity may be that most of the molecules consist of certain degrees of polynuclear aromaticity, as revealed in elemental analysis, H/C ratio or in NMR studies.

As a first step to understanding the precipitation of asphaltenes, it is important to understand the surface behaviour of asphaltenes and a full range of multiphase conditions through which asphaltene will behave, and relate these to a set of experimental data obtained from characterisation of North Sea asphaltene fractions and emulsification. Hence, an important aspect and contribution to this research, described in this chapter, is the multiphase molecular dynamics modelling of asphaltene structure and surface behaviour. For this investigation, molecular dynamics simulation to model the adsorption of model asphaltene structures at both air/water (a/w) and oil/water (o/w) interfaces has been used.

This allows a molecular level study of factors that may control the formation of asphaltene layers in water-in-crude oil emulsions, the objective being to gain insight into the relationship between these different structures and emulsion formation. Aggregation of molecules affects their mobility; this makes the molecular diffusion an excellent tool for exploring asphaltene aggregation (Mullins *et al.*, 2007). Typically, in the air/water interface model (a description of which is given in Section 6.2) the surfactant resides in the aqueous phase, and in the o/w interface model, the surfactants may reside in the aqueous or oil phase. The knowledge gained by investigating interfacial properties is considerably revealing, and extensively supports the information available from bulk emulsions studies, as previously given in Chapter 3. As stated by Spiecker (2001), from interfacial studies, one can determine the fundamental mechanisms and kinetics of film formation, surfactant adsorption, and film rupture that ultimately govern emulsion behaviour.

6.2 Relationship between surfactants (surface-active agents) and emulsification

Generally, a surfactant designates a substance which exhibits some superficial or interfacial activity, and is most acceptably and scientifically classified based on their dissociation in water (Salager, 2002). Interface is the boundary between two condensed phases. An amphiphilic substance or molecule exhibits a double affinity, which can be defined from the physico-chemical point of view as a polar-apolar duality, and typically consists of two parts namely: a polar group which contains heteroatoms such as O, S, P, or N included in functional groups such as alcohol, amide, sulfate, phosphate, esters, etc., and on the other hand, an essentially apolar group which is in general an hydrocarbon chain of the alkyl or alkylbenzene type, sometimes with halogen atoms and even a few non-ionized oxygen atoms (Salager, 2002). The polar portion exhibits a strong affinity for polar solvents, particularly water, and it is often called *hydrophilic* part or *hydrophile*. The apolar part is called *hydrophobe* or *lipophile*.

In general, the hydrophilic end consists of ionizing groups which may be cationic (cationic surfactants are dissociated in water into an amphiphilic cation and an anion, most often of the halogen type, with a large proportion corresponding to the nitrogen compounds such as quaternary ammoniums with one or several long chain of the alkyl type), or anionic (an anionic surfactant dissociates in an amphiphilic anion, and a cation, generally alkaline metals or quaternary ammonium), or even in some cases, non-ionic groups (non-ionic surfactants do not ionize in aqueous solution because their hydrophilic group is of non-dissociable type such as alcohol, phenol, amide). On the other hand, the hydrophobic end consists of alkyl or aryl hydrocarbon structures (Cormack, 1999; Salager, 2002). Due to its dual affinity, an amphiphilic molecule does not feel “at ease” in any solvent, be it polar or non-polar, since there is always one of the groups which “does not like” the solvent environment. This explains why amphiphilic molecules exhibits a very strong tendency to migrate to interface or surfaces and to orientate so that the polar group lies in water and the apolar group is placed out of it, and eventually in oil. According to Salager, 2002, all amphiphiles do not however display interfacial activity, stating that in effect, only the amphiphiles with more or less equilibrated hydrophilic and lipophilic tendencies are likely to migrate to the surface or interface and does not occur if the amphiphilic molecule is too hydrophilic or too hydrophobic, in which case it stays in one of the phases.

The surfactants are so named because they actively seek the interface between oil and water, with one end of the surfactant being oil compatible whereas the other is water compatible, i.e. it is both hydrophilic or lipophilic and the balance between the two, called the Hydrophilic – Lipophilic balance (HLB) is allocated a number from 0 – 40 which characterizes the tendency of the surfactant to dissolve preferentially in oil or in water, low or high values of HLB respectively (Griffins, 1954; Cormack, 1999). A practical application of the HLB system is in enhanced oil recovery (EOR), where weight percentage of each type of group on a molecule or in a mixture predicts what behaviour the molecular structure will exhibit. Water-in-oil emulsifiers have a low HLB numbers, typically around 4. Solubilizing agents have high HLB numbers. Oil-in-water emulsifiers have intermediate to high HLB numbers (Griffins, 1954).

Generally, industrial interest in emulsions relates to their formation and stability as products and so emulsifiers are chosen as additives to stabilize emulsions, especially if a high concentration of the dispersed phase is required. However, with water-in-oil emulsions arising from inadvertent oil spills, the interest shifts to finding and developing measures to destabilize and break the emulsions into their constituent parts as separate continuous phases.

Asphaltenes and wax are perhaps, the most important of the solid emulsifying agents which can precipitate from oils as very fine crystals which stick to the interface by surface tension forces. Cormack (1999) reported that mixed surfactant can have a synergistic effect on emulsion stability, in which the total effect is greater than the sum of the individual contributions. This was attributed to the inter-molecular complex formation at the interface. Specific explanation advanced was that one surfactant may reduce the surface tension of the film formed by the second at the interface, leading to greater film elasticity, or the interfacial viscosity may be increased, or diffusion rates in the surface film may be reduced. The “interfacial skins” produced are believed to provide mechanical stabilization of the water droplets and this effect increases with viscosity of the interfacial layer (Foordal *et al.*, 1996).

Considering water-in-oil emulsions, the natural emulsifiers contained in the oil stabilize the water droplets by locating at the oil-water interfaces. The total interfacial area of the

internal water droplets is, however, very much higher than the external surface of the emulsion itself, which is in contact with the sea. The surfactants in this case, therefore, are effectively trapped within the emulsion having their water compatibility properties internally satisfied, and the tendency to escape to the sea is small.

For the surfactants in dispersant formulations, which are expected to disperse oil or emulsion droplets into the sea, the situation is rather different. They need to reside external to the droplet with their hydrophilic ends in the surrounding seawater. For effectiveness, such surfactants tend to have high HLB numbers (i.e they are strongly water seeking and therefore, have a strong tendency to dissolve in water, i.e. to be preferentially lost to the sea water when applied to oil slick). In water-in-oil emulsion, the mechanism behind a destabilization with surfactants is probably an interfacial competition, a situation in which the indigenous crude oil film will be replaced by a surfactant layer which cannot stabilize the crude oil emulsion (Fordedal *et al.*, 1996).

Selection of Asphaltene structures for modeling

Asphaltenes were traditionally believed to be composed of 10 – 20 condensed aromatic and naphthenic rings with paraffin and naphthenic side chains. The structures were reported to contain variable amounts of nitrogen, oxygen and sulphur atoms with the open area in the asphaltene structures enabling the complexation of heavy metals such as nickel and vanadium (Hunt, 1979). More recent studies suggest that individual asphaltene molecules have a much lower molecular weight. Although structures have been proposed Mullins (2008), they lack detail of the heteroatoms known to be present.

For purposes of modelling for this research, structures were postulated based both on the literature and data obtained from the chemical characterisation of the asphaltenes extracted from the North Sea crude oils under investigation. Six “asphaltene” molecular structures (Fig.41) were used in the molecular dynamic simulations models, with varying aromatic content, polarity and alkyl chain length. This includes molecules with either a high or low degree of aromatic character (many conjugated aromatic rings or few aromatic rings), varying number of ring heteroatoms (1 or 2 ring Nitrogens), and the presence of alkyl side chains. These were:

High aromatic content, low polarity (one nitrogen)	ha1N
High aromatic content, high polarity (two nitrogens)	ha2N
High aromatic content, low polarity (one nitrogen), long alkyl side chain	ha1N_LC
Low aromatic content, low polarity (one nitrogen)	la1N
Low aromatic content, high polarity (two nitrogens)	la2N
Low aromatic content, high polarity (two nitrogens), long alkyl side chain	la2N_LC

The objective was to observe their behaviour at two different model interfaces and attempt to correlate this to the emulsification characteristics of the crude oils being studied.

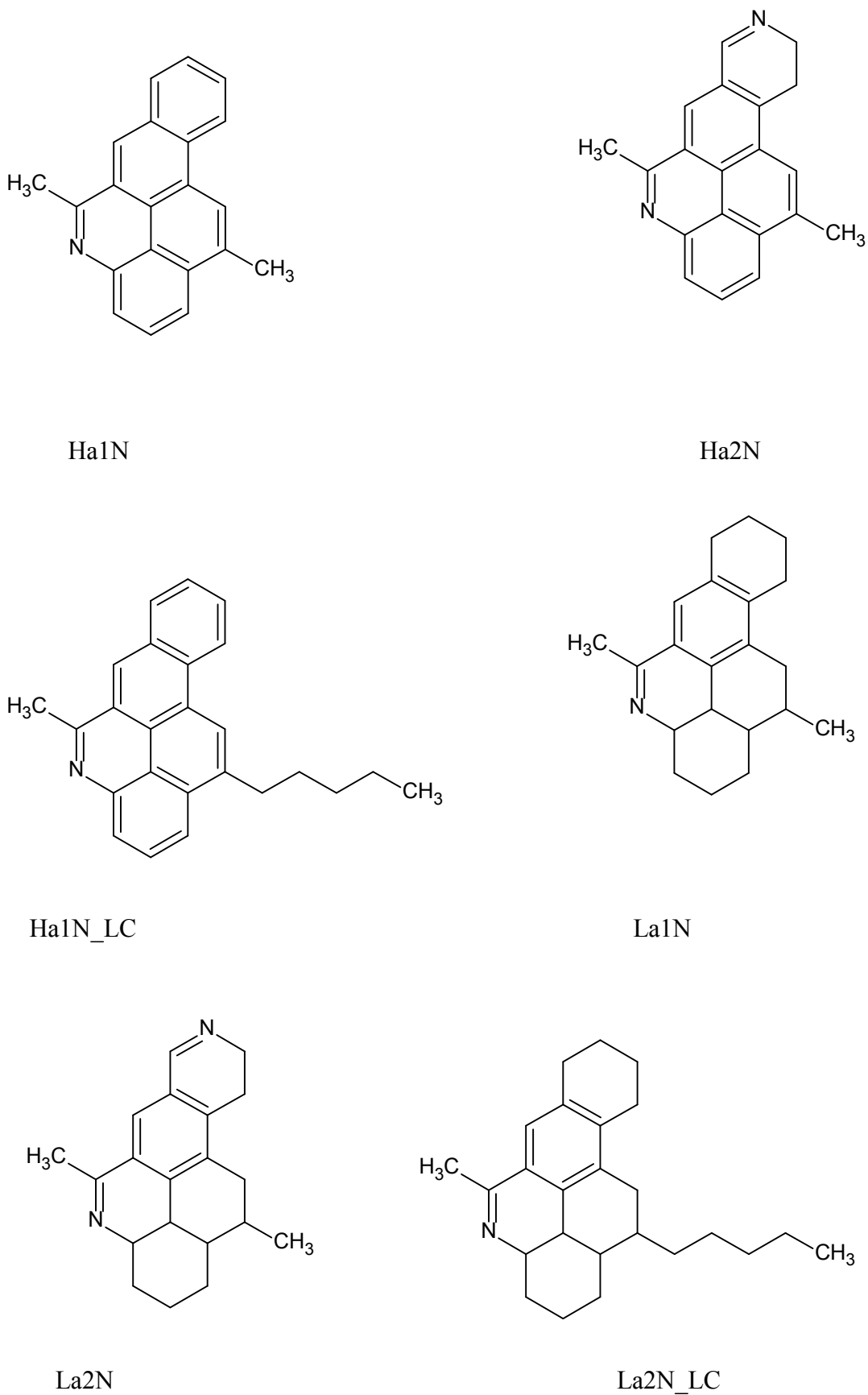


Fig. 41 Asphaltene molecular structures showing the high or low aromatic ring, ring heteroatoms and alkyl side chains. These structures were used in the molecular dynamic (MD) simulations.

6.3 Methodology

Molecular dynamics (MD) simulations were carried out using the GROMACS software package version 4.0 (Hess *et al.*, 2008). A description of the software is given in Appendix D. Simulations were carried out at a vacuum-water interface for the model asphaltenes: high aromaticity, low polarity 1N (ha1N); high aromaticity, high polarity (ha2N); low aromaticity, low polarity 1N (la1N); low aromaticity, high polarity 2N (la2N); ha1N-LC and la1N-LC, (the LC represents hydrocarbon chain), and at a decane water interface for ha2N and la2N. These structures are shown in Fig. 41. The significance of initially using the air/water interface was because the molecular simulation at this interface was believed to correctly approximate the result of what would be obtained in the simulation at other interfaces, such as the oil/water interface. For the water vacuum interface a simulation box of size 6.3 x 6.3 x 4 nm was set up containing twenty asphaltene molecules. The topology file for each asphaltene molecule was generated using the PRODRG server at Dundee University (Schuettelkopf and van Aalten., 2004). The topology file describes the connectivity in the molecule (i.e. which atoms are bonded to which), the atom type, atom mass and the partial charge on each atom. This data is required for calculation of bonded and non-bonded interactions.

The conformation was solvated with SPC (simple point charge) water (Berendsen *et al.* 1981; Berweger *et al.*, 1995). The box was expanded in the z-dimension to form a vacuum space and to give a final box of size 6.3 x 6.3 x 10 nm. The system was energy minimised using a conjugate gradients algorithm (Hestenes and Stiefel, 1952), as described in Appendix D. The system was further equilibrated for 1 ns using NVT (constant atom number, constant volume and constant temperature simulation in the Canonical ensemble) MD simulation with position restraints applied to the asphaltene molecule. In molecular dynamic simulation, an ensemble is a collection of all possible systems which have different microscopic states but have an identical macroscopic or thermodynamic state. The Canonical ensemble (NVT) is one of such statistical mechanics ensemble. It is a collection of all systems whose thermodynamic state is characterized by a fixed number of atoms, N, a fixed volume, V, and a fixed temperature, T.

Finally the position restraints were relaxed on the asphaltene molecules and an equilibration run of 20ns during which the asphaltene was allowed to adsorb freely at

the water-vacuum interface. The final conformation (after 20ns) from this run was used as the starting point for production runs of 20ns for each asphaltene molecule/ type.

The decane-water interface was set up in a similar way. A box of size 6.3 x 6.3 by 4 nm was set up containing either twenty ha2N or twenty la2N molecules. This box was solvated with SPC water and then the box was expanded in the z-dimension to form a water-vacuum interface in a box of size 6.3 x 6.3 x 6.3 nm. Four hundred and eighty two decane molecules were added to the vacuum space of the simulation box. This number was chosen by trial and error so as to give a decane density close to the expected density (720 g/L) under the simulation conditions being used. The topology for the decane molecules was generated by the PRODRG server. The simulation box was energy minimized using a conjugate gradients algorithm. The conformation was then equilibrated for 1ns with position restraints applied to the asphaltene molecules to allow the formation of a stable decane-water interface. The system was then equilibrated for a further 20ns with the position restraints relaxed and the asphaltene molecules were allowed to adsorb at the decane-water interface. The final conformation from this 20 ns simulation was used as the starting point for a 20ns production run. This procedure was carried out for both of the asphaltene molecules studied at the decane-water interface.

During the MD simulations the following parameters were used. Electrostatic interactions were modelled using the GROMOS 43a2 force field (Schuler *et al.*, 2001). The particle mesh Ewald summation method (Darden *et al.*, 1993; Essmann *et al.*, 1995) was used to sum coulomb interactions. Van der Waals interactions were represented by a switch function set to 0.8nm and a cut-off of 0.9 nm. The component molecules of the system were coupled to a V-rescale thermostat (Bussi *et al.*, 2007) to control temperature. Periodic boundary conditions were defined in all 3 coordinate directions. This is further described in Appendix D.

The MD trajectories for the asphaltene systems were analysed in two ways. The density profile of the asphaltene, water and decane, if present, was calculated as a function of the position along the z-dimension normal to the interface. The radial distribution function ($g(r)$) of the centres of mass of the asphaltene molecules was calculated for the adsorbed asphaltene molecules. The $g(r)$ is defined in terms of the density of molecules

a distance r from a central molecule, normalised by the density of the whole system. Mathematically the $g(r)$ is calculated using the equation:

$$g(r) = \rho(r) / \rho(ave)$$

where $\rho(r)$ is the number density of molecules a distance r from the central molecule, and $\rho(ave)$ is the average density for the molecules in the whole system.

6.4 RESULTS AND DISCUSSION

The results for the molecular dynamic (MD) simulations for the water - vacuum interface, decane – water interface and the ha2N asphaltene at the decane interface are given below:

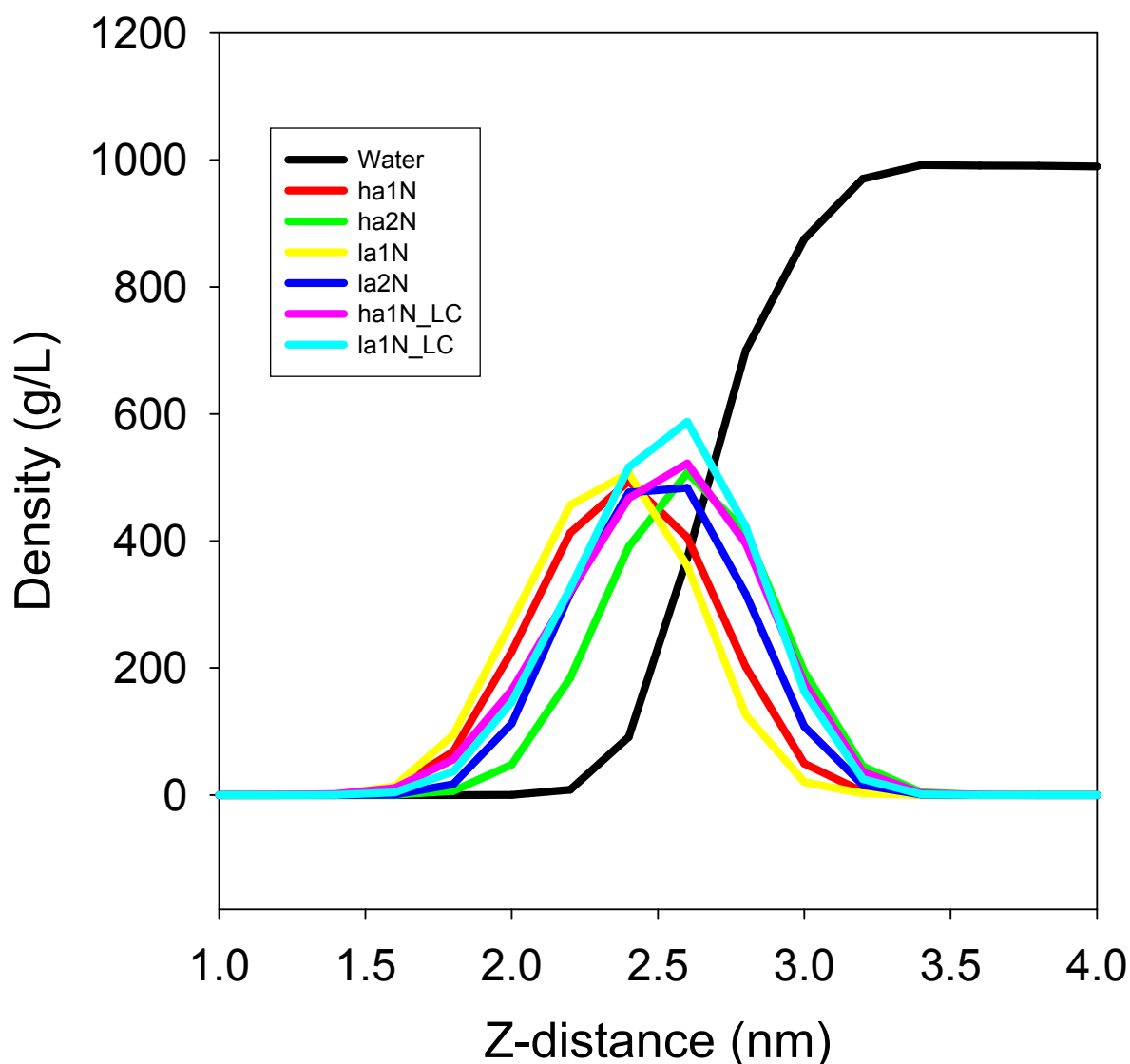


Fig. 42 Plot of density of asphaltene molecules at the water-vacuum interface. The Z-distance (nm) is the distance along the z-dimension normal to the interface

From the molecular dynamic simulation, the following general trends were indicated: All asphaltenes wet the vacuum side of the interface i.e. they are hydrophobic. Increasing the number of ring nitrogen atoms in the molecules leads to a larger proportion of the molecule sitting in the water phase i.e. they are less hydrophobic. Decreasing the aromaticity of the asphaltene molecules results in a complex behaviour. Ha1N compared to la1N there is little difference, although la1N sits slightly more in the vacuum phase. Comparing ha2N to la2N it is obvious that la2N sits much further into the vacuum phase than the ha2N which is unexpected. This may be a conformational entropy effect, i.e. more flexible molecules tend to sit further away from a surface due to an unfavourable entropy contribution to the free energy of adsorption. The high aromaticity molecules are flat and rigid due to the conjugated benzene ring system,

whilst the low aromaticity molecules adopt the normal chair conformation for non-aromatic 6-membered carbon rings. The extra flexibility will increase the conformational entropy of the molecule. Adding a hydrocarbon chain the ha1N and la1N molecules again leads to complex behaviour. Comparing the ha1N_LC molecule to ha1N and the la1N_LC to the la1N the extra hydrocarbon chain leads to the molecule sitting more into the aqueous phase.

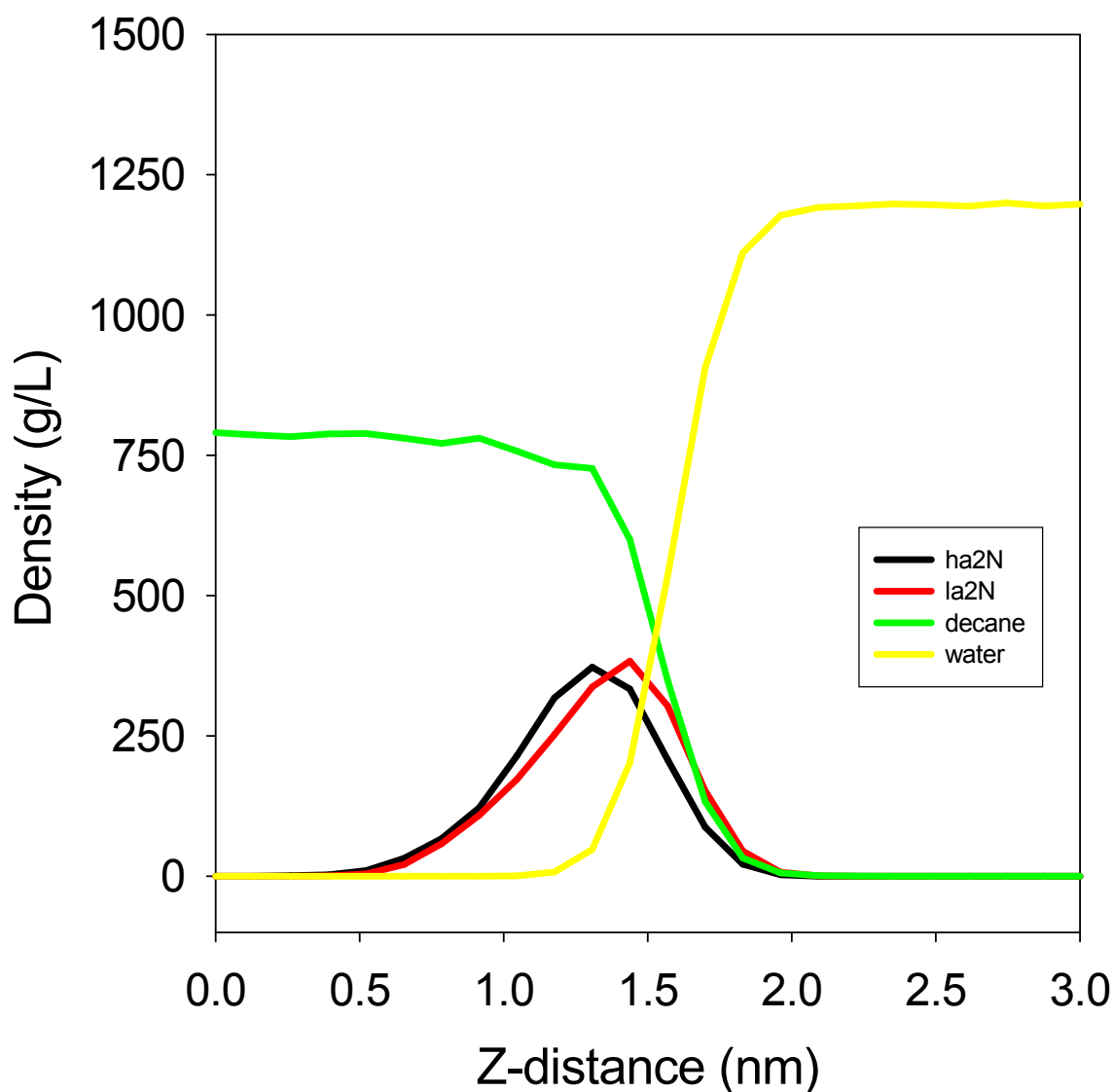
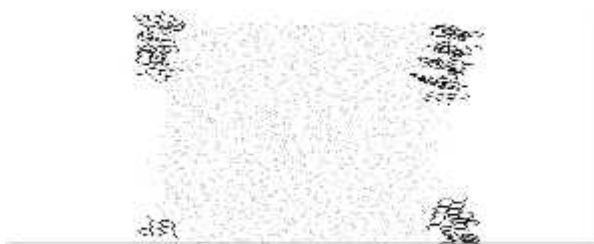
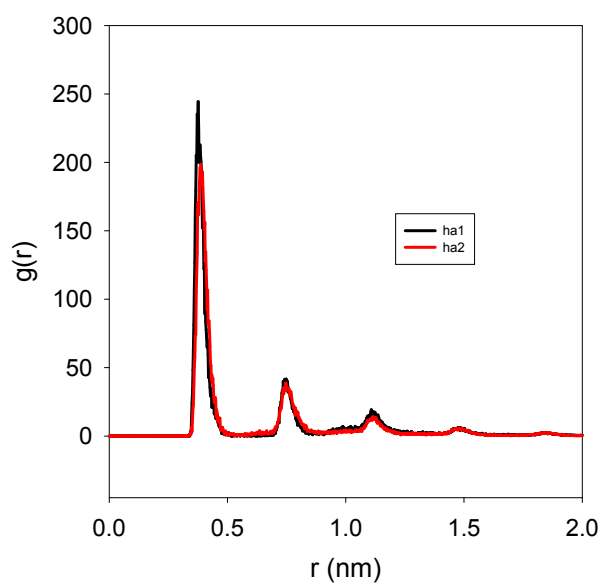


Fig 43 Plot of density of asphaltene molecules at the decane - water interface. The Z-distance (nm) is the distance along the z-dimension normal to the interface

For the decane - water interface only ha2N and la2N were simulated, in order to investigate the conformation of asphaltenes with higher heteroatoms. Both molecules sat fully in the decane phase with only a relatively small proportion of the molecule occupying the 2-phase decane-water interfacial layer, i.e. they wet the oil side of the interface. At the decane surface the low aromaticity molecule sits closer to the water phase, the opposite behaviour to that observed at the air-water interface. This suggests that penetration of the molecule into the decane phase reduces conformational entropy and allows for stronger adsorption to the surface.

(a)



(b)



(c)



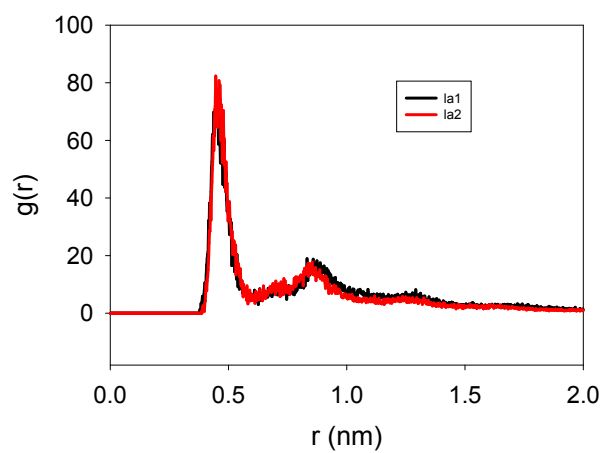
(d)



(e)

Fig 44 (b,c) of $Ha1N$ and (44d,e) of $ha2N$ showing the structural conformation at the water-vacuum interface and a plot of radial distribution ($g(r)$), (Fig 44a) for the adsorbed molecules

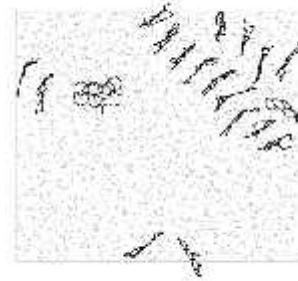
Ha1N (Fig. 44b,44c) and ha2N (44d,44e) both adopt a highly ordered conformation at the water-vacuum interface. This conformation is reminiscent of the π -stacking observed in porphyrin molecules (Spiecker, 2001; Zhou *et al.*, 2005). π -Stacking is one of the possible mechanisms for adsorption proposed by Fingas and Fieldhouse (2008). Although the simulation should not be taken as definitive proof of π -stacking, the configurations are highly suggestive of this mechanism. This highly ordered structure is confirmed by looking at the radial distribution function ($g(r)$) for the adsorbed molecules (Fig.44a). Both ha1N and ha2N show a large initial peak at a separation of approximately 0.4nm, with 2nd, 3rd and 4th coordination peaks evenly spaced at greater separations. This is characteristic of semi-solid or liquid-like ordering at the interface. Highly ordered adsorbed asphaltene layers could be expected to behave as highly rigid surface layers. Intuitively, it could be imagined that a more rigid adsorbed asphaltene layer would be better at stabilizing water-in-oil emulsions. Thus, from the simulation results, it was possible to predict that increasing the polar character of asphaltenes by including extra heteroatoms will reduce the degree of surface ordering of the asphaltenes, which would lead to a less stable adsorbed layer.



(a)



(b)



(c)



(d)



(e)

Fig 45 (b,c) of La1N and (45d,e) of la2N showing the structural conformation at the water-vacuum interface and a plot of radial distribution ($g(r)$), (Fig45a), for the adsorbed molecules

The low aromaticity asphaltenes, la1N and la2N have a more disordered structure at the interface – the first peak in the $g(r)$ is lower for the low aromaticity molecules than for the high aromaticity ones. Also the peaks are wider, and there are less of them. These are features that indicate a more disordered structure at the interface. These differences between the high and low aromaticity molecules are apparent if we compare the $g(r)$ of the two types,

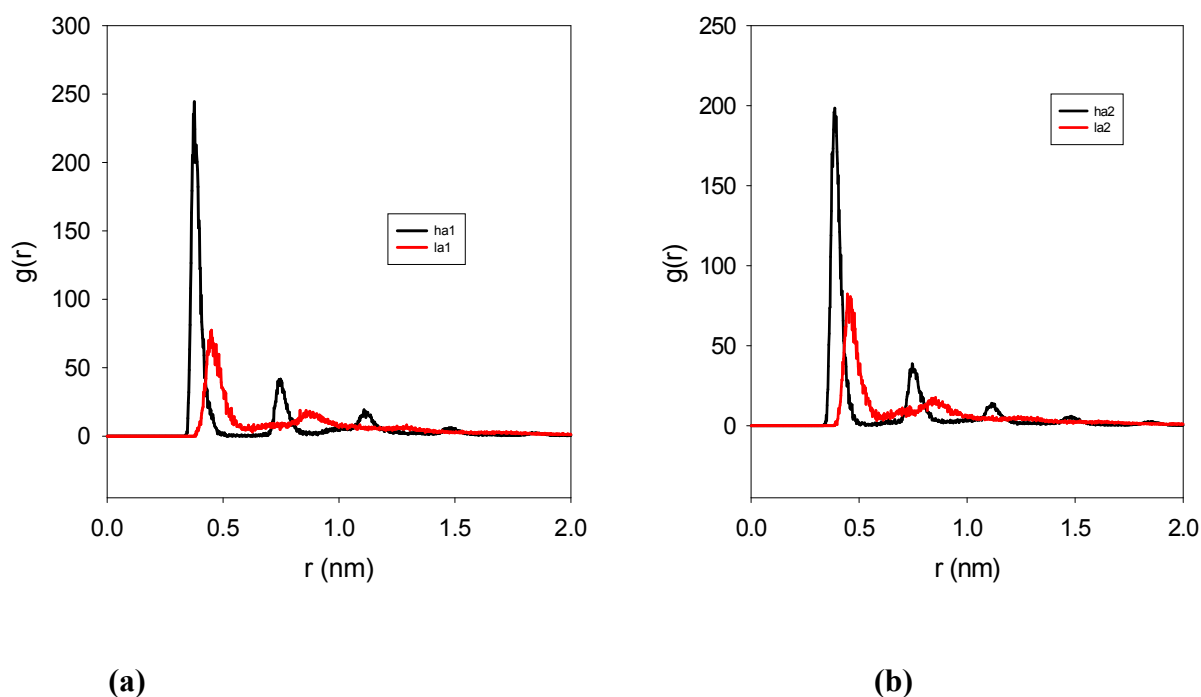
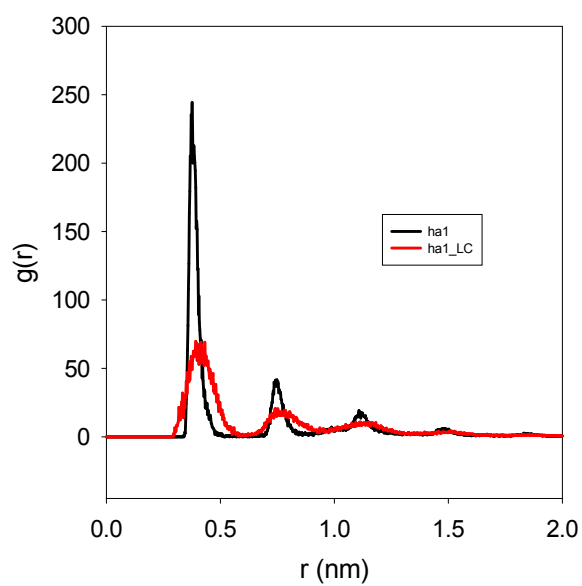
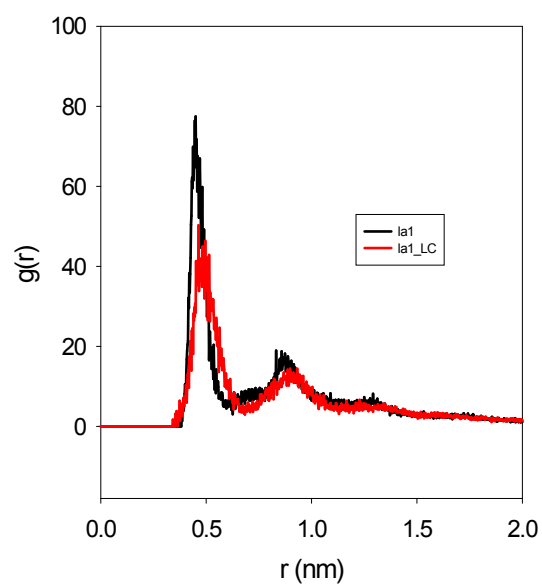


Fig 46(a,b) showing the comparison of the ha1N with la1N and ha2N with la2N

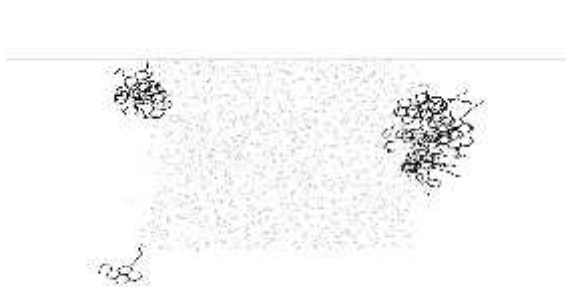
From the comparison of the ha1N with la1N and ha2N with la2N it is obvious from the $g(r)$ that the la1N and la2N adopt more disordered structure at the surface. Therefore, using the same argument as proposed earlier, it might be expected that the low aromaticity molecules would form a less stable adsorbed layer, and would not be as good at stabilizing the interface as would the highly aromatic structures.



(a)



(b)



(c)



(d)



(e)



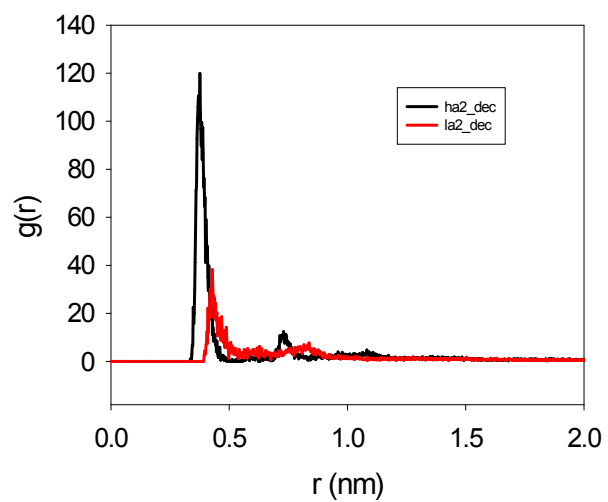
(f)

Fig 47 Showing the effect of addition of hydrocarbon chains to the ha1N (Fig 47c,d) and la1N (Fig 47e, f) molecules to the asphaltene layer

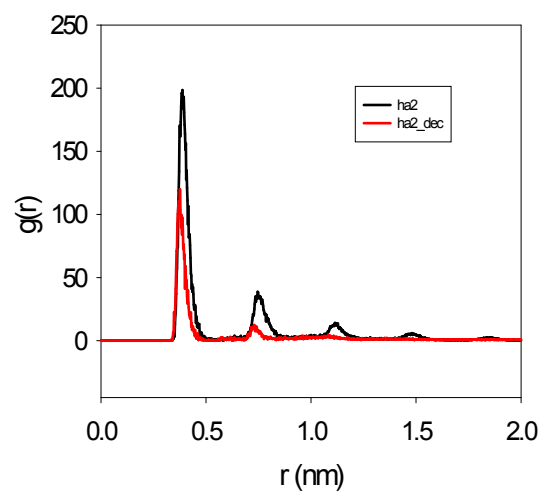
If hydrocarbon chains are added to the ha1N and la1N molecules as shown above, this leads to a further disordering of the adsorbed asphaltene layer i.e. when comparing ha1N to ha1N_LC (top conformations) and la1N to la1N_LC (bottom conformations) the $g(r)$ shows smaller, broader peaks and a reduced number of peaks when the LC chain is added. Again, we would expect these to form stable adsorbed layers compared to the equivalent structures that do not have chains attached (Ha1N and La1N), and presumably would not be as good at stabilizing water-in-oil emulsions.

High aromaticity 2N (ha2N) and Low aromaticity 2N (la2N) conformation at the decane-water interface

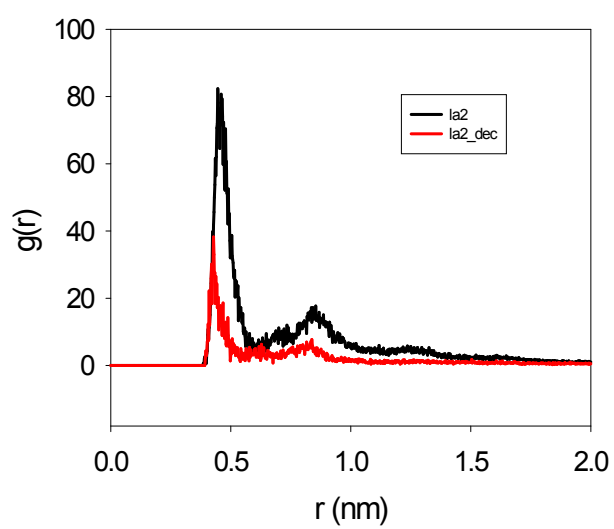
Molecular dynamic simulation was performed for the ha2N and la2N at the decane-water interface in order to compare this to that of the water- vacuum interface and to investigate the effect that the ha2N asphaltene has on the decane at the interface. This is illustrated in the figures below:



(a)



(b)



(c)

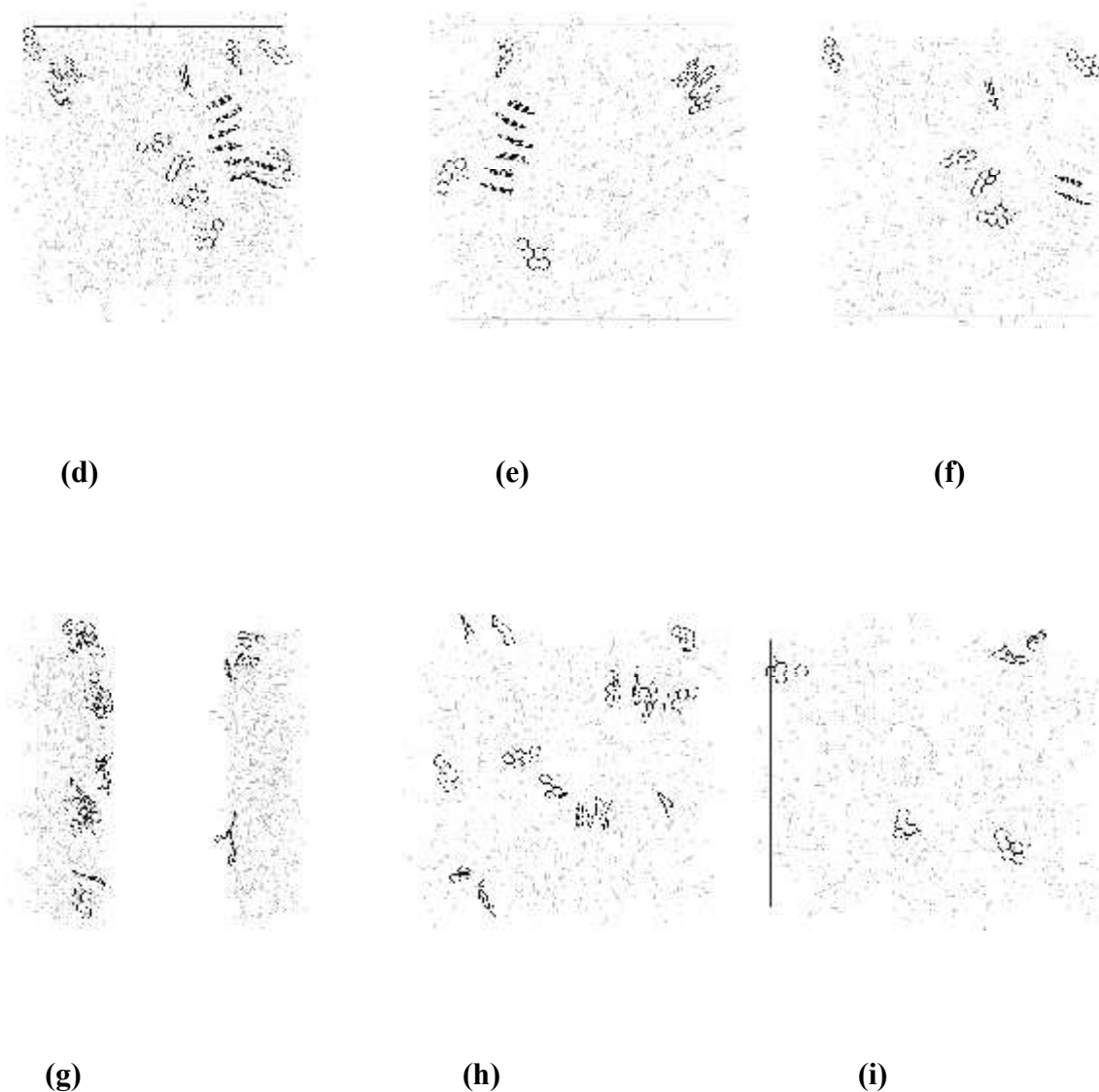


Fig 48 Ha2N and la2N showing the structural conformation of asphaltenes at the decane-water interface and a plot of radial distribution ($g(r)$), (Fig 48a,b,c), for the adsorbed molecules

The ha2N and la2N asphaltenes are less ordered at the decane-water interface than at the water-vacuum interface (the $g(r)$ has lower peaks and less of them at the decane-water interface). La2N is less ordered than ha2n at the decane-water interface in a similar way to that at the water-vacuum interface.

The most noticeable observation is the effect that the ha2N asphaltene has on the decane at the interface. There is considerable ordering of the decane molecules as well when the ha2N molecules are present. This suggests that ha2N ordering at the surface acts as a template for “crystallization” of the decane molecules. This could be a form of phase

separation, or thermodynamic incompatibility. The aromatic nature of the ha2N means that they are very rigid, and they will dictate the structure of the immediate surroundings, i.e. the structure of the decane. This introduces an ordering of the decane molecules which decreases the entropy of the decane layer. This should be unfavourable. It is somewhat uncertain what could be the interaction in the system to allow for this enthalpy penalty. However, the phase separation at the interface as obtained from the results of molecular simulation in this work extensively supports the characteristic property of asphaltene by several authors where it is stated that asphaltenes generally are characterized by fused ring aromaticity, small aliphatic side chains, and polar heteroatoms containing functional groups and trace metals, and also form colloidal suspensions in the oil (Stankiewicz *et al*, 2002; Mullins *et al*, 2007), as given earlier in Section 6.1 of this Chapter.

The results obtained from this work, as given in this Chapter, are strongly supported by previous studies by Singh *et al.* (1999). Singh and co-workers studied the effect of the fused-ring solvents including naphthalene, phenanthrene, and phenanthridine in destabilizing emulsions (Singh *et al.*, 1999). They noted that the primary mechanism for emulsion formation is the stability of asphaltene films at the oil-water interface. They suggested that the mechanism is one in which planar, disk-like asphaltene molecules aggregate through lateral intermolecular forces to form aggregates. This is similar to the results obtained from molecular dynamic simulations of asphaltene interfacial behavior, described in this work, and presented in this Chapter.

The aggregates form a viscoelastic network after absorption at the oil-water interface. The network is sometimes called a film or skin and the strength of this film correlates with emulsion stability. Singh *et al.* (1999) further probed the film-bonding interactions by studying the destabilization by aromatic solvents. It was found that fused-ring solvents, in particular, were effective in destabilizing asphaltene-stabilized emulsions. It is suggested that both π -bonds between fused aromatic sheets and H-bonds play significant roles in the formation of the asphaltene films (Fingas, 2010).

The effect of ha2N asphaltene on the decane interface can be related to formation and behaviour of water-in-oil emulsification, and the stability of the emulsion. The result indicates however, that this may very likely lead to an increase in the viscosity of the hydrocarbon phase since it is starting to crystallize. It should be noted that if the viscosity of the continuous phase of an emulsion is higher, then it is expected that the emulsion will be more stable i.e. more difficult to break since the water droplets can not move around as much to coalesce. The mechanism of coalescence is that non-deforming surfaces makes emulsion stable (McClements, 1998). As reported by Fingas (2010), the oleic medium plays an important role in the surface activity of asphaltenic aggregates and in the resulting emulsion stability.

In all the four crude oil types analysed, the viscosity of the Stirling crude was high. Also, Stirling crude was more aromatic, and the least polar compared to Forties, Brent and Brae A crude oil types. Moreover, the emulsions obtained from it were more stable, which tends to support the result demonstrated by simulation of the behaviour of the high aromaticity asphaltene 2N on the decane at the interface.

6.5 Conclusion

1. At the water-vacuum interface, all “asphaltenes” wet the vacuum side of the interface i.e. they are hydrophobic
2. Increasing the number of ring nitrogen atoms in the molecules leads to a larger proportion of the molecule to reside in the water phase i.e. they are less hydrophobic.
3. Decreasing the aromaticity of the “asphaltene” molecules results in a complex behaviour. The low aromaticity 2N (la2N) unexpectedly resides much further into the vacuum phase than the high aromaticity 2N (ha2N).
4. The addition of a hydrocarbon chain to the ha1N and la1N molecules again leads to complex behaviour, with the extra hydrocarbon chain leading to the molecule to reside more into the aqueous phase.
5. Ha1N and ha2N molecular dynamic simulations both adopted a highly ordered conformation at the water-vacuum interface, similar to the π -Stacking observed in porphyrin molecules. This is evident in the orientation of the molecules. They tended to prefer an almost parallel packing conformation, as similarly reported by Fingas and Fieldhouse (2008).
6. The low aromaticity “asphaltenes”, la1N and la2N have a more disordered structure at the interface, compared to the high aromaticity asphaltenes.
7. A simulation of the ha2N and la2N at the decane-water interface resulted in the both molecules residing fully in the decane phase i.e. they wet the oil side of the interface.
8. Ha2N “asphaltene” has an effect on the decane at the decane-water interface, where the ha2N appears to promote crystallization of the decane molecules. This may very likely lead to an increase in the viscosity of the hydrocarbon phase in water-in-oil emulsification, with a resultant effect on the stability and behaviour of the emulsion.
9. The ability of North Sea crude oil asphaltenes to form stable w/o emulsions correlated to a number of structural factors (aromaticity, polarity and degree of total alkylation including aliphatic chain length and branching).

10. The experimental design and results from the molecular dynamic simulation of the interactions and conformations of asphaltene structures at the interface, obtained from this work may significantly enhance and contribute a step forward in the design of chemical demulsifiers.

CHAPTER 7

CORRELATION ANALYSIS OF VARIABLES MEASURED IN A STUDY OF NORTH SEA CRUDE OILS

7.1 Introduction

Chapters 2-5 describe a series of chemical and physical investigations which were carried out on four North Sea crude oils. The techniques used have given significant information on the physicochemical properties of the different oils. A correlation analysis was carried out to investigate which of the many parameters measured correlated with one another. The objectives were: a) to see whether the correlated values agreed with experimental observations; b) to see whether the correlated values agreed with those reported in the literature; c) to see whether new correlations could be found. Although a large number of parameters were compared only a small sample number of crudes (4) were investigated. This was taken into account when evaluating the relevance of the findings.

It is necessary to correlate crude oil properties in order to ascertain and gain insight into emulsion stability and behaviour. A correlation analysis was performed to cull the variance from a data set of measured parameters in the four North Sea crude oils samples. The correlation follows from properties related to the compositions of the oils such as: alkyl side chain, carbon type, polarity, hydrogen/ carbon ratio (H/C) ratio, condensed aromatic rings, % asphaltenes, and chemical and physical properties of the emulsions such as water content and viscosity.

7.2 Background

Crude oil physico-chemical properties and SARA compositions have been correlated to emulsion stability by several researchers. The results from these studies have found that stability increased as viscosity increased and viscosity also correlated with SARA data (Fingas and Fieldhouse, 2009; Hemmingston *et al.*, 2005; Sjoblom *et al.*, 2002). Further correlations with their respective references are given below:

Significant positive correlations reported in the literature

1. *Emulsion viscosity and asphaltene contents* - References: Abdurahman and Yunus, 2009; Fingas, and Fieldhouse, 2009; Kokal, 2002; Spiecker, 2001; Schorling *et al.*, 1999; Sjoblom *et al.*, 1992.
2. *Emulsion viscosity (stability) and water contents* - Spiecker, 2001; Kilpatrick and Spiecker, 2001; Gu *et al.*, 2002; Dicharry *et al.*, 2006; Yarranton *et al.*, 2007; Fingas and Fieldhouse, 2009; Abdurahman and Yunus, 2009.
3. *Asphaltene content and water content* - Fingas and Fieldhouse, 2009.
4. *Stability and wax or sulphur content* – Sjoblom *et al.*, 1990a,b; Mingyuan *et al.*, 1992a, b; Nordli *et al.*, 1991;
5. *Asphaltene / resin content and emulsion stability* – Xia *et al.*, 2004; Fingas and Fieldhouse, 2009; Abdurahman and Yunus, 2009.
6. *Viscosity and emulsion stability* – Hemmingston *et al.*, 2005; Sjoblom *et al.*, 2002.
7. *Amount of asphaltene / resin (A/R ratio) contents and emulsion stability* - Elsharkawy *et al.*, 2008; Schorling *et al.*, 1999; Kallevik *et al.*, 2000; Fingas and Fieldhouse, 2009.
8. *Density and water content* - Fingas and Fieldhouse, 2009; Elsharkawy *et al.*, 2008.
9. *Density and viscosity* - Fingas and Fieldhouse, 2009.
10. *Emulsion viscosity and SARA composition* - Hemmingston *et al.*, 2005; Fingas and Fieldhouse, 2009.
11. *H/C ratio in asphaltene and amount (%) hydrogen content in asphaltene* - Elsharkawy *et al.*, 2008; Spiecker, 2001.
12. *Polarity and % Nitrogen* - McLean and Kilpatrick, 1997; Speight, 2004.
13. *Aromaticity (condensed aromatic ring) and H/C ratio* - McLean and Kilpatrick, 1997; Speight, 2004; Elsharkawy *et al.*, 2008; Spiecker, 2001.
14. *Interfacially active fractions of crude oil and high (rich) acidic functional groups*- Sjoblom *et al*; Mingyuan, 1992.
15. *High (rich) acidic functional groups and emulsion stability* - Sjoblom *et al*; Mingyuan, 1992.
16. *Amount of asphaltene and interfacial elasticity* – Cormack, 1999; Sjoblom *et al.*, 2003; Fingas and Fieldhouse, 2009.
17. *Amount of asphaltene and interfacial modulus (tension/elasticity)* – Yarranton *et al.*, 2007a, b.

Significant negative correlations reported in the literature

1. *H/C ratio in asphaltene and the H/C ratio in resin* - Elsharkawy *et al.*, 2008; Spiecker, 2001;
2. *H/C ratio in asphaltene and the H/C ratio in aromatic* - Elsharkawy *et al.*, 2008
2. *Stability and wax or sulphur content* - Berridge, 1968.
3. *Emulsion stability and only resins of crude* – Schorling *et al.*, 1998.
4. *Fresh crude emulsion viscosity and weathered crude emulsion viscosity* – Fingas and Fieldhouse, 2009.
5. *Fresh crude emulsion water content and SARA % asphaltene* - Fingas and Fieldhouse, 2009.
6. *SARA % asphaltenes and SARA % aliphatic* - Elsharkawy *et al.*, 2008; Fingas and Fieldhouse, 2009.
7. *SARA % asphaltenes and SARA % resins* - Elsharkawy *et al.*, 2008; Fingas and Fieldhouse, 2009.
8. *SARA % asphaltenes and SARA % aromatic* - Fingas and Fieldhouse, 2009.

The results are discussed in the light of these reported correlations.

7.3 RESULTS AND DISCUSSION

The correlation analysis performed here highlights some differences between the variables in the North Sea crude oils studied. Important factors that may influence the stability of water-in-oil emulsions stability are given in the correlation Table 7.1

Table 7.1 showing the correlation of variables in the analyses of some North Sea crude oils

Variable	Correlations (Joachim PCA data)																													
	Marked correlations are significant at $p < 0.0001$																													
Variable	N=4 (Casewise deletion of missing data)																													
	side chain	aromatic	type aromatic	type aromatic	Polarity	Density	asphaltenes %	resins %	carbon %	aromatic %	resins %	hydrogen %	hydrogen %	hydrogen %	hydrogen %	hydrogen %	hydrogen %	hydrogen %	hydrogen %	hydrogen %	hydrogen %	hydrogen %	hydrogen %	hydrogen %	hydrogen %	hydrogen %	hydrogen %	hydrogen %	hydrogen %	hydrogen %
Alkyl side chain	1.00	-0.50	-0.33	-0.30	0.99	0.95	-0.24	-0.35	0.77	0.33	0.72	0.61	0.74	-0.95	0.95	0.80	0.72	-0.35	0.98	0.85	-0.04	-0.33	-0.94	-0.09	-0.92	-0.70	-0.58	-0.31	-0.77	-0.77
Condensed aromatic rings	-0.50	1.00	0.83	0.71	-0.40	-0.63	-0.24	0.33	-0.29	0.34	-0.95	-0.61	-0.00	0.54	-0.60	-0.98	-0.96	-0.62	-0.65	-0.13	-0.79	-0.10	0.76	0.00	0.80	0.44	0.73	0.01	0.10	0.10
Carbon type asphaltene	-0.33	0.83	1.00	0.94	-0.20	-0.32	-0.72	0.89	-0.51	0.93	-0.69	-0.86	0.37	0.54	-0.96	-0.91	-0.81	-0.65	-0.44	0.20	-0.89	-0.55	0.56	-0.55	0.57	-0.07	0.23	-0.49	-0.30	-0.30
Carbon type aromatic	0.00	0.71	0.94	1.00	0.14	0.00	-0.85	0.82	-0.27	0.30	-0.47	-0.70	0.65	0.24	-0.83	-0.58	-0.60	-0.82	-0.12	0.51	-0.96	-0.77	0.26	-0.61	0.28	-0.32	0.04	-0.33	-0.59	-0.59
Carbon type resin	0.99	-0.40	-0.20	0.14	1.00	0.94	-0.36	-0.24	0.72	0.17	0.65	0.50	0.82	-0.90	0.97	0.71	0.62	-0.47	0.95	0.91	-0.18	-0.33	-0.90	-0.18	-0.87	-0.74	-0.57	-0.39	-0.84	-0.84
Polarity	0.95	-0.63	-0.32	0.00	0.94	1.00	-0.38	-0.19	0.55	0.36	0.85	0.46	0.76	-0.63	0.95	0.81	0.79	-0.23	0.98	0.85	0.05	-0.33	-0.96	-0.34	-0.90	-0.67	-0.81	-0.52	-0.81	-0.81
Density	-0.24	-0.24	-0.72	-0.35	-0.36	-0.38	1.00	-0.82	0.32	-0.39	-0.01	0.63	-0.81	-0.08	-0.28	0.23	0.17	0.57	-0.21	-0.70	0.70	0.36	0.11	0.92	0.11	0.74	0.35	0.35	0.80	0.80
Asphaltenes % carbon	-0.35	0.53	0.86	0.32	-0.24	-0.19	-0.82	1.00	-0.75	0.35	-0.42	-0.86	0.36	0.63	-0.31	-0.59	-0.59	-0.35	-0.37	0.17	-0.66	-0.51	0.45	-0.82	0.44	-0.30	-0.13	-0.73	-0.32	-0.32
Resins % carbon	0.77	-0.29	-0.51	-0.27	0.72	0.55	0.32	-0.75	1.00	-0.30	0.39	0.87	0.28	-0.92	0.67	0.59	0.51	-0.31	0.69	0.44	0.07	0.31	-0.67	0.55	-0.62	-0.09	0.02	0.34	-0.29	-0.29
Aromatics % carbon	0.03	0.64	0.93	0.99	0.17	0.05	-0.89	0.85	-0.30	1.00	-0.43	-0.71	0.69	0.23	0.61	-0.54	-0.55	-0.73	-0.07	0.55	-0.93	-0.32	0.21	-0.69	0.23	-0.40	-0.06	-0.70	-0.26	-0.26
Asphaltenes % hydrogen	0.72	-0.95	-0.69	-0.47	0.65	0.85	-0.01	-0.42	0.39	-0.40	1.00	0.58	0.32	-0.69	0.81	0.93	0.98	0.35	0.85	0.44	0.56	-0.20	-0.91	-0.17	-0.94	-0.68	-0.35	-0.28	-0.41	-0.41
Resins % hydrogen	0.61	-0.61	-0.86	-0.70	0.50	0.43	0.83	-0.96	0.37	-0.71	0.53	1.00	-0.08	-0.82	0.56	0.94	0.72	0.13	0.61	0.11	0.35	0.35	-0.67	0.67	-0.65	0.04	-0.07	0.52	0.04	0.04
Aromatics % hydrogen	0.74	-0.60	0.37	0.55	0.82	0.75	-0.81	0.36	0.28	0.39	0.32	-0.08	1.00	-0.50	0.73	0.24	0.20	-0.71	0.68	0.98	-0.61	-0.36	-0.56	-0.61	-0.54	-0.84	-0.55	-0.77	-1.09	-1.09
Asphaltenes % nitrogen	-0.85	0.54	0.54	0.24	-0.90	-0.83	-0.08	0.83	-0.92	0.23	-0.69	-0.82	-0.50	1.00	-0.91	-0.97	-0.75	0.24	-0.52	-0.66	-0.14	0.24	0.91	-0.23	0.88	0.45	0.38	-0.31	0.53	0.53
Resins % nitrogen	0.99	-0.60	-0.36	-0.30	0.97	0.99	-0.28	-0.31	0.67	0.31	0.81	0.56	0.73	-0.91	1.00	0.93	0.78	-0.25	1.00	0.84	0.04	-0.55	-0.97	-0.20	-0.96	-0.79	-0.70	-0.40	-0.78	-0.78
Aromatics % nitrogen	0.80	-0.88	-0.81	-0.58	0.71	0.81	0.23	-0.69	0.66	-0.54	0.93	0.84	0.24	-0.67	0.83	1.00	0.97	0.25	0.88	0.41	0.56	-0.33	-0.94	0.17	-0.94	-0.47	-0.60	0.01	-0.31	-0.31
H/C ratio asphaltenes	0.72	-0.96	-0.81	-0.50	0.62	0.79	0.17	-0.59	0.51	-0.55	0.93	0.72	0.20	-0.75	0.78	0.97	1.00	0.43	0.83	0.35	0.65	-0.34	-0.90	0.03	-0.93	-0.53	-0.72	-0.39	-0.28	-0.28
H/C ratio resins	-0.36	-0.62	-0.65	-0.32	-0.47	-0.23	0.57	-0.35	-0.31	-0.78	0.35	0.19	-0.71	0.24	-0.25	0.25	0.40	1.00	-0.18	-0.66	0.92	0.56	0.03	0.19	-0.03	0.23	-0.15	0.31	0.64	0.64
H/C ratio aromatics	0.98	-0.65	-0.44	-0.12	0.95	0.99	-0.21	-0.37	0.66	-0.37	0.85	0.61	0.68	-0.92	1.00	0.98	0.83	-0.13	1.00	0.80	0.11	-0.49	-0.99	-0.15	-0.96	-0.76	-0.70	-0.35	-0.73	-0.73
SARA % aliphatics	0.85	-0.13	0.20	0.51	0.91	0.85	-0.70	0.17	0.44	0.55	0.44	0.11	0.98	-0.66	0.84	0.41	0.35	-0.65	0.80	1.00	-0.49	-0.39	-0.70	-0.49	-0.67	-0.84	-0.58	-0.58	-0.99	-0.99
SARA % aromatics	-0.04	-0.79	-0.86	-0.36	-0.18	0.05	0.70	-0.68	0.07	-0.30	0.55	0.55	-0.61	-0.14	0.84	0.56	0.65	0.92	0.11	-0.49	1.00	0.37	-0.27	0.39	-0.31	0.17	-0.23	0.43	0.53	0.53
SARA % resins	-0.53	-0.70	-0.58	-0.77	-0.63	-0.61	0.95	-0.41	0.01	-0.32	-0.20	0.35	-0.96	0.24	-0.55	-0.33	-0.04	0.65	-0.49	-0.89	0.67	1.00	0.37	0.81	0.37	0.85	0.57	0.90	0.95	0.95
SARA % asphaltenes	-0.54	0.76	0.56	0.26	-0.90	-0.95	0.11	0.45	-0.67	0.21	-0.91	-0.67	-0.56	0.91	-0.97	-0.94	-0.90	0.03	-0.99	-0.70	-0.27	0.37	1.00	0.10	1.00	0.71	0.73	0.28	0.63	0.63
Fresh oil crude oil emulsion viscosity	-0.09	0.00	-0.55	-0.51	-0.18	-0.34	0.92	-0.32	0.35	-0.59	-0.17	0.67	-0.61	-0.23	-0.20	0.17	0.03	0.19	-0.15	-0.49	0.39	0.31	0.10	1.00	0.13	0.76	0.67	0.97	0.97	0.97
Fresh crude emulsion water content	-0.62	0.80	0.57	0.28	-0.87	-0.95	0.11	0.44	-0.62	0.23	-0.94	-0.65	-0.54	0.88	-0.96	-0.94	-0.93	-0.03	-0.58	-0.67	-0.31	0.37	1.00	0.13	1.00	0.73	0.77	0.30	0.61	0.61
11% weathered crude emulsion viscosity	-0.70	0.44	-0.07	-0.32	-0.74	-0.87	0.74	-0.30	-0.09	-0.40	-0.68	0.04	-0.84	0.45	-0.75	-0.47	-0.53	0.23	-0.76	-0.84	0.17	0.35	0.71	0.75	0.73	1.00	0.91	0.97	0.89	0.89
11% weathered crude emulsion water content	-0.58	0.73	0.25	0.34	-0.57	-0.81	0.49	-0.13	0.02	-0.36	-0.85	-0.07	-0.55	0.58	-0.70	-0.50	-0.72	-0.19	-0.70	-0.58	-0.23	0.57	0.73	0.67	0.77	0.61	1.00	0.73	0.63	0.63
20% weathered crude emulsion viscosity	-0.31	0.07	-0.49	-0.53	-0.39	-0.52	0.95	-0.73	0.34	-0.70	-0.23	0.52	-0.77	-0.01	-0.40	0.01	-0.09	0.31	-0.35	-0.68	0.43	0.30	0.28	0.97	0.30	0.67	0.73	1.00	0.79	0.79
20% weathered crude emulsion water content	-0.77	0.70	-0.30	-0.59	-0.84	-0.81	0.80	-0.32	-0.26	-0.53	-0.41	0.04	-1.00	0.53	-0.78	-0.33	-0.28	0.64	-0.73	-0.99	0.53	0.36	0.63	0.63	0.61	0.69	0.83	0.79	1.00	1.00

The raw correlation data set is given in Tables 7.1. In the analysis, values for variables between 0.95 – 1.00 indicated significant correlation; values below 0.95 are not significant ($p < 0.05$). The significant positive and negative correlations are listed in Table 7.2. The variables showed both significant positive correlation and significant negative correlation. In general, the analysis showed that there was a high correlation between viscosity, asphaltenes, resins, aliphatic and aromatics. However, for analysis of the variables that are likely to influence crude oil emulsification, a correlation of the crude oils unique polarity, aromaticity and alkyl side chain length with the oil emulsions viscosities enabled a better understanding in addition to the complex strong interactions among the crude oil subclasses (resins, asphaltenes etc.) and other variables. The properties of the four crude oil types can be further understood using the inputs of oil properties such as H/C ratio and emulsion water contents.

Table 7.2 showing a summary of the significant and not significant correlated variables in the correlation analysis ($p < 0.05$)

Significant positive correlation (≥ 0.95)	Significant negative correlation (≤ -0.98)
<ul style="list-style-type: none"> Alkyl side chain / carbon type resin Alkyl side chain / resins % nitrogen Alkyl side chain / H/C ratio aromatics Carbon type aromatic / aromatic % carbon Carbon type resin / alkyl side chain Carbon types resin / resins % nitrogen Carbon types resins / H/C ratio aromatic Polarity / resins % nitrogen Aromatic % carbon / carbon type aromatic Resins % nitrogen / alkyl side chain Resins % nitrogen / polarity Resins % nitrogen / H/C ratio aromatics H/C ratio aromatic / resins % nitrogen SARA % Asphaltenes / fresh crude emulsion water content Fresh crude emulsion water content / SARA % Asphaltenes Asphaltenes % hydrogen / H/C ratio asphaltenes H/C ratio asphaltenes / asphaltenes % hydrogen H/C ratio asphaltenes / aromatics % nitrogen H/C ratio aromatics / alkyl side chains H/C ratio aromatics / carbon type resins Aromatics % nitrogen / H/C ratio asphaltenes Aromatics % hydrogen / SARA % aliphatics H/C ratio aromatics / polarity SARA % aliphatics / aromatics % hydrogen Fresh crude oil emulsion viscosity / 20% weathered crude emulsion viscosity 20% weathered crude emulsion viscosity / fresh crude emulsion viscosity 	<ul style="list-style-type: none"> Condensed aromatic ring/ H/C ratio asphaltene Carbon type aromatic/ SARA % aromatic Polarity / SARA % asphaltenes Asphaltenes % carbon / resins % hydrogen Resins % hydrogen / Asphaltenes % carbon Aromatics % hydrogen / SARA % resins Aromatics % hydrogen / 20% weathered crude emulsion water content Resins % nitrogen / SARA % asphaltenes Resins % nitrogen / fresh crude emulsion water content H/C ratio asphaltenes / condensed aromatic rings H/C ratio aromatics / SARA % asphaltenes H/C ratio aromatics / fresh crude emulsion water content SARA % aliphatics / 20% weathered crude emulsion water content SARA % aromatics / carbon type aromatics SARA % resins / aromatics % hydrogen SARA % asphaltenes / polarity SARA % asphaltenes / resins % nitrogen SARA % asphaltenes / H/C ratio aromatics Fresh crude emulsion water content / polarity Fresh crude emulsion water content / resins % nitrogen Fresh crude emulsion water content / H/C ratio aromatics 20% weathered crude emulsion water content / aromatics % hydrogen 20% weathered crude emulsion water content / SARA % aliphatics Polarity / fresh crude emulsion water content

Expected correlations in the literature (EE)

1. *Emulsion viscosity and asphaltene contents* - References: Abdurahman and Yunus, 2009; Fingas, and Fieldhouse, 2009; Kokal, 2002; Spiecker, 2001; Schorling *et al.*, 1999; Sjoblom *et al.*, 1992.
2. *Emulsion viscosity (stability) and water contents* - Spiecker, 2001; Kilpatrick and Spiecker, 2001; Gu *et al.*, 2002; Dicharry *et al.*, 2006; Yarranton *et al.*, 2007; Fingas and Fieldhouse, 2009; Abdurahman and Yunus, 2009.
3. *Asphaltene content and water content* - Fingas and Fieldhouse, 2009.
4. *Stability and wax or sulphur content* – Sjoblom *et al.*, 1990a, b; Mingyuan *et al.*, 1992a, b; Nordli *et al.*, 1991;
5. *Asphaltene / resin content and emulsion stability* – Xia *et al.*, 2004; Fingas and Fieldhouse, 2009; Abdurahman and Yunus, 2009.
6. *Viscosity and emulsion stability* – Hemmingston *et al.*, 2005; Sjoblom *et al.*, 2002.
7. *Amount of asphaltene / resin (A/R ratio) contents and emulsion stability* - Elsharkawy *et al.*, 2008; Schorling *et al.*, 1999; Kallevik *et al.*, 2000; Fingas and Fieldhouse, 2009.
8. *Density and water content* - Fingas and Fieldhouse, 2009; Elsharkawy *et al.*, 2008.
9. *Density and viscosity* – Cormack, 1999; Fingas and Fieldhouse, 2009.
10. *Emulsion viscosity and SARA composition* - Hemmingston *et al.*, 2005; Fingas and Fieldhouse, 2009.
11. *H/C ratio in asphaltene and amount (%) hydrogen content in asphaltene* - Elsharkawy *et al.*, 2008; Spiecker, 2001.
12. *Polarity and % Nitrogen* - McLean and Kilpatrick, 1997; Speight, 2004).
13. *Aromaticity (condensed aromatic ring) and H/C ratio* - McLean and Kilpatrick, 1997; Speight, 2004; Elsharkawy *et al.*, 2008; Spiecker, 2001.
14. *Interfacially active fractions of crude oil and high (rich) acidic functional groups*- Sjoblom *et al*; Mingyuan, 1992.
15. *High (rich) acidic functional groups and emulsion stability* - Sjoblom *et al*; Mingyuan, 1992.
16. *Amount of asphaltene and interfacial elasticity* – Cormack, 1999; Sjoblom *et al.*, 2003; Fingas and Fieldhouse, 2009.
17. *Amount of asphaltene and interfacial modulus (tension/elasticity)* – Yarranton *et al.*, 2007a, b.

Non-expected correlations from the literature

1. *H/C ratio in asphaltene and the H/C ratio in resin* - Elsharkawy *et al.*, 2008; Spiecker, 2001;
2. *H/C ratio in asphaltene and the H/C ratio in aromatic* - Elsharkawy *et al.*, 2008
2. *Stability and wax or sulphur content* - Berridge, 1968.
3. *Emulsion stability and only resins of crude* – Schorling *et al.*, 1998.
4. *Fresh crude emulsion viscosity and weathered crude emulsion viscosity* – Fingas and Fieldhouse, 2009.
5. *Fresh crude emulsion water content and SARA % asphaltene* - Fingas and Fieldhouse, 2009.
6. *SARA % asphaltenes and SARA % aliphatic* - Elsharkawy *et al.*, 2008; Fingas and Fieldhouse, 2009.
7. *SARA % asphaltenes and SARA % resins* - Elsharkawy *et al.*, 2008; Fingas and Fieldhouse, 2009.
8. *SARA % asphaltenes and SARA % aromatic* - Fingas and Fieldhouse, 2009.

Expected positive correlations based on the experimental data in this thesis were:

1. Asphaltene content and emulsion stability
2. Viscosity and emulsion stability
3. Water contents and emulsion stability
4. Alkyl side chain and SARA % asphaltene (emulsion stability)*
5. Asphaltene/ Resin (A/R) ratio and emulsion stability
6. H/C ratio aromatic and emulsion stability
7. H/C ratio resin and emulsion stability
8. H/C ratio asphaltenes and emulsion stability
9. H/C ratio aromatic and polarity
10. Carbon type resin and emulsion viscosity
11. SARA % asphaltenes and emulsion stability
12. SARA % asphaltene and fresh crude emulsion water content
13. Polarity and emulsion stability (negative correlation)
14. Polarity and % Nitrogen
15. Aromaticity and emulsion stability
16. Density and viscosity

Expected negative correlations based on the experimental data in this thesis were:

1. Fresh crude oil emulsion viscosity and 20% weathered crude emulsion viscosity
2. SARA % asphaltene and fresh crude emulsion viscosity
3. SARA % asphaltene and asphaltene % nitrogen
4. Fresh crude emulsion water content and SARA % asphaltene
5. Fresh crude emulsion water content and emulsion stability
6. H/C ratio asphaltenes and H/C ratio resin
7. H/C ratio asphaltenes and H/C ratio aromatic
8. H/C ratio resin H/C ratio aromatic
9. SARA % aliphatic and SARA % aromatic
10. SARA % aliphatic and SARA % resin
11. SARA % asphaltenes and SARA % resins
12. SARA % asphaltenes and SARA % aromatic
13. SARA % asphaltenes and SARA % aliphatic
14. SARA % aromatic and SARA % resins

The correlation analysis indicated the following trends: A significant correlation was obtained between H/C ratio of aromatics and resins % nitrogen (1.00), alkyl side chain (0.98) and polarity (0.98) respectively. SARA % asphaltenes showed a significant positive correlation (1.00) with fresh crude emulsion water content. This was considered an important result in the analyses of the variables, particularly as several researchers have used water content as an index to determine the stability of water-in-oil emulsions (Spiecker, 2001; Gu *et al.*, 2002; Dicharry *et al.*, 2006; Yarranton *et al.*, 2007; Fingas and Fieldhouse, 2009; Abdurahman and Yunus, 2009).

Based on several studies on emulsion viscosity and asphaltene contents (Abdurahman and Yunus, 2009; Fingas, and Fieldhouse, 2009; Kokal, 2002; Spiecker, 2001; Schorling *et al.*, 1999; Sjoblom *et al.*, 1992), it would be expected that SARA % asphaltene would yield a significant positive with 20% weathered emulsion viscosity. However, with no obvious outlier in the data set that could account for this, the result given here (0.28) showed no correlation of the two variables in the crude oils investigated in this work. This may probably be related to the limited size of the sample set. This result was unexpected, although in the analysis, SARA % asphaltene yielded a significant positive correlation with fresh crude emulsion water content. Water content

has been used by many researchers (Fingas and Fieldhouse, 2009; Abdurahman and Yunus, 2009, Spiecker; Dicharry *et al.*, 2006) as an index of emulsion stability.

The study, interestingly also yielded a positive correlation (0.97) between fresh crude oil emulsion viscosity and 20% weathered crude emulsion viscosity in the analysis. This was considered as an important previously unreported result in available literature, for the North Sea crude oils studied in these experiments. This is because as would be expected, the experiments had yielded lower viscosity values for the fresh crude emulsions viscosity compared to the higher viscosity values for the 20% weathered crude emulsions, and therefore a positive correlation would not have been expected in these samples. However, it has been reported by other authors that some crude oils do not form stable water-in-oil emulsions until they lose a certain amount of volatile compounds through evaporation (Cormack, 1999; Fingas and Fieldhouse, 2009). The fresh crude oils investigated in this work formed unstable emulsions, confirming the results obtained by other authors.

Alkyl side chain yielded a significant positive correlation with carbon type resin at 0.99, and similarly with resins % nitrogen at 0.99. Carbon type aromatics showed a significant positive correlation with aromatic % carbon at 0.99. This result agreed well with studies reported by other authors stating that some of the carbon and hydrogen atoms are bound in ring-like, aromatic groups in crude oil asphaltene, in particular Mullins *et al.* (2007). Hence, it is expected that the carbon types in aromatic fraction would yield a significant positive correlation with aromatic % carbon, as shown in the analysis of these variables. A correlation was expected between alkyl side chain with SARA % asphaltene, however, the analysis showed no correlation of these two variables in this study. The density of crude oils showed no correlation with both the fresh and weathered crude oil emulsion viscosities although a positive correlation was expected based on the experimental data. The North Sea crude oils investigated were of moderate densities and contained significant amount of asphaltenes to some extent, and these strongly related to the emulsion viscosities. A positive correlation has been reported between the density of the starting oil (i.e. fresh oil) and viscosity, both parameters influencing crude oil emulsions (Cormack, 1999; Fingas and Fieldhouse, 2009). Thus, a strong correlation was expected between density and the emulsions.

As expected in the analysis, H/C ratio of aromatics yielded a significant positive correlation with polarity ($r = 0.98$). Similarly, polarity yielded a significant positive correlation with resins % nitrogen at 0.99. This strong correlation was observed to be in good agreement with similar results reported by McLean and Kilpatrick, 1997; Speight, 2004, on crude oil polarity studies. The authors reported that nitrogen content may indicate the polarity in oil fractions. Experimental results from this study, as reported in Chapter 4, Section 4.5.3 also indicated that nitrogen content was higher in the resins compared to the asphaltene and aromatics fractions with the exception of the Stirling oil fractions.

However, interesting results were obtained in the positive correlations of carbon type resin with resins % nitrogen (0.97), and carbon type resins with H/C ratio of aromatics (0.95) respectively. As shown in the analysis of the variables in this study, the significant positive correlations of carbon types in crude oil resin with the resins % N, and also with H/C ratio of crude oil aromatics have not been previously reported in available literature. The correlation of aromatic % carbon with carbon type aromatic was good, with a significant positive correlation at 0.99.

The correlation analysis showed that some variables both yielded significant positive correlations with some variables, and on the other hand also yielded a significant negative correlation with other variables. For instance, H/C ratio of asphaltene showed a positive correlation with asphaltene % hydrogen at 0.98 and with aromatics % nitrogen at 0.97 respectively, whereas the same variable (H/C) ratio of asphaltene, showed a significant negative correlation at -0.96 with condensed aromatic rings. The H/C ratio of resins similarly yielded a significant negative correlation with condensed aromatic rings. These results agreed with findings by other researchers who have reported the correlation of aromaticity with H/C (Elsharkawy *et al.*, 2008; McLean and Kilpatrick, 1997; Speight, 2004; Spiecker, 2001).

Asphaltenes % hydrogen yielded a positive correlation ($r = 0.98$) with H/C ratio of asphaltenes, whereas aromatic % hydrogen showed a negative correlation at -0.96 with SARA % resin. Also, aromatics % hydrogen showed a positive correlation with SARA % aliphatics at 0.98.

Carbon type aromatic yielded a negative correlation with SARA % aromatic fraction of the sample. This negative correlation was unexpected in the sample between the carbon type aromatic and SARA % aromatic. It would be expected in the analysis that the carbon type aromatic which is determined based on the overall SARA fractions, would yield a significant positive correlation with the SARA % aromatic, but this was not the case between the two variables. This may be as a result of the limited amount of samples in the correlation of the two variables, resulting in a significant negative correlation.

It is clear that key factors relating to water-in-oil emulsification process in crude oils (particularly, North Sea crudes) can be adequately understood, with the significant variables including polarity, condensed aromatic rings and alkyl side chain and the difference between the oils/emulsions. However, it is also apparent that emulsion formation, viscosity/water contents relationships and stability, are much more complex and dependent on several oil parameters, in addition to density, which change in value from oil to oil. Although the understanding of emulsions is much less thorough and presently inconclusive compared to other weathering factors, the overall approach outlined in this chapter provides insight into the nature and scope of challenges which arise when emulsions are encountered on the sea surface. They also enhance the understanding of persistence of emulsions as surface slicks and possible countermeasures (dispersant application, etc.) that may be applied.

7.4 Conclusion

1. SARA % asphaltenes showed a significant positive correlation with fresh crude emulsion water content.
2. H/C ratio of aromatics yielded a significant positive correlation with polarity.
3. SARA % asphaltenes yielded no correlation with 20% weathered emulsion viscosity.
4. Alkyl side chain showed no correlation with SARA % asphaltene.
5. Fresh crude oil emulsion viscosity showed a positive correlation with 20% weathered crude emulsion viscosity.
6. The factors that may influence water-in-oil emulsification (particularly in North Sea crude oils) can be understood with the knowledge of variables such as polarity, condensed aromatic rings and alkylation (alkyl side chain), in oils/emulsions.

CHAPTER 8

INTEGRATED DISCUSSION OF THE EXPERIMENTAL RESULTS

8.1 Introduction

The results from each of the previous chapters (Chapters 2 – 5), an investigation of the weathering, emulsification behaviour and chemistry of the North Sea crude oils; Chapter 6, modeling of proposed asphaltene structures; and Chapter 7, a correlation analysis of measured parameters), have been discussed in light of the literature. This chapter aims to pull together the results from the previous chapters and discuss them in an integrated manner, again comparing the data to the literature, to see what conclusions can be drawn.

8.2 Background to Oil pollution incidents

Oil pollution at sea, either as a result of anthropogenic or natural sources, has been the focus of many researches over the past years by scientists, consultancies and governments due to a number of serious accidents involving the release of large volumes of oil at sea. Oil released as a consequence of human activity such as ship cleaning operations, refinery activities, sunken ship, well blow-outs and accidental spills have the potential to cause significant impact on the environment. Accidents which may result in the discharge of relatively large quantities of oil near to sensitive coastal marine environment are of great concern. A review of some of the well known and reported cases has been given in Chapter 1, Section 1.4, with the most recent of such occurrence being the Deepwater Horizon offshore installation accident which occurred on 20th April, 2010 in the Gulf of Mexico. The short and long-term economic and environmental implications of these accidents has led to studies aimed at understanding and quantifying the spill processes, in order to predict the behaviour of the spilled oil with a view to developing realistic options and contingency plans for an effective response and countermeasure. It is important to note that the efficiency of these response measures lies in prior and in-depth knowledge of the compositional properties of the spilled substance, and also the understanding of the fundamental physicochemical processes that begins immediately oil is spilled on the sea surface.

Spilled hydrocarbon in the marine environment is subjected to various simultaneous, inter-acting phenomena. The transformation of spilled oil, also known as weathering, associated with these wide varieties of physicochemical and biological processes that changes the composition and behaviour of crude oil, has been previously given in Chapter 1, Section 1.5. Evaporation has been identified as one of the foremost weathering processes that primarily cause a rapid volume reduction of spilled oil, especially in the first few hours of an oil spill. The loss of volatile components by evaporation leads to an increase in the viscosity and density of the remaining residue. Evaporation can also cause changes in the oil properties such as precipitation of asphaltenes that may alter the flow properties of the residue and the stability of water-in-oil emulsions.

8.3 Discussion of experimental results

A major parameter that governs the rate of evaporation of crude oil is temperature. This research has extensively studied the weathering of four North Sea crude oil types over a wide range of temperature and time. Evaporative weathering was carried out on Forties crude oil. The rates of evaporation at different temperatures at timed intervals are shown in Chapter 2, Section 2.4.1, Fig 4a and b. The results indicated a rapid rate of evaporation in the initial duration (0-6 h), for all experimental temperatures (12°C to 50°C), which progressed at a constant rate with time of evaporation, with an increased rate of evaporation at the higher temperatures (40°C - 50°C). The rate of evaporation of the volatile components was slower after the initial 0-6hrs at the temperature range of 12°C - 30°C, and the evaporation thereafter, progressed at a steady rate at these temperatures comparable to the evaporative rate at the higher temperatures (40°C - 50°C). The results indicated that temperature plays a significant role in the evaporation process in crude oil weathering phenomena, and generally agrees well with studies reported by other researchers, as given in Chapter 2, Section 2.4.1 of this work. The relationship and dependence of temperature and time in respect of the North Sea crude oils evaporation was established, and showed a trend which increased with increasing temperature and time. The rate of evaporation increased with temperature and this was modelled, in order to predict the rate of evaporation at other temperatures.

From the results of investigations demonstrated in this work, a proposed numerical algorithm for a modelling scheme to predict the rate of evaporation of crude oil on seawater was given. The experiments were conducted to determine the rates of evaporation of Forties crude on seawater at pre-determined times and temperatures (0-110 h; 12-50°C), and the proposed model is presented to predict the rate of evaporation at other temperatures and time for the sample tested in this research. In the conceptual evaporation model given in Chapter 2, Fig 16-25 showed a good agreement between model predictions and experimental data. The model results are within the values expected for Forties crude, which is a fairly volatile crude oil and is expected to evaporate more than 40% in the initial 24 h for a relatively small spill (Cormack, 1999), even at low evaporative temperatures as indicated in Fig 4b. Also, a good agreement was expected with experimental data, because the sample was allowed naturally to decrease by evaporation during the simulation, and that slightly improved the estimation of the fraction evaporated.

The simulation demonstrated the factors that affect the rate of oil spill on seawater, as a function of various physical variables such as temperature and time at constant wind speed. The model proposed showed the rates of evaporation of Forties crude as a result of these two variables. The algorithms reproduced a satisfactory agreement with results of other researchers (Riazi and Edalat, 1996; Riazi and Al-Enezi, 1999; Daling and Strom, 1999; Wang and Fingas, 2007; Nazir *et al.*, 2008), in which the rates of evaporation were correlated with dissolution, temperature and time. The comparisons of the model predictions with the experimental data were satisfactory since the combined effect and interactions between the variables are accounted for. This should therefore further the understanding of evaporation as a major parameter in crude oil weathering, particularly for spills in tropical climates.

The rate of evaporation using oil on seawater was compared to oil on its own, and was measured by both gravimetric and gas chromatography. Oil on its own evaporated more quickly than oil on seawater. This suggests that evaporating oil on seawater, a more realistic scenario, may give a more realistic evaporation rate.

A weathering experiment was further conducted to investigate the rate of evaporation of Brent crude oil on seawater, at a temperature of 30°C and time interval of 0-48 h. The evaporative rate is illustrated in Chapter 2, Fig 5. A comparison of the rate of evaporation of volatile components of Brent crude with Forties at these temperatures and time intervals indicated that both crude oils types evaporated at similar rapid rates over the initial 0-6 h duration. The mass loss (g) measured for Forties at 1hr and 48hrs evaporation were 1.23 ± 0.15 and 2.52 ± 0.22 , whereas the mass loss for Brent crude at the same interval were 2.12 ± 0.41 and 4.53 ± 0.74 respectively. This strongly suggests that the North Sea crude oils may evaporate at different rates on seawater.

The results showed marked variations in the rate of mass loss from two oils, where Brent crude exhibited a faster evaporation rate compared to Forties crude, from the onset of the experiment to completion (0-48 h). Evaporation loss is controlled most importantly, by the composition and physical properties specific to individual crude oil. These properties are however, extensively affected by evaporation whereby in some instances up to 70% of low molecular weight volatile components can be readily removed by evaporation in the first few hours days of an oil spill, particularly for light crude oil types. It should also be noted that crude oils contain many different compounds ranging from light hydrocarbons such as pentane to heavy compounds in the C₂₀₊ to C₃₀₊ fractions. The light compounds evaporate quickly. Hence, the variation in volatility characteristics between Forties and Brent crude oil can be attributable to the differences in the chemistry of each crude oil type. This may have implications for the evaporation behaviour of other crude oils produced in the North Sea.

Gas chromatography – flame ionisation detection (GC-FID) was used to determine the extent of weathering by molecular carbon number of the Forties and Brent crudes as a consequence of evaporation. The hydrocarbon evaporation signature was ascertained by inspection of the GC-FID chromatograms and the distribution of the saturated hydrocarbons in the chromatograms (Fig 7a-15c). These indicated the changes in the chemical compositions of the crude oils. The modification of the oil's composition provided information on the hydrocarbon fraction that has been eliminated by volatilisation. The crude oil compositional changes, as previously discussed in Section 2.4.5 highlighted the weathering trends between Forties and Brent crudes for the experimental conditions used. The GC chromatograms clearly indicated a unique

physical weathering of Forties and Brent crudes, in which each crude oil type exhibited variability in the evaporation of volatile components.

An investigation to determine the rate of evaporation of volatile components in a water-in-oil emulsion was carried out using Brent crude at the same experimental conditions, and a comparison drawn with the rate of evaporation from the unemulsified Brent crude. The difference in the rate of evaporation is shown in Fig.14 and indicated a higher evaporation in the Brent crude emulsion, compared to Brent crude floating on seawater. Again, using the same argument stated in Chapter 2, Section 2.4.6, it can be theorised, that in a water-in-oil emulsion, the concentration of the lighter hydrocarbon in the oil phase tends to be increased, the heavier molecules with surfactant properties concentrating at the oil - water interface. This hypothesis may explain the higher rate of evaporation in the emulsified oil.

A comparison of the GC chromatograms from the Brent crude and Brent emulsion showed distinct chemical compositional changes as a result of evaporative weathering (Fig 11b; 13b) and (Fig 15a-c) respectively. The GC-FID chromatograms revealed the aliphatic samples of the four crude oil types contained a homologous series of normal alkanes but each indicated a distinct normal alkane profile. Close inspection of the chromatograms also revealed some differences in the relative abundance of the *n*-alkanes, measured by the peak heights in the four oil fractions. The chromatograms suggest that all four crudes contained the same compounds but with differing abundance. Other researchers (Cormack, 1999; Xie *et al.*, 2007; Fingas and Fieldhouse, 2009) have also reported that formation of emulsions resulted in significant changes in properties and characteristics of crude oil. Some of the reported changes include change in viscosity in particular (Fingas and Fieldhouse, 2009). The differences, in the rate of evaporation and compositional changes between Brent crude and Brent emulsion as discussed in Section 2.4.6 highlighted that volatile components will evaporate at different rates with time, based on the nature or surface of the same evaporating substance.

Water-in-oil emulsions were formed with fresh and weathered Forties, Brent, Brae A and Stirling North Sea crude oil types and rheological measurements and properties investigated. Four distinct water-in-oil emulsion types, based on varying stabilities were formed. The emulsion types were: stable, meso-stable, entrained water and unstable emulsion. The effects of degree of weathering on emulsion states were assessed. In general, it was found that the more weathered the oil, the more viscous the emulsions formed. An exception was in Brent crude oil. The parameters known to influence the stability of crude oil emulsions investigated included viscosity, water content, crude oil type, shear rate of formation, volume fraction of internal phase and temperature, as previously reported in Section 3.4.1 - 3.4.7. It has been reported that emulsion types may also depend on the volume fraction of internal phase (Cormack, 1999; Chen and Tao, 2005). The stability of the emulsions were gauged by their viscosities and water content. The stability of the emulsions increased with water content. Viscosity also provides a reliable measure of water-in-oil emulsion stability. Fingas *et al.* (2003) had investigated the stabilities of crude oil emulsions based on the viscosity of the emulsions. Water content has also been used as a convenient and reliable measure to test the stability of water-in-oil emulsions as reported by Fingas and Fieldhouse, 2008. An investigation on the influence of chemical composition on the stability of crude oil emulsions have been reported by Lynch (1987), where Forties crude oil was weathered in an open sea surface experiment and water content of 60.0% and a viscosity of 1200 mPas⁻¹ was measured. The same author had also reported an unstable emulsion with a viscosity of 910 mPas⁻¹ and a relatively high water content of 60.0%.

Significant differences in viscosities and water contents were recorded for the various emulsion types investigated and were correlated with the stability of the emulsions formed from each crude oil type, as given in Section 3.5. It was evident that crude oil types which formed stable emulsions had water contents ranging from 60.0 - 83.0% and high viscosities. However, 11% weathered Stirling crude was an exception as its emulsion remained unstable even at a high water content of 78.0%. The stability of the w/o emulsions based on viscosities and water contents followed the trend: Forties > Stirling > Brae A > Brent.

The key hydrocarbon classes such as asphaltenes, resins and the distribution and proportions of other component organic fractions, in crude oil emulsification were characterized using a variety of analytical techniques such as Saturates, Aromatics, Resins and Asphaltenes (SARA) analyses, elemental microanalysis, UV-fluorescence, FT-IR spectroscopy, ^1H and ^{13}C NMR and GC-FID/GC-MS. The isolation and analyses of the crude oil sub-fractions were uniform in procedure and is therefore comparable. This is broadly presented in Chapter 4, Section 4.5. These techniques were used to investigate the crude oil compositions and establish their role and impact on emulsion stability in the four crude oil emulsion types.

The results of the chemical compositions analyses as shown in Appendix C (Table 1-3 and Table 5-6) and summarised in this Chapter, clearly indicated varied yields of chemically distinct fractions in each of the crude oil type. Notable variations occurred in proportions of the hydrogen and carbon ratios and nitrogen hetero element. The elemental compositions of the crude oil sub-fractions appeared to vary over a narrow range, although the variations were considerable in some fractions. There were notable increases in H/C ratios of the resins relative to asphaltenes and the aromatics fractions as shown in Fig 37. This variation in H/C ratios is in agreement with findings by Speight (2004), where higher H/C ratios were reported for resins comparable to asphaltene fractions. Structural differences between polar fraction (asphaltenes, resins) and aromatics isolated from the four crude oil types were also analysed, and gave unique characteristics in the peripheral and internal carbon in aromatic ring systems, polarity, alkyl side chain and aromaticity. These structural factors appeared to contribute to the emulsion forming capacity and correlate to the stability of the emulsions. A summary of other component organic fractions in terms of functional group distribution in the crude oils and major chemical differences is given in Table 4.2-4.3.

The fractionation process and analytical techniques were able to effectively separate the various fractions from the crude oils. The yields from the SARA analyses were compared for the four oil types. The compositions of the four oils also differed to one another.

For the aliphatic fractions, the four techniques used (GC-FID, FT-IR, ^{13}C NMR and CHN analyses) gave different results for each of the oils. It can be concluded that the chemistry of the aliphatic fractions differed for the four crude oils as confirmed by all four analytical techniques used.

The ^{13}C NMR indicated different amounts of carbon in the structures. This was confirmed by the CHN analysis. The higher carbon contents of the aromatic fractions indicated by NMR and CHN analyses strongly suggested that the fraction contained more cyclic compounds compared to the resin fractions.

The aromatic fractions (analyzed by CHN, FT-IR, NMR, UV-fluorescence and GC-MS) gave different spectra for each of the oils. The NMR data indicated that the carbon content of some oil fractions were higher than others, indicating an increased aromaticity. For the aromatic fractions, the increased aromaticity seen in the NMR corresponds to a change in the H/C ratio in the CHN analysis.

For the resin analysis, the FT-IR, NMR and CHN values differed between the crude oils. The UV-fluorescence analysis gave broad spectra for all crudes samples and these were not considered appropriate for use in the characterization. The increased aromaticity shown for the resin also corresponded to an increased aromaticity for the aromatic fraction using both NMR and CHN analytical methods.

The analytical techniques used (UV-fluorescence, FT-IR, NMR and CHN) gave different data for each of the crude oils. For the asphaltenes, an increased number of carbons shown by the NMR was reflected in the CHN data. The polarity value given by the NMR corresponded to the nitrogen contents given by the CHN analysis. In the UV-f analysis, the emission wavelength maxima for the peaks differed between the four oils. A series of PAH standard compounds were run by UV-fluorescence to see where the emission maxima appeared for each compound. The asphaltenes for the crude oils had an emission maxima that broadly corresponded to coronene (7-ring PAH). The results of these experiments were in good agreement with reported studies (Martinez-Haya *et al.*, 2007; Hortal *et al.*, 2007; Yosandra and Mullins, 2009), on the absorption and emission spectra of asphaltenes.

These differences in terms of aromaticity, polarity and alkyl side chain in Forties, Brae A, Brent and Stirling crude oils were further probed by molecular dynamic modelling using proposed asphaltene structures based on the analytical results. The effect of these model “asphaltenes” on the stability of emulsions formed by the North Sea crude oils were assessed, based on their emulsification data (given in Chapter 3). The experimental results broadly supported the observations from the modelling.

One aspect of asphaltene characterisation that has provided strong evidence for the complexity of crude oil asphaltene constituents arises from composition studies using fractionation techniques (Cimino *et al.*, 1995; Acevedo *et al.*, 1995). The solvent-based fractionation of the asphaltene component of crude oil showed that it is possible to study asphaltene fractions characterised by different aromaticity or hetero-atom content by using heptane/toluene mixtures in variable ratios. Other solvents that have been used to fractionate asphaltenes from crude oil include toluene/methanol (Anderson, 1997). The use of mixtures of a polar and a nonpolar solvent in order to fractionate an asphaltene sample will tend to direct the fractionation by introducing polar forces and hydrogen bonding, as well as dispersion forces, as factors determining which components of the asphaltene sample are soluble in the mixture.

Molecular weight, aromaticity, and polarity combine to determine asphaltene solubility in hydrocarbon media and the solubility properties of the asphaltene fractions of different crude oils can vary markedly (Acevedo *et al.*, 1995). The fractionation of asphaltenes constituents of the different oils into a variety of functional (and polar) types confirmed the complexity of the asphaltene fraction. Speight (1994) had also used High Performance Liquid Chromatography (HPLC) to illustrate the diversity of the structural and functional types in asphaltene constituents to the extent that different HPLC profiles can be expected for different asphaltene constituents.

Three main criteria that are identified as necessary for crude oil emulsion formation are: two immiscible or mutually insoluble liquids must be brought in contact; surface - active components or a combination of emulsifiers must be present as the emulsifying agent and sufficient mixing or agitation must be applied to enable the dispersion of one

liquid into another as droplets (Schubert and Armbruster, 1992; Chen and Tao, 2005). Many researchers (Speight, 2004; Fingas and Fieldhouse, 2008), have suggested that water-in-oil emulsions can be produced by a variety of compounds and mixtures. While asphaltenes and resins play an important role in the formation of stable emulsions, there are oils with sufficient amount of asphaltenes, which do not produce stable emulsions. Certain types of compounds in the asphaltenes and resins with surfactant properties likely play a major role in producing stable emulsions. Compounds with higher solubility in the oil phase than in the aqueous phase are the most likely emulsifying agents to produce stable water-in-oil emulsions.

In order to investigate the effect of varying the asphaltene/ resin ratios and the influence of the various asphaltene types on the emulsification characteristics, 'synthetic oils' and 'model oils' systems were formed using the method previously described in Chapter 5, Section 5.3.2.

Briefly, synthetic oils were formed using decahydronaphthalene (DHN) and *n*-heptane and the asphaltene and resin extracted from the four North Sea crudes. The objective was to see whether emulsions could be produced using different ratios of asphaltene/resin (A/R).

Emulsions could be produced but they were of low viscosity and unstable. For each of the crudes, the highest viscosity and most stable emulsions were obtained using the A/R ratio of 2:1. This suggested that increasing the ratio of A/R produced a more stable emulsion.

The characteristics of the synthetic oils emulsions revealed significant effect of the asphaltene/resin ratios on the emulsion stability. In the synthetic oil emulsions, the results showed the increase in emulsion stability from a level comparable to the sample with low A/R ratios to stability levels with higher A/R ratios. It is reasonable to explain and attribute the increasing stability as a process in which the emulsion stabilising ability of the interfacial surfactants films changes from one dominated by the resins to one dominated by the asphaltenes (but whose strength is influenced by the resins) as similarly reported by Fordedal *et al.* (1996). McLean and Kilpatrick (1997) had also found that some resin fractions can give an enhanced stability in regions of A/R ratios

larger than about 1:3, while others were found to reduce the emulsion stability at all A/R ratios. The increase in stability may be further explained as follows: if the resins are present in the synthetic oil containing both asphaltenes and resins, they disperse some of the asphaltene particles. The amount dispersed depends on the A/R ratio and the character of the resin and asphaltene fractions (Barre *et al.*, 1997; Bardon *et al.*, 1996; McLean and Kilpatrick, 1997).

It has also been reported that when water is added to the water-in-oil system, the highly interfacially active resins reach the oil-water interface first, followed by the asphaltenes. Thus a new equilibrium condition is established in which a complex interfacial layer of resins and asphaltenes decides the stability of the emulsion (Fordedal *et al.*, 1996; Midttun *et al.*, 2000). The results from the characterisation analyses in this research has also showed that resins with very low polarity in the polar functional groups (such as the type obtained in Stirling crude), also have a strong interaction with the asphaltenes, aided by the type of intermolecular forces which promote the solubilization of the asphaltenes.

Brent crude oil was fractionated into the asphaltenes and the deasphalted fractions. This was then re-combined and the emulsion characteristics determined. The emulsion characteristics of the re-constituted crude corresponded to that of the original crude. This method confirmed that the approach used in this thesis was able to re-constitute separated oil to its original form.

The asphaltene fractions from the four crude oils were extracted and combined between the oils to investigate the effects it would have on emulsification behaviour. The ‘model oils’ formed from the combinations had different viscosities and water contents to the original crudes. In general, the viscosities of the model oils were changed to be more similar to that of the crudes where the asphaltenes were obtained or extracted from.

The substitutions and recombination of the asphaltenes from one oil to another to form model oils, yielded emulsions of distinct stabilities as described in Sections 5.4.1- 5.4.2. The rheological measurements and properties of the model oils varied over a wide

margin and have been given in Chapter 5, Table 5.5. The model oil emulsions stabilities as discussed in Section 5.4.2 revealed significant changes in the viscosities and water contents when the asphaltenes were isolated from the whole crude, and combined with deasphaltened (maltenes) fraction of another crude oil type. The water contents of the model oils differed to that of the original crudes. The viscosities and water content of the ‘model oil’ emulsions tended to either reduce, or increase following addition of asphaltene fractions from another crude oil type. It was evident that the stability of the model oil emulsions, as gauged by the viscosities and water contents, correlated to a large extent with, and were dependent on the asphaltene type.

Molecular dynamics (MD) simulation was carried out to study the multiphase modelling and surface behaviour at both air/water (a/w) and oil/water (o/w) interfaces to study their behaviour (i.e. how the molecules orientate at the interfaces) of six possible asphaltene structures. The objective was to investigate which of the structures has surfactant-strong emulsifying properties. Asphaltene structures were designed *ab initio*, based on polarity, aromaticity, and alkyl side chain. (CH stretch at approx. 2930 cm^{-1} (peak height) from FT-IR, and NMR and CHN characterisations. These parameters were selected based on the analyses carried out on the asphaltene molecules in this study.

The simulation results showed conformations for asphaltenes where orientations between neighbouring molecules were affected by molecule structure. The molecules located at the interface (wetting non-aqueous side of the interface), therefore more likely to form water-in- oil emulsion. The simulation also showed that some molecules do not penetrate as deeply into the non-aqueous phase. To give a more stable w/o emulsion, we need compounds that reside more at the outer-surface, and penetrate as much into the aqueous phase. The implications for phase behavior at the interfaces on emulsion formation were correlated with the asphaltenes characterized in this study in order to gain insight into the stability of the emulsions.

With increased polarity, the molecules reside more in the aqueous phase, giving a less stable emulsion (i.e. conferring a lesser emulsion stability). The effect of heteroatoms in the asphaltene on interfacial behaviour was seen where an increase in the number of

ring nitrogen atoms in the molecules led to a larger proportion of the molecule to reside in the water phase i.e. they are less hydrophobic. From the MD simulation results, it was possible to predict that increasing the polar character of asphaltenes, by including extra heteroatoms, will reduce the degree of surface ordering of the asphaltenes, which would lead to a less stable adsorbed layer. The theoretical observations agreed with the experimental data, i.e. the asphaltenes with the highest polarity (Brent crude), gave a less stable (unstable) emulsion, whereas the Stirling crude with the least polarity gave a more stable emulsion in the study.

With increased aromaticity, there was more ordering of the structures at the interface and that would result in a better (stable) emulsification. The MD simulation showed that high aromaticity, two nitrogen (Ha2N) “asphaltene” had an effect on the decane at the decane-water interface, where the ha2N appeared to promote crystallization of the decane molecules. In fact, the aromatic nature tended to dictate the structure of the immediate surroundings, i.e. the structure of the decane. This interfacial behaviour was seen to very likely lead to an increase in the viscosity of the hydrocarbon phase in water-in-oil emulsification, with a resultant effect on the stability and behaviour of the emulsion. The aromatic molecules in asphaltenes will stack into a sandwich-like structure when they associate (Jones, 1978). The presence of solid particles (waxes or organic clays) at the interface will further increase the rigidity of the film and hence make it even more difficult to break the emulsions (Mullins and Sheu, 1998). From the crude oils studied in this work, Stirling crude oil which had the highest aromaticity gave a stable w/o emulsion whereas Brae A gave the less stable (unstable) w/o emulsion. The results from this work agrees well with the studies by Zhang and Greenfield (2007), where molecular orientation in model asphaltenes were reported that for nearest asphaltene molecules, orientations between neighboring molecules were affected by molecule structure and that highly aromatic asphaltene molecules preferred to pack almost parallel to each other.

Increasing the alkyl side chain length pushed the molecules into the aqueous phase. This observation was difficult to explain. However, Zhang and Greenfield (2007), had also reported that asphaltene molecules with long alkane branches preferred to pack almost

parallel. Based on alkyl side chain, Stirling crude with the least alkylation gave the highest viscosity or more stable emulsion.

The results from this work are fully consistent with studies by other researchers (Sjoblom *et al.*, 1990a, b; Mingyuan, 1992; Nordli *et al.*, 1991; Sjoblom *et al.*, 1992) who reported that emulsion stability correlates to asphaltenes, wax, and resin/asphaltene ratio. Their studies observed that the interfacially active fractions of crude oils which give rise to emulsion stability are rich in acidic functional groups. Therefore, the results of this study are consistent and have demonstrated that the ability of asphaltenes to form stable w/o emulsions correlated to a number of structural factors (aromaticity, polarity and degree of total alkylation including aliphatic chain length and branching). Evidence from these results, as outlined here, strongly suggests that the complex nature of crude oils and perhaps, some product oils may provide a number of natural components for the stabilization of their water-in-oil emulsions. Specifically, it was shown that the asphaltenes (and crude oil resins) provide the polar properties for location at the oil-water interface with the asphaltenes doing so preferentially. Within the asphaltenes themselves, two classes may be distinguished, namely; the asphaltene “precipitators” (i.e. asphaltenes with increased aromaticity) and the asphaltene “dissolvers” (i.e. asphaltenes with increased polarity).

Hydrophile-lipophile balance (HLB) of the emulsifier

Formation of an emulsion results from the agitation of oil and water in the presence of a surface active agent as emulsifier. The nature and type of emulsion formed, i.e oil-in-water (O/W) or water-in-oil (W/O) is dependent on a number of factors. Apart from the particular surface active agent chosen, these factors such as the method of dispersion, the phase volume and relative viscosities of the phases may greatly influence the type of the resultant emulsion (Clayton, 1954; Davies, 1957; Williams, 1991; Akay, 1997). The concept of HLB has been given in Chapter 6, Section 6.2 and this concept essentially characterizes the tendency of the surface active agents to dissolve preferentially in oil/water interface (Griffin, 1954; Davies, 1957; Cormack, 1999). Emulsifying agents have been classified numerically on the ‘HLB’ scale (Griffin, 1950), which refers to the HLB balance of the emulsifier molecule, and is related to oil and water solubilities. The

correlation of HLB and emulsion type is based on direct experimental tests, although for some systems the HLB value can be estimated by empirical rules from the surface analysis of the surface active agent (Griffin, 1950; 1956). It must be emphasised that the HLB system is not concerned with the stability of the emulsion once formed, but it is only a correlation of function (Table 8.1), not of efficacy (Griffin, 1954).

Table 8.1 Classification of emulsifiers according to HLB values

<i>Range of HLB values</i>	<i>Application</i>
3.5 - 6	<i>W/O emulsifier</i>
7 - 9	<i>Wetting agent</i>
8 -18	<i>O/W emulsifier</i>
13-15	<i>Detergent</i>
15-18	<i>Solubilization</i>

(Griffin, 1954)

Table 8.2 HLB group numbers used in equation (1) calculation for the model asphaltene compounds.

<i>Hydrophilic groups</i>	<i>Group Number</i>
-SO ₄ ⁻ Na ⁺	38.7
-COO ⁻ K ⁺	21.1
-COO ⁻ Na ⁺	19.1
N (tertiary amine)	9.4
Ester (sorbitan ring)	6.8
Ester (free)	2.4
-COOH	2.1
Hydroxyl (sorbitan free)	1.9
-O-	1.3
Hydroxyl (sorbitan ring)	0.5
<i>Lipophilic groups</i>	
-CH-	-0.475
-CH ₂ -	
CH ₃ -	
=CH-	
<i>Derived groups</i>	
-(CH ₂ -CH ₂ -O)-	+0,33
-(CH ₂ -CH ₂ -CH ₂ -O)-	- 0.15

(Davies, 1957).

Davies (1957) has extensively outlined and discussed a quantitative kinetic theory of emulsion type in relation to emulsifying agent and has found that HLB values for surface active agents can be consistently calculated directly from the chemical formulae, using *group numbers*. Tables 8.1 and 8.2 respectively shows a classification of emulsifiers according to HLB values and HLB group numbers, from which the HLB values for the model asphaltene compounds have been calculated using the equation:

$$\text{HLB} = \sum (\text{hydrophilic group numbers}) - n (\text{group number per CH}_2 \text{ group}) + 7 \dots\dots\dots (1)$$

(Davies, 1957)

Where n = the number of -CH₂- groups in the molecule of emulsifying agent.

Hydrophile-lipophile balance (HLB) of the model asphaltene compounds

Using the approach and HLB equation given above, example calculations for the HLB values for high aromatic content, low polarity (Ha1N) and high aromatic content, high polarity (Ha2N) model asphaltene compounds in this study are given below:

For Ha1N model compound: 20 carbon; 1N; 15H

$$\begin{aligned} \text{HLB} &= \sum (\text{hydrophilic group numbers}) - n (\text{group number per CH}_2 \text{ group}) + 7 \\ &= 7 + \sum \text{hydrophilic} + \sum \text{hydrophobic} \\ &= 7 + 9.4 + 20(-0.475) \\ &= 6.9 \text{ (Marginally W/O emulsion)} \end{aligned}$$

With the ring oxygen (-O-)

$$\begin{aligned} &= 7 + 1.3 + 20(-0.475) \\ &= -1.2 \end{aligned}$$

Hence, the HLB = -1.2 – 6.9

For Ha2N model compound: 19 carbon; 1N; 15H

$$\begin{aligned} &= 7 + \sum \text{hydrophilic} + \sum \text{hydrophobic} \\ &= 7 + 9.4 + 20(-0.475) \\ &= 16.4 \end{aligned}$$

With the ring oxygen (-O-)

$$= 7 + 9.4 + 20(-0.475)$$

$$= 0.1$$

Hence, the HLB = 0.1 – 16.4

The group number for tertiary amine and for ring oxygen was used to obtain limiting values of HLB, and it can be suggested that true value is likely to be between these. The calculation above shows that the concept is not easily applied to heterocyclic amine rings. The HLB numbers calculated depends on the group number for the ring nitrogen (N), and we do not have a good estimate of this. From the foregoing, it can be concluded that further work would be needed to parameterize the -N- in the ring in order to be able to estimate a group number for it so that a better estimate of HLB number could be calculated.

The MD simulations enabled conclusions to be drawn on the structural conformation of North Sea crude oil asphaltenes and in general, the knowledge gained by investigating interfacial properties considerably supported the information available from bulk emulsions studies, as previously given in Chapter 3 of this work. This is because from interfacial studies, one can determine the fundamental mechanisms and kinetics of film formation, surfactant adsorption, and film rupture that ultimately govern emulsion behaviour. This premise is fully supported and has been strongly emphasized by Sjöblom *et al.*, 2003, underpinning the importance of understanding the interfacial properties of crude oils when correlating and assessing emulsion stabilization/destabilization.

Following from analyses carried out for the different North Sea crude oils, in order to further investigate and obtain information on the interrelated variables from the large number of physicochemical properties of the crude oils investigated by use of various analytical techniques, a correlation analysis was performed to distil the variance from the data set. Results from the correlation analysis indicated a trend which showed that the variables yielded both significant positive correlations and significant negative correlations between the various variables. A detailed correlation table is given in Chapter 7, Table 7. The analysis showed the complex relationships between these key variables and parameters which may influence water-in-oil emulsions. Some of the

correlations that have not been reported previously in the literature include that: SARA % asphaltenes showed a significant positive correlation with fresh crude emulsion water content, fresh crude oil emulsion viscosity yielded a positive correlation with 20% weathered crude emulsion viscosity, and the SARA % asphaltenes which showed no positive correlation with the 20% weathered emulsion viscosity. An understanding of these would provide insight into correlation of the physicochemical properties, emulsification behaviour and stability of emulsions of the crude oils studied.

CHAPTER 9

Conclusions and suggestions for further work

Following from the studies, the following conclusions can be made:

1. Brent crude oil exhibited a faster evaporation rate than Forties crude oil and this can be attributable to the differences in the chemistry of each crude oil type. This may have important implications for the evaporation behaviour of other North Sea crude oils.
2. The relationship and dependence of temperature and time in respect of the North Sea crude oils' evaporation was established by this study, and showed a trend which increased with increasing temperature and time. This was modelled, in order to predict the rate of evaporation at other temperatures. These results may therefore enhance the understanding of evaporation as a major factor in crude oil weathering process, particularly in tropical climates.
3. Oil on its own evaporated more quickly than oil on seawater. This suggests that evaporating oil on seawater, a more realistic scenario, may give a more realistic evaporation rate.
4. Emulsified oil evaporates more quickly than unemulsified oil.
5. The four North Sea crude oils investigated (Forties, Brent, Brae A and Stirling), produced four different states of emulsions (stable, unstable, meso-stable and entrained water), and the stability generally increased with water content. The stability of the water-in-oil emulsions are affected by the asphaltene/resin ratio.
6. North Sea crude oils investigated by several analytical methods revealed that the chemistry of the oils differ from one to another.
7. Emulsions could be produced from synthetic oils, although they were unstable and depended on the asphaltene/resin (A/R) ratios.

8. The behaviour of “model oil” emulsions produced from combinations of North Sea crude asphaltenes was a function of rheological properties (viscosity and water content), and depended on the asphaltene type.
9. The ^{13}C NMR analysis of asphaltenes indicated that the NMR analytical method may be a potential indicator for oil spill identification / fingerprinting. More detailed analysis of asphaltene chemistry by mass spectrometric techniques may help confirm the correctness of the structures proposed for the modelling study based on the analytical data in this thesis.
10. Molecular dynamics (MD) simulation and modelling of surface behaviour of “asphaltene” structures at two interfaces revealed structural conformations and surfactant properties based on polarity, aromaticity, and alkyl side chain length, from the analyses of the asphaltene molecules in this study. Further work may be proposed to calculate the free energy of adsorption (potential of mean force (PMF) of the asphaltene molecules (i.e. binding energy between two species), using umbrella sampling method.
11. A correlation analyses showed a complex relationships between polarity, aromaticity, alkyl side chain, SARA percentages of crude oil fractions and other key variables and parameters which may influence water-in-oil emulsions. Some of the correlations shown in this work have not been reported yet in available literature. Extension of studies to cover a wider range of crude oil types may improve the data set and enrich the correlation analyses, and will enable a more robust chemometrics and principal component analysis (PCA) of the variables.
12. The results of this study may significantly enhance and give insight into the fundamentals of water-in-oil emulsion formation/destabilisation, and crude oil asphaltenes interfacial characteristics, with implications that ultimately determine emulsion behaviour. The information from this work may find useful industrial applications, including in oil spill countermeasures.
13. The knowledge of interfacial behaviour of asphaltene and its implications for phase separation and reservoir wettability can also be widely applied in the geochemical process of crude oil production.

These results will complement the understanding of the profound effects of crude oil compositions and other key parameters on emulsification, stability and persistence as surface slicks. By continuing to fractionate and characterize the fractions from various North Sea crude oils, and oils from other production reservoirs and regions, it is possible to run a comprehensive array of properties and stability test to further the understanding of the mechanism of crude oil emulsification.

APPENDIX A
Experimental measurements of Forties crude oil evaporation on Seawater

Table 2.1 Forties evaporation at 12°C

	Weight of petridish (g) measured at intervals of evaporation at 12°C												
	Duration												
Sample	0hr	1hr	2hrs	3hrs	4hrs	5hrs	6hrs	12hrs	24hrs	48hrs	72hrs	96hrs	110hrs
Dish 1	72.00	71.48	71.28	71.07	70.95	70.85	70.75	70.66	70.41	70.22	70.09	69.96	69.87
<i>Subt. Wt</i>		0.52	0.72	0.93	1.05	1.15	1.25	1.34	1.59	1.78	1.91	2.04	2.13
Dish 2	70.13	69.59	69.41	69.21	69.11	69.01	68.92	68.87	68.62	68.47	68.39	68.26	68.15
<i>Subt. Wt</i>		0.54	0.72	0.92	1.02	1.12	1.21	1.26	1.51	1.66	1.74	1.87	1.98
Dish 3	70.93	70.48	70.35	70.21	70.11	70.03	69.95	69.92	69.66	69.52	69.37	69.28	69.14
<i>Subt. Wt</i>		0.45	0.58	0.72	0.82	0.9	0.98	1.01	1.27	1.41	1.56	1.65	1.79
Mean Wt. loss		0.50	0.67	0.85	0.96	1.05	1.14	1.20	1.45	1.61	1.73	1.85	1.96

Table 2.2 Forties evaporation at 20°C

	Weight of petridish (g) measured at intervals of evaporation at 20°C												
	Duration												
Sample	0hr	1hr	2hrs	3hrs	4hrs	5hrs	6hrs	12hrs	24hrs	48hrs	72hrs	96hrs	110h
Dish 1	71.49	70.65	70.52	70.42	70.32	70.26	70.18	70.09	69.92	69.76	69.64	69.54	69.4
<i>Subt. Wt</i>		0.84	0.97	1.07	1.17	1.23	1.31	1.40	1.57	1.73	1.85	1.95	2.09
Dish 2	70.12	69.4	69.26	69.15	69.02	68.95	68.91	68.79	68.61	68.49	68.34	68.24	68.14
<i>Subt. Wt</i>		0.72	0.86	0.97	1.10	1.17	1.21	1.33	1.51	1.63	1.78	1.88	1.98
Dish 3	70.93	70.18	70.06	69.95	69.86	69.78	69.68	69.55	69.40	69.26	69.13	69.03	68.91
<i>Subt. Wt</i>		0.75	0.87	0.98	1.07	1.15	1.25	1.38	1.53	1.67	1.80	1.90	2.02
Mean Wt. loss		0.77	0.90	1.00	1.11	1.18	1.25	1.37	1.53	1.67	1.81	1.91	2.03

Table 2.3 Forties evaporation at 25 °C

	Weight of petridish (g) measured at intervals of evaporation at 25°C												
	Duration												
Sample	0hr	1hr	2hrs	3hrs	4hrs	5hrs	6hrs	12hrs	24hrs	48hrs	72hrs	96hrs	110hrs
Dish 1	72.04	71.0	70.76	70.61	70.49	70.43	70.35	70.25	70.03	69.79	69.58	69.38	69.17
Subt. Wt		1.04	1.28	1.43	1.55	1.61	1.69	1.79	2.01	2.25	2.46	2.66	2.87
Dish 2	72.73	71.52	71.22	71.07	70.97	70.88	70.81	70.7	70.5	70.28	70.05	69.86	69.71
Subt. Wt		1.21	1.51	1.51	1.76	1.85	1.92	2.03	2.23	2.45	2.68	2.87	3.02
Dish 3	71.72	70.61	70.4	70.30	70.20	70.12	70.01	69.93	69.72	69.45	69.25	69.06	68.9
Subt. Wt		1.11	1.32	1.42	1.52	1.60	1.71	1.79	2.00	2.27	2.47	2.66	2.82
Mean Wt. loss		1.12	1.37	1.5	1.61	1.68	1.77	1.87	2.08	2.32	2.53	2.73	2.90

Table 2.4 Forties evaporation at 30 °C

	Weight of petridish (g) measured at intervals of evaporation at 30°C												
	Duration												
Sample	0hr	1hr	2hrs	3hrs	4hrs	5hrs	6hrs	12hrs	24hrs	48hrs	72hrs	96hrs	110hrs
Dish 1	71.49	70.11	69.75	69.68	69.57	69.51	69.43	69.25	69.05	68.85	68.66	68.48	68.26
Subt. Wt		1.38	1.74	1.81	1.92	1.98	2.06	2.24	2.44	2.64	2.83	3.01	3.23
Dish 2	70.11	68.80	68.48	68.31	68.21	68.14	68.00	67.84	67.60	67.38	67.16	66.96	66.78
Subt. Wt		1.31	1.63	1.80	1.90	1.97	2.11	2.27	2.51	2.73	2.95	3.15	3.33
Dish 3	70.92	69.9	69.66	69.57	69.48	69.38	69.28	69.12	68.88	68.71	68.5	68.35	68.11
Subt. Wt		1.02	1.26	1.35	1.44	1.54	1.64	1.8	2.04	2.21	2.42	2.57	2.81
Mean Wt. loss		1.23	1.54	1.65	1.75	1.83	1.93	2.1	2.33	2.52	2.73	2.91	3.12

Table 2.5 Forties evaporation at 40 °C

	Weight of petridish (g) measured at intervals of evaporation at 40°C												
	Duration												
Sample	0hr	1hr	2hrs	3hrs	4hrs	5hrs	6hrs	12hrs	24hrs	48hrs	72hrs	96hrs	110hrs
Dish 1	72.01	70.9	70.7	70.53	70.36	70.23	70.13	69.65	68.93	67.92	67.23	66.7	66.1
<i>Subt. Wt</i>		<i>1.11</i>	<i>1.31</i>	<i>1.48</i>	<i>1.65</i>	<i>1.78</i>	<i>1.88</i>	<i>2.36</i>	<i>3.08</i>	<i>4.09</i>	<i>4.78</i>	<i>5.31</i>	<i>5.91</i>
Dish 2	72.71	71.95	71.64	71.38	71.15	70.91	70.65	69.72	67.29	63.77	59.71	56.78	53.98
<i>Subt. Wt</i>		<i>0.76</i>	<i>1.07</i>	<i>1.33</i>	<i>1.56</i>	<i>1.80</i>	<i>2.06</i>	<i>2.99</i>	<i>5.42</i>	<i>8.94</i>	<i>13.00</i>	<i>15.93</i>	<i>18.73</i>
Dish 3	71.7	70.53	70.23	70.04	69.84	69.64	69.45	68.79	67.2	65.75	64.81	64.16	63.49
<i>Subt. Wt</i>		<i>1.17</i>	<i>1.47</i>	<i>1.66</i>	<i>1.86</i>	<i>2.06</i>	<i>2.25</i>	<i>2.91</i>	<i>4.50</i>	<i>5.95</i>	<i>6.89</i>	<i>7.54</i>	<i>8.21</i>
Mean Wt. loss		1.01	1.28	1.49	1.69	1.88	2.06	2.75	4.33	6.32	8.22	9.59	10.95

Table 2.6 Forties evaporation at 50°C

	Weight of petridish (g) measured at intervals of evaporation at 50°C												
	Duration												
Sample	0hr	1hr	2hrs	3hrs	4hrs	5hrs	6hrs	12hrs	24hrs	48hrs	72hrs	96hrs	110hrs
Dish 1	72.06	69.46	68.79	68.41	68.04	67.68	67.32	65.94	-	-	-	-	-
									-	-	-	-	-
<i>Subt. Wt</i>		2.6	3.27	3.65	4.02	4.38	4.74	6.12	-	-	-	--	-
									-	-	-	-	-
Dish 2	72.06	69.55	68.98	68.62	68.31	68.09	67.82	66.92	-	-	-	-	-
									-	-	-	-	-
<i>Subt. Wt</i>		2.51	3.08	3.44	3.75	3.97	4.24	5.14	-	-	-	-	-
									-	-	-	-	-
Dish 3	72.22	69.60	69.03	68.58	68.16	67.80	67.46	66.3	-	-	-	--	-
									-	-	-	-	-
<i>Subt. Wt</i>		2.62	3.19	3.64	4.06	4.42	4.76	5.92	-	-	-	-	-
									-	-	-	-	-
Mean Wt. loss		2.58	3.18	3.58	3.94	4.26	4.58	5.73	-	-	-	-	-

Subt. Wt. represents subtracted weight.

Table 2.7 Mean evaporative mass loss (g) of Forties crude on seawater

	Mean weight loss at temperatures and durations of evaporation					
Duration (hrs)	12°C Mean Wt. loss	20°C Mean Wt. loss	25°C Mean Wt. loss	30°C Mean Wt. loss	40°C Mean Wt. loss	50°C Mean Wt. loss
1	0.5	0.77	1.12	1.23	1.01	2.58
2	0.67	0.9	1.37	1.54	1.28	3.18
3	0.85	1.00	1.50	1.65	1.49	3.58
4	0.96	1.11	1.61	1.75	1.69	3.94
5	1.05	1.18	1.68	1.83	1.88	4.26
6	1.14	1.25	1.77	1.93	2.06	4.58
12	1.2	1.37	1.87	2.1	2.75	5.73
24	1.45	1.53	2.08	2.33	4.33	-
48	1.61	1.67	2.32	2.52	6.32	-
72	1.73	1.81	2.58	2.73	8.22	-
96	1.85	1.91	2.73	2.91	9.59	-
110	1.96	2.03	2.90	3.12	10.95	-

Table 2.8 Percentage (%) evaporation of sample at 12°C

	% Evaporation of Sample at 12°C		
Time (hrs)	D1	D2	D3
1	2.13	2.38	1.92
2	2.95	3.17	2.48
3	3.81	4.05	3.07
4	4.3	4.50	3.5
5	4.71	4.94	3.84
6	5.12	5.33	4.18
12	5.49	5.55	4.31
24	6.51	6.65	5.42
48	7.29	7.32	6.02
72	7.82	7.67	6.66
96	8.35	8.24	7.04
110	8.72	8.73	7.64

Table 2.9 Percentage (%) evaporation of sample at 20°C

	% Evaporation of Sample at 20°C		
Time (hrs)	D1	D2	D3
1	3.51	3.17	3.20
2	4.06	3.79	3.71
3	4.48	4.28	4.18
4	4.89	4.85	4.57
5	5.14	5.16	4.91
6	5.48	5.34	5.34
12	5.86	5.86	5.89
24	6.57	6.66	6.53
48	7.24	7.19	7.13
72	7.74	7.85	7.68
96	8.16	8.29	8.11
110	8.74	8.73	8.62

Table 2.10 Percentage (%) evaporation of sample at 25°C

	% Evaporation of Sample at 25°C		
Time (hrs)	D1	D2	D3
1	4.34	4.91	4.69
2	5.34	6.13	5.57
3	5.97	6.74	5.99
4	6.47	7.14	6.42
5	6.72	7.51	6.75
6	7.06	7.79	7.22
12	7.47	8.24	7.56
24	8.39	9.05	8.44
48	9.39	9.94	9.58
72	10.27	10.88	10.43
96	11.1	11.65	11.23
110	11.98	12.26	11.90

Table 2.11(a) Percentage (%) evaporation of sample at 30°C

	% Evaporation of Sample at 30°C		
Time (hrs)	D1	D2	D3
1	5.77	5.78	4.36
2	7.28	7.20	5.38
3	7.57	7.94	5.76
4	8.03	8.38	6.15
5	8.28	8.69	6.58
6	8.61	9.31	7.00
12	9.37	10.01	7.69
24	10.2	11.07	8.71
48	11.04	12.04	9.44
72	11.84	13.01	10.33
96	12.59	13.9	10.97
110	15.51	14.69	12.00

Table 2.11(b) Mean weight loss (g) for Forties evaporation on seawater at 30°C

Time (hr)	Weight loss (g)
1	1.23 ± 0.15
2	1.54 ± 0.20
3	1.65 ± 0.21
4	1.75 ± 0.22
5	1.83 ± 0.20
6	1.93 ± 0.21
12	2.10 ± 0.21
24	2.33 ± 0.20
48	2.52 ± 0.22

Table 2.12 Percentage (%) evaporation of sample at 40°C

Time (hrs)	% Evaporation of Sample at 40°C		
	D1	D2	D3
1	4.64	3.09	4.94
2	5.48	4.35	6.21
3	6.19	5.4	7.01
4	6.9	6.33	7.86
5	7.44	7.31	8.7
6	7.86	8.37	9.51
12	9.87	12.14	12.29
24	12.88	22.01	19.01
48	17.1	36.31	25.13
72	19.98	52.8	29.11
96	22.2	64.7	31.85
110	24.71	76.08	34.69

Table 2.13 Percentage (%) evaporation of sample at 50°C

Time (hrs)	% Evaporation of Sample at 50°C		
	D1	D2	D3
1	10.62	10.19	10.60
2	13.36	12.51	12.90
3	14.91	13.97	14.72
4	16.42	15.23	16.42
5	17.89	16.13	17.88
6	19.36	17.22	19.26
12	25.00	20.88	23.95
24	-	-	-
48	-	-	-
72	-	-	-
96	-	-	-
110	-	-	-

D1, D2, D3 indicates petridishes 1, 2 and 3 respectively.

Table 2.14 Evaporation of Brent crude oil on Seawater at 30°C and measurement of weight loss (g) at intervals

Sample	Duration								
	0hr	1hr	2hrs	3hrs	4hrs	5hrs	6hrs	24hrs	48hrs
Dish 1	76.61	73.77	73.15	72.69	72.53	72.45	72.36	71.88	71.29
<i>Subt. Wt.</i>		2.84	3.46	3.92	4.08	4.16	4.25	4.73	5.32
Dish 2	76.63	74.51	73.77	73.23	72.89	72.70	72.53	72.03	71.39
<i>Subt. Wt.</i>		2.12	2.86	3.4	3.74	3.93	4.1	4.6	5.24
Dish 3	76.61	75.19	75.02	74.89	74.79	74.70	74.63	74.17	73.56
<i>Subt. Wt.</i>		1.42	1.59	1.72	1.82	1.91	1.98	2.44	3.05
Mean Wt. loss		2.12	2.63	3.01	3.21	3.33	3.44	3.92	4.53

Table 2.15 Evaporation of Brent crude oil (without seawater) at 30°C and measurement of weight loss (g) at intervals

Sample	Duration								
	0hr	1hr	2hrs	3hrs	4hrs	5hrs	6hrs	24hrs	48hrs
Dish 1	51.56	50.76	50.64	50.57	50.54	50.51	50.48	50.29	50.21
<i>Subt. Wt</i>		0.8	0.92	0.99	1.02	1.05	1.08	1.27	1.35
Dish 2	51.56	50.74	50.62	50.56	50.52	50.48	50.48	50.27	50.20
<i>Subt. Wt</i>		0.82	0.94	1.0	1.04	1.08	1.08	1.29	1.36
Dish 3	51.57	50.69	50.56	50.50	50.43	50.42	50.42	50.20	50.12
<i>Subt. Wt</i>		0.88	1.01	1.07	1.14	1.15	1.15	1.37	1.45
Mean Wt.loss		0.83	0.95	1.02	1.06	1.09	1.10	1.31	1.38

Table 2.16 Evaporation of seawater on petridishes at 30°C and measurement of weight loss (g) at intervals

Sample	Duration								
	0hr	1hr	2hrs	3hrs	4hrs	5hrs	6hrs	24hrs	48hrs
Dish 1	70.43	66.57	62.80	58.62	54.51	50.82	0	0	0
<i>Subt. Wt.</i>		3.86	7.63	11.81	15.92	19.61	0	0	0
Dish 2	70.42	65.84	61.37	56.49	52.12	49.36	0	0	0
<i>Subt. Wt.</i>		4.58	9.05	13.93	21.06	3.93	0	0	0
Dish 3	70.42	64.12	58.86	53.32	49.61	48.89	0	0	0
<i>Subt. Wt.</i>		6.3	11.56	17.1	20.81	21.53	0	0	0
Mean Wt. loss		4.91	9.41	14.28	18.34	20.73	0	0	0

(*Subt.wt* represents subtracted weight)

Table 2.17 Mean weight loss (g) for Brent evaporations on seawater; Brent (no seawater) and seawater at 30°C

Time (hr)	Samples		
	Brent on Seawater (B on SW)	Brent (without Seawater)	Seawater (SW)
	wt. loss(g)	Wt. loss(g)	wt. loss(g)
1	2.12 ± 0.41	0.83 ± 0.02	4.91 ± 0.72
2	2.63 ± 0.55	0.95 ± 0.02	9.41 ± 1.15
3	3.01 ± 0.66	1.02 ± 0.25	14.28 ± 1.54
4	3.21 ± 0.77	1.06 ± 0.04	18.34 ± 1.41
5	3.33 ± 0.71	1.09 ± 0.03	20.73 ± 0.58
6	3.44 ± 0.73	1.1 ± 0.02	0
24	3.92 ± 0.74	1.31 ± 0.03	0
48	4.53 ± 0.74	1.38 ± 0.03	0

(Data presented as mass ± S.E)

Table 2.18 Mean weight loss for weathering (evaporation) of Brent crude emulsion on Seawater at 30°C

Time (hr)	Sample weight loss (g)
0	0.00
1	1.0 ± 0.34
2	1.15 ± 0.36
3	1.23 ± 0.37
4	1.40 ± 0.36
5	1.43 ± 0.36
6	1.51 ± 0.36
24	2.03 ± 0.36
48	2.55 ± 0.33

(Data presented as mass ± S.E)

APPENDIX B

Table 3a Effect of temperature on emulsion stability

Emulsion property	11% Weathered (B)				20% Weathered (C)			
	Forties	Brent	Brae A	Stirling	Forties	Brent	Brae A	Stirling
Viscosity (PaS)	3.29	1.98	2.36	3.01	10.0	2.04	4.06	4.61
Water content (%)	63.1	40.1	35.0	60.0	82.9	54.0	75.0	78.0

*Note: Viscosity selected at shear rate of 8.90 (S⁻¹) in PaS

Table 3b Water content (%) of water-in-oil emulsions

Emulsion sample	Fresh emulsion				11% weathered (B)				20% weathered (C)			
	1	2	Mean	S.D	1	2	Mean	S.D	1	2	Mean	S.D
Forties	25.5	24.5	25.0	0.707	64.2	62.0	63.1	1.1	84.5	81.2	82.9	1.650
Brent	33.9	35.0	34.5	0.777	42.1	38.0	40.1	2.050	55.0	53.0	54.0	1.0
Brae A	19	21.0	20.0	0.714	36.0	34.0	35.0	1.0	73.5	75.6	75.0	1.081
Stirling	16.9	18.6	17.8	1.202	59.0	61.0	60.0	1.0	76.5	79.5	78.0	1.5

Determination of water content:

$$\% \text{ Water content} = \frac{\text{volume of water resolved in trap}}{\text{Weight (vol.) of sample}} \times 100$$

Table 3c Density of crude oil with viscosity of emulsions

	Fresh Crude				11% weathered				20% weathered			
	Forties	Brent	Brae A	Stirling	Forties	Brent	Brae A	Stirling	Forties	Brent	Brae A	Stirling
Viscosity	3.47	1.71	1.89	1.90	3.29	1.98	2.36	3.01	10.0	2.04	4.06	4.61
Density	0.87	0.83	0.85	0.84	0.87	0.83	0.85	0.84	0.87	0.83	0.85	0.84

APPENDIX C

Table 1 Elemental Analysis (wt. %) of crude oil fractions*

Fraction	Asph. (wt.%)				Resin (wt.%)				Aromatic (wt.%)			
<i>Crude oil type</i>	C	H	N	H/C	C	H	N	H/C	C	H	N	H/C
Forties	78.01	9.53	0.48	1.44	79.24	9.51	1.01	1.43	83.23	8.93	0.80	1.28
	79.45	9.62	0.48		71.56	8.70	0.91		84.12	9.01	0.71	
	78.75	9.58	0.49		75.46	9.13	0.98		84.34	9.13	0.61	
	Mean	78.73	9.57		75.42	9.11	0.96		83.89	9.02	0.7	
SD	0.7200	0.0450	0.0057		3.84	0.4	0.05		0.58	0.10	0.09	
Brae A	82.37	11.36	0.62	1.64	69.90	8.80	1.05	1.48	84.72	9.22	0.75	1.29
	82.59	11.43	0.59		67.53	8.37	1.06		85.06	9.02	0.96	
	82.49	11.38	0.61		68.75	8.62	1.07		82.79	9.14	0.68	
	Mean	82.48	34.17		68.72	8.59	1.06		84.19	9.12	0.79	
SD	0.1101	0.0360	0.0152		1.1851	0.2159	0.01		1.22	0.10	0.14	
Brent	83.93	10.46	0.36	1.50	77.45	9.08	1.36	1.37	86.68	9.52	0.78	1.31
	83.43	10.92	0.41		71.25	8.62	1.22		86.04	9.72	0.80	
	84.54	10.33	0.34		74.33	8.04	1.28		86.11	9.25	0.65	
	Mean	83.96	10.57		74.34	8.58	1.28		86.27	9.49	0.74	
SD	0.5559	0.31	0.0360		3.1000	0.5211	0.0702		0.35	0.23	0.08	
Stirling	86.37	8.14	0.89	1.09	62.78	7.46	0.71	1.41	86.81	9.01	0.19	1.25
	87.69	7.85	0.92		67.97	8.03	0.68		85.56	9.11	0.45	
	87.04	8.00	0.90		65.40	7.76	0.70		86.24	9.23	0.10	
	Mean	87.03	7.99		65.38	7.75	0.69		86.20	9.11	0.24	
SD	0.6600	0.1450	0.0152		2.5950	0.2851	0.0152		0.62	0.11	0.18	

*All numbers are weight percentages of the mean values of the weighted parameters except H/C ratio which represents an atomic ratio calculated from the elemental microanalysis.

Table 2 Summary of mean yield (wt.%) of CHN of crude oil fractions by elemental analysis

Crude oil type	Forties	Brae A	Brent	Stirling
		%Carbon		
Asphaltenes	78.73 ± 0.72	82.48 ± 0.11	83.96 ± 0.55	87.03 ± 0.66
Resins	75.42 ± 3.84	68.72 ± 1.18	74.34 ± 3.10	65.38 ± 2.59
Aromatics	83.89 ± 0.58	84.19 ± 1.22	86.27 ± 0.35	86.20 ± 0.62
		%Hydrogen		
Asphaltenes	9.57 ± 0.04	11.39 ± 0.03	10.57 ± 0.31	7.99 ± 0.14
Resins	9.11 ± 0.40	8.59 ± 0.21	8.58 ± 0.52	7.75 ± 0.28
Aromatics	9.02 ± 0.10	9.12 ± 0.10	9.49 ± 0.23	9.11 ± 0.11
		%Nitrogen		
Asphaltenes	0.48 ± 0.00	0.60 ± 0.01	0.37 ± 0.03	0.90 ± 0.01
Resins	0.96 ± 0.05	1.06 ± 0.01	1.28 ± 0.07	0.69 ± 0.01
Aromatics	0.7 ± 0.09	0.79 ± 0.14	0.74 ± 0.08	0.24 ± 0.18

Table 3

Hydrogen/Carbon (H/C) ratios in Asphaltene, Resin and Aromatic fractions of Forties, Brae A, Brent and Stirling crude oils.

Crude oil type/ fraction	Asph.	Resin	Aromatic
Forties	1.44	1.43	1.28
Brea A	1.64	1.48	1.29
Brent	1.5	1.37	1.31
Stirling	1.09	1.41	1.25

Calculation of Hydrogen/Carbon ratio (H/C) in Elemental Analyses of Asphaltenes and Resins in crude oils:

Atomic weight of Carbon = 12.0107

Atomic weight of Hydrogen = 1.00794

*Wt. (%) of Carbon measured is divided by atomic weight of Carbon (a)

Wt. (%) of Hydrogen measured is divided by atomic weight of Hydrogen (b)

Then to determine the H/C ratios in asphaltenes and resins:

Divide the value in (b) by the value in (a), *i.e.* H/C

N/B: *Wt.(%) is the mean of the three replicate weights of asphaltene and resin fractions.

Fig 1(a – f) showing the fluorescence emission spectrum obtained for the various PAH compounds. The measured emission spectrum ranged from ~340 nm – 445 nm. All compounds were in dilute cyclohexane solution.

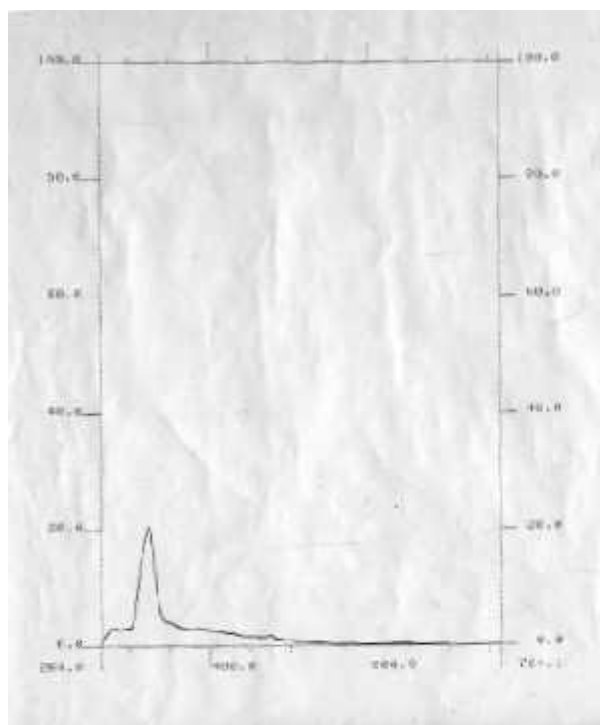


Fig 1(a) 1- Methylnaphthalene

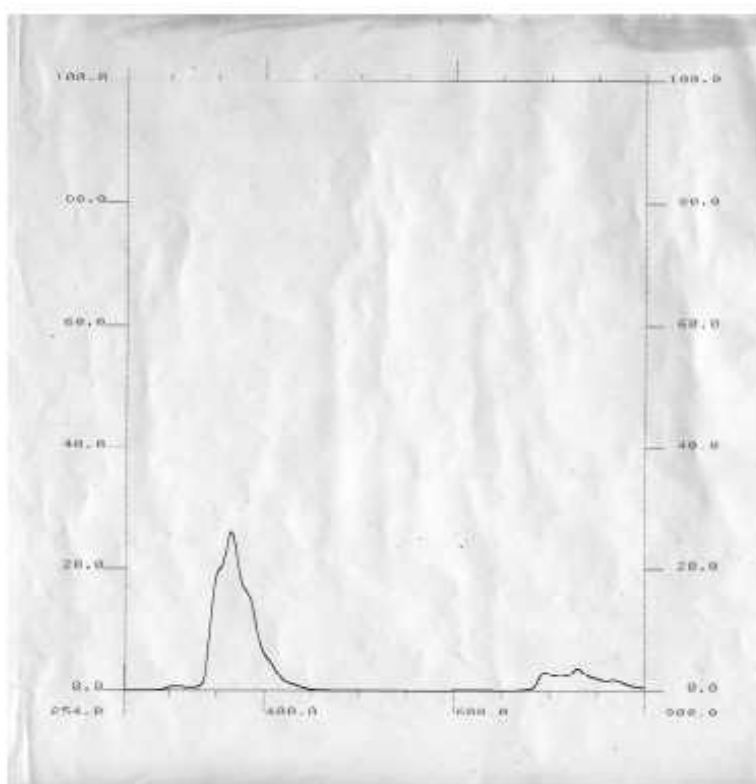


Fig 1(b) Phenanthrene

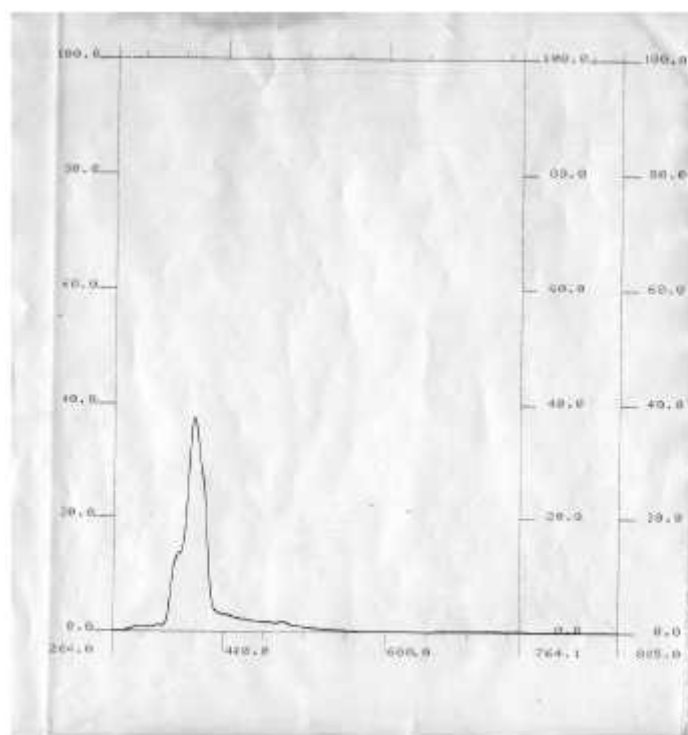


Fig 1(c) Chrysene

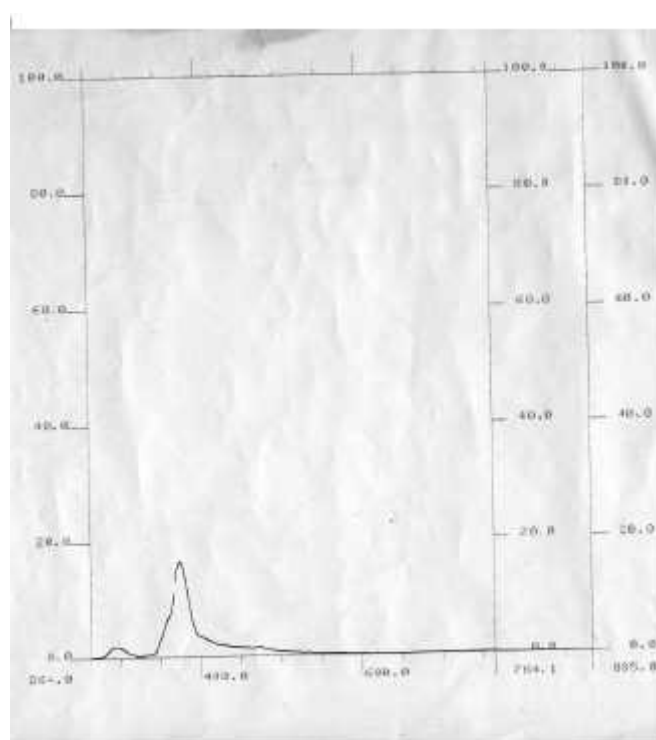


Fig 1(d) Pyrene

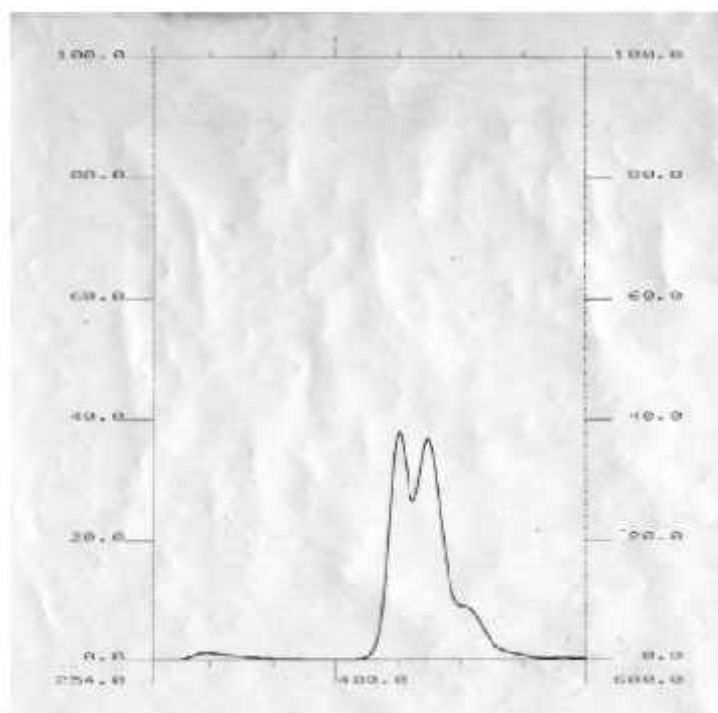


Fig 1(e) Perylene

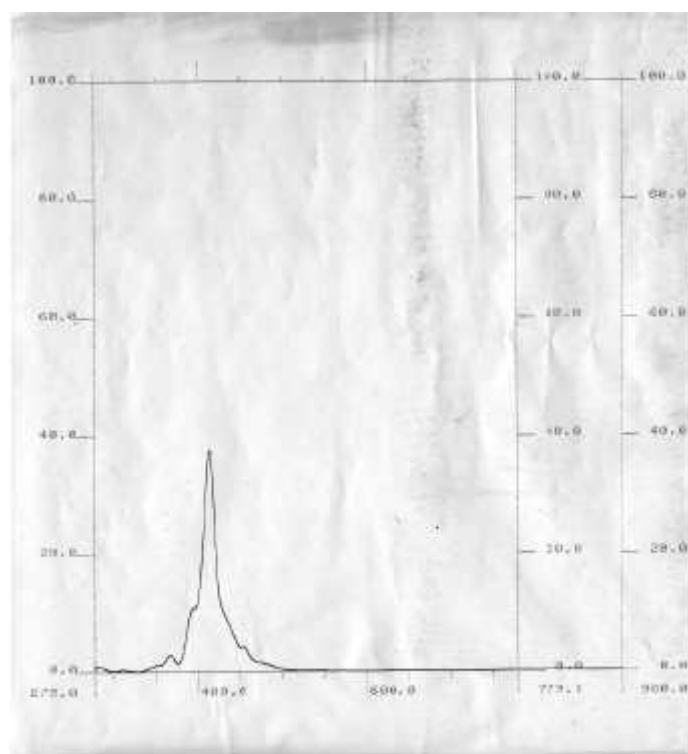


Fig 1(f) Coronene in cyclohexane

Fig 2 (a – c) shows the measured fluorescence emission spectra for Asphaltenes of Forties, Brae A and Brent. The spectra indicate the fluorescence ranging from ~ 300 – 600 nm.

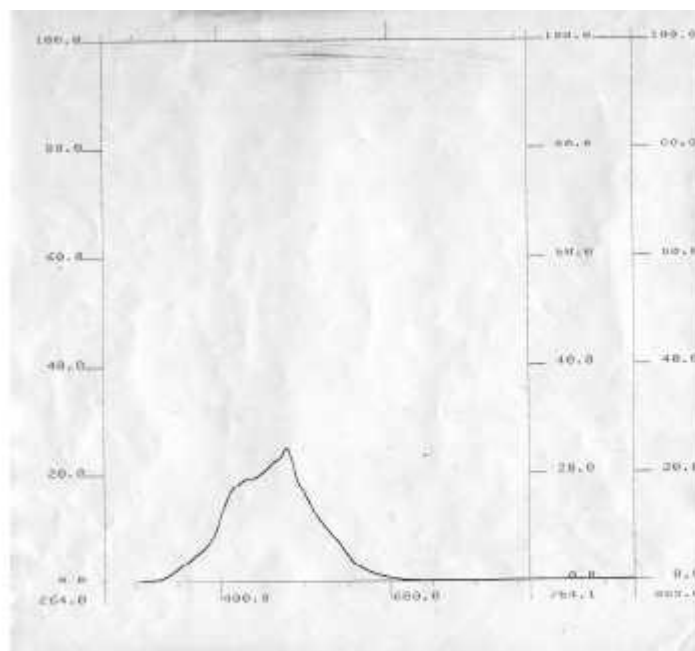


Fig 2 (a) Forties asphaltene in cyclohexane

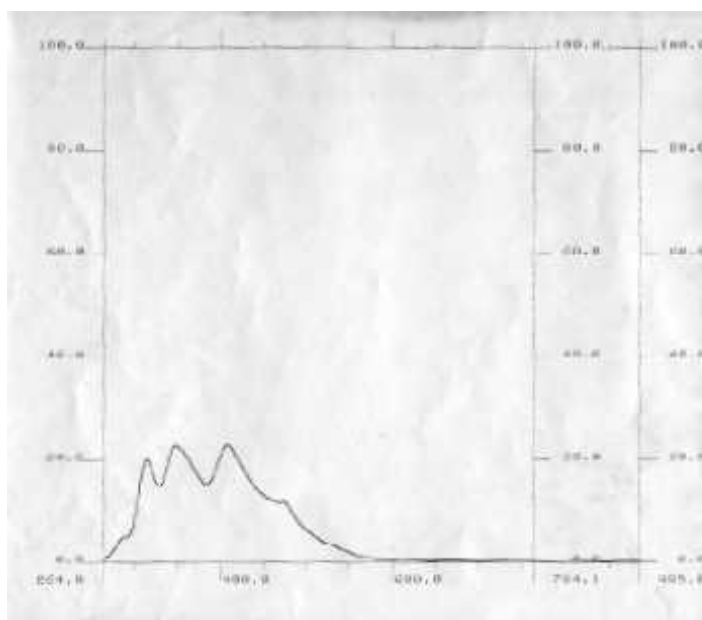


Fig 2(b) Brae A asphaltene in cyclohexane

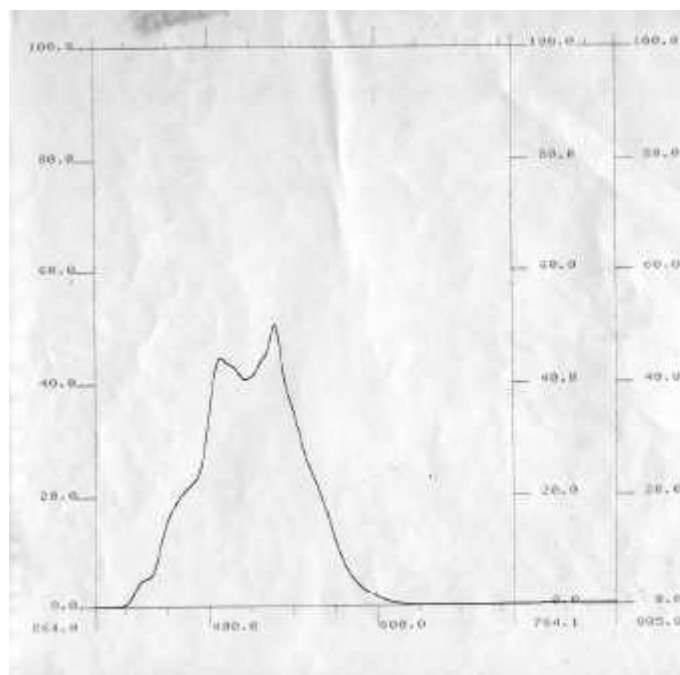
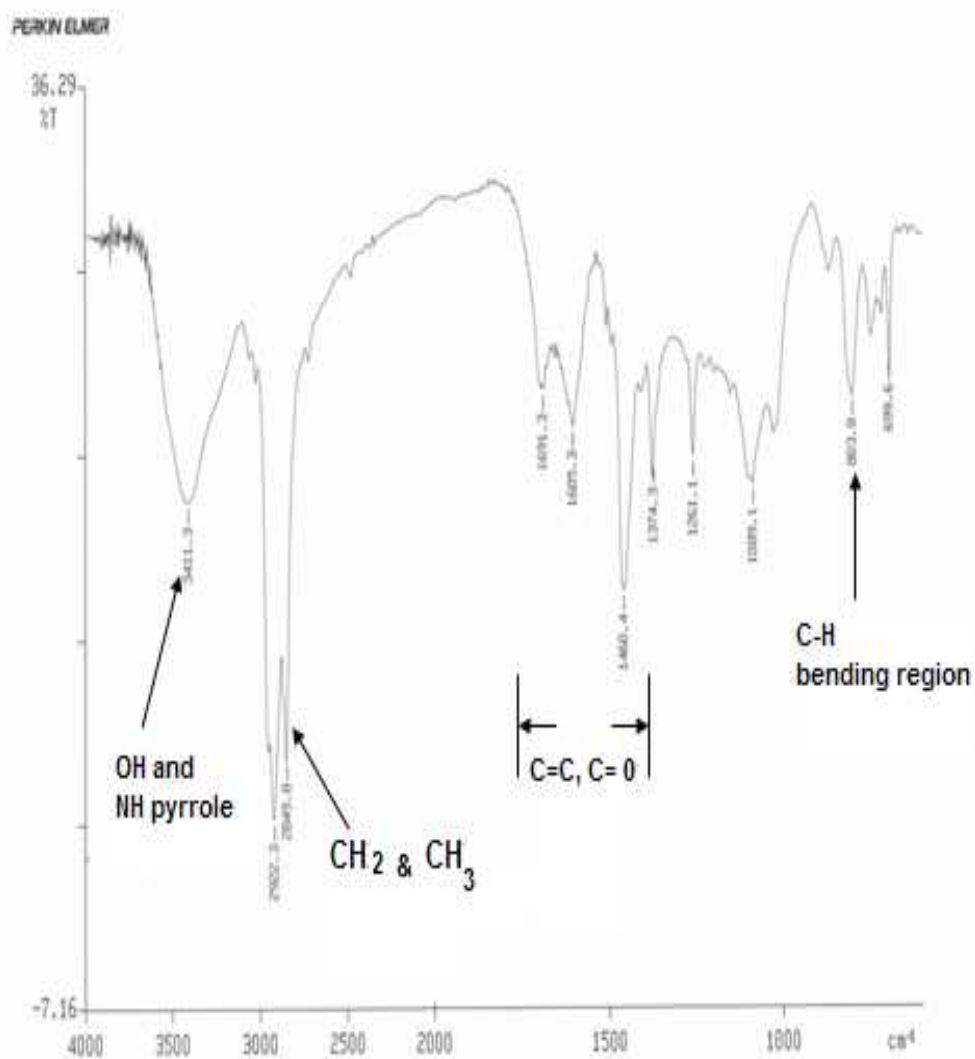


Fig 2(c) Brent asphaltene in cyclohexane

Fig 3 (a) Showing the FT-IR spectra of Forties asphaltene



09/07/09 12:36 Organic Teaching Lab
Z: 4 scans, 4.0cm-1, flat
FORTIES ASPHALTENE

Fig 3 (b) Showing the FT-IR spectra of Brae A asphaltene

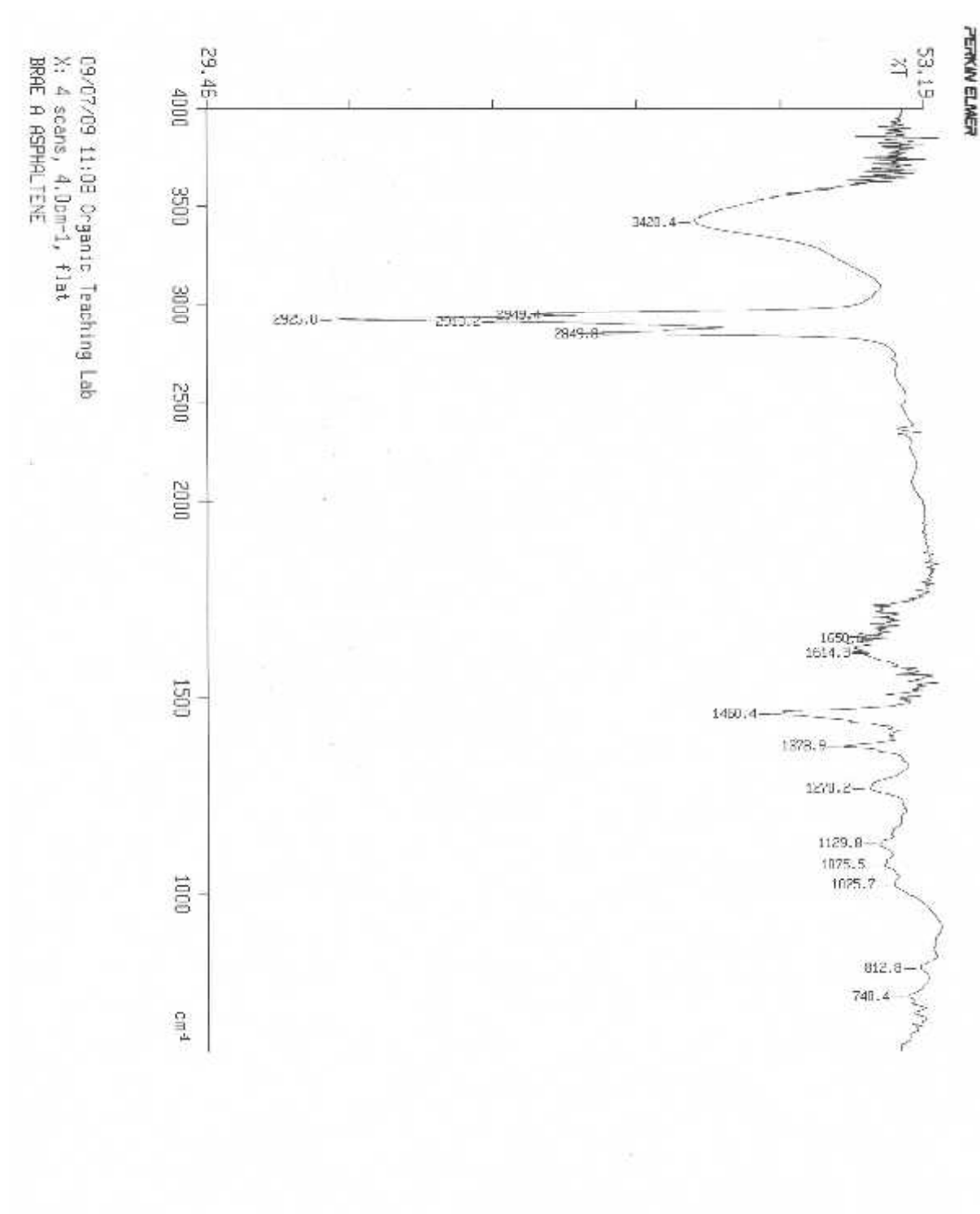


Fig 3 (c) Showing the FT-IR spectra of Brent asphaltene

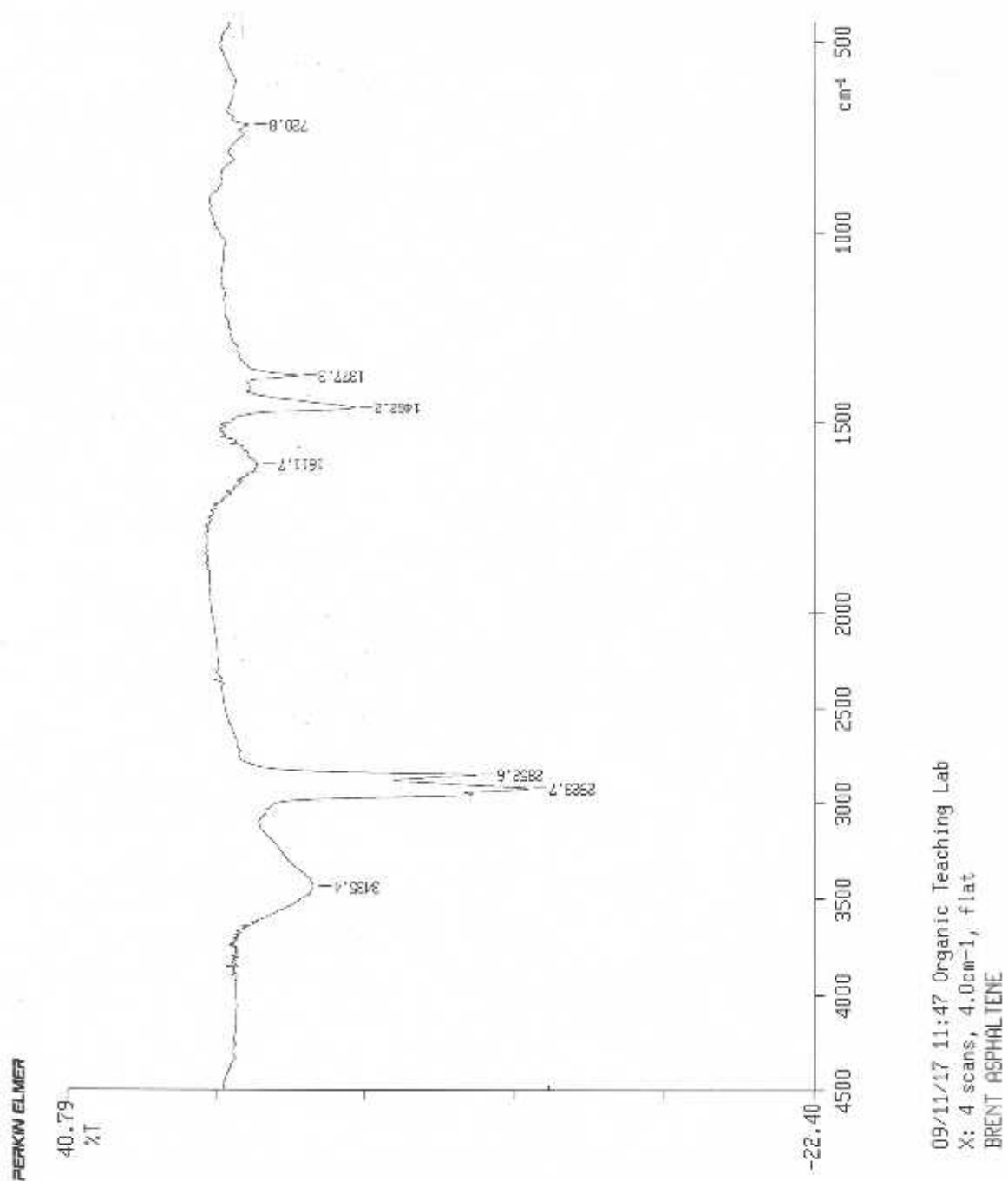
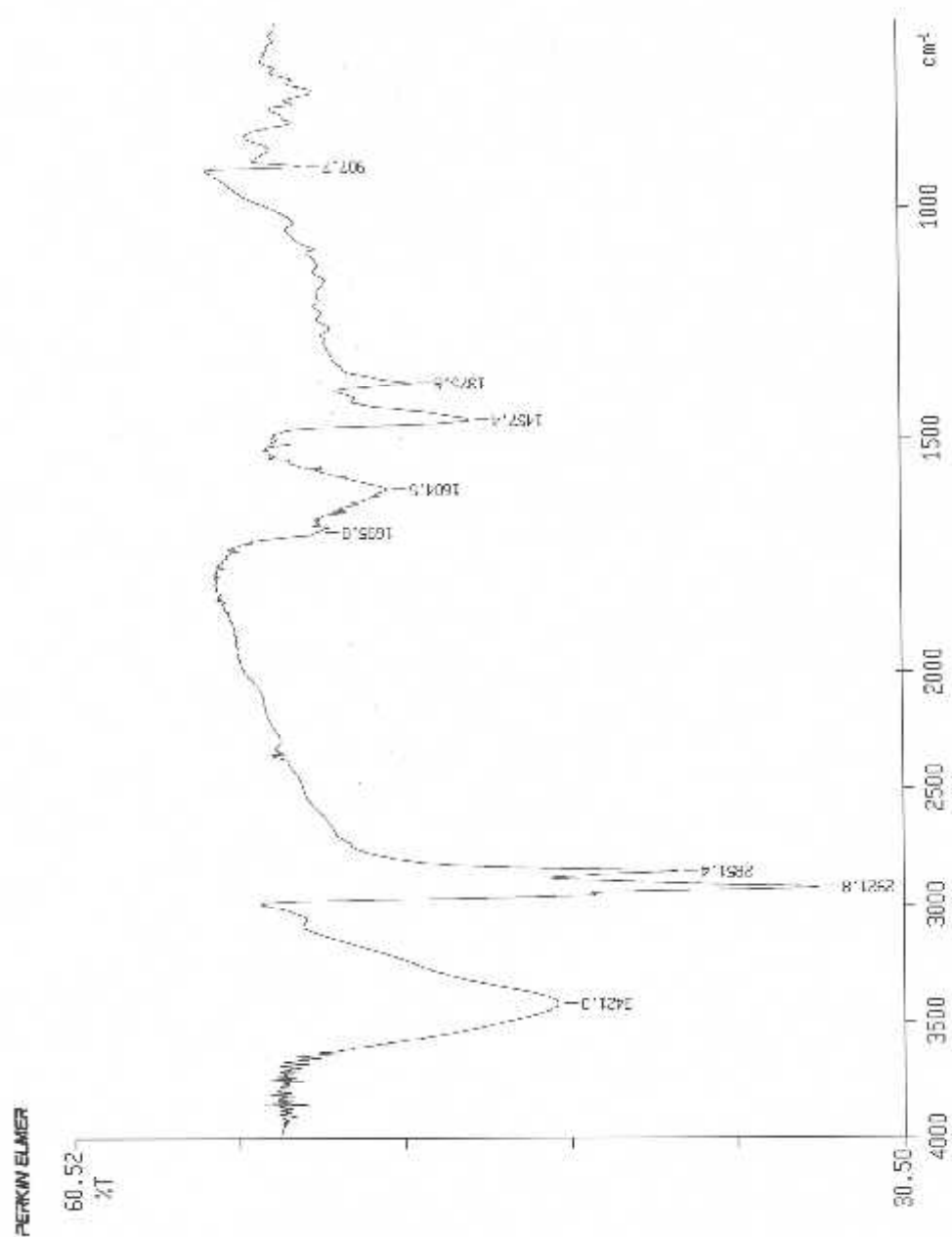


Fig 3 (d) Showing the FT-IR spectra of Stirling asphaltene



05/07/08 12:09 Organic Teaching Lab
X: 4 scans, 4.0cm-1, flat

STIRLING ASPH.

Fig 4 (a) Showing the FT-IR spectra of Forties resin

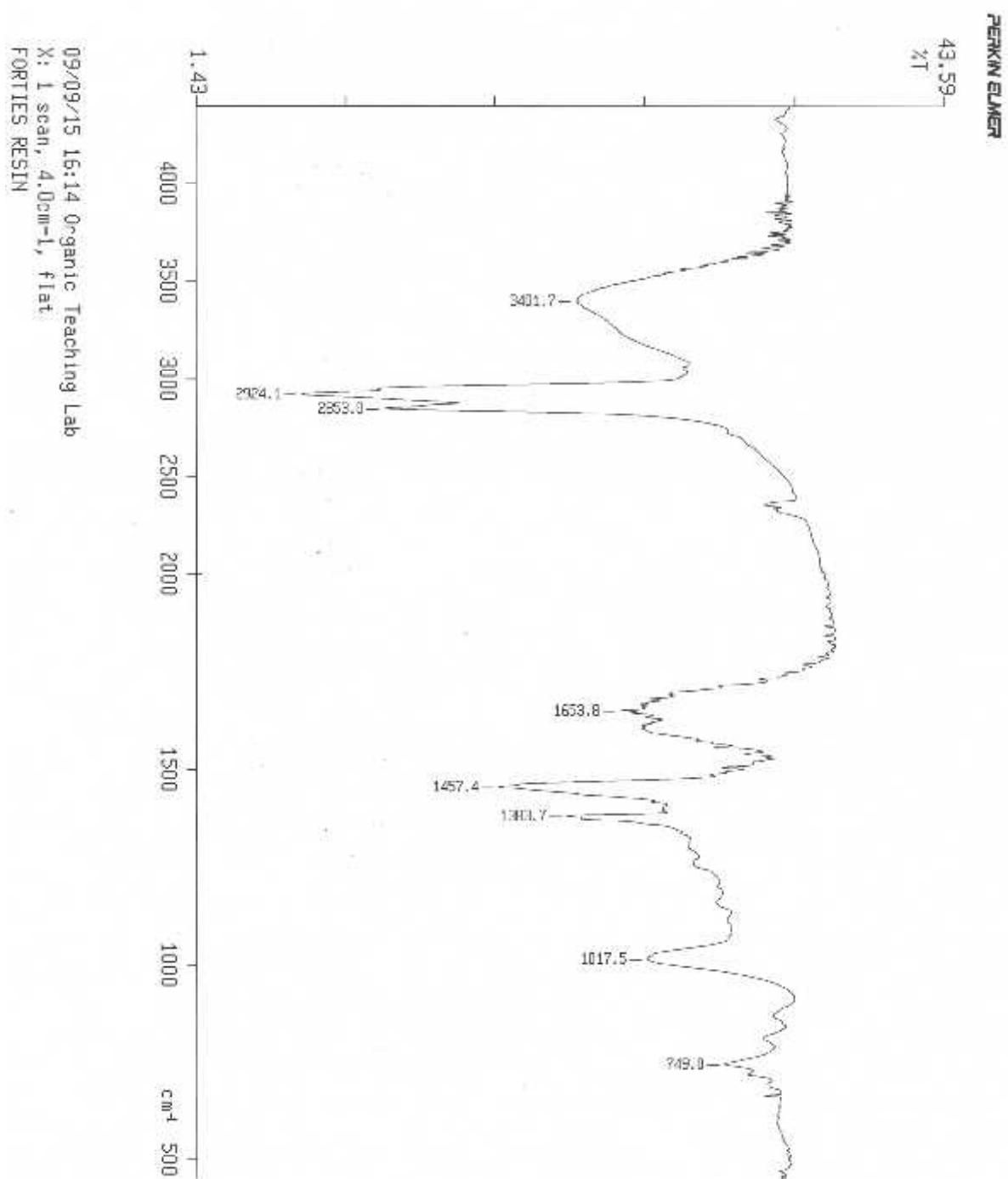


Fig 4 (b) Showing the FT-IR spectra of Brae A resin

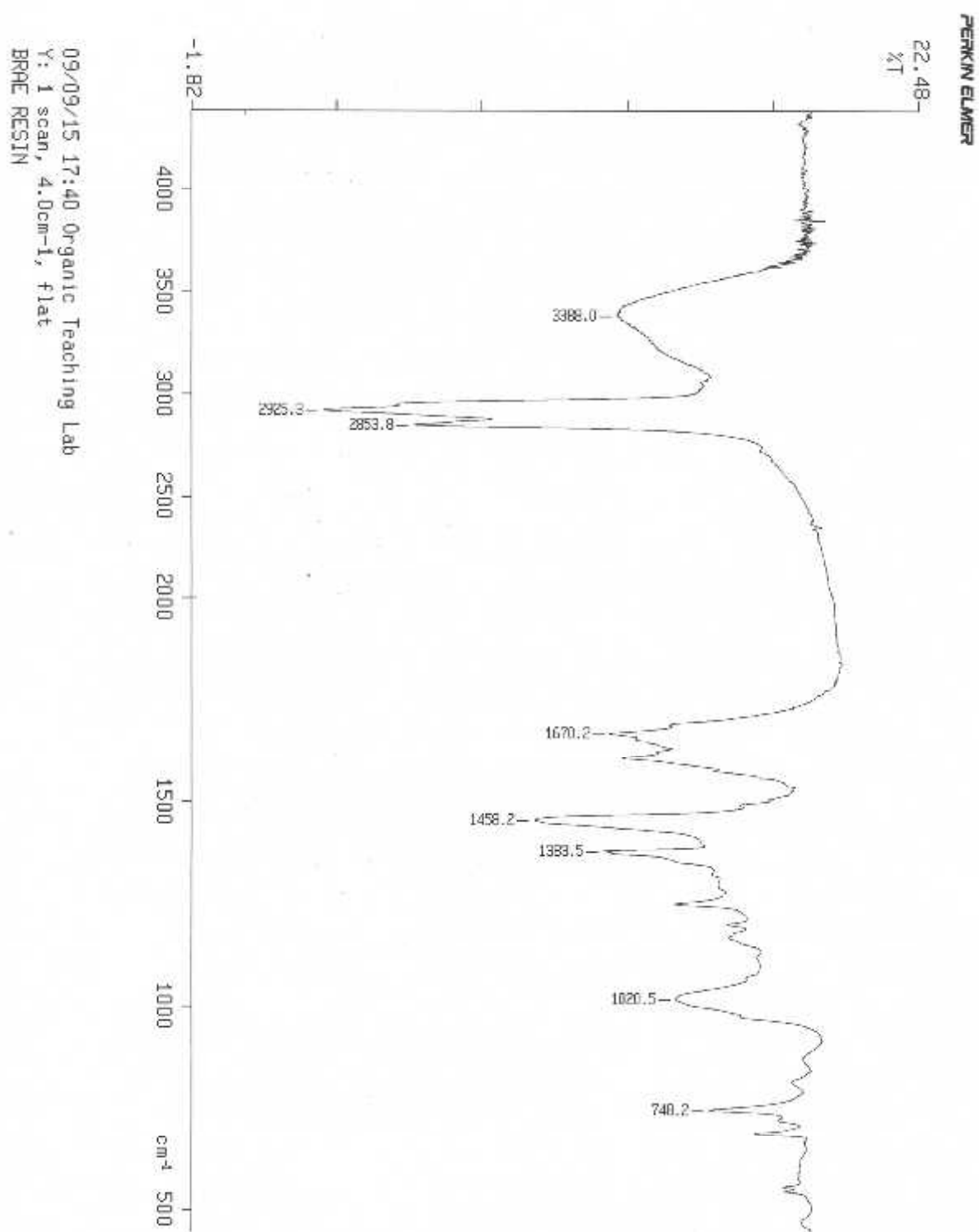


Fig 4 (c) Showing the FT-IR spectra of Brent resin

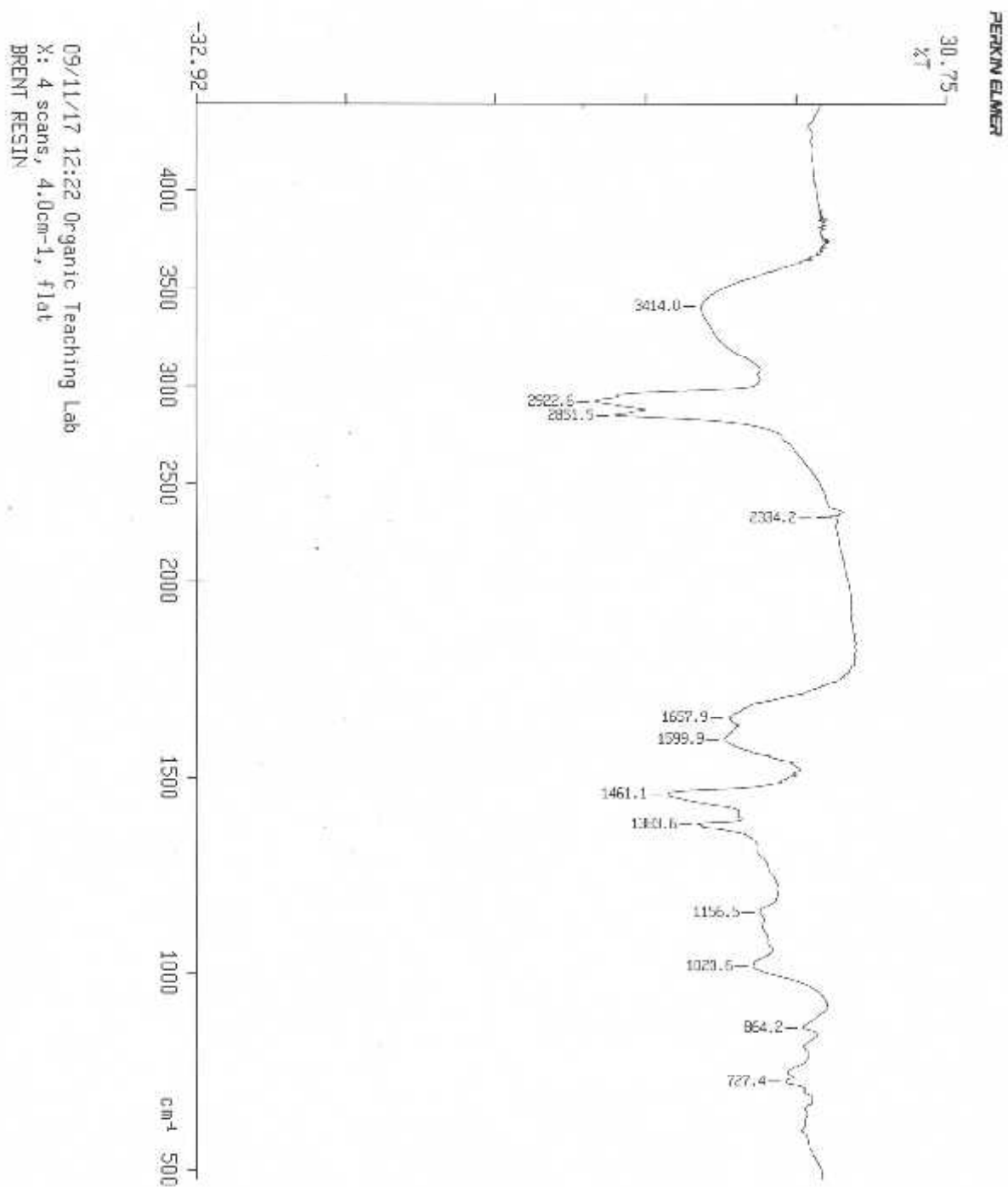


Fig 4 (d) Showing the FT-IR spectra of Stirling resin

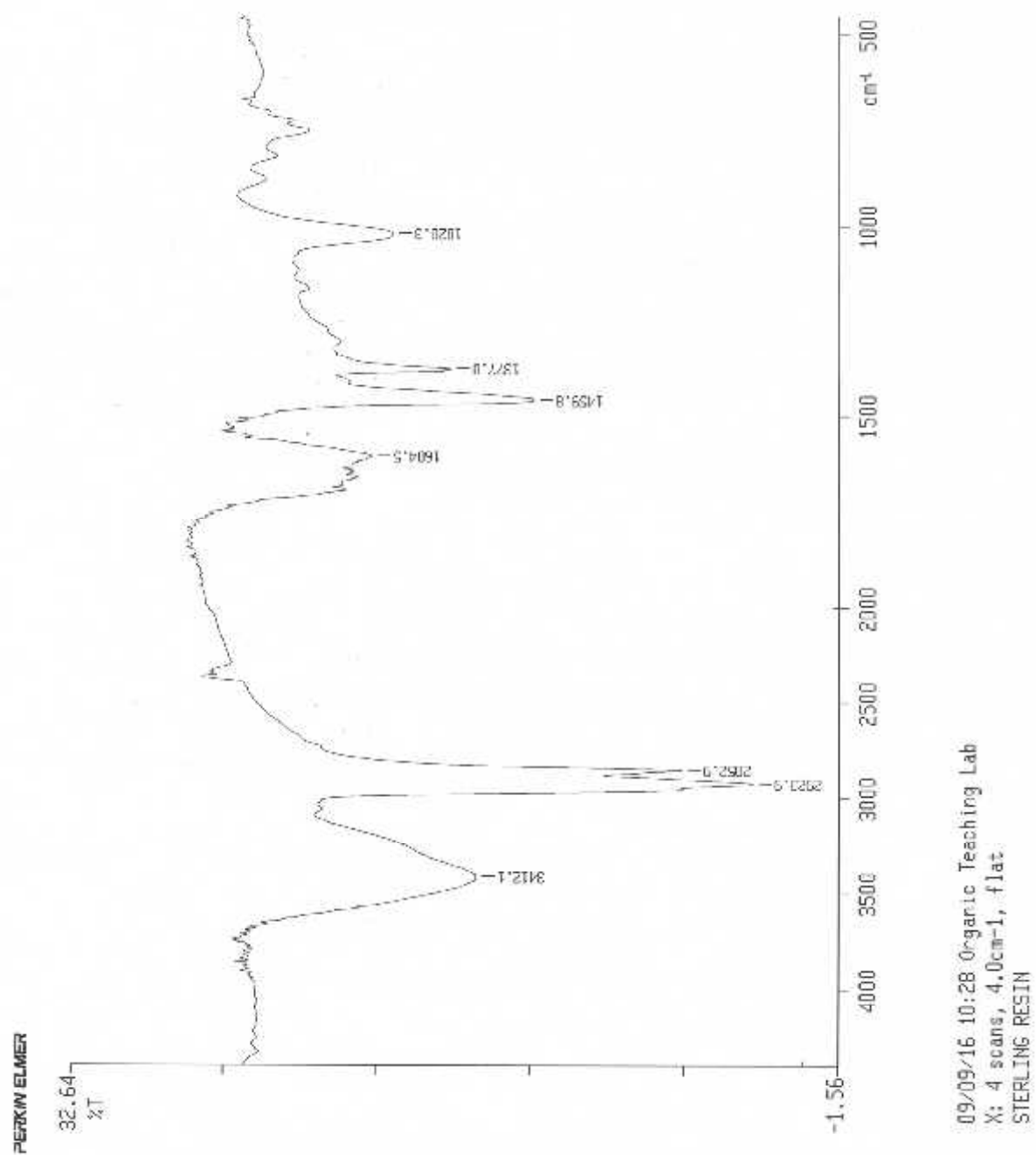


Fig 5 (a) Showing the FT-IR of Forties aromatic

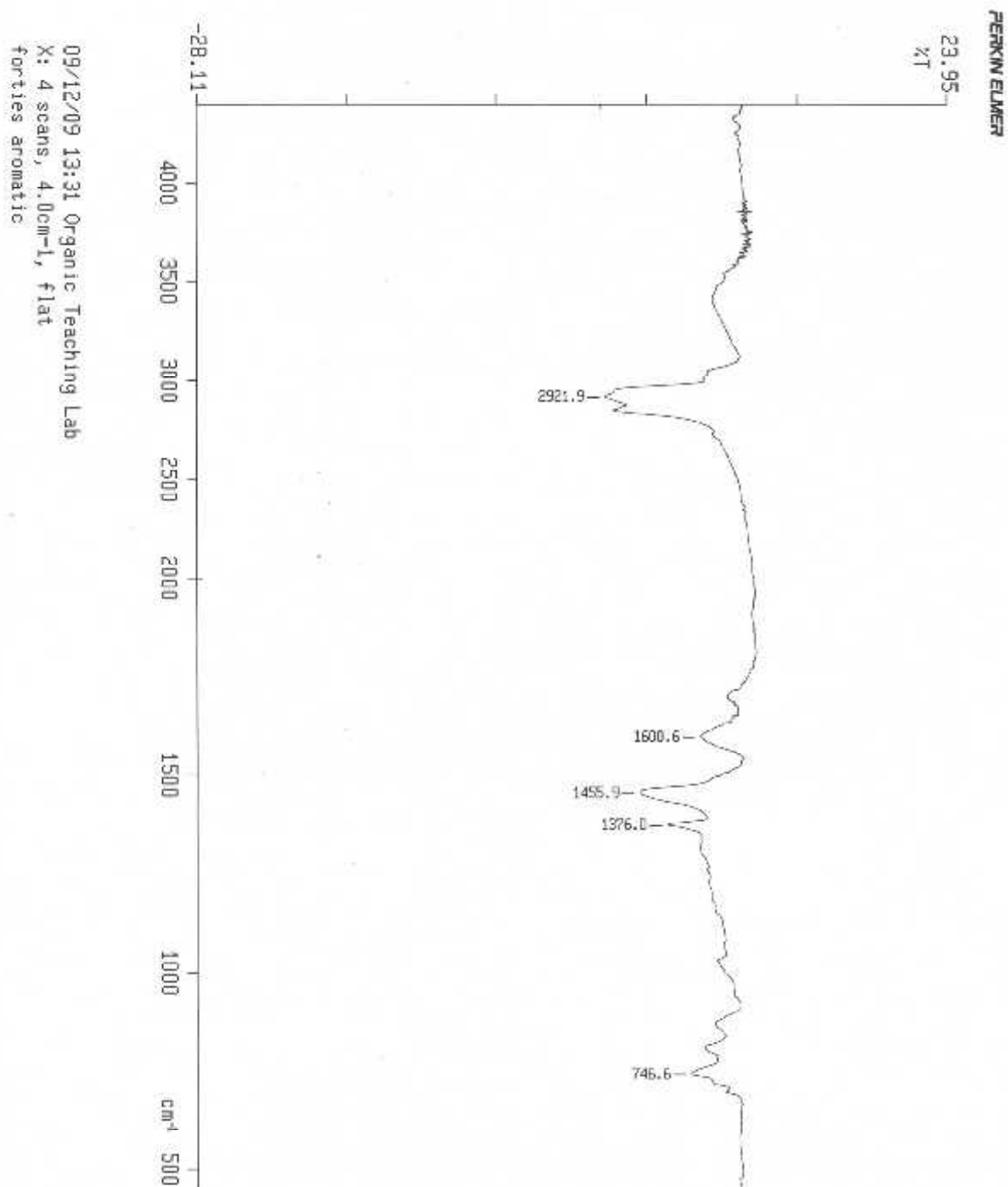
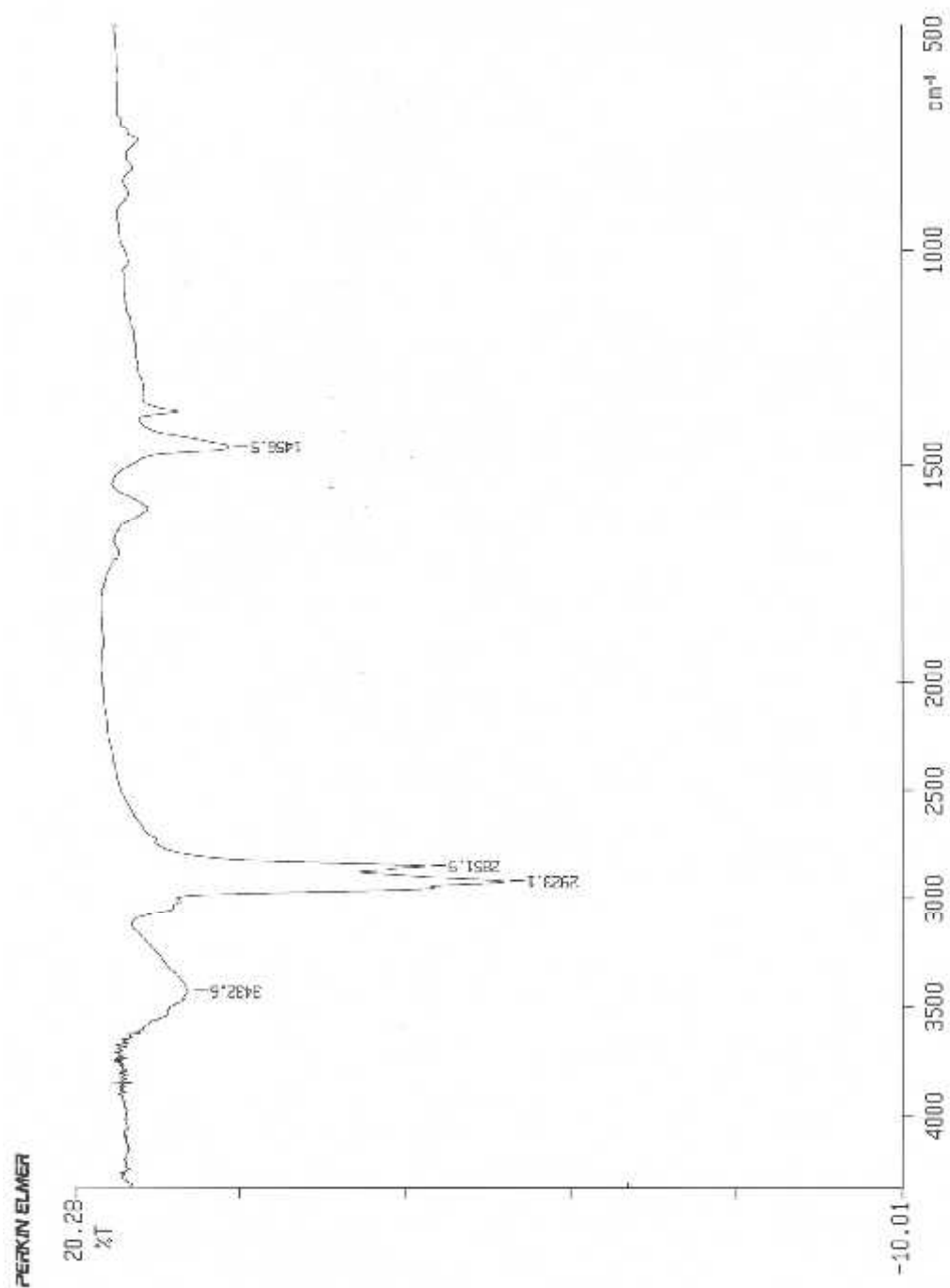


Fig 5 (b) Showing the FT-IR spectra of Brae A aromatic



09/12/09 14:12 Organic Teaching Lab
X: 4 scans, 4.0cm⁻¹, flat, atr
BRAE A AROMATIC

Fig 5 (c) Showing the FT-IR spectra of Brent aromatic

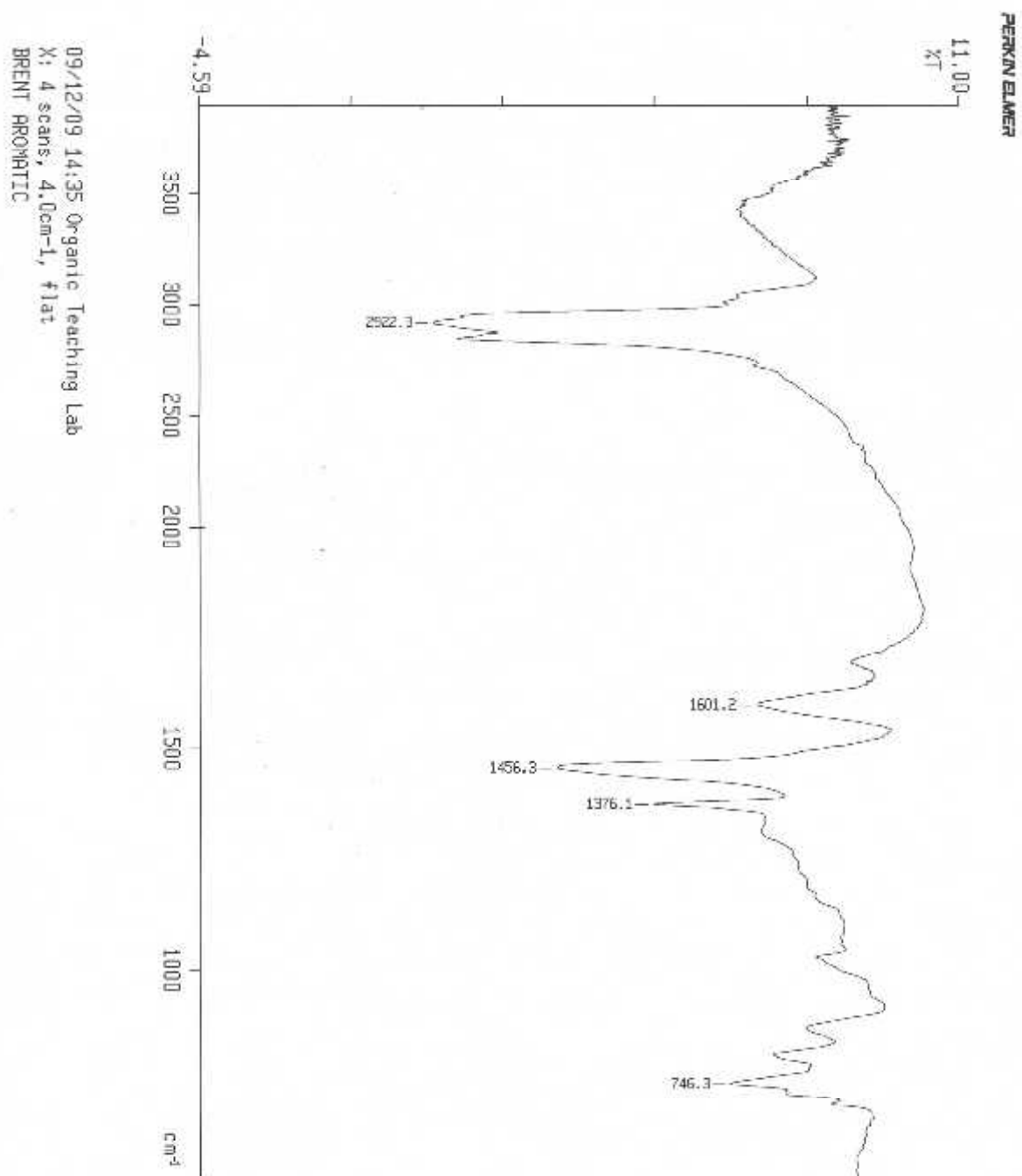
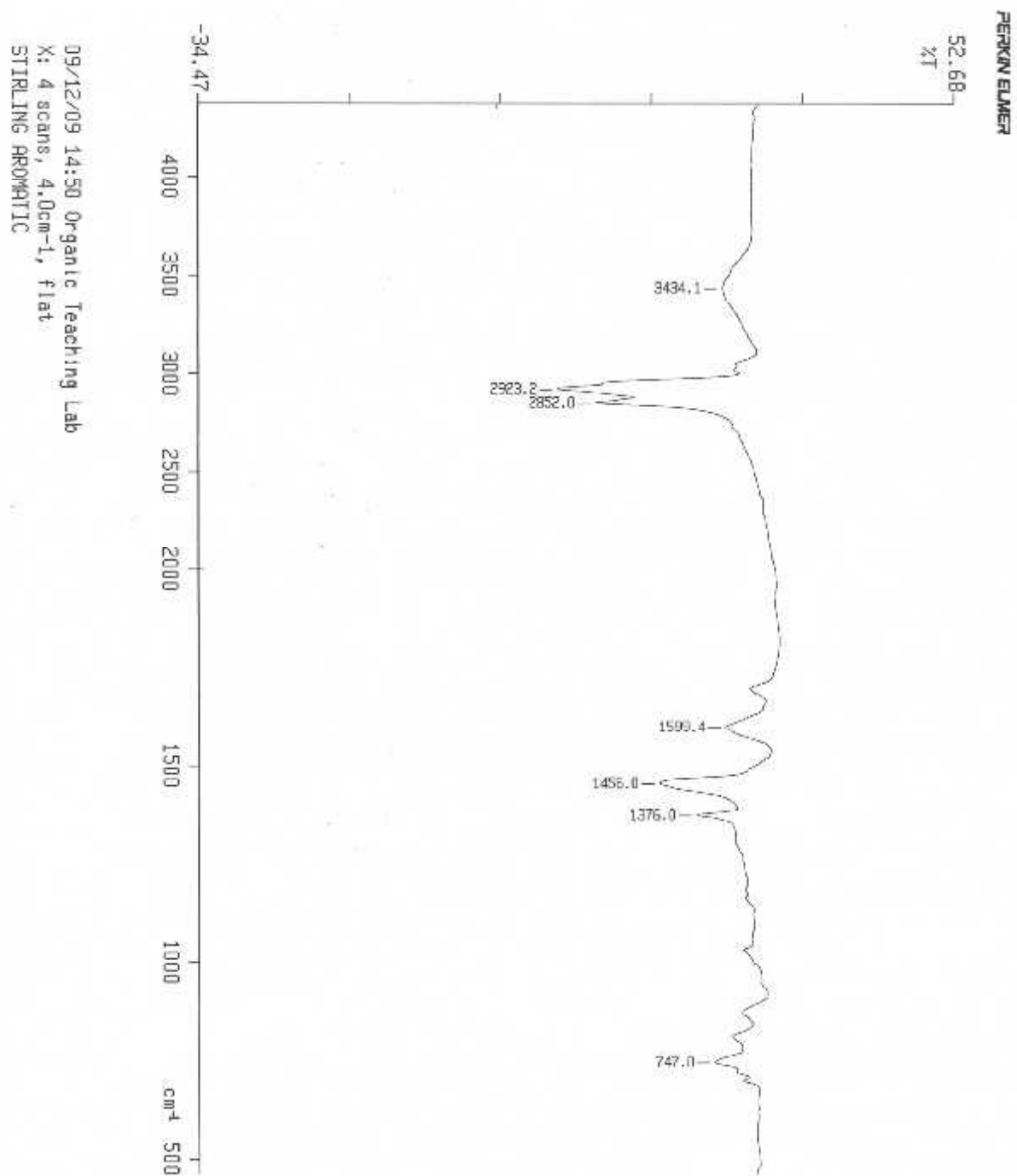


Fig 5 (d) Showing the FT-IR spectra of Stirling aromatic



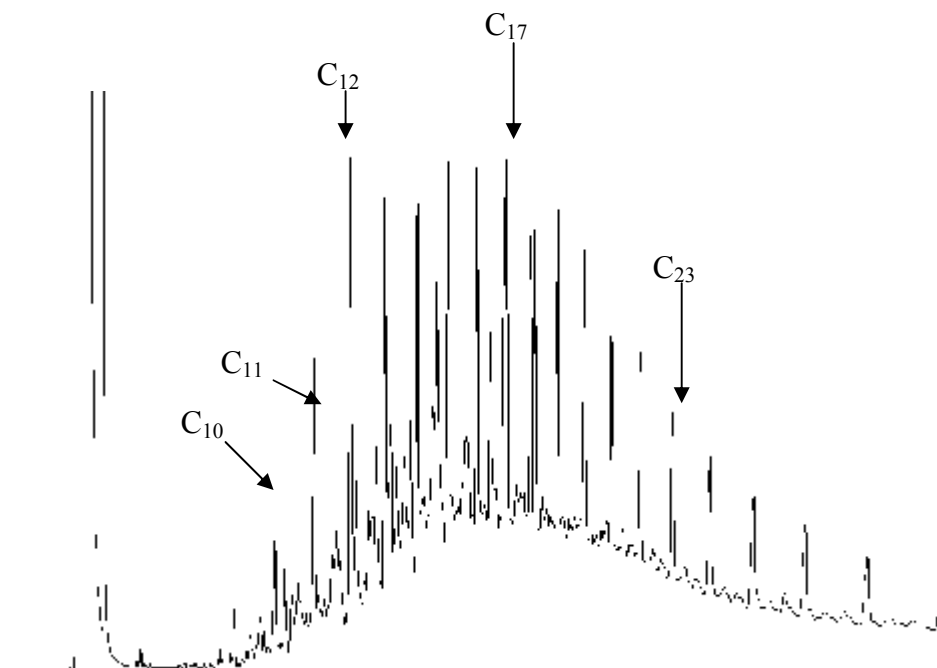
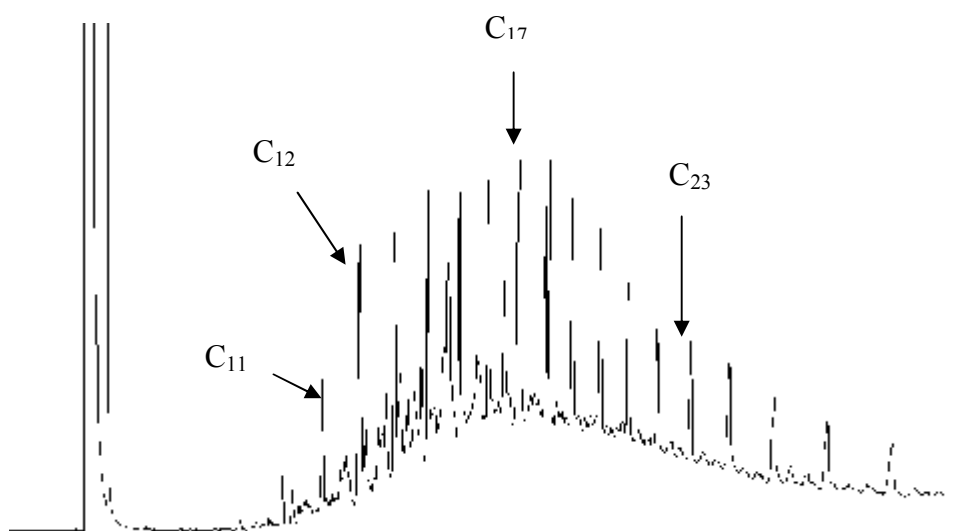
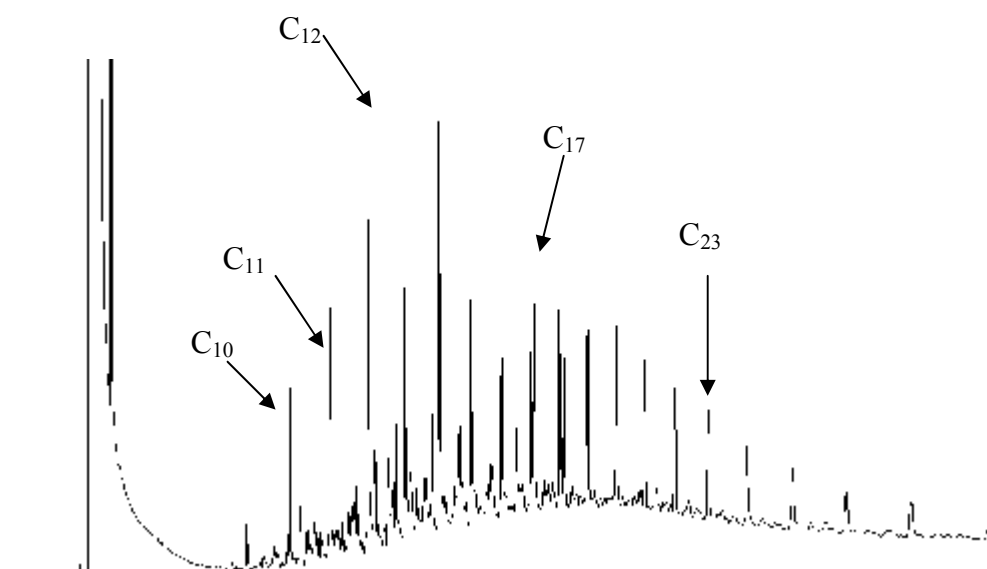


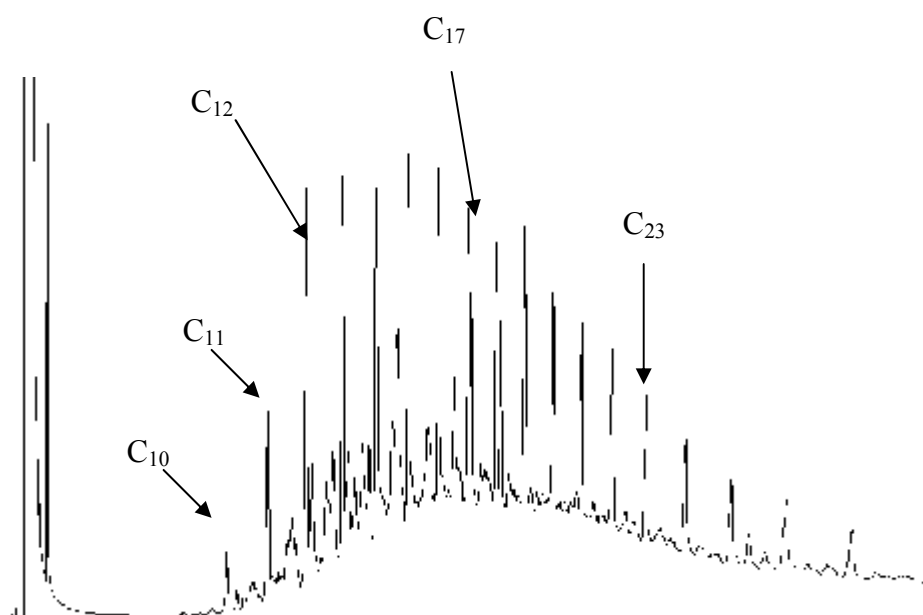
Fig 6 (a) GC-FID of Forties aliphatic fraction



6 (b) GC-FID of Brae A aliphatic fraction



6 (c) GC-FID of Brent aliphatic fraction



6 (d) GC-FID of Stirling aliphatic fraction

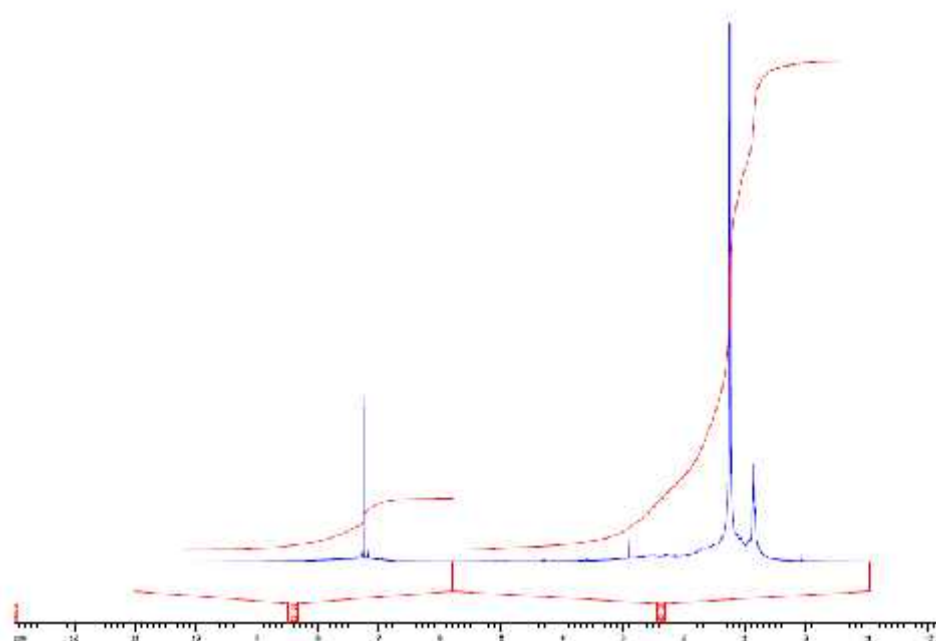
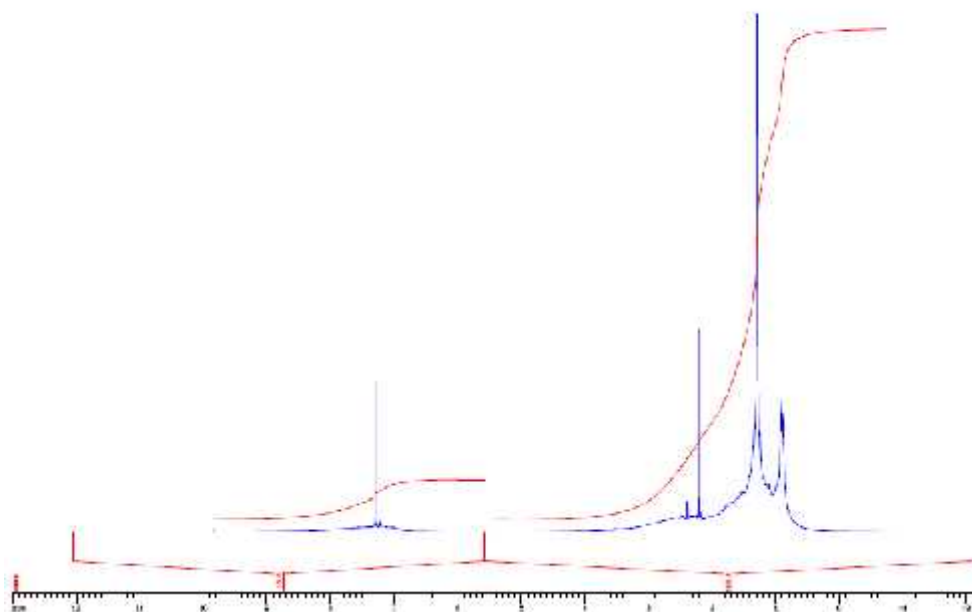
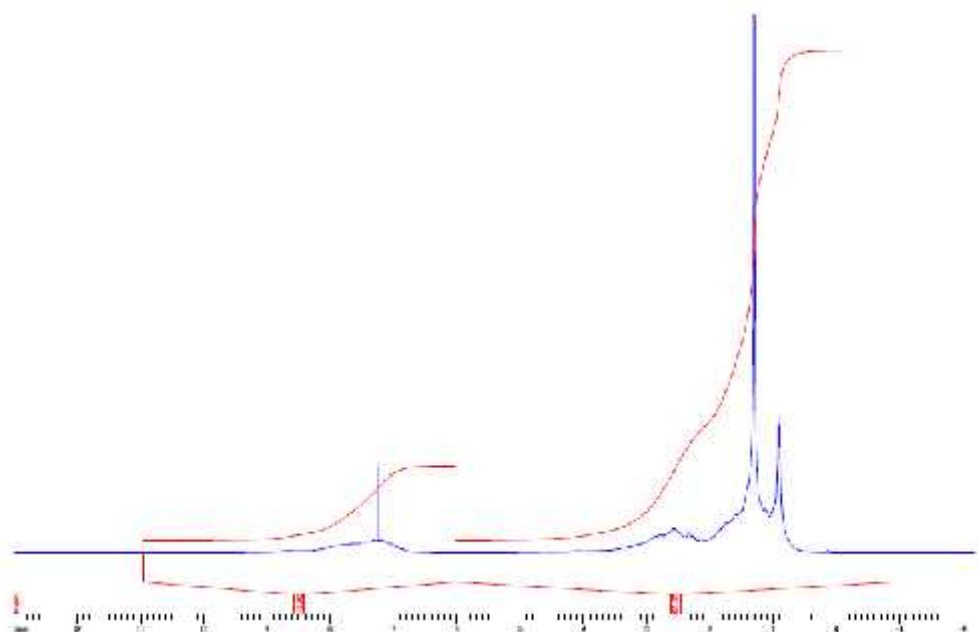


Fig 7 (a) ^1H NMR spectrum of Forties asphaltene showing signals at different intensities



7(b) ^1H NMR spectrum of Forties resins showing signals at different intensities



7 (c) ^1H NMR spectrum of Forties Aromatics showing signals at different intensities

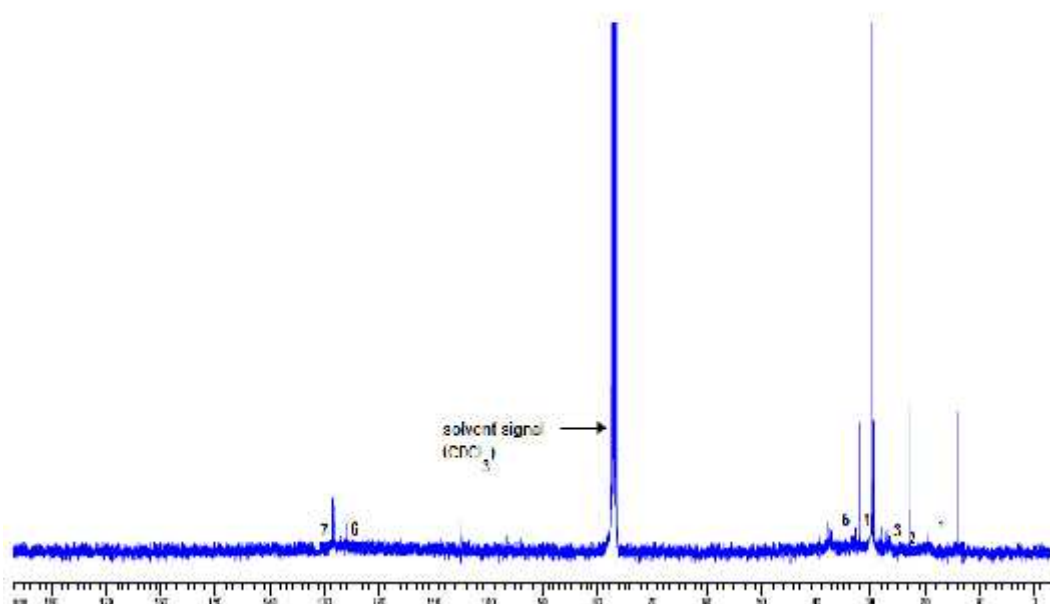


Fig 7(d) ^{13}C NMR spectrum of Forties asphaltene showing 7 signals corresponding to the different carbon environments, numbered (1-7) in the sample in CDCl_3 .

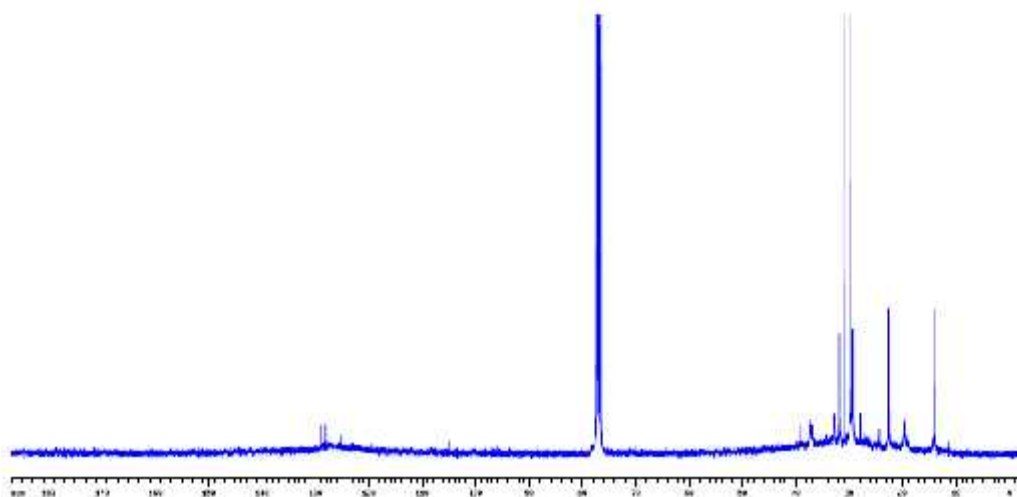


Fig 7 (e) ^{13}C NMR spectrum of Forties Resin showing signals corresponding to the different carbon environments in the sample.

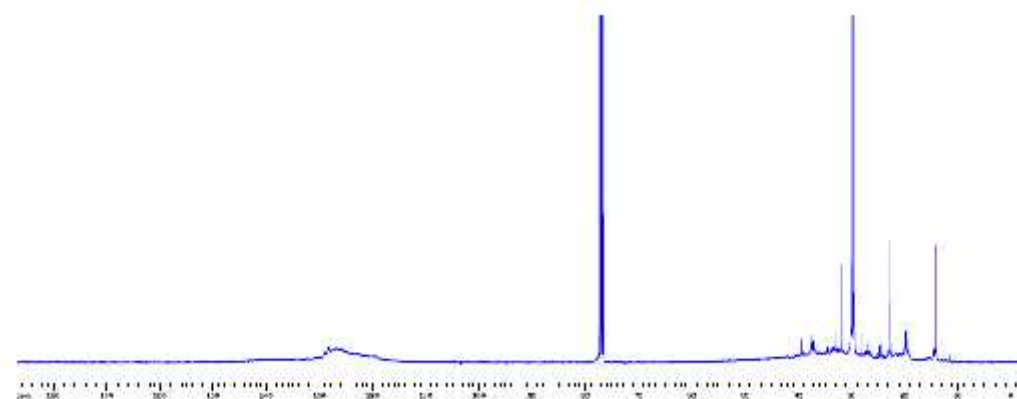


Fig 7(f) ^{13}C NMR spectrum of Forties Aromatics showing signals corresponding to the different carbon environments in the sample.

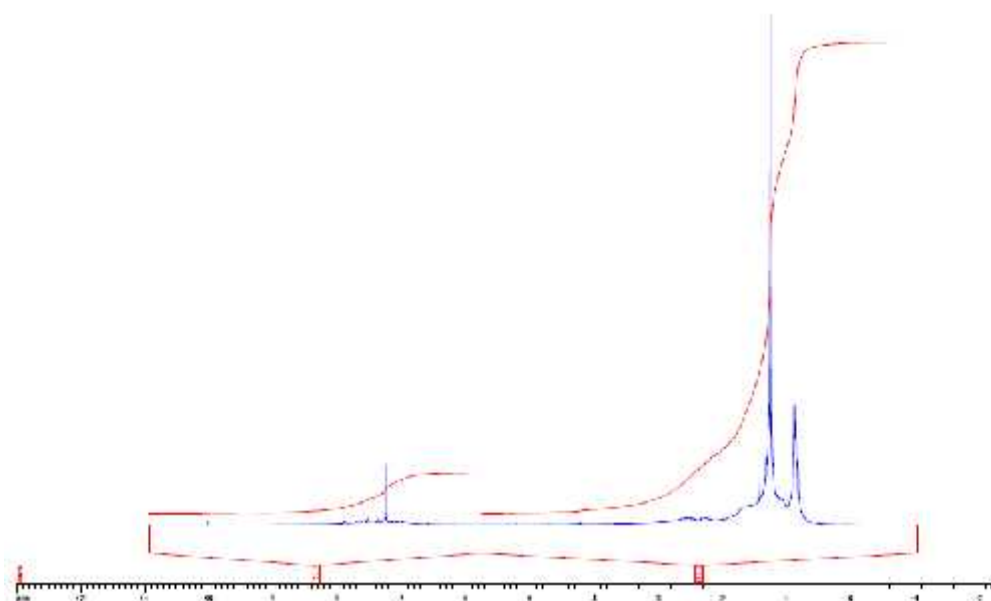


Fig 8 (a) ^1H NMR of Brae A asphaltene showing signals at different intensities

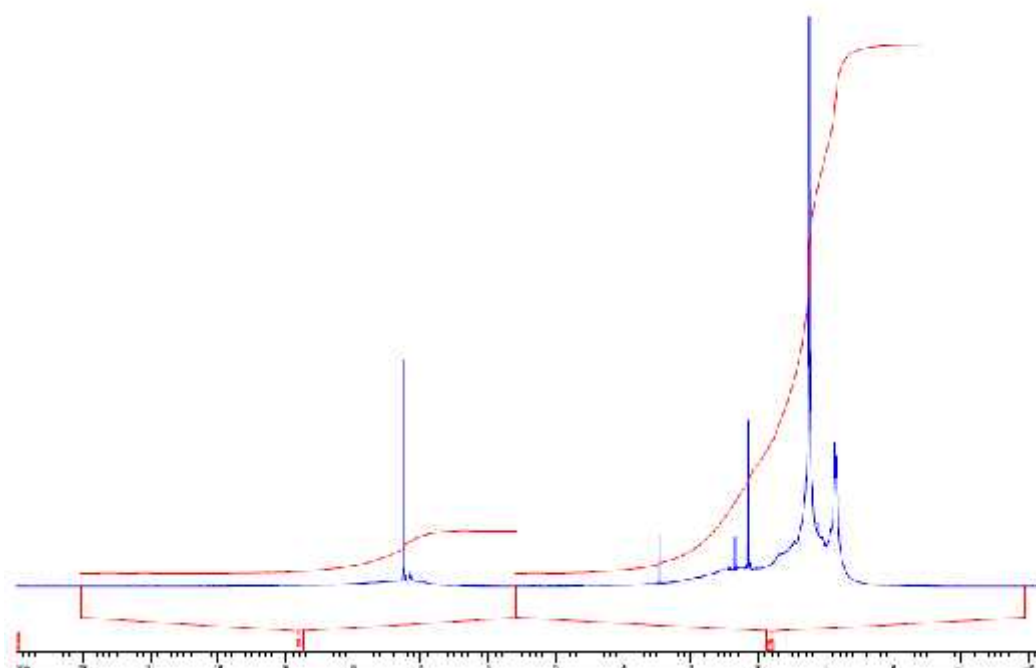


Fig 8(b) ^1H NMR of Brae A Resin showing signals at different intensities

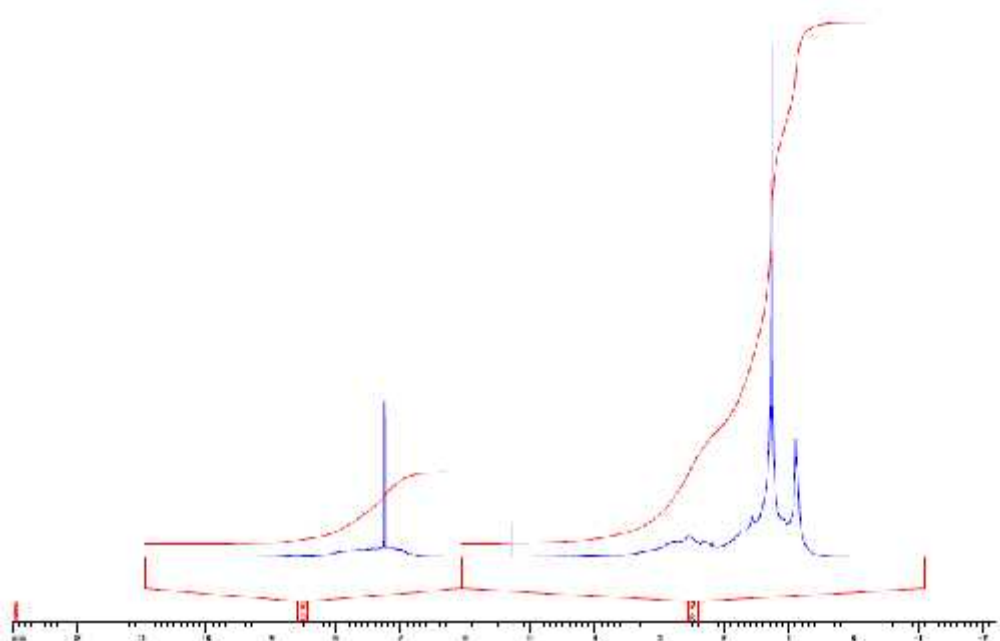


Fig 8(c) ^1H NMR of Brae A Aromatics showing signals at different intensities

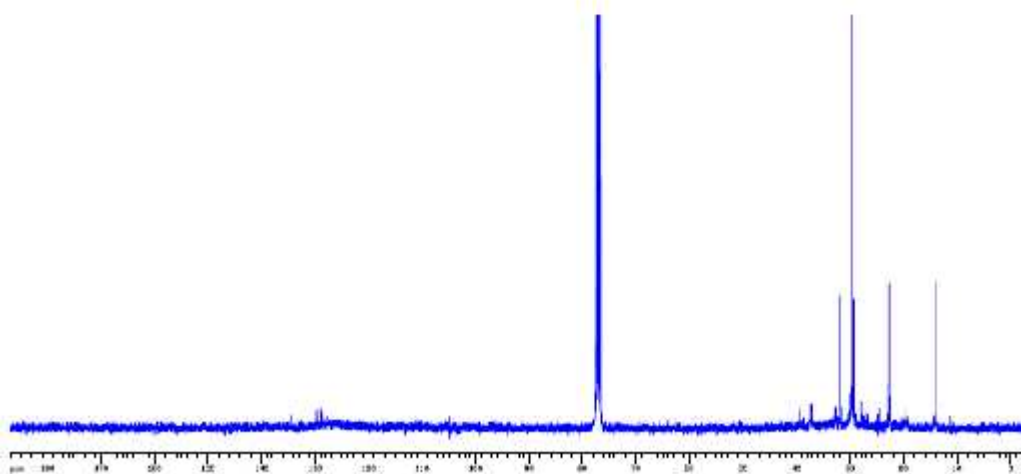


Fig 8(d) ^{13}C NMR spectrum of Brae A asphaltene showing signals corresponding to the different carbon environments in the sample.

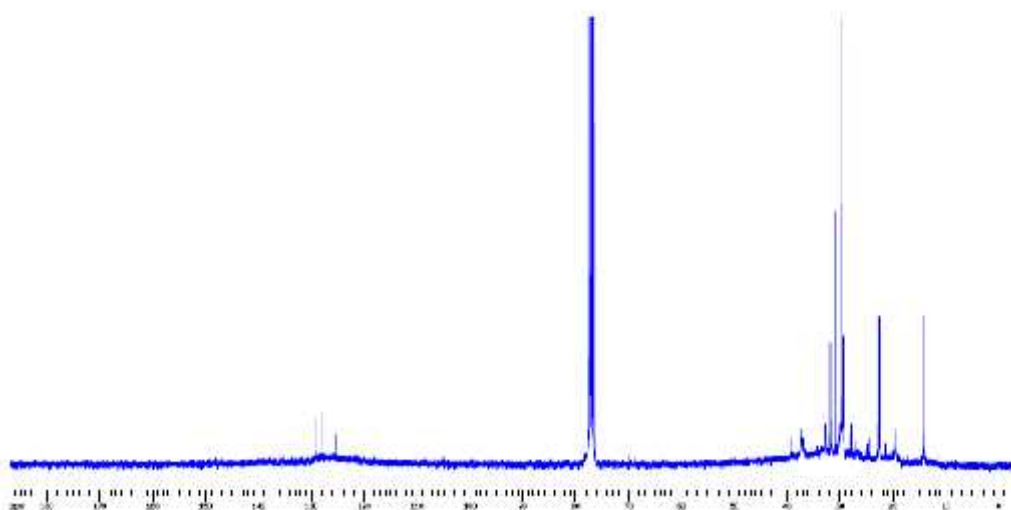


Fig 8(e) ^{13}C NMR spectrum of Brae A Resin showing signals corresponding to the different carbon environments in the sample.

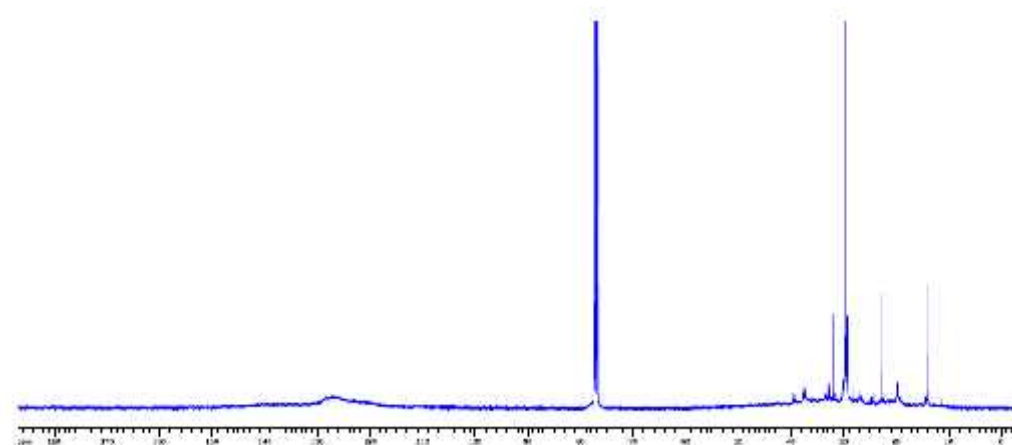


Fig 8(f) ^{13}C NMR spectrum of Brae A Aromatics showing signals corresponding to the different carbon environments in the sample.

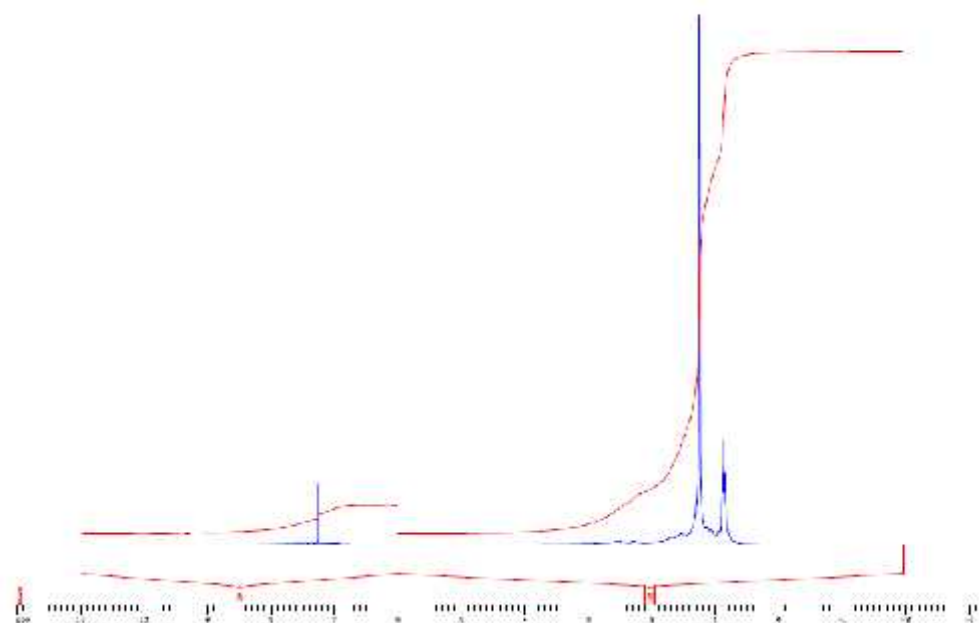


Fig 9(a) ^1H NMR of Brent asphaltene showing signals at different intensities

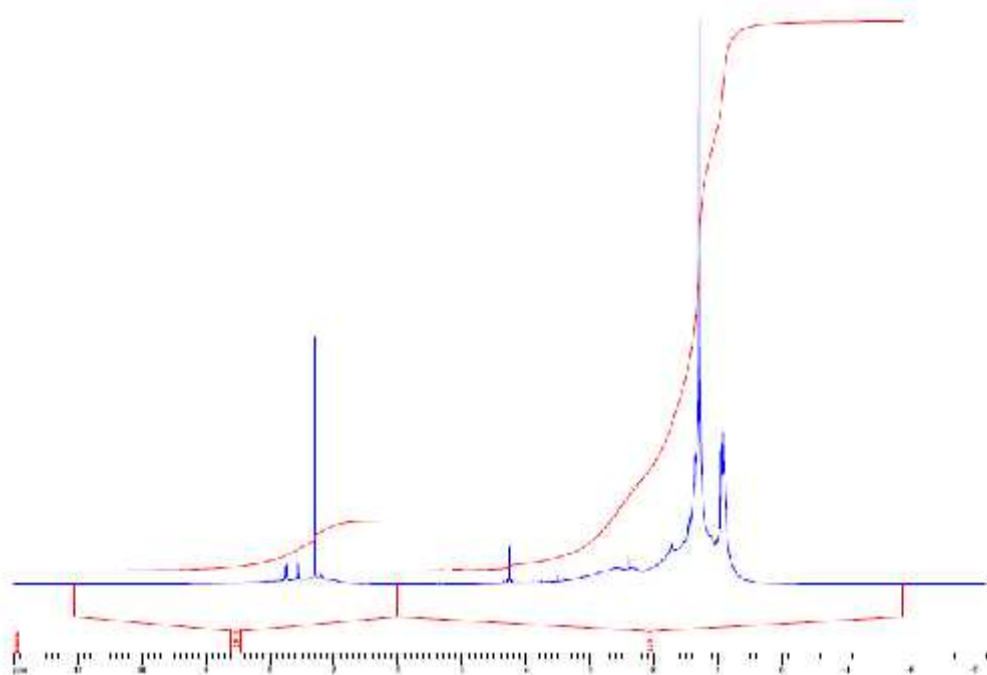


Fig 9(b) ^1H NMR of Brent Resin showing signals at different intensities

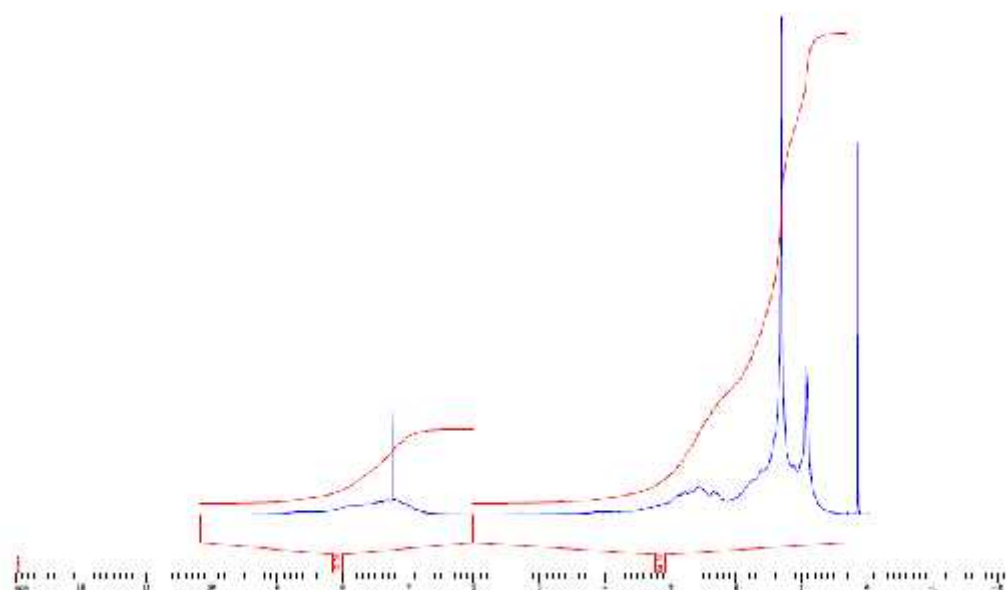


Fig 9(c) ^1H NMR of Brent Aromatics showing signals at different intensities

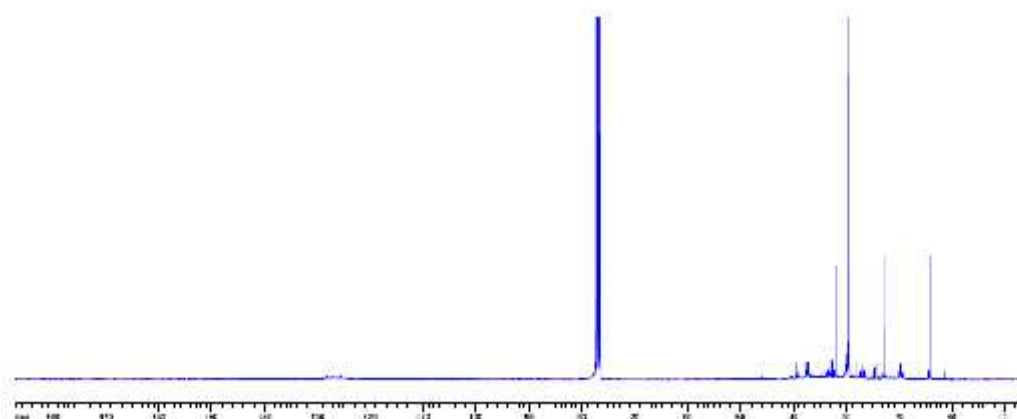


Fig 9(d) ^{13}C NMR spectrum of Brent asphaltene showing signals corresponding to the different carbon environments in the sample.

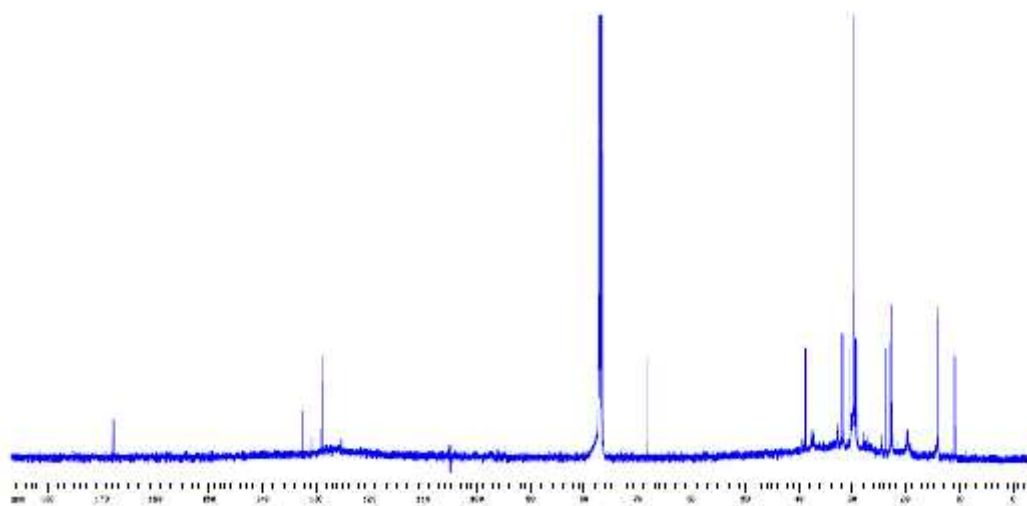


Fig 9(e) ^{13}C NMR spectrum of Brent Resin showing signals corresponding to the different carbon environments in the sample.

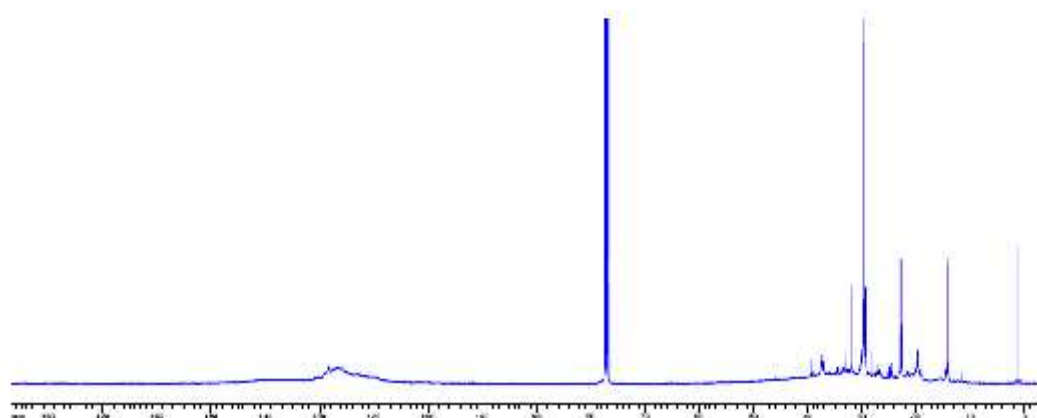


Fig 9(f) ^{13}C NMR spectrum of Brent Aromatics showing signals corresponding to the different carbon environments in the sample.

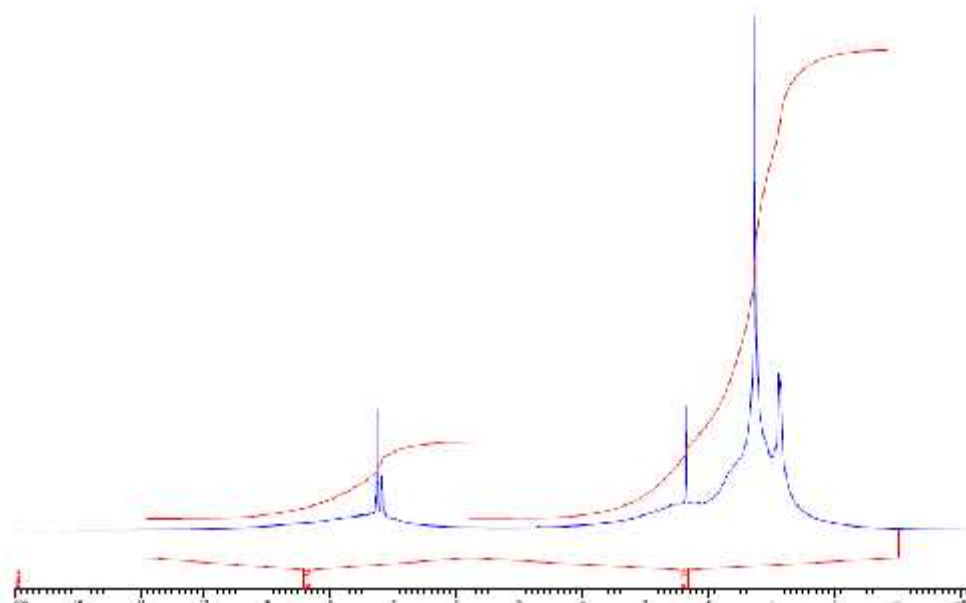


Fig 10(a) ^1H NMR of Stirling asphaltene showing signals at different intensities

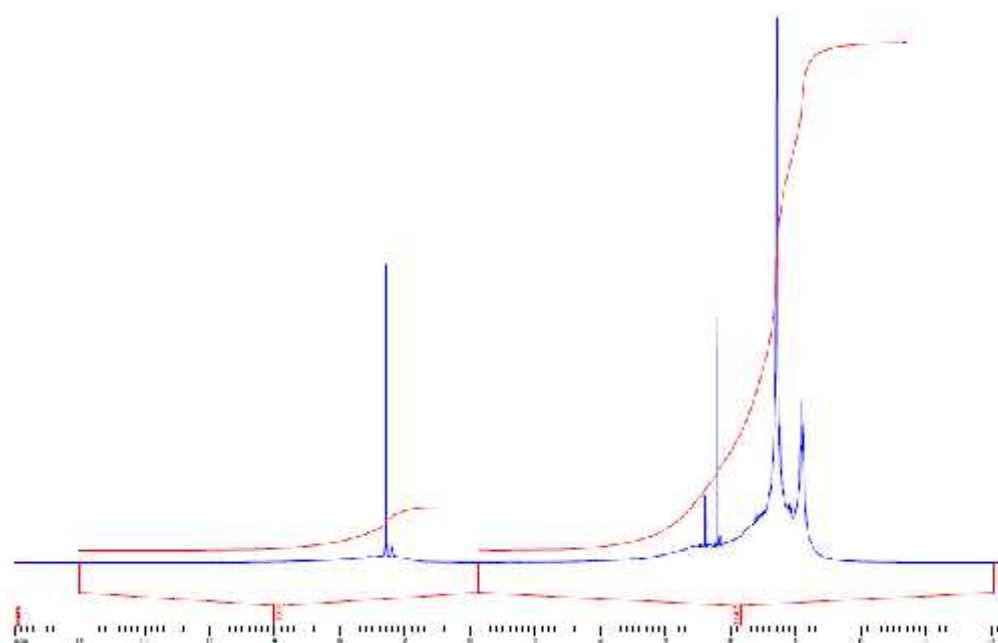


Fig 10(b) ^1H NMR of Stirling resins showing signals at different intensities

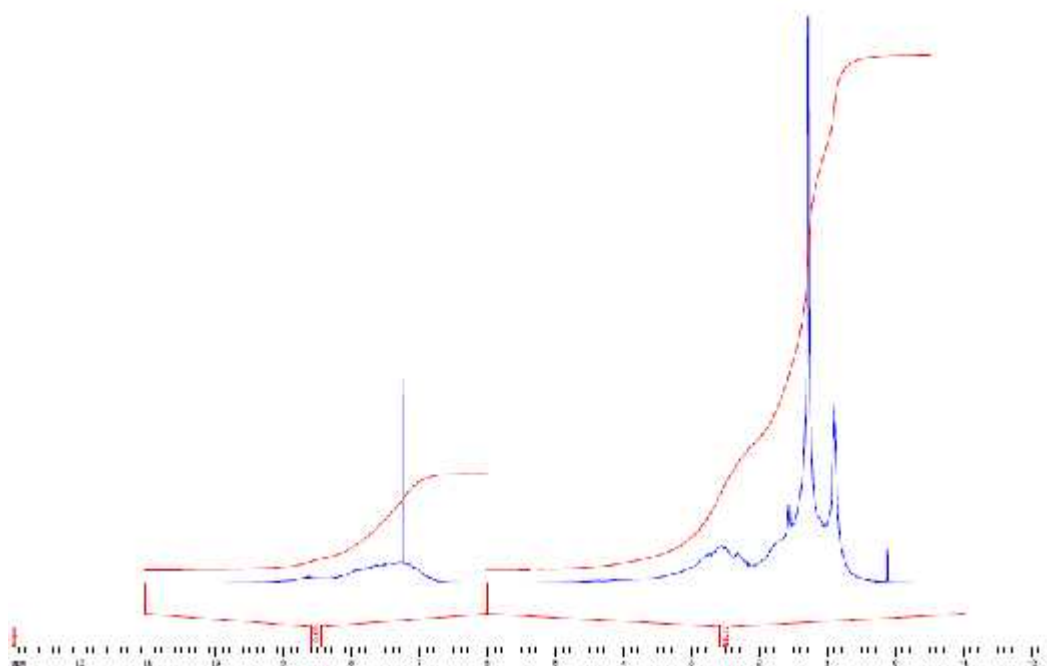


Fig 10(c) ^1H NMR of Stirling Aromatics showing signals at different intensities

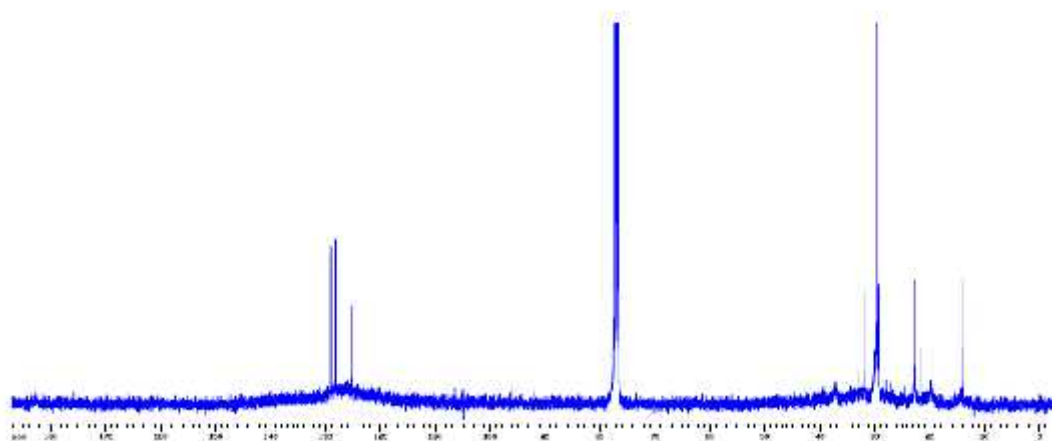


Fig 10(d) ^{13}C NMR spectrum of Stirling asphaltene showing signals corresponding to the different carbon environments in the sample.

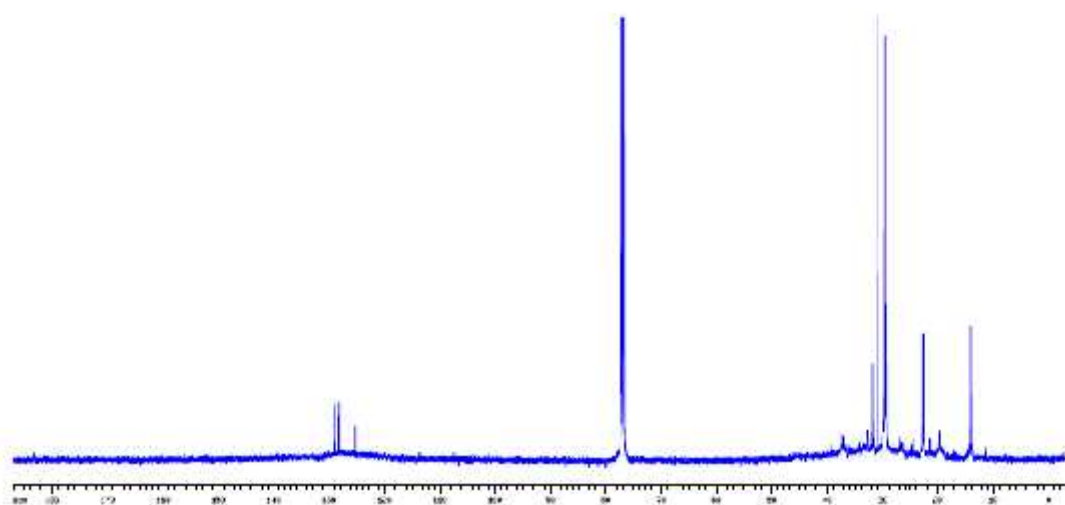


Fig 10(e) ^{13}C NMR spectrum of Stirling resins showing signals corresponding to the different carbon environments in the sample.

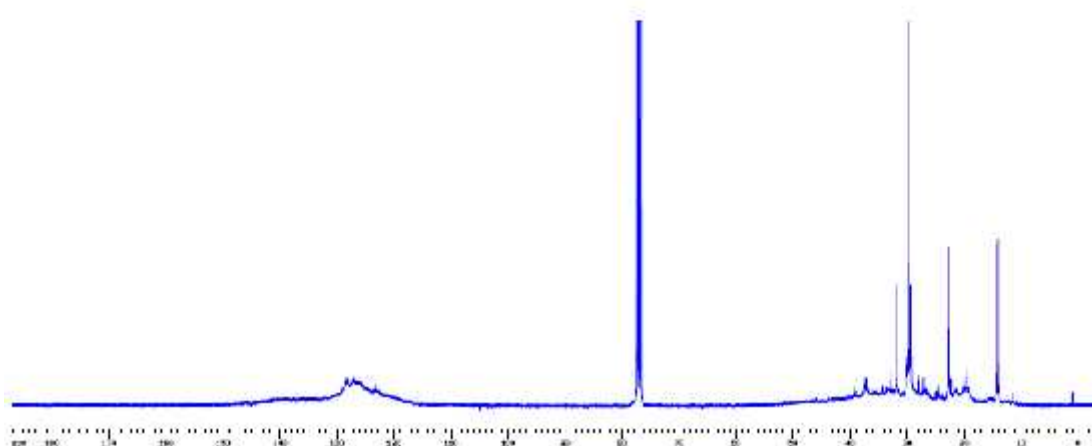


Fig 10(f) ^{13}C NMR spectrum of Stirling Aromatics showing signals corresponding to the different carbon environments in the sample.

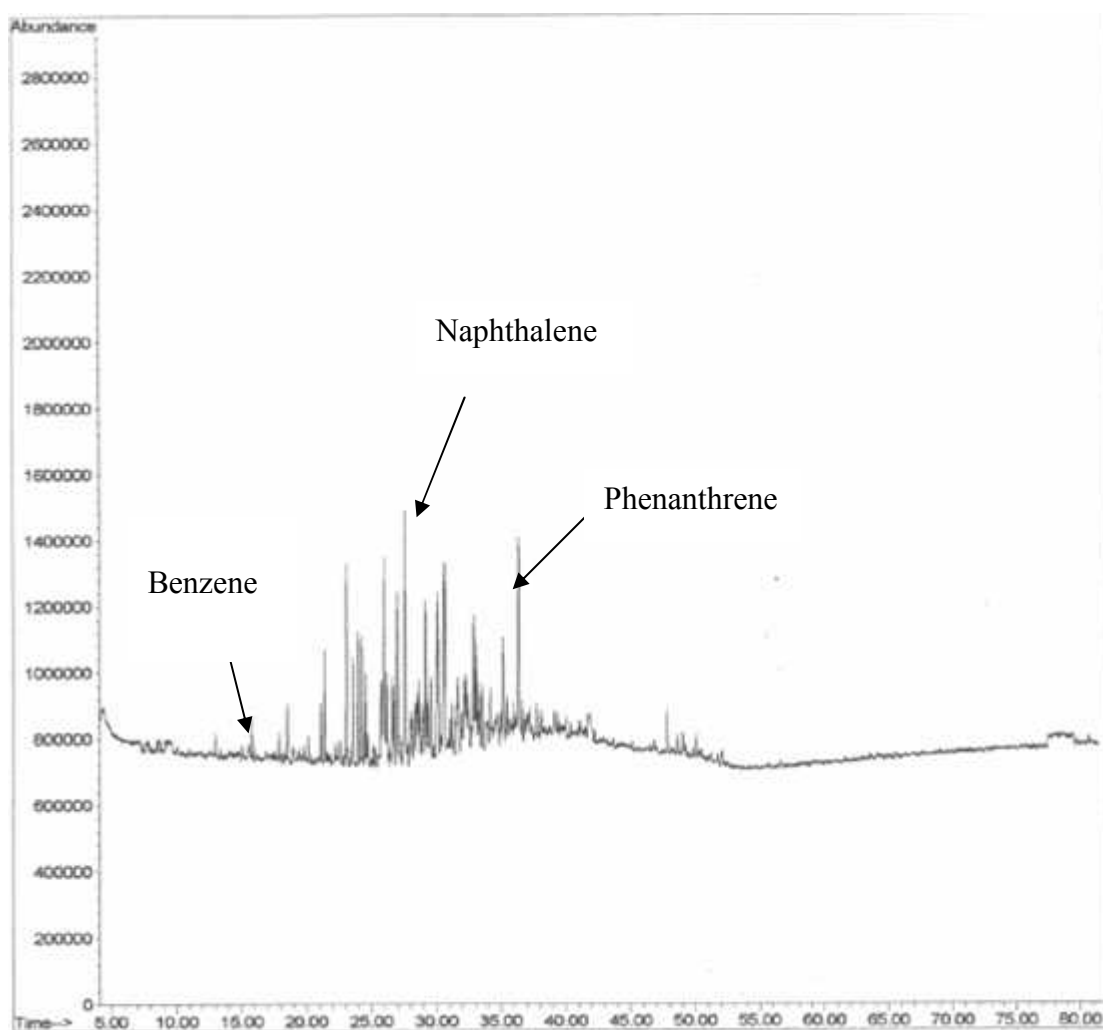


Fig 11 (a) GC-MS of Forties aromatic fraction

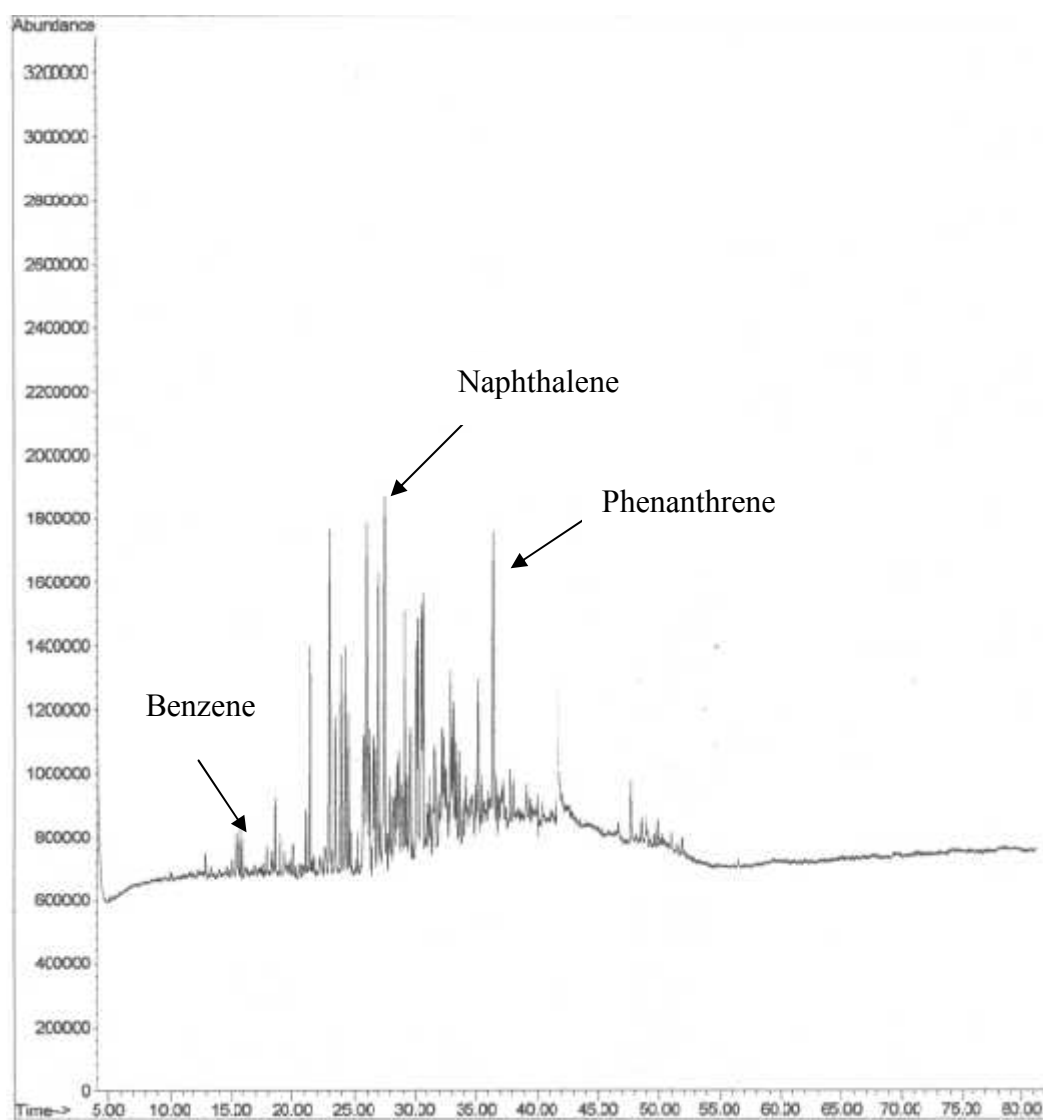


Fig 11 (b) GC-MS of Brae A aromatic fraction

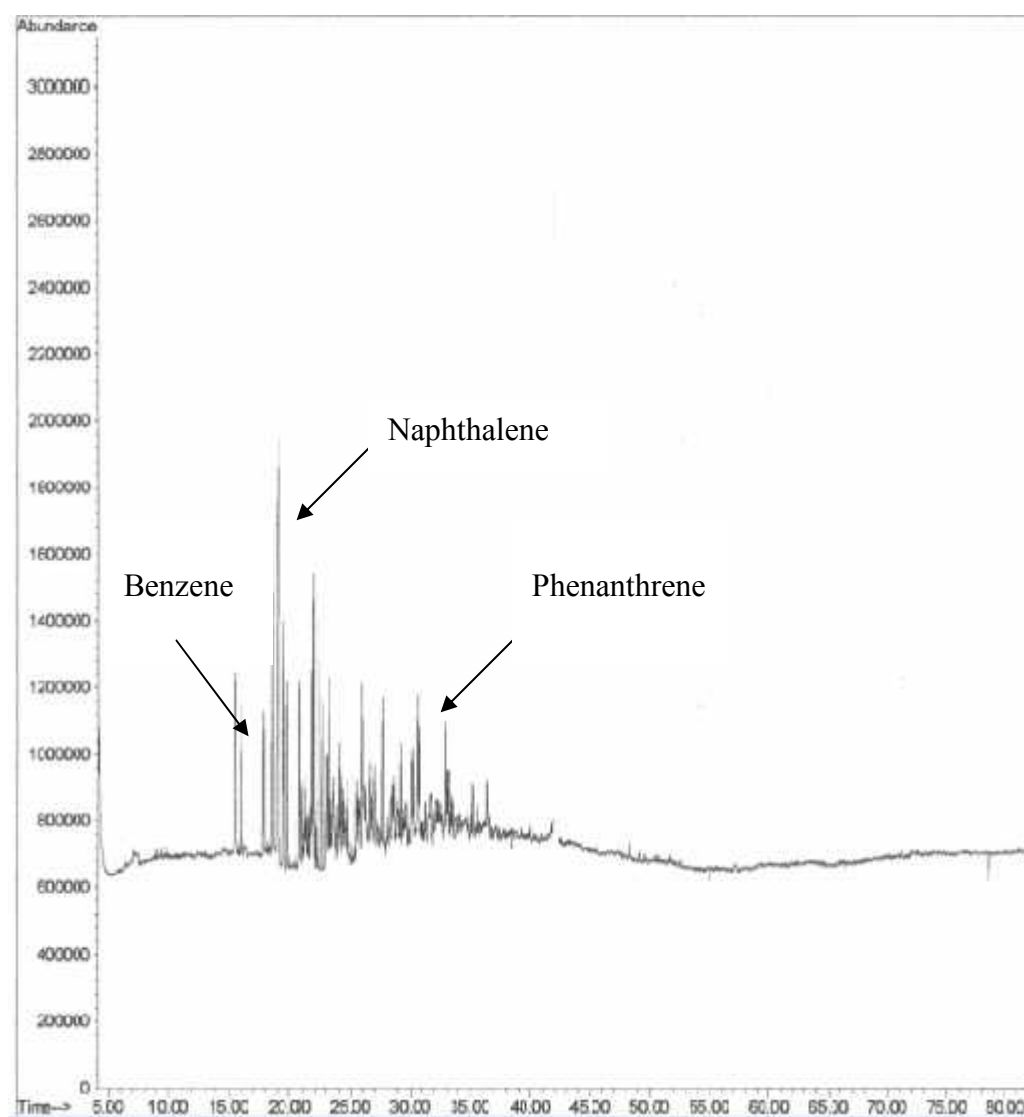


Fig 11 (c) GC-MS of Brent aromatic fraction

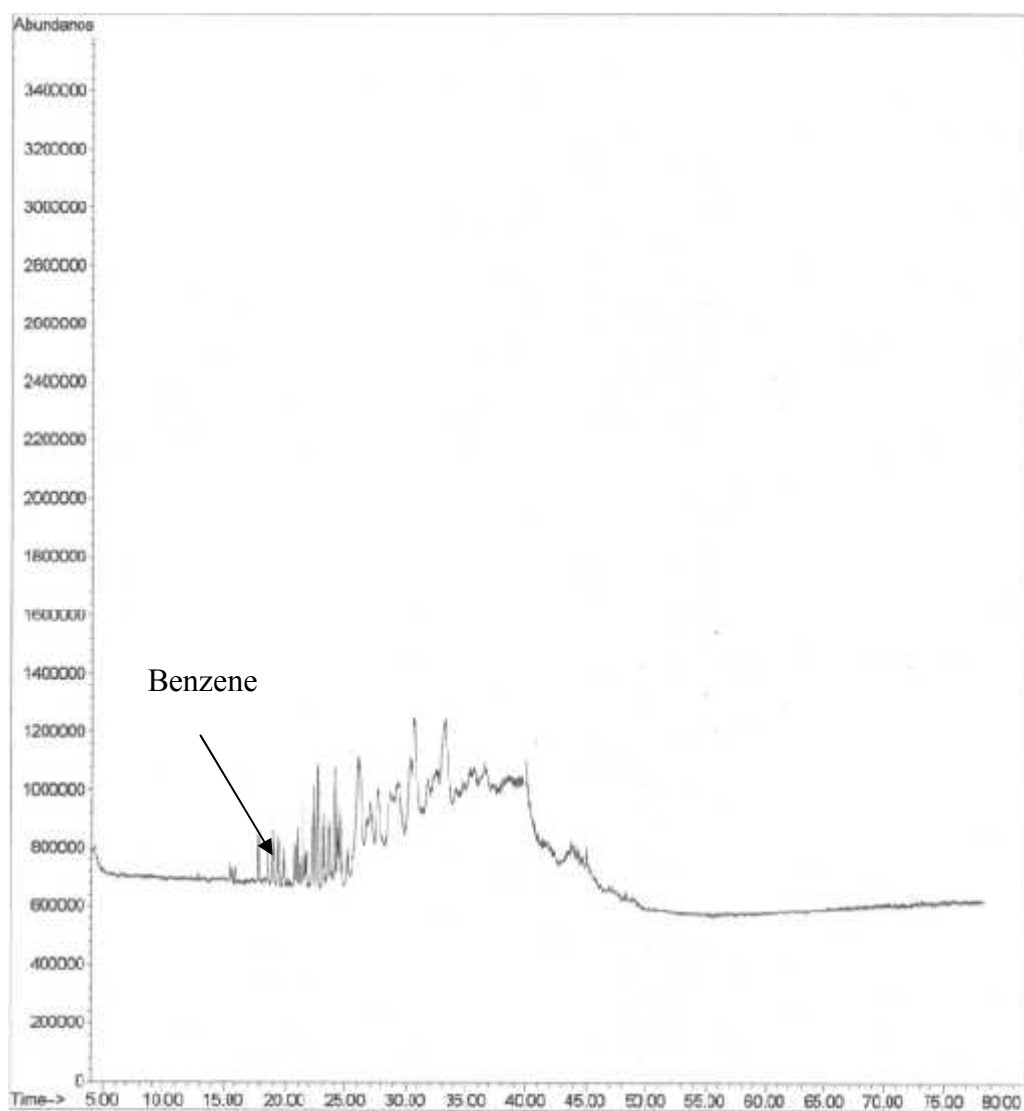


Fig 11 (d) GC-MS of Stirling aromatic fraction

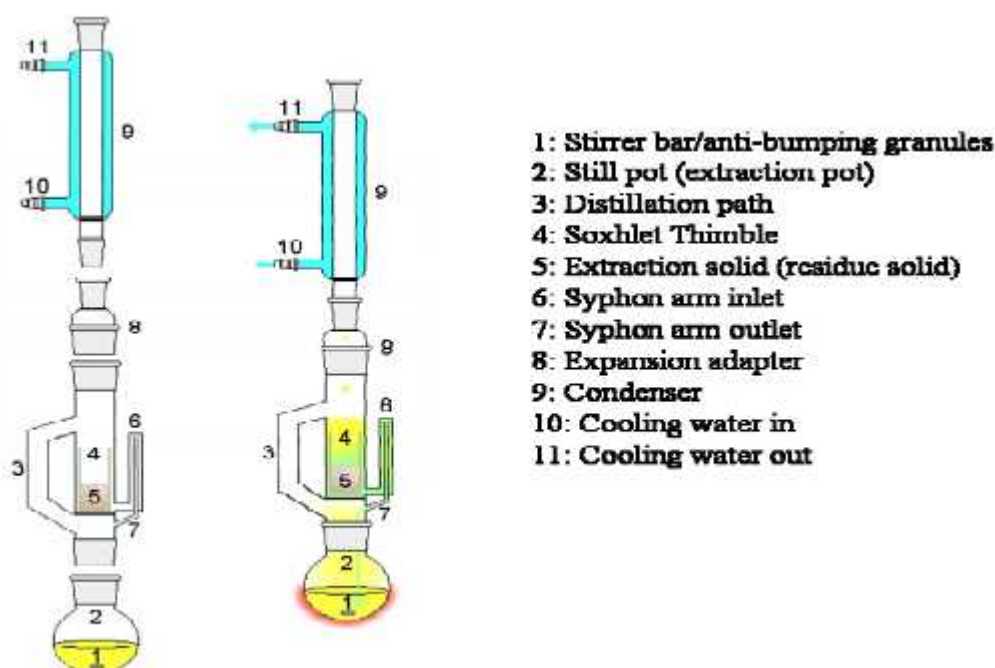


Fig. 12 A schematic representation of a Soxhlet extractor (Wikimedia Foundation, 2006), used in the separation and purification of crude oil asphaltenes

Table 4 Yield of various fractions from chromatographic fractionation (SARA analysis) of crude oils*

<i>Crude Sample</i>	<i>Aliphatic(Saturates) (mg)</i>	<i>Aromatics (mg)</i>	<i>Resins (mg)</i>	<i>Asphaltene (mg)</i>
Forties	510.79	93.39	52.29	24.58
	461.20	89.40	30.40	42.05
	426.60	81.20	34.10	31.10
Mean	466.19	87.99	38.93	32.57
SD	34.55	5.07	9.56	7.20
Brae A	524.10	116.15	34.28	27.74
	504.30	102.30	34.40	27.07
	523.40	96.60	36.10	21.00
Mean	517.26	105.01	34.92	25.27
SD	9.17	8.20	0.83	3.03
Stirling	515.93	73.79	34.35	46.76
	458.70	81.50	31.4	77.55
	489.30	71.30	28.80	55.00
Mean	487.97	75.53	31.51	59.77
SD	23.38	4.342	2.26	13.01
Brent	534.10	72.80	19.00	16.10
	537.80	72.40	21.60	13.20
	549.30	75.40	22.40	18.40
Mean	540.40	73.53	21.00	15.90
SD	6.47	1.32	1.45	2.13

*Results of three replicate fractionations are shown above.

Table 5 Summary of mean yield (mg) of crude oil fractions from 3 replicate fractionations:

Crude oil fraction	Mean yield (mg)			
	Forties	Brae A	Stirling	Brent
Aliphatic(saturates)	466.20 ± 34.551	517.26 ± 9.173	487.97 ± 23.382	540.4 ± 6.4719
Aromatics	87.99 ± 5.074	105.016 ± 8.209	75.53 ± 4.342	73.53 ± 1.3299
Resin	38.93 ± 9.566	34.926 ± 0.831	31.516 ± 2.267	21.00 ± 1.4514
Asphaltene	32.576 ± 7.208	25.27 ± 3.031	59.77 ± 13.014	15.9 ± 2.1275

Table 6 Summary of weight percentage (%) yields of fractions from SARA separation of crude oils*

Crude oil	Density (g cm ⁻³)	Aliphatics (saturates) (% wt/wt)	Aromatics (% wt/wt)	Resins (% wt/wt)	Asphaltenes (% wt/wt)	Total Polars (Asphaltenes + Resins)
Forties	0.8713	74.51±0.0345	14.06±0.050	6.22±0.0095	5.21±0.0072	11.43
Brae A	0.8576	75.79±0.0095	15.39±0.0081	5.12±0.0008	3.71±0.0030	8.83
Stirling	0.8434	74.52±0.0233	11.54±0.0043	4.81±0.0022	9.13±0.0130	13.94
Brent	0.8342	83.03±0.0064	11.30±0.0013	3.23±0.0014	2.44±0.0021	5.67

*All numbers are weight percentages of the mean values of the weighted parameters. Weights converted to grams.

Table 7 Physical appearance of crude oil fractions from chromatographic fractionation

Crude oil fraction	Visual appearance			
	Forties	Brae A	Brent	Stirling
Asphaltene	Dark brown	Dark brown	Dark brown	Brownish - black
Aliphatics	Pale yellow; gelatinous	Pale yellow; gelatinous	Pale yellow; gelatinous	Pale yellow; gelatinous
Aromatics	Brown solid	Brown solid	Brown solid	Brown solid
Resins	Dark brown crystalline solid	Dark brown crystalline solid	Dark brown crystalline solid	Dark brown crystalline solid

Determination of percentage (%) yield of each fraction in the oil

The yield of each fraction can be calculated as a percentage (%) by weight on the original sample as follows:

$$\text{Asphaltene content} = \frac{\text{weight of dried asphaltene (g)}}{\text{Crude oil volume (ml)}} \times 100$$

1g of oil = 1ml

The mean yield from three replicates results are used in calculating the percentage yield of fraction separated in the oil samples. The weights of dried asphaltenes from each of the yields are converted to grammes (g) by dividing the value by 1000.

APPENDIX D

ASPHALTENE. ANNOTATED mdp FILE FOR THE MOLECULAR DYNAMICS (MD) SIMULATION

```
;
;    ** Option for preprocessor    **
;
```

title = all atom asphaltene

```
;
;    ** Option for run control    **
;
```

integrator = md

this tells the programme to do a molecular dynamics simulation using a leapfrog Verlet algorithm to integrate the equations of motion

dt = 0.002 ; dt x nsteps = simulation time (1ns)

dt is the time step for the simulation. This means that system is “moved” to a new conformation dt ps more advanced in time than the previous. The typical time step for GROMACS is 2 fs. It has to be a very small time interval because a condition of the simulation is that the forces on each atom must not change significantly from one time step to the next. The very small time step ensures this condition is met by only allowing the atoms to move a very small distance each time step.

nsteps = 5000000; max no of steps to integrate

Total number of time steps in the simulation. The total simulation time is dt x nsteps

comm_grps = system
comm_mode = linear
nstcomm = 1

The integrators used for MD simulations do not give total conservation of the kinetic energy of the system. This is not a problem for many systems, but for ones containing surfaces or interfaces it can be problematic. It manifests itself such that the whole system or parts of acquire a systematic centre of mass motion in one direction. With time the whole system can be seen to move across the simulation box en masse. To get around this, it is usual to remove the centre of mass motion. Comm_grps sets the parts of the simulation from which COM movement is removed (here the whole system),

comm_mode is the method of removal (here only linear motion and not angular motion is removed) and *nstcomm* = 1 removes the motion after every step.

```
;
; ** Options for Neighbour Searching **
;
```

In MD simulation the interactions between atoms are summed and from this the force acting on this atom (as a vector, i.e. magnitude and direction) is calculated. The force is used to predict the distance and direction each atom moves in the time step dt by integration of Newton's equation of motion ($F = m \cdot a = m \cdot d^2r/dt^2$). Strictly since electrostatic interactions are very long-ranged (infinite) you should sum these interactions over infinite distances. This is not practical since the summing of interactions is very time consuming and is the part of a simulation that takes the longest time.

*For systems with a large number of atoms (N) the cpu time required for the simulation scales as $N(N-1)$ because of the need to sum the interaction of each atom with all $N-1$ others. To reduce the time taken for a simulation it is usual to truncate the interactions at a certain distance *rcoulomb*, above which interaction equal zero. Then a neighbour list is set up which contains only those atoms which are close enough to be able to interact with an atom i.e. for each atom a list is constructed that has all interacting neighbour atoms in it. All atoms within a cut-off distance *rlist* (nm) from an atom are deemed to be in the neighbour list for that atom. When interactions are summed, only the neighbours in the list are counted. This can reduce the time taken to count interactions by a large degree. Since the system is evolving, atoms will enter and leave the neighbour list, and so it has to be updated regularly so that the correct forces on each atom can be counted. The frequency of updating is chosen by trial and error (and a certain degree of experience). To further reduce the time needed for a simulation it is also common to use periodic boundary conditions, i.e. a finite box size is chosen, but the edges of the box are permeable, and if an atom or molecule moves across the box at one edge, it then disappears from that edge and enters the box with the same motion at the opposite edge. This is equivalent to surrounding, say, a cubic box with 6 identical images of itself at each side of the cube. In this way a small, finite sized box can be made to behave as if it were a much larger system. In this simulation the periodic boundary conditions have been turned on in all three coordinate directions.*


```

nstlist      = 5      ; nblist update frequency
ns_type      = grid   ; nb search type (simple or grid)
pbc          = xyz    ; periodic boundary condition
rlist        = 1.0    ; neighbour list cut-off in nm

```

```

;
;      ** Options for electrostatics and VDW/LJ **
;      we want the ordering rlist <= rvdw <= rcoulomb

```

Electrostatic and van der Waals interactions are problematic because they are long range. Since as mentioned above it is not practical to count all interactions at large separations we have to decide whether we are simply going to ignore these (i.e. truncate or cut them off over a certain distance) or if we are going to use more sophisticated methods to include long range interactions. Options for the later include a full Ewald summation which is an accurate way of summing interactions over very long range, or the particle mesh Ewald (PME) summation which uses approximations to estimate long range contributions to the interaction force.

The Ewald summation is extremely time consuming, and simulations including this can easily be several orders of magnitude longer than those using a cut-off. For most simulations this is not practical and leads to simulations that may take several years to run for a modest “real” time. Ewald summation is only used when accurate results are required for comparison with experiment. The particle mesh ewald summation is our method of choice and only leads to a modest increase in cpu time (typically 50-75%). PME sets a cut off value for the range of the coulombic interactions, and then makes a long range correction for interactions at a greater distance than this.

For van der Waals interactions we chose a different option to sum these called a switch function. In this use the normal form of the van der Waals force out to a certain separation (rvdw-switch) and then turn on the switch function which makes the VDW forces decay exponentially and are then turned off completely (set to zero) at separations greater than the VDW cut off distance (rvdw). For all electrostatic interactions the cut off distances rcoulomb and rvdw must be less than or equal to the neighbour list cut off rlist so that we do not try to count interactions outside of the neighbour list.

```

coulombtype      = PME
rcoulomb         = 1.0 ; electrostatic cutoff in nm
vdwtype          = switch ;cut-off
rvdw-switch      = 0.8
rvdw             = 0.9 ; vdw/lj cutoff in nm

;
;    ** Options for temp coupling **
;

```

Temperature control in the simulation is achieved by coupling the simulation box to a thermostat. A simple way of explaining this is to think of it as a water bath in which you immerse the simulation. The thermostat soaks up excess heat if the simulation has too much energy, and gives heat to the simulation if the energy of the system drops. In this simulation the V-rescale thermostat is used, which gives good conservation of kinetic energy in the simulation compared to other simple thermostats. It works by rescaling the velocities of the atoms after each time step to keep the total kinetic energy in the system constant. It is usual to couple each part of the simulation (here the asphaltene HA1 and the water, sol) separately.

The parameter tau_t is the coupling time constant and it controls how quickly the thermostat responds to perturbations in the system temperature. A large coupling constant will cause a greater response to a change in temperature, but there is danger that the system will overshoot the target temperature and then oscillate about that temperature before it returns to its set value. Too low a couple constant leads to a slow response to temperature changes. Tau_t = 0.1 has been found to give the optimum response for a wide range of systems. (There are parallels between the method used to control T in a thermostat and the type of controllers use to control T in a water batch). The target temperature is set as ref_T, here 300K.

```

Tcoupl          = V-Rescale
tc_grps         = HA1 Sol
tau_t           = 0.1 0.1
ref_t           = 300 300

;
;    ** Option for pressure coupling **
;

```

Pressure control is turned off in this simulation, but it can be achieved using a barostat, working with a similar principle to the thermostat.

```
Pcoupl      = no ;Berendsen
pcoupltype  = isotropic
tau_p       = 0.5 0.5; time constant for coupling
compressibility = 4.5e-5 4.5e-5
ref_p       = 1.0 1.0
```

```
;
;  **  Option for bonded interactions  **
;      which groups are constrain
```

The bonds present in molecules cause a particular problem to MD simulation. If two atoms are joined by a covalent bond then their motion is restricted by the bond length and rotational constraints. This means that if they are acted on by forces from surrounding atoms then how far and fast they can move is restricted by the bonds between them. Rather than including the bond constraints as extra forces holding the atoms at a fixed distance and rotation it has been found that it is much quicker to use a constraints algorithm. This algorithm treats the n=bonded and non-bonded forces as separate and then uses mathematical methods that search for solutions that satisfy both sets of forces. GROMACS typically uses a solver called LINCS which is much faster than other solvers and allows a longer time step to be used compared to other MD packages.

```
constraints      = all-bonds
constraint_algorithm = Lincs
```

References

- Aamo, O. M., Reed, M., Daling, P. S., Johansen, O. (1993). A laboratory based weathering model. PC version for coupling to transport models. In: Proceedings of the 16th AMOP Technical Seminar, Environment Canada, Ottawa, Canada, 617-626.
- Abdurrahman, H. N. and Yunus, R. M. (2009). Coalescence of Water Droplets in Water-in-Crude Oil Emulsions. *International Journal of Chemical Technology*, **1** (1), 19-25.
- Abdurrahman, H. N., and Yunus, R. M., (2006). Stability Investigation of Water-in-Crude Oil Emulsion. *Journal of Applied Sciences*, **6** (14), 2895-2900.
- Acevedo, S., Ranaudo, M.A., Escobar, G., Gutierrez, L.B., and Gutierrez, X. (1995) In: *Asphaltene Constituents: Fundamentals and Applications*, Chapter IV, E.Y. Sheu and O.C. Mullins (eds.), Plenum Press, New York.
- Akay, G. (1998). Flow-induced phase inversion in the intensive processing of concentrated emulsions. *Chemical Engineering Science*, **53**, 2, 203-223.
- Akbarzadeh, K., Hammami, A., Kharrat, A., and Zhang, D. (2007). Asphaltenes – Problematic but Rich in Potential. *Oilfield Review*, **19**, (2) 22-43.
- Al Darouich, T., F. Behar., C. Largeau., and H. Budzinski (2005). Separation and Characterization of the C₁₅ Aromatic Fraction of Safaniya Crude Oil. *Oil & Gas Science and Technology – Rev. IFP*, **60**, 4, 681-695.
- Ali, L. N., Mantoura, R. F., Rowland, S. J., (1995). The dissolution and photo-degradation of Kuwaiti crude oil in seawater. Part 2: A laboratory photo-degradation apparatus and photo-degradation kinetics of a model seawater soluble hydrocarbon (Phenanthrene). *Marine Environmental Research*, **40**, 4, 319-335.

- Ali, M. A. and Nofal, W. A. (1994). Application of high performance liquid chromatography for hydrocarbon group type analysis of crude oils. *Fuel Science Technology International*, **12**(1), 21-23.
- Andersen, S.I. (1997). Separation of Asphaltenes by polarity using liquid-liquid extraction. *Petroleum Science and Technology*, **15**, 185-198.
- Andreatta, G., Bostrom, N., and Mullins, O. C. (2005). High- Q ultrasound determination of the critical nanoaggregate concentration of asphaltene and the critical micelle concentration of standard surfactants. *Langmuir* **21**, 2728
- API (1999). Fate of spilled oil in marine waters (American Petroleum Institute). Publication Number 4691.
- Arey, J. S., Nelson, R. K., Reddy, C. M. (2007). Disentangling Oil Weathering Using GC x GC. 1. Chromatogram Analysis. *Environ. Sci. Technol.*, **41**, 5738-5746.
- Arey, J. S., Nelson, R. K., Xu, L., Reddy, C. M. (2005). Using comprehensive two-dimensional gas chromatography retention indices to estimate environmental partitioning properties for a complete set of diesel fuel hydrocarbons. *Analytical Chemistry*, **77**, 7172-7182.
- ASCE Task Force. (1996). State-of-the-art review of modeling transport and fate of oil spills. Water Resources Engineering Division. *Journal of Hydraulic Engineering*. **122**, (11), 594-609.
- Aske, N., H., Kallevik, and J. Sjoblom (2001). Determination of Saturate, Aromatic, Resin, and Asphaltenic (SARA) Components in Crude Oils by Means of Infrared and Near –Infrared Spectroscopy. *Energy Fuels*. **15**(5), 1304-1312.
- Aske, N., Kallevik, H. and Sjoblom, J. (2002). Water-in-crude oil stability studied by critical electric field measurements. Correlation to physicochemical parameters and near-infrared spectroscopy. *Journal of Petroleum Science and Engineering*, **36**, 1-17.

- ASTM 5291. *Standard Test Methods for Instrumental Determination of Carbon, Hydrogen, and Nitrogen in Petroleum Products and Lubricants.*
- ASTM D2007 (1993). *Annual Book of ASTM Standards, American Society for Testing and Materials.*
- ASTM D4124 (1991). *Annual Book of ASTM Standards, American Society for Testing and Materials.*
- ASTM D95. Standard Test Method for Water in Petroleum Products and Bituminous Materials.
- Atlas, R. M., Bartha, R. (1993). *Microbial Ecology: Fundamentals and Applications.* 3rd ed. Reading, Ma: Addison-Wesley publishing Company.
- Atlas, R.M., Boehm, P. D., and Calder, J. A. (1981). Chemical and biological weathering of oil from the *Amoco Cadiz* spillage within the littoral zone. *Estuarine Coastal Shelf Science*, **12**, 589-608.
- Atlas, Ronald M. (1995). Petroleum Biodegradation and Oil Spill Bioremediation. *Marine Pollution Bulletin*, **31**, 178-182.
- Auflem, I. H. (2002). Influence of Asphaltene Aggregation and Pressure on Crude Oil Emulsion Stability. PhD Thesis.
- B.S 733 (1987). *Methods for calibration and use of pyknometers.*
- Baker, E.W., Louda, J.W., (1986). Porphyrins in the geological record. In: R.B. Johns (Ed.), *Biological Markers in the Sedimentary Record. Elsevier*, 121-223.
- Bardon, Ch., Barre, L., Espinat, D., Guille, V., Li, M. H., Lambard, J., Ravey, J. C., Rosenberg, E., and Zemb, T., (1996). *Fuel Science Technology International*. **14** (1 & 2), 203-242
- Barre, L., Espinat, D., Rosenberg, E., and Scarsella, M., (1997). *Rev. Inst. Fr. Petrole*, **52** (2). 161- 175.

- Bastow, T. P., Ben, G. K., van Aarssen, G. K., Dale, L. (2007). Rapid small-scale separation of saturate, aromatic and polar components in petroleum. *Organic Geochemistry*. **38**, 1235-1250.
- Bastow, T. P., van Larsson, B. G. K., Herman, R., Alexander, R., and Kagi., R. I. (2003). The effect of oxidation on the distribution of alkylphenols in crude oils. *Organic Chemistry*. **34**, 1103-1111.
- BBC news World edition, (2002). Brazil oil rig straightened. Available on <http://news.bbc.co.uk/1/hi/world/americas/2331817.stm>
- Becher, P. (1983). *Encyclopedia of Emulsion Technology*, (ed.), **1**, Marcel Dekker Inc, New York.
- Behar, F., Saint-Paul, C. and Leblond, C. (1989) Analyse quantitative des effluents de pyrolyse en milieu ouvert et fermé. *Rev. Inst. fr. Pét.*, **44**, 3, 387-411.
- Bertilsson, S. and Widenfalk, A. (2002). Photochemical degradation of PAHs in freshwaters and their impact on bacterial growth – influence of water chemistry. *Hydrobiologia*, **469**, 23-32.
- Berweger, C. D., van Gunsteren, W. F. and Muller-Plathe, F. (1995). Force Field Parametrisation by Weak Coupling: Re-engineering SPC water. *Chem. Phys. Lett.*, **232**, 429-436.
- Bibette, J., Leal-Calderon, F., Schmitt, V. and Poulin, P. (2002). Introduction, In: *Emulsion Science - Basic Principles*. Springer.
- Bidleman, T. F. (1984). Estimation of vapor pressure for nonpolar organic compounds by capillary gas chromatography. *Analytical Chemistry*, **56**, 2490-2496.
- Boduszynski, M. M., J. F. McKay and D. R. Latham (1980). Asphaltenes, Where Are You? *Proceedings of the Association of Asphalt Paving Technologists*, **49**, 123-143.

- Boehm, P. D., and Fiest, D. L. (1982). Subsurface distributions of petroleum from an offshore well blowout. The Ixtoc 1 Blowout, Bay of Campeche. *Environmental Science Technology*, **16**, 67-74.
- Bragg, J. R., Prince, R. C., Harner, E. J., and Atlas, R. M. (1994). Effectiveness of bioremediation for the *Exxon Valdez* oil spill. *Nature*, **368**, 413-418.
- Brandvik, P. J., and Liv-Guri Faksness (2009). Weathering processes in Arctic oil spills: Meso-scale experiments with different ice conditions. *Cold Regions Science and Technology*, **55**, 160-166.
- Bridie, A. L., Th.H. Wanders, W. Zegveld and H. B. Van der Heijde. (1980b). Formation and Prevention and Breaking of Sea Water in Crude Oil Emulsions: Chocolate Mousses Marine Pollution Bulletin, **2**, 343-348.
- Bridie, A. L., Wanders, Th. H., Zegveld, W., and Van der Heijde, H. B. (1980a). The formation and Breaking of Sea Water-in Crude-Oil Emulsions: Chocolate Mousse. International Research Symposium, Chemical Dispersion of Oil Spills. Nov. 17-19. Toronto, Canada.
- Buenrostro-Gonzalez, E., Groenzin, H. H., Lira- Galeana, C., and Mullins, O. C. (2001). The Overriding Chemical Principles that Define Asphaltenes. *Energy Fuels*. **15**(4), 972-978.
- Burns, G. H., Benson, C. A., Kelly, S., Eason, T., Benggio, B., Michel, J., and Ploen, M. (1995). Recovery of Submerged Oil at San Juan, Puerto Rico 1994. Proceedings of the 1995 International Oil Spill Conference. American Petroleum Institute, Washington DC, 551-557.
- Burns, W. A., Mankiewicz, P. J., Bence, A. E., Page, D. S., and Parker, K. R. (1997). *Environmental Toxicology Chemistry*, **16**, 1119-1131.
- Bussi, G., Donadio, D., and Parrinello, M. (2007). Canonical sampling through velocity-rescaling. *J. Chem. Phys.* **126**, 014101.

- Butler, E. L., Douglas, G. S., and Steinhauer, W. G. (2001). On-Site Bioreclamation, *Microbial Ecology*, **42**, 4, 515-521.
- Casper, J., Meyer, T. J. (1983). Application of the energy gap law to non-radiative, excited state decay. *Journal of Physical Chemistry*, **87**, 952- 957.
- Chao, X. B., Shankar, N. J., and Cheong, H. F. (2001). Two-and three-dimensional oil spill model for coastal waters. *Ocean Engineering*, **28**, 1557-1573.
- Charter, R. (2002). Prepared Statement. Field Hearing of the subcommittee on Energy House Committee on Science. The Renewable Roadmap to Energy Independence. Sonoma State University, Rohnert Park, California. Democratic caucus Committee on Science. 107th Congress. Available on: http://www.house.gov/science_democrats/subcoms/woolsey/
- Chen, Gonglun and Daniel, Tao. (2005). An experimental study of stability of oil-water emulsion. *Fuel Processing Technology*, **86**, 5, 499-508.
- Christensen, J. H. (2002). Application of multivariate data analysis for assessing the early fate of petrogenic compounds in the marine environment following the Baltic Carrier oil spill. *Polycyclic Aromatic Compounds*, **22**, 703-714, 2002.
- Christensen, J. H., Hansen, A. B., Tomasi, G., Mortensen, J., and Andersen, O. (2004). Integrated methodology for forensic oil spill identification. *Environmental Science Technology*, **38**(10), 2912 –2918.
- Christensen, Jan H. (2005). Chemometrics as a tool to analyze complex chemical mixtures Environmental forensics and fate of oil spills. PhD Thesis.
- Cimino, R., Correria, S., Del Bianco, A. and Lockhart, T. P. (1995) In: *Asphaltene constituents: Fundamentals and Applications*, Chapter 111, E. Y. Sheu and O. C. Mullins (eds.), Plenum Press, New York.

- Clayton, G. Sumner (1954). The theory of Emulsions and their Technical Treatment, 5th ed., London.
- Clint, J. H., Fletcher, P. D. I., and Todorov, I. T., (1999). Evaporation rates of water from water-in-oil microemulsions. *Physical Chemistry*, **1**, 5005-5009.
- Cormack, Douglas (1999). Response to Marine Oil Pollution – Review and Assessment. Kluwer Academic Publishers.
- Creek, J. L. (2005). Freedom of action in the state of asphaltenes: Escape from conventional wisdom. *Energy Fuels* **19** (4), 1212-1224.
- Crick, F. (1988). *What mad pursuit, a personal View of Scientific Discovery*, Basic Books, New York.
- Daling, P. S. and Brandvik, P. J. (1991). Characterisation and prediction of the weathering properties of oil at sea – a manual for the oil investigated in the DIWO project. Continental Shelf and Petroleum Technology Research Institute. IKU SINTEF GROUP. HWU library reference: 628: 168 DIW.
- Daling, P. S. and Strøm-Kristiansen, T. (1999). Weathering of Oils at Sea: Model/Field Data Comparison. *Spill Science & Technology Bulletin*, **5**, (1), 63-74.
- Daling, P. S., Aamo, O. M., Lewis, A., and Strom-Kristiansen, T. (1997). IKU Weathering Oil Model- predicting oil's properties at sea. In: *Proceedings of the 1997 International Oil Spill Conference*, Fort Lauderdale, Florida, 2-10 April, 297-307.
- Daling, P. S., and Brandvik, P. J. (1988). A study of the formation and stability of water-in-oil emulsions. In: Proc. 11th AMOP Technical Seminar, Vancouver, BC, Canada. 488 - 499.
- Daling, P. S., Brandvik, P. J., Mackay, D., Johansen, O. (1990). Characterization of crude oils for environmental purposes. *Oil and Chemical Pollution*, **7**, 199-224.

- Daling, P. S., Faksness, L. G., Hansen, A. B., and Stout, S. A. (2002). Improved and standardized methodology for oil spill fingerprinting, *Environmental Forensics*, **3**, 263-278.
- Daling, P. S., Moldestad, M. O., Johansen, O., Lewis, A., and Rodal, J. (2003). Norwegian Testing of Emulsion Properties at Sea – The Importance of Oil Type and Release Conditions. *Spill Science & Technology Bulletin*, **8**, (2), 123-136.
- Daling, P. S., Moldestad, M. O., Johansen, O., Lewis, A., Rodal, J. (2003). Norwegian Testing of Emulsion Properties at Sea – The Importance of Oil Type and Release Conditions. *Spill Science & Technology Bulletin*, **8**, 123-136.
- Darden, T., York, D., and Pedersen, L. (1993) Particle Mesh Ewald-an N.Log(N) method for Ewald sums in large systems. *J Chem Phys* **98**, 10089-10092
- Davies, J. M. and Topping, G. (1997). The impact of an oil spill in turbulent waters: The Braer. Proceedings of a symposium held at the Royal Society of Edinburgh, 7-8 September, 1995. Stationery Office, Edinburgh, UK.
- Davies, J .T. (1957). A quantitative kinetic theory of emulsion type. 1. Physical chemistry of the emulsifying agent. Gas/Liquid and Liquid/Liquid Interfaces. Proceedings of 2nd International Congress Surface Activity. Butterworths, London.
- Davies, L. (2001). Weathering and dispersibility of Azeri crude oil. A report produced for Dames & Moore Group. National Chemical Emergency Centre. AEA Technology Oxfordshire. Report no. AEAT/R/ENV/0739/A Issue 1.
- De Groot, S. J. D. (1996). Quantitative assessment of the development of the offshore oil and gas industry in the North Sea. *ICES Journal of Marine Science*, **53**, 1045-1050.
- Dickie, J. P. and Yen, T. F. (1967). Macrostructures of the Asphaltic Fractions by Various instrumental Methods. *Analytical Chemistry*, **39**, 14, 1847–1852.

- Dicharry, C., Arla, D., Sinquin, A., Graciaa, A., Bouriat, P. (2006). Stability of water/crude oil emulsions based in interfacial dilational rheology. *J. Colloid Interf. Sci.* **297**, 785.
- Doerffer, J. W. (1992). Oil spill response in the marine environment. Technical University of Gdansk, Poland. Pergamon Press Limited, Oxford, England.
- Douglas, G. S., Bence, A. E., Prince, R. C., McMillen, S. J., and Butler, E. L. (1996). Environmental stability of selected petroleum hydrocarbon source and weathering ratios. *Environmental Science Technology*, **30**, 2332-2339.
- Douglas, G. S., Owens, E. H., Hardenstine, J., and Prince, R. C. (2002). The OSSA 11 pipeline oil spill: the character and weathering of the spilled oil. *Spill Science & Technology Bulletin*, **7**, 135-148.
- Durell, G. S., Ostazeski, S. A., Uhler, A. D., and Nordvik, A. B. (1993). Transfer of crude oil weathering technology. Technical Report No. 93-027; Marine Spill Response Corporation, Washington, D.C.
- Dutta, T. K. and Harayama, S. (2000). Fate of crude oil by the combination of photo-oxidation and biodegradation. *Environmental Science & Technology*, **34**, 1500-1505.
- Dutta, T. K. and Harayama, S. (2001). Analysis of long side chain alkylaromatics in crude oil for evaluation of their fate in the environment. *Environmental Science & Technology*, **35**, 102-107.
- E&P Forum/ UNEP Technical Publication (1997). Environmental Management in oil & gas exploration and Production: An overview of issues and management approaches. UNEP IE/PAC Technical Report 37.
- Edwards, R., and White, I. (1999). Proceedings of the International oil spill conference. 7-12 March, 1999. Seattle, USA, 97-102, American Petroleum Institute, Washington DC, USA.

- Ehrhardt, M. and Douabul, A. (1989). Dissolved petroleum residues and alkylbenzene photo-oxidation products in the upper Arabian Gulf. *Marine Chemistry*, **26**, 363-370.
- Ehrhardt, M. G., and Burns, K. A. (1990). Petroleum-derived dissolved organic compounds concentrated from inshore waters in Bermuda. *Journal Experimental Marine Biology Ecology*, **138**, 35-47.
- Ehrhardt, M. G., Burns, K. A., and Bicego, M. C. (1992). Sunlight-induced compositional alterations in the seawater-soluble fraction of a crude oil. *Marine Chemistry*, **37**, 53-64.
- Elsharkawy, A. M., Alsahhal, T. A., Fahim, M. A., and Harvey W. Yarranton (2008). Characterization of Asphaltenes and Resins Separated from Water-in-Crude Oil Emulsions. *Petroleum Science and Technology*, **26**, (2) 153-169.
- Espinat, D. (1993). In: *SPE International Symposium on Oilfield Chemistry*, New Orleans, LA, USA, March 2-5, SPE 25187.
- Essmann, U., Perera, L., Berkowitz, M.L., Darden, T., Lee, H. and Pedersen, L.G. (1995). A smooth particle mesh Ewald method, *J. Chem. Phys.* **103**, 8577-8593
- Etkin, D. S. (2001). Analysis of Oil Spill Trends in the United States and Worldwide. International Oil Spill Conference. 1291-1300.
- Evdokimov, I. N., Nikolay Yu Eliseev., and Bulat R. Akhmetov (2006). Asphaltene dispersions in dilute oil solutions. *Fuel*, **85**, 1465-1572.
- Evers, K.-U., Jensen, H.V., Resby, J. M., Ramstad, S., Singsaas, I., Dieckmann, G. and Gerdes, B. (2004): State-of-the-Art Report on Oil Weathering and on Effectiveness of Response Alternatives, Report of ARCOP Work package 4 Environmental Protection and Management System for the Arctic, GROWTH Project GRD2-2000-30112 "ARCOP".
- Exxonmobil (2010). The Outlook for Energy: A view to 2030.

- Ezra, S., Feinsten, S., Pelly, I., Bauman, D., Miloslavsky, I. (2000). Weathering of fuel oil spill on the Mediterranean coast, Ashdod, Israel. *Organic Geochemistry*, **31** (12), 1733-1741.
- Fan, T. G. and Buckley, J. S. (2002). Rapid and accurate SARA analysis of medium gravity crude oils. *Energy Fuels*, **16**(6), 1571-1575.
- Fernandez-Varela, R., Suarez-Rodriguez, D., Gomez-Carrecedo, M. P., Andrade, J. M., Fernandez, E., Muniategui, S., Prada, D. (2005). Screening the origin and weathering of oil slicks by attenuated total mid- IR spectrometry. *Talanta*, **68**, 116-125.
- Fingas, M. (1994). Studies on the evaporation of oil spills. 17th Environment Canada Arctic and Marine oil spill program (AMOP) technical seminar. Vancouver, Canada. June 8-10, **1**, 189.
- Fingas, M. (2007). Estimation of oil spill behaviour parameters from readily-available oil properties. In Proceedings of the Thirtieth Arctic Marine Oil Spill Program, Technical Seminar. 1-34.
- Fingas, M. (2010b). Oil Spill Science and Technology: Prevention, Response and Clean Up. Gulf Professional Publishing.
- Fingas, M. and Fieldhouse, B. (2004). Formation of Water-in-oil emulsions and application to oil spill modeling. *Journal of Hazardous Materials*, **107**, 37-50.
- Fingas, M. and Fieldhouse, B. (2009). Studies on crude oil and petroleum product emulsions: Water resolution and rheology. *Colloids and Surfaces A: Physicochem Engineering Aspects*, **333** (67-81).
- Fingas, M. F. (1995a). A literature review of the physics and predictive modeling of oil spill evaporation. *Journal of Hazardous Materials*, **42**, 157-175.
- Fingas, M. F. (1997). Studies on the evaporation of crude oil and petroleum products: 1. The relationship between evaporation rate and time. *Journal of hazardous materials*, **56**, 227-236.

- Fingas, M. F. (2004). Modeling evaporation using models that are not boundary-layer regulated. *Journal of Hazardous Materials*, **107**, 27-36.
- Fingas, M. F. and Fieldhouse, B. (2003). Studies of the formation of water-in-oil emulsions. *Marine Pollution Bulletin*, **47**, 369-396.
- Fingas, M., and Fieldhouse, B. (2006). A review of knowledge on water-in-oil emulsions. In Proceedings of the Twenty-ninth Arctic and Marine Oilspill Program Technical Seminar, June 6-8, 1-56.
- Fingas, M. F. (2010). Review of the North Slope Oil properties relevant to environmental assessment and prediction. Spill Science, Edmonton, Alberta, Canada.
- Fordedal, H., Scildberg, Y., Sjoblom, J., and Volle, J. L. (1996). Crude oils in high electric fields as studied by dielectric spectroscopy. Influence of interaction between commercial and indigenous surfactants. *Colloids and Surfaces A: physicochemical and Engineering Aspects*. **106**, 33-47.
- Frysiner, G. S. and Gaines, R. B. (2002). Separation and identification of petroleum biomarkers by comprehensive two dimensional gas chromatography. *Journal of Separation Science*, **24**, 87-96.
- Garrett, R. M., Pickering, I. J., Haith, C. E., and Prince, R. C. (1998). Photooxidation of crude oils. *Environmental Science & Technology*, **32**, 3719-3723.
- Glaser, J. A., Venosa, A. D.; Opatken, E. J. (1991). Development and Evaluation of Application Techniques for Delivery of Nutrients to Contaminated Shoreline in Prince William Sound. International Oil Spill Conference; 1991 March 4-7; San Diego, California: U.S. Coast Guard, American Petroleum Institute, and U.S. Environmental Protection Agency: 1991: 559-562.
- Goodwin, J. W. (1987). The rheology of colloidal dispersions. In *Solid/Liquid Dispersions*, ed. Th. Tadros, Chap. 10. Academic Press, London, U.K

- Gomha, F. M. (2004). Compositional changes in crude oil as a consequence of evaporative losses. PhD Dissertation. University of Tulsa, USA.
- Goncalves, S., Castillo, J., Fernandez, A., and Hung, J. (2004). Absorbance and Fluorescence Spectroscopy on the aggregation behaviour of asphaltene-toluene solutions. *Fuels*, **83**(13), 1823-1828.
- Gough, M.A., Rhead, M. M., and Rowland, S. J. (1992). Biodegradation studies of unresolved complex mixtures of hydrocarbons: Model UCM hydrocarbons and the aliphatic UCM. *Organic Geochemistry*, **18**, 17-22.
- Gray, M. R. (2003). Consistency of Asphaltene Chemical Structures with Pyrolysis and Cooking Behavior. *Energy & Fuels*, **17**, (6), 1566-1569.
- Griffin, W. C. (1950). Emulsions, Encyclopedia of Chemical Technology, ed., Kirka and Othmer. **5**, 692. New York
- Griffin, W. C (1954). Calculation of HLB Values of Non-Ionic Surfactants. *Journal of the Society of Cosmetic Chemists* **5**, 259.
- Griffin, W. C (1956). Official Digest (Fed. Paint Vanish Production Clubs)
- Groenzin, H., Mullins, O.C., (2001). Molecular size and structure of asphaltenes. *Petroleum Science and Technology*, **19** (1&2), 219-230.
- Groenzin, H. and Mullins, O. C. (2000). Molecular Size and Structure of Asphaltenes from Various Sources. *Energy and Fuels*. **14**(3), 677-684.
- Groenzin, H., Mullins, O. C., Eser, S., Mathews, J., Yang, M. G., Jones, D. (2003). Asphaltene molecular size for solubility subfractions obtained by fluorescence depolarization. *Energy Fuel* **17**, 498.

- Gu, G., Xu, Z., Nandakumar, K., Masliyah, J. H. (2002). Influence of water-soluble and water-insoluble natural surface active components on the stability of water-in-toluene –diluted bitumen emulsion. *Fuel*, **81**, 1859.
- Gutman, I. and Ruiz-Morales, Y. (2007). Note on the Y-rule. *Polycyclic Aromatic Compounds*, **27** (1), 41.
- Hagen, A. P., Johnson, M. P., Randolph, B. B. (1989). 13-C NMR Studies on Roadway Asphalts. *Fuel Science Technology International*, **7** (9), 1289-1326.
- Hamid, S. H. (2000). Development of High-Performance Heavy Oil Hydrocracking Catalysts: Characterization of Atmospheric Residue Feed. *Petroleum Science and Technology*, **18** (7& 8), 871-888.
- Hammami, A., Ferworn, K. A., Nighswander, J. A., Overa, S., Stange, E. (1998). Asphaltenic crude oil characterization: An experimental investigation of the effect of resins on the stability of asphaltenes. *Fuel Science Technology International*, **16**(3,4), 227-249.
- Hammami, A., Phelps, C. H., Monger-McClure, T. and Little, T. M. (2000). Asphaltene Precipitation from Live Oils: An experimental Investigation of Onset and Reversibility. *Energy Fuels* **14**(1), 14-18.
- Hasan, M., Siddiqui, M. N., and Arab, M. (1988). Chromatographic Separation and Characterization of Asphaltene Subfractions from Saudi Arabian Crudes, *Fuel*, **67**, (9), 1307-1309.
- Helgeson, H., Knox, A., Owens, C., and Shock, E. (1993) Petroleum, oil field waters, and authigenic mineral assemblages: Are they metastable equilibrium in hydrocarbon reservoirs? *Geochimica et Cosmochimica Acta*, **57**, 3295-3339.
- Hemmingston, P. V., A. Silset, A. Hannisdal, J. Sjöblom, Emulsions of heavy crude oils. I. (2005). Influence of viscosity, temperature and dilution. *Journal of Dispersion Science Technology*, **26**, 615.

- Henderson, S. (1999). An Investigation into the Effect on Total Toxicity Predictions of Interactions between Components of a Typical North Sea Produced Water. A PhD Thesis submitted to the Heriot-Watt University, Edinburgh.
- Hess, B., Kutzner, C., van der Spoel, D. and E. Lindahl, E. (2008). GROMACS 4: Algorithms for Highly Efficient, Load-Balanced, and Scalable Molecular Simulation. *J. Chem. Theory Comput.*, **4**, 435–447.
- Hestenes, M. R. and Stiefel, E. E (1952). Methods of conjugate gradients for solving linear systems. *J. Research Natl. Bur. Standards* , **49**, 409–436.
- Hokstad, J. N., Daling, P. S., Lewis, A., Strom-Kristiansen, T. (1993) Methodology for testing water-in-oil emulsions and demulsifiers. Description of laboratory procedures. In: Proceedings Workshop on the Formation and Breaking of W/O Emulsions. MSRC, Alberta, June 14-15, 24p.
- Hortal, A. R., Hurtado, P. M., Martinez-Haya, B., and Mullins, O. C. (2007). Molecular weight distributions coal and petroleum asphaltenes from laser desorption ionization experiments. *Energy Fuels*, **21**, 2863-2868.
- Hunt, J. M. (1979). Petroleum Geochemistry and Geology, Ch.3, Freeman, San Francisco.
- Hurford, N. (1989). The Behaviour of Flotta and Forties Crude Oils: Results of Small-Scale Sea Trials. Warren Spring Laboratory Report LR 699 (MPBM).
- Ignasiak, T., O.P. Strausz and D.S. Montgomery (1977). Oxygen Distribution and Hydrogen Bonding in Athabasca Asphaltene. *Fuel*, **56**, 359-365.
- IP 143/90 (1985). Asphaltene (Heptane Insolubles) in Petroleum Products. *Standards for Petroleum and Its Products*; Institute of Petroleum: London, 143, 1.
- Irvine, G. V., Mann, D. H., and Short, J. W. (1999). Multi-year persistence of oil mousse on high energy beaches distant from *Exxon Valdez* oil source. *Marine Pollution Bulletin*, **38**. 572-584.

- ITOPF (1987). Response to Marine Oil spills. The International Tanker Owners Pollution Federation, London.
- ITOPF (2004). Oil spill statistics. Available on: <http://www.itopf.org/stats.html>.
- Jenkins, R.H., Grigson, S, J, W., McDougall, J. (1991). The formation of emulsions at marine oil spills and the implications for response strategies. Proceedings of the First International Conference on Health, Safety and Environment in the Oil and Gas Exploration and Production, 11-14 November, The Hague, Netherlands, 437-443.
- Jennings, P. W.; Desando, M. A.; Raub, M. F.; Moats, R.; Mendez, T. M.; Stewart, F. F.; Hoberg, J. O.; Pribanic, J. A. S.; Smith, J. A. (1992). NMR Spectroscopy in the Characterization of Eight Selected Asphalts. *Fuel Science Technology International*, **10**, (4-6), 887-907.
- Jiang, C., Li, M., Duin, A.C.T., (2000). Inadequate separation of saturate and monoaromatic hydrocarbons in crude oils and rock extracts by alumina column chromatography. *Organic Geochemistry*, **31**, 751-756.
- Johansen, O. (1991). Numerical modeling of physical properties of weathered North Sea Crude oils. DIWO Report No. 15, IKU-report 02.0786.00/15/91.
- Jones, T. P., Neustadter, E. L., Whittingham, K. P. (1978). Water-in-oil crude oil emulsion stability and emulsion destabilization by Chemical Demulsifiers. *Journal of Canadian Petroleum Technology*, **17**, 2, 100-108.
- Jordan, R. E. and Payne, J. R. (1980). Fate and Weathering of Petroleum Spills in the Marine Environment: A Literature Review and Synopsis. Ann Arbor Science Publishers, Ann Arbor, MI.
- Kaplan, I. R., Galperin, Y., Lu, S., and Lee, R. (1997). Differentiation of fuel-types, their sources and release time. *Forensic Environmental Geochemistry*. **27**, 5-6, 289-299, 301-317.
- Kemp, William (1991). Organic Spectroscopy. Third Edition. Macmillan Press, London, UK.

- Khadim, M. A., and Sarbar, M. A. (1999). Role of asphaltene and resin in oil field emulsions. *Journal of Petroleum Science and Engineering*, **23**, 213-221.
- Kilpatrick, P. K., Spiecker, P. M. (2001). In: Encyclopedic Handbook of Emulsion Technology. Sjoblom, J. (Ed.). New York. Marcel Dekker, **30**: 707.
- Kircher, C.C. (1989). Separations and Characterisations of Fractions from Mayan, Heavy Arabian, and Hondo Crude Oils. *Prepr. American Chemical. Society, Division Petroleum. Chemistry*, **34** (2), 416-420.
- Klein, A.E., Pilpel, N., (1974). The Effects of Artificial Sunlight Upon Floating Oils. *Water Resources*, **8**, 79, and Photo-oxidisation of alkylbenzenes indicated by 1. Naphthol, J., *Chem. Society, Faraday Trans.*, **1**, **70**, 1250
- Kloff, S., and Wick, C. (2004). Environmental management of offshore oil development and maritime oil transport. Commission on Environment, Economic and Social Policy.
- Kokal, S. (2002). Crude oil emulsions: A state-of-the-art review. Paper SPE 77497 presented at the SPE Annual Technical Conference and Exhibition, San Antonio, TX, USA.
- Krieger, I. M. (1972). Rheology of monodispersed lattices. *Adv. Colloid Interface Sci.* **3**, 111-136.
- Laane, R. W. P. M., Southward, A. J., Slinn, D. J., Allen, J., Groeneveld, G., and de Vries, A. (1996). Changes and causes of variability in salinity and dissolved inorganic phosphate in the Irish Sea, English Channel, and Dutch coastal zone. *ICES Journal of Marine Science*, **53**, 933-944.
- Lakowicz, J. R. (2010). Principles of fluorescence spectroscopy. 4th Edition. Springer Science. NY, US.

- Larson, R. A., Hunt, L. L., and Blakenship, D. W. (1977). Formation of toxic products from #2 fuel oil by photooxidation. *Environmental Science Technology*, **11**, 492-496.
- Law, R. J. and Kelly, C. (2004). The impact of the Sea Empress oil spill. *Aquatic Living Resources*. **17**, 389-394.
- Leahy, J.G., and Colwell RR (1990). Microbial degradation of hydrocarbons in the environment. *Microbial Rev.*, 54: 300-315.
- Lee, R. F. (1999). Agents which Promote and Stabilize Water-in-oil Emulsions. *Spill Science & Technology Bulletin*. Elsevier Science Ltd. **5** (2), 117-126.
- Lee, R. F. (2003). Photo-oxidation and Photo-toxicity of Crude and Refined Oils. *Spill Science & Technology Bulletin*, **8**, (2), 157-162.
- Leonataritis, K. J., (1997). SPE International Symposium on Oilfield Chemistry, Houston, Texas., 18-21 February, 421 – 440.
- Lewis, A., Daling, P., Strom-Kristiansen, T., Brandvik, P. J. (1995a). The behavior of Sture blend crude oil spilled at sea and treated with dispersants: 18th AMOP Technical Seminar. June 14-15, Edmonton, Canada. 453-469.
- Lewis, A., Strom-Kristiansen, T., Brandvik, P. J., Daling, P. S., Jensen, H., Durrell, G., (1995b). Dispersant Trials- NOFO Exercise, June 6th-9th. Main Report. IKU Report No.22.2050.00/14/95.
- Li, S., Liu, C., Que, G., Liang, W. and Zhu, Y. (1997). A Study of the Interactions Responsible for Colloidal Structures on Petroleum Residua. *Fuel*, **76**, 1459.
- Lira-Galeana, C. and Hammami, A. (2000). In: T.F. Yen and G. Chillingarian (eds.), *Asphaltenes and Asphalts*. Elsevier Science Publishers, Amsterdam. Chapter, 21.

- Lundanes, E., Greibokk, T., (1994). Separation of fuels, heavy fractions, and crude oils into compound classes: a review. *Journal of High Resolution Chromatography*, **17**, 197-202.
- Ma, Q., Xia, L. and Zhigang, Y. (2007). Changes in the chemical components of light crude oil during simulated short term weathering. *Journal of Ocean University of China*, **6**, (3) 231-236.
- Mackay, D. (1987). Formation and stability of water in oil emulsions. Environment Canada Manuscript Report EE-93, Ottawa, Ontario, 97-99.
- Mackay, D., Buist, I., Mascarenhas, R. and Paterson, S. (1980). Oil Spill Processes and Models. (Environmental Protection Service, Environment Canada).
- Malmquist, L. (2006). Chemometric Analysis of In Vitro Weathering of a Heavy fuel oil. M.Sc. Thesis. Roskilde University and National Environmental Research Institute (NERI).
- Marquez, N., Ysambertt, F., de la Cruz, C., (1999). Three analytical methods to isolate and
characterize vanadium and nickel porphyrins from heavy crude oil. *Analytica Chimica Acta*, **395** (3), 343-349.
- Martinez-Haya, B., Hortal, A. R., Hurtado, P. M., Lobato, M. D., Pedrosa, J. M. (2007). Laser desorption/ionization determination of molecular weight distributions of polyaromatic carbonaceous compounds and their aggregates. *J. Mass Spectrom*, **42**, 701-713.
- Michel, J., and Galt, J. A. (1995). Conditions under which floating slicks can sink in marine settings. Proceedings of the 1995 International Oil Spill Conference. American Petroleum Institute, Washington DC, 573-576.
- Mansoori, G. (1997). Modeling of asphaltene and other heavy organics depositions. *Journal of Petroleum Science Engineering*, **17**, 101-111.

- Mansuy, L., Philp, R. P., and Allen, J. (1997). *Environmental Science Technology*, **31**, 3417-3425.
- Masuda, K., Okuma, O., Nishizawa, T., Kanaji, M., and Matsumura, T. (1996). High-temperature NMR Analysis of Aromatic units in Asphaltenes and Preasphaltenes derived from Victorian brown coal. *Fuel*, **75**, 295-299.
- McClements, D. J. (1998). *Food Emulsions: Principles, Practice, and Techniques*. CRC Press.
- McLean, J. D., and Kilpatrick, P. K. (1997). Comparison of Extrography in the Fractionation of Crude Oil Residua. *Energy & Fuels*. **11**, 570-585.
- McLean, J.D. and Kilpatrick, P. K. (1997). Effects of asphaltene aggregation in model heptane- toluene mixtures on stability of water-in-oil emulsions," *Journal of Colloid and Interface Science*, **196** (1), 23-34.
- McLean, J.D., P.M. Spiecker, A.P. Sullivan, and P.K. Kilpatrick (1998). The Role of Petroleum Asphaltenes in the Stabilization of Water-in-Oil Emulsions", in *Structure and Dynamics of Asphaltenes*, Mullins and Sheu (eds.), Plenum Press, New York, NY. 377-422.
- Mearns, Alan J., and Simecek-Beatty, D. (2003). Long-term weathering - Research Needs in Perspective. *Spill Science & Technology Bulletin*, **8**, (2.), 223-227.
- Mehta, S. D. (2005). Making and Breaking of Water in crude oil emulsions. M. Sc Thesis. Texas A & M University.
- Merdrignac, I., and Espinat, D. (2007). Physicochemical characterization of Petroleum Fractions: the State of the Art. *Oil & Gas Science and Technology – Rev. IFP*, **62**, (1), 7-32.

- Merlin, F. X., and Poutchkovsky, A. (2004). Behavior of Crude Oils: New Experimental Devices. SPE 86766. The Seventh SPE International Conference on Health, Safety, and Environment in Oil and Gas Exploration and Production. Calgary, Alberta, Canada.
- Midttun, Oivind., Kallevik, H., Sjoblom, J., Olav, M. K. (2000). Multivariate Screening Analysis of Water-in-oil Emulsions in High External Fields as Studied by Means of Dielectric Time Domain Spectroscopy. 111. Model Emulsions Containing Asphaltenes and Resins. *Journal of Colloid and Interface Science*, **227**, 262-271.
- Mille, G., Munoz, D., Jacquot, F., Rivet, L., and Bertrand, J. C. (1998). *Estuarine Coastal Shelf Science*, **47**, 547-559.
- Miller, R. (1982). Hydrogen Class Fractionation with Bonded-Phase Liquid Chromatography. *Analytical Chemistry*, **54** (11), 1742-1746.
- Mingyuan, L., Christy, A. A. and Sjoblom, J. (1992). Emulsion – A Fundamental and Practical Approach. NATO ASI Ser. **363**, Kluwer Academic Publishers, Dordrecht, 157.
- Mingyuan, L., A. A. Christy, and J. Sjöblom (1992). Water-in-Crude Oil Emulsions from the Norwegian Continental Shelf: Part VI. Diffuse Reflectance Fourier Transform Infrared Characterization of Interfacially Active Fractions from North Sea Crude Oil: In *Emulsions – A Fundamental and Practical Approach*, J. Sjöblom (ed.), Kluwer Academic Publishers, Dordrecht, The Netherlands, 157-172.
- Moldowan, J. M., Dahl, J., McCaffery, M. A., Smith, W. J., Fetzer, J. C. (1995). Application of biological marker technology to bioremediation of refinery by-products. *Energy and Fuel*, **9**, 155-162.
- Mullins, O. C. (2008). Review of the Molecular Structure and Aggregation of Asphaltenes and Petroleomics. SPE Journal. SPE (95801), **13**, (1), 48-57.

- Mullins, O. C. and Sheu, E. Y. (1998). Structures and Dynamics of Asphaltenes. Plenum Press, New York.
- Mullins, O. C., Sudipa, M., and Zhu, Y. (1992). The Electronic Absorption Edge of Petroleum. *Applied Spectroscopy*, **46**, 1405-1411.
- Mullins, O. C. (2009). Rebuttal of Strausz et al Regarding Time Resolved-Fluorescence Depolarization of Asphaltenes. *Energy & Fuels*, **23** (5), 2845-2854.
- Mullins, O. C. (2010). The Modified Yen Model. *Energy & Fuels*, **24** (4), 2179-2207.
- Mullins, O. C., Sheu, E. Y., Hammami, A., and Marshall, A. G. (2007). Asphaltenes, Heavy Oils, and Petroleomics. Springer Science + Business Media, LLC.
- Munoz, D., Doumenq, P., Guiliano, M., Jacquot, F., Scherrer, P., and Mille, G. (1997). *Talanta*, **45**, 1-12.
- Murgich, J., Strausz, O. P. (2002). Molecular mechanics of aggregates of asphaltenes and resins of the Athabasca oil. *Petroleum Science and Technology*. **19** (1-2). 231-243.
- Nagata, S. and Kondo, G. (1977). Photo-oxidation of crude oils. Oil spill Conference Proceedings.
- Nalwaya, V., Tangtayakom, V., Piumsomboon, P., Fogler, S. (1999). Studies of Asphaltenes through analyses of polar fractions. *Industrial & Engineering Chemistry Research*, **38** (3), 964-972.
- National Research Council (2003). Oil in the Sea 111: Inputs, Fates, and Effects. National Academies Press, Washington, DC.
- Nazir, M., Khan, F., Amyotte, P., and Sadiq, R. (2008). Multimedia fate of oil spills in a marine environment - An integrated modeling approach. *Process Safety and Environmental Protection*, **86**, 141-148.
- New Scientist (2003). Prestige oil spill far worse than thought. New Scientist.com news service, 27 August.

- Nicodem, D. E., Fernandes, M. C. Z., Guedes, C. L. B., and Correa, R. J. (1997). Photochemical processes and the environmental impact of petroleum spills. *Biogeochemistry*, **39**, 121-138.
- NOOA (2005). Office of Response and Restoration, GNOME. response.restoration.gov/software/gnome.html
- Nordli, K. G., Sjoblom, J., Kizling, J., and Stenius, P. (1991). Water-in-Crude Oil Emulsions from the Norwegian Continental Shelf 4. Monolayer Properties and the Interfacially active crude oil fraction. *Colloids and Surfaces*, **57**, 83-98.
- Nordvik, A. B. (1995). The Technology Windows-of-Opportunity for Marine Oil Spill Response as related to Oil Weathering and Operations. *Spill Science & Technology Bulletin*, **2**, (1) 17-46.
- Okpokwasili, G.C., Nnubia C (1995). Effects of drilling fluids on marine bacteria from a Nigerian offshore oilfield. *Environmental Management*, **19**, 923-929.
- OLF (2000). The Norwegian Oil Industry Association. Guidelines for characterization of offshore drill cuttings piles.
- OSPAR (2002). Quality status report 2000 for the North East Atlantic. <http://www.ospar.org/eng/html/welcome.html>
- Ostlund, J. A., Lofroth, J. E., Holmerg, K., Nyden, M., and Fogler, H. (2002). Flocculation behavior of asphaltenes in solvent/nonsolvent system. *Journal of Colloid Interface Science*, **253**, 150.
- Oudot, J., Merlin, F. X., and Pinvidic, P. (1998). Weathering rates of oil components in a bioremediation experiment in estuarine sediments. *Marine Environmental Resource*, **45**, 113-125.
- Oudut, J. (1984). Rates of microbial degradation of petroleum components as determined by computerized capillary gas chromatography and computerized mass spectrometry. *Marine Environmental Resources*, **13**, 277-302.

- PAC (2007). **79**, 1801. Definitions of terms relating to the structure and processing of sols, gels, networks, and inorganic-organic hybrid materials (IUPAC Recommendations 2007).
- Patin, Stanislav. (1999). Environmental impact of the offshore oil and gas industry, EcoMonitor Publishing East Northport, N.Y. Also available on www.offshore-environment.com
- Payne, J. R. and G. D. McNabb (1985). Weathering of petroleum in the marine environment. *Marine Technology Society*. **18**, 1-19.
- Payne, J. R., and Phillips, C. R. (1985). Petroleum Spills In the Marine Environment. The Chemistry and Formation of Water-in-Oil Emulsions and Tar Balls. Lewis Publishers Inc. USA.
- Peng, P., Fu, J., Sheng, G., Morales-Izquierdo, A., Lown, E. M. and Strausz, O. P. (1999). Ruthenium-Ions-Catalyzed Oxidation of an Immature Asphaltene: Structural Features and Biomarker Distribution. *Energy & Fuels*, **13**, 2, 266–277.
- Peters, K. E. and Moldowan J. M. (1993). The Biomarker Guide: Interpreting Molecular Fossils in Petroleum and Ancient Sediments, Prentice Hall, Englewood Cliffs, New Jersey.
- Peters, K. E., Walters, C. C., Moldowan, J. M. (2005). The Biomarker Guide Volume 1. Biomarkers and Isotopes in the Environment and Human History. Second ed. University Press, Cambridge.
- Premovic, P. I., Dordevic, D. M., Pavlovic, M. S., (2002). Vanadium of petroleum asphaltenes and source kerogens (La Luna Formation, Venezuela): isotopic study and origin. *Fuel* **81** (15), 2009-2016.
- Premovic, P. I., Jovanovic, L. S., (1997). Are vanadyl porphyrins products of asphaltene/kerogen thermal breakdown? *Fuel* **76** (3), 267-272

- Premuzic, E. T, and Lin, M. S. (1999). *Journal of Petroleum Science and Engineering*, **22**, (1), 171-180.
- Prince, R. C., Garrett, R. M., Bare, R. E., Grossman, M. J., Townsend, T., Suflita, J. M., Lee, K., Owens, E. H., Sergy, G. A., Braddock, J. F., Lindstrom, J. E., and Lessard, R. R. (2003). The roles of photooxidation and biodegradation in long-term weathering of crude oil and heavy fuel oils. *Spill Science Technology Bulletin*, **8**, 145-156.
- Prince, R. C., Stibrany, R. T., Hardenstine, J., Douglas, G. S., and Owens, E. H. (2002). Aqueous evaporation: A previously unrecognized weathering process affecting oil spills in vigorously aerated water. *Environmental Science & Technology*, **36**, 2822-2825.
- Prince, R.C., Elmendorf, D. L., Lute, J. R., Hsu, C. S., Halth, C. E., Senius, J. D., Dechert, G. J., Douglas, G. S., and Butler, E. L. (1994). *Environmental Science & Technology*, **28**, 142-145.
- Rainey, G., Lehr, W., Johnson, W. (2003). Longer-term Weathering Workshop: An Overview. *Spill Science and Technology Bulletin*, **8**, 2.
- Rajagopal, K., and Silva, S. M. C. (2004). An Experimental Study of Asphaltene Particle Sizes in *n*-Heptane –Toluene Mixtures by Light Scattering. *Brazilian Journal of Chemical Engineering*. **21**, (04), 601-609.
- Ralston, C.Y., Mitra-Kirtley, S., and Oliver C. Mullins (1996). Small Population of One to Three Fused-Aromatic Ring Moieties in Asphaltenes. *Energy Fuels*, **10**, 623-630.
- Ramade F. (1978). *Elements D.ecologie Appliquee*. McGraw Hill Publ., 497 p.
- Reddy, C. M., Eglinton, T. I., Hounshell, A., White, H.K., Xu, L., Gaines, R. B., Frysiner, G. S. (2002). The West Falmouth Oil spill after thirty years: the persistence of petroleum hydrocarbons in marsh sediments. *Environmental Science and Technology*, **36**, 4754-4760.

- Reed, M. (1989). The physical fates component of the natural resource damage assessment model system. *Oil Chemistry Pollution*, **5**(2-3), 99-123.
- Reed, M. (2005). Numerical Models for Marine Environmental Risk Management. SINTEF Materials and Chemistry. Norwegian Institute of Technology (NTH), 1-6.
- Reed, M. (2007). State -of- the Art, The Future, Research Questions to be Addressed. Coastal Response Research Center. University of New Hampshire.
- Riazi, M. R and Al Enezi, G. A. (1999). Modeling of the rate of oil spill disappearance from seawater for Kuwaiti crude and its products. *Chemical Engineering Journal*, **73**, 161-172.
- Riazi, M. R., and M. Edalat. (1996). Prediction of the fate of oil removal from seawater by evaporation and dissolution. *Journal of Petroleum Science and Engineering*, **16**. 291- 300
- Rodgers, R. P., and Marshall, A. (2004). *Petroleomics: Advanced Characterization of Petroleum – Derived Materials by Fourier Transform Ion Cyclotron Resonance Mass Spectrometry (FT-ICR MS)*. In: *Asphaltenes, Heavy Oils, and Petroleomics*, (2007). Springer Science + Business Media, LLC.
- Rodgers, R. P., Schaub, T. M., and Marshall, A. G. (2005). Mass spectroscopy returns to its root. *Analytical Chemistry*, **77**, 20A-27A.
- Rodgers, R., Blumer, E. N., Freitas, M. A., and Marshall, A. G., (2000). Complete compositional monitoring of the weathering of transportation fuels based on elemental compositions from Fourier transform ion cyclotron resonance mass spectrometry. *Environmental Science & Technology*, **34**, 1671-1678.
- Rogers, K. M. and Savard, M. M. (1999). Detection of Petroleum contamination in river sediments from Quebec City region using GC-IRMS. *Organic Geochemistry*, **30**, 12, 1559-1569.

- Röling, W. F. M., Milner, M. G., Jones, D. M., Lee, K., Daniel, F., Swannell, R. J. P., and Head, I. M. (2002). Robust Hydrocarbon Degradation and Dynamics of Bacterial Communities during Nutrient-Enhanced Oil Spill Bioremediation. *Applied and Environmental Microbiology*. **68**, 5537-5548.
- Rønningsen, H. P. (1995). Correlations for predicting Viscosity of W/O Emulsions based on North Sea Crude Oils. SPE 28968. SPE International Symposium on Oilfield Chemistry. San Antonio. 14-17 February.
- Ross, S., Buist, I. (1995). Preliminary laboratory study to determine the effect of emulsification on oil spill evaporation. Proceedings, 18th Arctic Marine Oilspill Program Technical Seminar. Environment Canada, Edmonton, Alberta, 61-74.
- Ruiz-Morales, Y. (2004). The agreement between clar structures and nucleus-independent chemical shift values in pericondensed benzenoid polycyclic aromatic hydrocarbons: An application of the Y-rule. *Journal of Physical Chemistry. A*. **108**. 10873.
- Ruiz-Morales, Y. (2007). Molecular Orbital Calculations and Optical Transitions of PAH and Asphaltenes. *Asphaltenes, Heavy Oils and Petroleomics*: Mullins, O. C., Sheu, E. Y., Hammami, A.G., eds.; Springer: New York. Chapter 4.
- Ruiz-Morales, Y., and Mullins, O. C. (2009). Measured and Simulated Electronic Absorption and Emission Spectra of Asphaltenes. *Energy & Fuels*, **23**, 1169-1177.
- Ruiz-Morales, Y., Mullins, O. C. (2007). Polycyclic Aromatic hydrocarbons of Asphaltenes analyzed by Molecular Orbital Calculations with Optical Spectroscopy. *Energy & Fuels*. **21**. 256.
- Ruiz-Morales, Y., Xu, Wu., and Mullins, O. C. (2007). Electronic Absorption Edge of Crude Oils and Asphaltenes Analyzed by Molecular Orbital Calculations with Optical Spectroscopy. *Energy & Fuels*. **21**. 944-952.

- Salager, Jean-Louis (2002). Surfactants - Types and uses. Laboratory of Formulation, Interphases Rheology and Processes (FIRP). Escuela de Ingeniera Quimica, Universidad de los ANDES, Venezuela.
- Sasaki, T., Maki, H., Ishihara, M., and Harayama, S. (1998). Vanadium as an internal marker to evaluate microbial degradation of crude oil. *Environmental Science Technology*, **32**, 3618- 3621.
- Sauer, T. C. and Boehm, P. D. (1995). Guidance document on hydrocarbon chemistry analytical methods for oil spill assessments. Marine Spill Response Corporation, Tech. Report. 95 –032, Washington, D.C.
- Sauer, T. C., Michel, J., Hayes, M. O., and Aurand, D. V. (1998). Hydrocarbon characterization and weathering of oiled intertidal sediments along the Saudi Arabian Coast two years after the Gulf War oil spill, *Environment International*, **24**, 43-60.
- Scholten, M. C. Th., Karman, C. C., and Huwer, S. (2000). Ecotoxicological risk assessment related to chemicals and pollutants in off-shore oil production. *Toxicological Letters*, **112-113**, 283-288.
- Schorling, P. C., Kessel, D. G., Rahimian, I. (1999). Influence of the crude oil resin/asphaltene ratio on the stability of oil/water emulsions. *Colloids and Surfaces. A: Physicochemical and Engineering Aspects*, **152**, 95–102.
- Schuettelkopf, A, W. and van Aalten, D. M. F. (2004). "PRODRG: a tool for high-throughput crystallography of protein-ligand complexes", *Acta Crystallogr. D*, **60**, 1355-1363.
- Schuler, L. D., Daura , X. and van Gunsteren, W. F. (2001) An improved GROMOS96 force field for aliphatic hydrocarbons in the condensed phase. *J. Comput. Chem.*, **22**, 1205-1218.
- Sebastiao, P. and Soares, C. G. (1995). Modelling the fate of oil spills at sea. *Spill Science & Technology Bulletin*, **2**, 121-131.

- SEEEEC (1998). Sea Empress Environmental Evaluation Committee Final Report. The environmental impact of the Sea Empress. Stationery Office, London, UK.
- Seidl, P. R., Chrisman, E. C. A. N., Carvalho, C. C. V., Leal, K. Z., Menezes, S. M. C. de. (2004). *Journal of Dispersion Science and Technology*. **25** (3), 349-353.
- Short, J. W and Heintz, R. A. (1997). Identification of *Exxon Valdez* Oil in Sediments and Tissues from Prince William Sound and the Northwestern Gulf of Alaska Based on a PAH Weathering Model. *Environmental Science and Technology*, **31**, (8), 2375-2384.
- Short, J. W. (2002). Oil identification based on a goodness-of-fit metric applied to hydrocarbon analysis results. *Environmental Forensics*, **3**, 349-356. In: Sjoblom, J. (1996). *Emulsions and Emulsion Stability* (ed.). Marcel Dekker Inc, New York.
- Singh, S., McLean, J. D. and Kilpatrick, P. K. (1999). Fused Ring Aromatic Solvency in Destabilizing Water-in-Asphaltene-Heptane-Toluene Emulsion. *Journal of Dispersion Science and Technology*, **20** (1&2), 279-293.
- Sjoblom, J., Aske, N., Auflem, I. H., Brandal, O., Havre, T.E., Saether, O., Westvik, A., Johnson, E. E. and Kallevik, H. (2003). Our current understanding of water-in-crude oil emulsions. Recent characterisation techniques and high pressure performance. *Advanced Colloid Interface Science*, **399**, 100-102.
- Sjoblom, N. J., Hemmingsen, P. V., Kallevik, H. (2007). The role of asphaltenes in stabilizing water -in- crude oil emulsions, In: O.C. Mullins, E.Y. Sheu, A. Hammami, A.G. Marshall *Asphaltenes, Heavy Oils and Petroleumics*. Springer Publications, N.Y, 549.
- Sjoblom, J., Soderlund, H., Lindblad, S., Johansen, E. J., and Skjarvo, I. M. (1990). Water-in-Crude Oil Emulsions from the Norwegian Continental Shelf Part 11. Chemical Destabilization and interfacial Tension. *Colloids and Polymer Science*, **268**, 389-398.

- Sjoblom, J., Urdahl, O., Hoiland, H., Christy, A. A., Johansen, E. J. (1990). Water-in-Crude Oil. Formation, Characterisation, and Destabilisation. *Progress in Colloids and Polymer Science*, **82**, 131-139.
- Sjoblom, J., Urdahl, O., Borge, K. G. N., Mingyuan, L., Saeten, J.O., Christy, A. A., and Gu, T. (1992). Stabilization and Destabilization of Water-in-Crude Oil Emulsions from the Norwegian Continental Shelf. Correlation with Model Systems. *Advances in Colloids and Interface Science*, **41**, 241-271.
- Smith, D. F., Tanner, M. Schaub., Rahimi, P., Teclemariam, A., Ryan P. Rodgers, R. P., and Marshall, A. G. (2004). Self- Association of Organic Acids in Petroleum and Canadian Bitumen Characterized by Low- and High-Resolution Mass Spectroscopy. *Energy & Fuels*, **21**, 1309-1316.
- Speight, J. G. (2004). Petroleum Asphaltene Part 1. Asphaltenes, Resins and the Structure of Petroleum. *Oil & Gas Science and Technology – Rev. IFP*, **59**, 5, 467-477
- Spiecker, M. P., Gawrys, K. L., Trail, C. B., and Kilpatrick, P. K. (2003). Effects of petroleum resins on asphaltene aggregation and water-in-oil emulsion formation. *Colloids and Surfaces A: Physicochemical Engineering Aspects*, **220**, 9 – 27.
- Spiecker, P. M. (2001). The Impact Of Asphaltene Chemistry and Solvation On Emulsion And Interfacial Film Formation. PhD Thesis.
- Spiecker, P.M., Gawrys, K.L., Kilpatrick, P.K. (2003). Aggregation and solubility behavior of asphaltenes and their subfractions. *Journal of Colloid Interface Science*, **267**. 179.
- Spiecker, P.M., Gawrys, K.L., Trail, C.B., Kilpatrick, P.K. (2003). Effects of petroleum resins on asphaltene aggregation and water-in-oil emulsion formation, *Colloids Surfaces. A: Physicochemical Engineering Aspects*, **228**, 131.
- Spiecker, P.M., Kilpatrick, P. K. (2004). Interfacial Rheology of Petroleum Asphaltenes at the oil-water interface. *Langmuir*, **20**, 4022.

- Stankiewicz, A.B., Flannery, M. D., Fuex, N. A., Broze, G., Couch, J. L., Dubey, S. T., Iyer, S. D., Ratulowski, J. and Westerich, J. T. (2002). Prediction of asphaltene deposition risk in E&P operations. In: *Proceedings of 3rd International Symposium on Mechanisms and Mitigation of Fouling in Petroleum and Natural Gas Production, AIChE 2002 Spring National Meeting*, New Orleans, USA, **47C**, 410-416.
- Steiner, R., (2003). Background document on offshore oil for Stakeholders of the Baltic Sea region. Unpublished report available via the authors.
- Stiver, W. and Mackay, D. (1984). Evaporation rates of spills of hydrocarbon and petroleum mixtures. *Environmental Science and technology*. **18**, 834-840.
- Stout, S. A., Uhler, A. D., and McCarthy, K. J. (2001). A strategy and methodology for defensibly correlating spilled oil to source candidates. *Environmental Forensics*, **2**, 87-98.
- Strausz, O. P., Safarik, I., Lown, E. M., and Morales- Izquierdo, A. (2008). A Critique of Asphaltene Fluorescence Decay and Depolarisation – Based Claims about Molecular weight and Molecular Architecture. *Energy & Fuels*, **22** (2), 1155 – 1166.
- Strom-Kristiansen, T., Daling, P. S., Lewis, A. (1993). Weathering Properties and Chemical Dispersibility of Crude oils Transported in US Waters. IKU Report, No. 22. 2142.00/94. Marine Spill Response Corporation. Washington DC. MRSC Technical Report Series No. 93-032. p. 214.
- Strom-Kristiansen, T., Lewis, A., Daling, P. S., Hokstad, J, N., Singsaas, I. (1997). Weathering and dispersion of naphthenic, asphaltenic and waxy crude oils. In: Paper to 1997 Oil Spill International Conference, Fort Lauderdale, Florida, 2-10 April, 631-636.
- Syndes, L.K., Hemmingsen, T. H., Skare, S., Hansen, S. H., Falk-Petersen, I. B., Lonning, S., and Ostgaard, K. (2001). Seasonal variations and toxicity in weathering of crude oil on seawater under arctic conditions. *Environmental Science Technology*, **19**, 1076-1081.

- Tanaka, R., Sato, E., Hunt, J., Winans, R., Sato, S., and Takanohashi, T. (2004). Characterisation of asphaltene aggregates using X-ray diffraction and small-angle X-ray scattering. *Energy Fuels*, **18**, 1118.
- The Institute of Petroleum (1983). *Methods for Analysis and Testing*. Chichester, John Wiley.
- The Institute of Petroleum. (1983). *Methods for Analysis and Testing*. Chichester, John Wiley.
- The Institute of Petroleum. Guidelines on the use of oil spill dispersants (1986). London, Institute of Petroleum.
- The Leading Edge. Society of Exploration Geophysicists (SEG)*, (2004). Special Section- Heavy Oil. **27**, 8.
- Thominette, F. and Verdu, J. (1984). Photo-oxidative behaviour of crude oils relative to sea pollution. Part1. Comparative studies of various crude oils and model systems. *Marine Chemistry*, **15**, 91-104.
- Thominette, F. and Verdu, J. (1984). Photooxidative behaviour of crude oils relative to sea pollution. Part 11. Photo-induced phase separation. *Marine Chemistry*. **15**, 105-115.
- Tissot, B. P. and Welte, D. H. (1984). *Petroleum Formation and Occurrence*. Springer-verlag, Berlin.
- Trejo, F., G. Centeno., J. Ancheyta (2004). Precipitation, fractionation and characterization of Asphaltenes from heavy and light crude oils. *Fuel*, **83**, 2169-2175.
- UNEP (2011). Environmental Assessment of Ogoniland. United Nation Environment Programme. Nairobi, Kenya. (www.unep.org/nigeria).

- U.S. Environmental Protection Agency (1990). Interim Report, Oil Spill Bioremediation Project. U.S. Environmental Protection Agency, Office of Research and Development, Washington
- van der Meer, J. R. (2005). Sixth Framework Programme Priority (3). Fast Advanced Cellular and Ecosystem Information Technologies. Project no. 018391. Global Change and Ecosystem (FP6-2004-Global-3-3.111.3.1).
- Vanquez, D. and Mansoori, G. A. (2000). Identification and Measurement of petroleum precipitates. *Journal of Petroleum Science and Engineering*. **26**: 49-55.
- Venosa, D., Suidan, M. T., King, D., and Wrenn, B. A., (1997). *Journal of Industrial Microbiology and Biotechnology*, **18**, 131-139.
- Walker, M. I., Albone, D. J., McDonagh, M., Wilkinson, A. O., Baron, G. R., and Grigson, S. J. W. (1992). Final Report on the Joint Programme of Research on Source Identification, Behaviour and Modelling of North Sea Crudes at Sea. Stevenage: Warren Spring Laboratory. Report CR 3698. IOE Report 89/790/R4.
- Walker, M., McDonaugh, M., Albone, D., Grigson, S., Wilkinson, A., Baron, G. (1993b). Comparison of observed and predicted changes to oil after spills. *In Proceedings of the 1993 Oil Spill Conference*. 389-393.
- Wang, X., and Mullins, O. C. (1994). Fluorescence lifetime of crude oils. *Applied Spectroscopy*, **48**, (8), 977-984.
- Wang, Z. and Fingas, M. (1994). Study of the effects of weathering on the chemical composition of a light crude oil. 17th Environment Canada arctic and marine oil spill program (AMOP) technical seminar. Vancouver, Canada. June 8-10, **1**, 133-171.
- Wang, Z. and Fingas, M. (1995). Use of methyldibenzothiophenes as markers for differentiation and source identification of crude and weathered oils. *Environmental Science Technology*, **29**, 2842 –2849.

- Wang, Z. and Fingas, M. (1995). Study on the effects of weathering on the chemical composition of a light crude using GC/MS GC/FID, *Journal of Microcolumn Separations*, **76**, 617-639.
- Wang, Z. D. and Fingas, M. (2003). Fate and identification of spilled oils and petroleum products in the environment by GC-MS and GC-FID, *Energy Sources*, **25**, 491-508.
- Wang, Z. D. and Fingas, M. F. (2003). Development of oil hydrocarbon fingerprinting and identification techniques, *Marine Pollution Bulletin*, **47**, 423-452.
- Wang, Z. D., Fingas, M., Lambert, P., Zeng, G., Yang, C., and Hollebone, B. (2004) Characterization and identification of the Detroit River mystery oil spill (2002), *Journal of Chromatography A*, **1038**, 201-214.
- Wang, Z., and Stout, S. A. (2007). *Oil Spill Environmental Forensics: Fingerprinting and Source Identification*. Academic Press, London, UK.
- Wang, Z., Fingas, M., and Sigouin, L. (2000). Characterization and source identification of an unknown spilled oil using fingerprinting techniques by GC-MS and GC-FID. *LC GC N. Am.*, **18**, 1058 – 1067.
- Wang, Z., Fingas, M., Blenkinsopp, S., Sergy, G., Landriault, M., Sigouin, L., Foght, J., Semple, K., Westlake, D. W. S. (1998). Comparison of oil changes due to biodegradation and physical weathering in different oils. *Journal of Chromatography A*, **809**, 89-107.
- Wang, Z.D. and Fingas, M. (1995). Study of the effects of weathering on the chemical composition of a light crude oil using GC/MS and GC/FID. *Journal of Microcolumn Separation*, **7**, 617-639.
- Weast, R. C., (1980). *CRC Handbook of Chemistry and Physics*, 60th ed. CRC Press, Boca Raton, FL.

- Weaver, J. W. (2004). Characteristics of spilled Oils, Fuels, and Petroleum Products: 3a. Simulation of Oil Spills and Dispersant Under Conditions of Uncertainty. EPA 600/R-04/120.
- Whittaker, M., Pollard, S. J. T., Fallick, A. E., and Preston, T. (1996). Characterization of refractory waste at hydrocarbon-contaminated sites - 11. Screening of reference oils by stable carbon isotope fingerprinting. *Environmental Pollution*, **94**, 195-203.
- Wikimedia Foundation, (2006). Soxhlet extractor. In: *Wikipedia* online encyclopedia.
- Williams, J. (1991). High internal phase water-in-oil emulsions: influence of surfactants on emulsion stability and foam quality. *Langmuir* **7**, 437-444
- Wills, J. W. G. (2002). Muddied Waters – A survey of Offshore Oilfield Drilling Wastes and Disposal Techniques to Reduce the Ecological Impact of Sea Dumping. *Ekologicheskaya Vahkta Sakhalina*, Yuzhno-Sakhalinsk, Russia, **139**, 1977.
- Xie, H., Yapa, P. D., Nakata, K. (2007). Modeling emulsification after an oil spill in the sea. *Journal of Marine Systems*, **68**. 489-506.
- Yanfei, Ma; Xuedong, Feng; Menghong, Li (2010). Volatilization rates of oils spills on porous media. *Environmental Science and Information Application Technology (ESIAT), International Conference*. 343-346.
- Yarranton, H.W., Urrutia, P., Sztukowski, D. M. (2007). Effect of Interfacial Rheology on model emulsion Coalescence. 1. Interfacial Rheology. *Journal of Colloid Interface Science*. **310**, 246.
- Yarranton, H.W., Urrutia, P., Sztukowski, D. M. (2007). Effect of Interfacial Rheology on model emulsion Coalescence. 11. Emulsion Coalescence, *Journal of Colloid Interface Science*. **310**. 253.

- Zagoski, W., and D. Mackay. (1982). Studies of Water-in-oil emulsions. EPS Report EE-34. Environment Canada. Ottawa.
- Zhang, L. and Greenfield, M. L. (2007). Molecular Orientation in Model Asphalts Using Molecular Simulation. *Energy Fuels*, **21** (2), 1102–1111
- Zhou, Y. S., Wang, B., and Zhu, M. Z. (2005). Observation of existence of ‘face-on’ and ‘edge-on’ stacking styles in a porphyrin monolayer. *Chemical Physics Letters*, **403** (1-3). 140-145.
- Zhu, Y. and O. C. Mullins (1992). Temperature dependence of fluorescence of crude oils and related compounds.